SYNTHETIC BIOLOGY OF YEASTS FOR THE PRODUCTION OF NON-NATIVE CHEMICALS, 2nd Edition

EDITED BY: Farshad Darvishi, Mark Blenner and Rodrigo Ledesma-Amaro

PUBLISHED IN: Frontiers in Bioengineering and Biotechnology

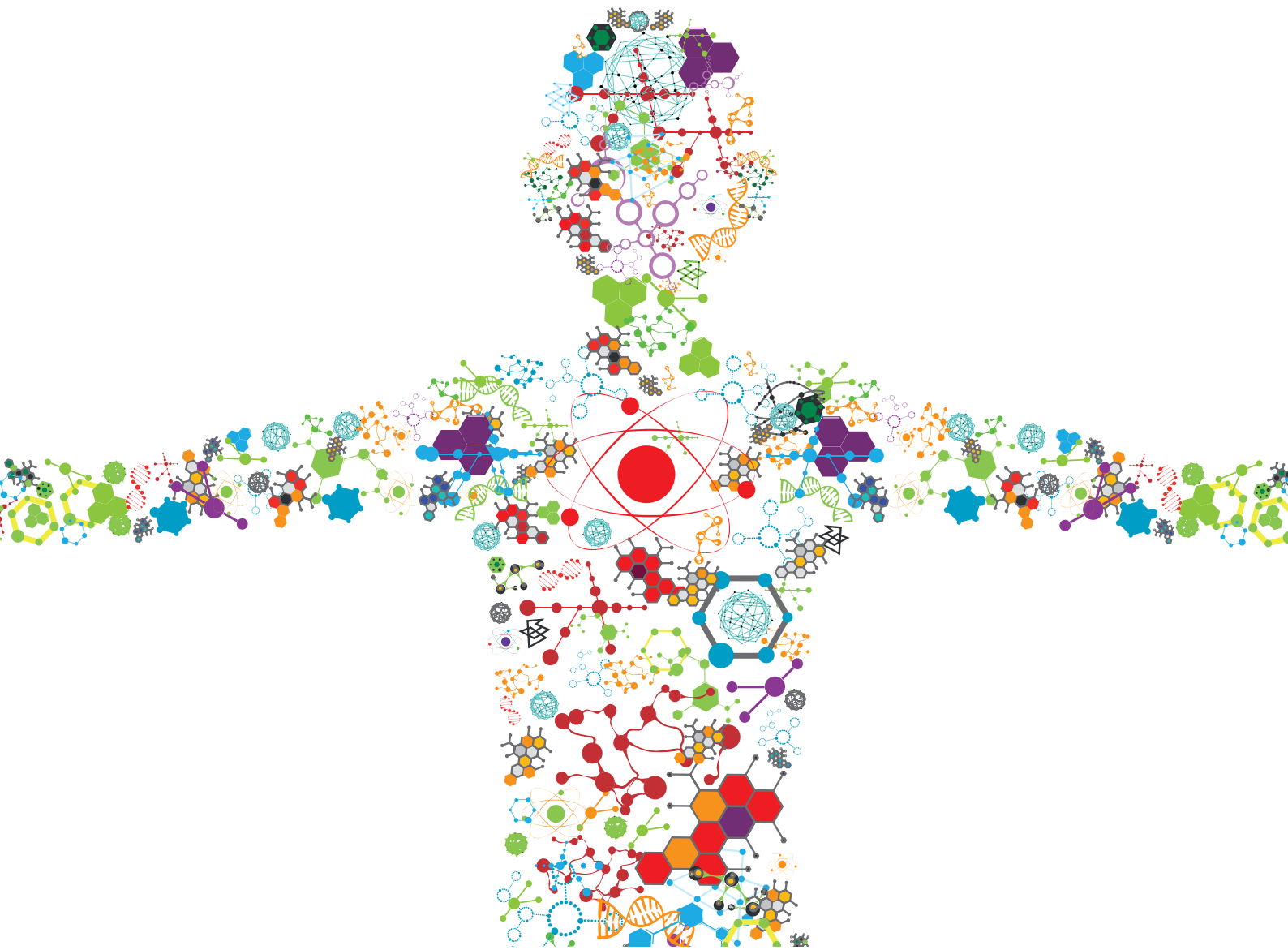

frontiers Research Topics

frontiers

ISSN 1664-8714
ISBN 978-2-88971-324-0
DOI 10.3389/978-2-88971-324-0

About Frontiers

Frontiers is more than just an open-access publisher of scholarly articles: it is a pioneering approach to the world of academia, radically improving the way scholarly research is managed. The grand vision of Frontiers is a world where all people have an equal opportunity to seek, share and generate knowledge. Frontiers provides immediate and permanent online open access to all its publications, but this alone is not enough to realize our grand goals.

Frontiers Journal Series

The Frontiers Journal Series is a multi-tier and interdisciplinary set of open-access, online journals, promising a paradigm shift from the current review, selection and dissemination processes in academic publishing. All Frontiers journals are driven by researchers for researchers; therefore, they constitute a service to the scholarly community. At the same time, the Frontiers Journal Series operates on a revolutionary invention, the tiered publishing system, initially addressing specific communities of scholars, and gradually climbing up to broader public understanding, thus serving the interests of the lay society, too.

Dedication to Quality

Each Frontiers article is a landmark of the highest quality, thanks to genuinely collaborative interactions between authors and review editors, who include some of the world's best academicians. Research must be certified by peers before entering a stream of knowledge that may eventually reach the public - and shape society; therefore, Frontiers only applies the most rigorous and unbiased reviews.
Frontiers revolutionizes research publishing by freely delivering the most outstanding research, evaluated with no bias from both the academic and social point of view. By applying the most advanced information technologies, Frontiers is catapulting scholarly publishing into a new generation.

What are Frontiers Research Topics?

Frontiers Research Topics are very popular trademarks of the Frontiers Journals Series: they are collections of at least ten articles, all centered on a particular subject. With their unique mix of varied contributions from Original Research to Review Articles, Frontiers Research Topics unify the most influential researchers, the latest key findings and historical advances in a hot research area! Find out more on how to host your own Frontiers Research Topic or contribute to one as an author by contacting the Frontiers Editorial Office: frontiersin.org/about/contact

SYNTHETIC BIOLOGY OF YEASTS FOR THE PRODUCTION OF NON-NATIVE CHEMICALS, 2nd Edition

Topic Editors:
Farshad Darvishi, Alzahra University, Iran
Mark Blenner, University of Delaware, United States
Rodrigo Ledesma-Amaro, Imperial College London, United Kingdom

Publisher's note: In this 2nd edition, the following article has been added: Darvishi F, Blenner M and Ledesma-Amaro R (2021) Editorial: Synthetic Biology of Yeasts for the Production of Non-Native Chemicals. *Front. Bioeng. Biotechnol.* 9:730047. doi: 10.3389/fbioe.2021.730047

Citation: Darvishi, F., Blenner, M., Ledesma-Amaro, R., eds. (2021). Synthetic Biology of Yeasts for the Production of Non-Native Chemicals, 2nd Edition. Lausanne: Frontiers Media SA. doi: 10.3389/978-2-88971-324-0

Table of Contents

frontiers in Bioengineering and Biotechnology

EDITORIAL
published: 11 August 2021
doi: 10.3389/fbioe.2021.730047

Editorial: Synthetic Biology of Yeasts for the Production of Non-Native Chemicals

Farshad Darvishi[1,2]*, *Mark Blenner*[3]* and *Rodrigo Ledesma-Amaro*[4,5]*

[1]Department of Microbiology, Faculty of Biological Sciences, Alzahra University, Tehran, Iran, [2]Research Center for Applied Microbiology and Microbial Biotechnology (CAMB), Alzahra University, Tehran, Iran, [3]Department of Chemical and Biomolecular Engineering, University of Delaware, Newark, DE, United States, [4]Department of Bioengineering, Imperial College London, London, United Kingdom, [5]Imperial College Centre for Synthetic Biology, Imperial College London, London, United Kingdom

Keywords: synthetic biology, yeast, metabolic engineering, bulk and fine chemicals, biotechnology, *Yarrowia lipolytica*, *Saccharomyces cerevisiae*

Editorial on the Research Topic

Synthetic Biology of Yeasts for the Production of Non-Native Chemicals

OPEN ACCESS

Edited and reviewed by:
Jean Marie François, Institut Biotechnologique de Toulouse (INSA), France

***Correspondence:**
Farshad Darvishi
f.darvishi@ymail.com
f.darvishi@alzahra.ac.ir
Mark Blenner
blenner@udel.edu
Rodrigo Ledesma-Amaro
r.ledesma-amaro@imperial.ac.uk

Specialty section:
This article was submitted to Synthetic Biology, a section of the journal Frontiers in Bioengineering and Biotechnology

Received: *24 June 2021*
Accepted: *31 July 2021*
Published: *11 August 2021*

Citation:
Darvishi F, Blenner M and Ledesma-Amaro R (2021) Editorial: Synthetic Biology of Yeasts for the Production of Non-Native Chemicals. Front. Bioeng. Biotechnol. 9:730047. doi: 10.3389/fbioe.2021.730047

Yeasts are now considered attractive microbial cell factories for the production of a wide range of bulk and fine chemicals, including biofuels, pharmaceuticals, agrochemicals, fragrances, additives, pigments, and so on. Yeasts are easy to manipulate and scale-up and have a short generation and production time. However, metabolic engineering of yeasts is needed to make robust cell factories that produce the desired chemicals at high titers, rates, and yields. Synthetic biology techniques such as computational tools for metabolic modeling and pathway design, synthesis and assembly of standardized DNA parts, powerful genome editing methods and optimization of synthetic pathways, have been developed to improve the metabolic engineering of yeasts and to construct novel pathways for the production of non-native chemicals in a faster and more reliable manner without any additional metabolic burden.

This topic focuses on approaches of rewiring metabolism in yeasts to produce non-native chemicals, overcoming potential bottlenecks and on the identification of key challenges and future research trends. A short description of the articles included in this topic can be found below.

Meng et al. provided an overview of the latest research progress in the use of CRISPR/Cas9 systems in genome editing with a focus on the applications in synthetic biology of *Saccharomyces cerevisiae*.

Kim et al. reviewed synthetic pathways diverging from the distinctive cellular metabolism of bioethanol-producing *S. cerevisiae* and biodiesel-producing *Yarrowia lipolytica* to guide future directions for product-specific engineering strategies for the sustainable production of non-native chemicals.

Yocum et al. summarized the colocalization strategies of enzymes, including enzyme scaffolding, construction of synthetic organelles, and organelle targeting, in metabolic and synthetic pathways of yeast to ensure sufficient carbon flux towards the desired product.

Bradley et al. reviewed the recent progress in the biosynthesis of plant-derived natural products in yeasts, especially medically relevant halogenated alkaloids. The halogenated alkaloids are rare in nature. The introduction of halogenated substrates or halogenation enzymes enables the production of non-natural halogenated chemicals in yeast.

Arnesen et al. engineered *Y. lipolytica* for the production of terpenoids, including mono, sesqui-, tri-, di- and tetraterpenoids. They provided the first report for the production of β-farnesene and the highest reported titer of valencene (sesquiterpenoid) in *Y. lipolytica*.

Furthermore, platform strains produced limonene, squalene, 2,3-oxidosqualene, or β-carotene.

The platform strains can be used for the evaluation of terpenoid biosynthetic pathways and it is a good starting point for constructing efficient cell factories of terpenoids.

López et al. produced β-ionone and β-carotene in engineered *S. cerevisiae*. The multiple expression of heterologous genes producing β-ionone and β-carotene were examined. Then, they carried out the tuning of the expression conditions to improve the production of β-ionone and β-carotene in the engineered *S. cerevisiae*, which resulted in the highest production of β-ionone in this yeast. Finally, a genome-scale metabolic model of *S. cerevisiae* was used to better understand β-ionone production in the engineered yeast and propose strategies to further enhance β-ionone titers.

Lajus et al. reported the production of poly-D-lactic acid (PDLA) in an engineered strain of *Y. lipolytica*. First, they identified and interrupted the pathway for lactic acid consumption in this yeast. Then, the heterologous pathway for PDLA production was introduced into the engineered strain. After that, PDLA homopolymer accumulated in the cells with the highest reported amount of produced PDLA *in vivo* so far.

Foo et al. generated strains of *S. cerevisiae* with the highest reported cytosolic aliphatic aldehyde and alkane/alkene production from fatty acyl-CoA by protein engineering of a fatty acyl-CoA reductase to alter its activity and metabolic engineering of *S. cerevisiae*.

Hambalko et al. reported the production of a fatty alcohol mixture by expressing bumble bee reductases in *Y. lipolytica*. A mixture of aliphatic unbranched fatty alcohols with eight or more carbons is naturally found in bumble bee as sex pheromones. A high titer and yield of fatty alcohols were obtained in the engineered strains by functional expression of bumble bee reductases from *B. lapidarius* (*Blap*Far) and *B. lucorum* (*Bluc*Far).

Park et al. engineered *Y. lipolytica* to produce ω-hydroxy palmitic acid from glucose using evolutionary metabolic engineering and synthetic FadR promoters for cytochrome P450 expression. They demonstrated *de novo* production of ω-hydroxy palmitic acid in batch fermentation containing nitrogen-limited media.

Overall, the collected works in this Research Topic present fabulous examples of advanced yeast metabolic engineering using synthetic biology in order to produce non-native chemicals of industrial interests.

Despite these exciting advances, the successful translation of non-native production of chemicals in yeast into the industrial practice is still limited. Just a few non-native chemicals are produced by yeasts on a commercial scale using metabolic engineering and synthetic biology tools. One of the major bottlenecks is making robust yeast strains to produce the chemicals at high titer, rate, and yield. The synthetic biology tools to construct synthetic pathways and rewire metabolism in yeasts are actively being developed to overcome these barriers.

Further advances in strain engineering technologies and computational guided synthetic biology are expected to streamline the strain creation process, but much work still need to be done. The creation of chassis strain, enriched in a particular type of products or their precursors can accelerate the number of successful stories. Interestingly, the type of yeasts being explored for bioproduction has expanded massively in recent years and we now see more and more examples of chemicals being made in non-*S. cerevisiae* microbes, as we can see in this issue. These non-conventional and non-model yeast hold great potential for overcoming the challenges associated with commercializing biotechnology when combined with the nascent and accelerating pace of synthetic biology tools across yeast platofrms.

In summary, there is a great potential in yeast biotechnology to address current sustainable manufacturing challenges and the scientific community is working hard and moving the field in the right direction.

AUTHOR CONTRIBUTIONS

All authors listed have made a substantial, direct, and intellectual contribution to the work and approved it for publication.

Conflict of Interest: The authors declare that the research was conducted in the absence of any commercial or financial relationships that could be construed as a potential conflict of interest.

Publisher's Note: All claims expressed in this article are solely those of the authors and do not necessarily represent those of their affiliated organizations, or those of the publisher, the editors and the reviewers. Any product that may be evaluated in this article, or claim that may be made by its manufacturer, is not guaranteed or endorsed by the publisher.

frontiers in Bioengineering and Biotechnology

ORIGINAL RESEARCH
published: 14 August 2020
doi: 10.3389/fbioe.2020.00945

Yarrowia lipolytica Strains Engineered for the Production of Terpenoids

*Jonathan Asmund Arnesen†, Kanchana Rueksomtawin Kildegaard†, Marc Cernuda Pastor, Sidharth Jayachandran, Mette Kristensen and Irina Borodina**

The Novo Nordisk Foundation Center for Biosustainability, Technical University of Denmark, Kongens Lyngby, Denmark

Terpenoids are a diverse group of over 55,000 compounds with potential applications as advanced fuels, bulk and fine chemicals, pharmaceutical ingredients, agricultural chemicals, etc. To facilitate their bio-based production, there is a need for plug-and-play hosts, capable of high-level production of different terpenoids. Here we engineer *Yarrowia lipolytica* platform strains for the overproduction of mono-, sesqui-, di-, tri-, and tetraterpenoids. The monoterpene platform strain was evaluated by expressing *Perilla frutescens* limonene synthase, which resulted in limonene titer of 35.9 mg/L and was 100-fold higher than when the same enzyme was expressed in the strain without mevalonate pathway improvement. Expression of *Callitropsis nootkatensis* valencene synthase in the sesquiterpene platform strain resulted in 113.9 mg/L valencene, an 8.4-fold increase over the control strain. Platform strains for production of squalene, complex triterpenes, or diterpenes and carotenoids were also constructed and resulted in the production of 402.4 mg/L squalene, 22 mg/L 2,3-oxidosqualene, or 164 mg/L β-carotene, respectively. The presented terpenoid platform strains can facilitate the evaluation of terpenoid biosynthetic pathways and are a convenient starting point for constructing efficient cell factories for the production of various terpenoids. The platform strains and exemplary terpenoid strains can be obtained from Euroscarf.

Keywords: terpenes, yeast, metabolic engineering, mevalonate pathway, isoprenoids

OPEN ACCESS

Edited by:
Mark Blenner,
Clemson University, United States

Reviewed by:
Xiaofeng Yang,
South China University of Technology, China
John Andrew Jones,
Miami University, United States

***Correspondence:**
Irina Borodina
irbo@biosustain.dtu.dk

†These authors have contributed equally to this work

Specialty section:
This article was submitted to Synthetic Biology, a section of the journal Frontiers in Bioengineering and Biotechnology

Received: *02 April 2020*
Accepted: *22 July 2020*
Published: *14 August 2020*

Citation:
Arnesen JA, Kildegaard KR, Cernuda Pastor M, Jayachandran S, Kristensen M and Borodina I (2020) Yarrowia lipolytica Strains Engineered for the Production of Terpenoids. Front. Bioeng. Biotechnol. 8:945. doi: 10.3389/fbioe.2020.00945

INTRODUCTION

Terpenoids comprise the largest class of secondary metabolites; many have biological activity and are used as nutra- and pharmaceutical agents and ingredients for cosmetics or food (Tetali, 2018). Several terpenoids, such as farnesene and bisabolene, have been developed as advanced biofuels. Terpenoids are categorized depending on the number of carbon atoms forming the core skeleton. The commonly studied classes are monoterpenoids (C_{10}), sesquiterpenoids (C_{15}), diterpenoids (C_{20}), triterpenoids (C_{30}), and tetraterpenoids (C_{40}) also known as carotenoids (Ashour et al., 2010). Other terpenoid classes include hemiterpenoids (C_5) and sesterterpenoids (C_{25}) (Janocha et al., 2015). The core hydrocarbon skeletons assembled from isoprene units are commonly modified by enzymes like cytochromes P450, hydrogenases, methyltransferases, and glycosyltransferases. Terpenoids content in natural sources is typically low and extraction

may result in by-products. As an example, the sweet wormwood *Artemisia annua* contains artemisinin, a terpene with anti-malarial properties, but the content is only 0.8% of the plant dry weight (Zyad et al., 2018). Similarly, to extract 1 kg of the flavoring and fragrance ingredient valencene, some sources estimate that 2.5 million kg of oranges is required (Evolva, 2020 Our valencene the natural choice for flavor and fragrance applications). Some terpenoids can be synthesized chemically, but these processes may be extremely complicated. For example, after two decades of research, a full chemical synthesis of azadirachtin, a triterpenoid with potent insect antifeedant properties, was performed with a yield of 0.00015% and no less than 71 steps (Fernandes et al., 2019). Therefore, production of complex terpenoids by chemical synthesis may be too expensive to be economically feasible (Zhang et al., 2017a). Production of terpenoids by fermentation using engineered cell factories can be cheaper and more sustainable than chemical synthesis. Indeed, hosts like the yeast *Saccharomyces cerevisiae* have been engineered to produce a variety of terpenoids and some of these cell factories are currently used industrially (Moser and Pichler, 2019). For example, the sesquiterpene β-farnesene is being produced industrially by highly engineered *S. cerevisiae* with titers of 130 g/L reported in the literature (Meadows et al., 2016). However, since these highly productive, industrial yeast chassis are proprietary, there is a need for accessible microbial terpenoid platform strains. Recently the oleaginous yeast *Yarrowia lipolytica* has attracted attention as a promising host for the production of hydrophobic compounds. The genome of *Y. lipolytica* has been sequenced and convenient toolkits for genetic engineering exists (Dujon et al., 2004; Christen and Sauer, 2011; Holkenbrink et al., 2018; Turck et al., 2019). Furthermore, several *Y. lipolytica* strains have been granted GRAS-status (Groenewald et al., 2014). The species naturally overproduces lipids and hence has a high acetyl-coenzyme A (CoA) flux, which makes it useful for terpenoid production. Terpenoids like limonene, linalool, α-farnesene, betulinic acid, and β-carotene have previously been produced in recombinant *Y. lipolytica* strains (Yang et al., 2016; Cao et al., 2017; Gao et al., 2017; Cheng et al., 2019; Jin et al., 2019). In yeasts, the C_5-precursor of terpenoids isopentyl diphosphate (IPP), is produced via the cytosolic mevalonate (MVA) pathway (**Figure 1**; Ashour et al., 2010; Cao et al., 2016). The initial steps of the MVA-pathway start with the condensation of three acetyl-CoA molecules forming 3-hydroxy-3-methylglutaryl-CoA (HMG-CoA). Subsequently, HMG-CoA is reduced to mevalonic acid, which is then phosphorylated twice and lastly decarboxylated, forming IPP which can isomerize to form dimethylallyl diphosphate (DMAPP). These phosphorylated C_5-precursors can condensate to form geranyl diphosphate (GPP), farnesyl diphosphate (FPP), geranylgeranyl diphosphate (GGPP) that then generate the backbones of monoterpenoids, sesqui- and triterpenoids, or diterpenoids and carotenoids, respectively. Although *Y. lipolytica* may be highly suited for the production of terpenoids, the yeast strains often require several cycles of engineering and optimization before high terpenoid titers can be reached. Since terpenoids are derived from the same basic IPP/DMAPP-building blocks, pre-engineered "platform" strains with high MVA-pathway flux could be engineered (Cravens et al., 2019). Upon integration of terpenoid biosynthetic genes, such platform strain could provide immediately improved titers, which would shorten the downstream engineering process considerably. Furthermore, platform strains tailored toward the production of specific terpenoid classes could be constructed, since the subsequent pathways from IPP/DMAPP diverge toward mono-, sesqui-, tri-, or diterpenoids and carotenoids. Therefore, this study aimed to develop pre-engineered platform strains of *Y. lipolytica* with improved production of GPP for monoterpene production, FPP for sesquiterpene production, squalene/2,3-oxidosqualene for triterpene production, or GGPP for diterpenoid and carotenoid production. While these platform strains require additional engineering before industrially relevant titers can be reached, they can serve as convenient plug-and-play hosts for testing new or improved enzymes toward various terpenoids and for testing new metabolic engineering strategies for improving terpenoid production in *Y. lipolytica*. By making the strains available via Euroscarf, we hope to initiate a scientific community effort of building superior platform strains together.

MATERIALS AND METHODS

Yeast Strains and Media

The W29-derived ST6512 (MatA ku70Δ:PrTEF1->Cas9-TTef12:PrGPD->DsdA-TLip2) expressing Cas9 for CRISPR/based DNA integration was used to construct the platform strains (Marella et al., 2019). This strain was based on the W29 *Y. lipolytica* (MatA) strain Y-63746, which was a kind gift from the ARS Culture Collection, NCAUR, United States. YPD-media containing 10 g/L yeast extract, 20 g/L peptone, and 20 g/L glucose were used to grow the *Y. lipolytica* strains at 30°C. 20 g/L agar was added for solid media. For selection, either nourseothricin (250 mg/L) or hygromycin (400 mg/L) was added to the media. Cultivation of strains for terpenoid production was done in YP-media with 80 g/L glucose. *Escherichia coli* strain DH5α was used for plasmid construction. The *E. coli* cells were cultivated at 37°C on Lysogeny Broth (LB) medium supplemented with 100 mg/L ampicillin for plasmid selection. The chemicals were obtained, if not indicated otherwise, from Sigma-Aldrich. Nourseothricin was purchased from Jena BioScience GmbH (Germany).

DNA Constructs

The primers, biobricks, plasmids, and primers used in this study are listed in **Supplementary Tables 1–4**, respectively. The biobricks were amplified with PCR using Phusion U polymerase (Thermo Scientific) and assembled into the EasyCloneYALI vectors with USER cloning (Holkenbrink et al., 2018). The USER reactions were transformed into *E. coli* and correct assemblies were verified by sequencing. Codon-optimized genes encoding *Citrus limon* limonene synthase (*ClLS*) (Accession: Q8L5K3.1), *Perilla frutescens* limonene synthase (*PfLS*) (Accession: AJW68081.1), *Artemisia annua* β-farnesene synthase (*AaBFS*) (MT276895.1), *Callitropsis nootkatensis* valencene synthase (*CnVS*) (Accession: AFN21429.1),

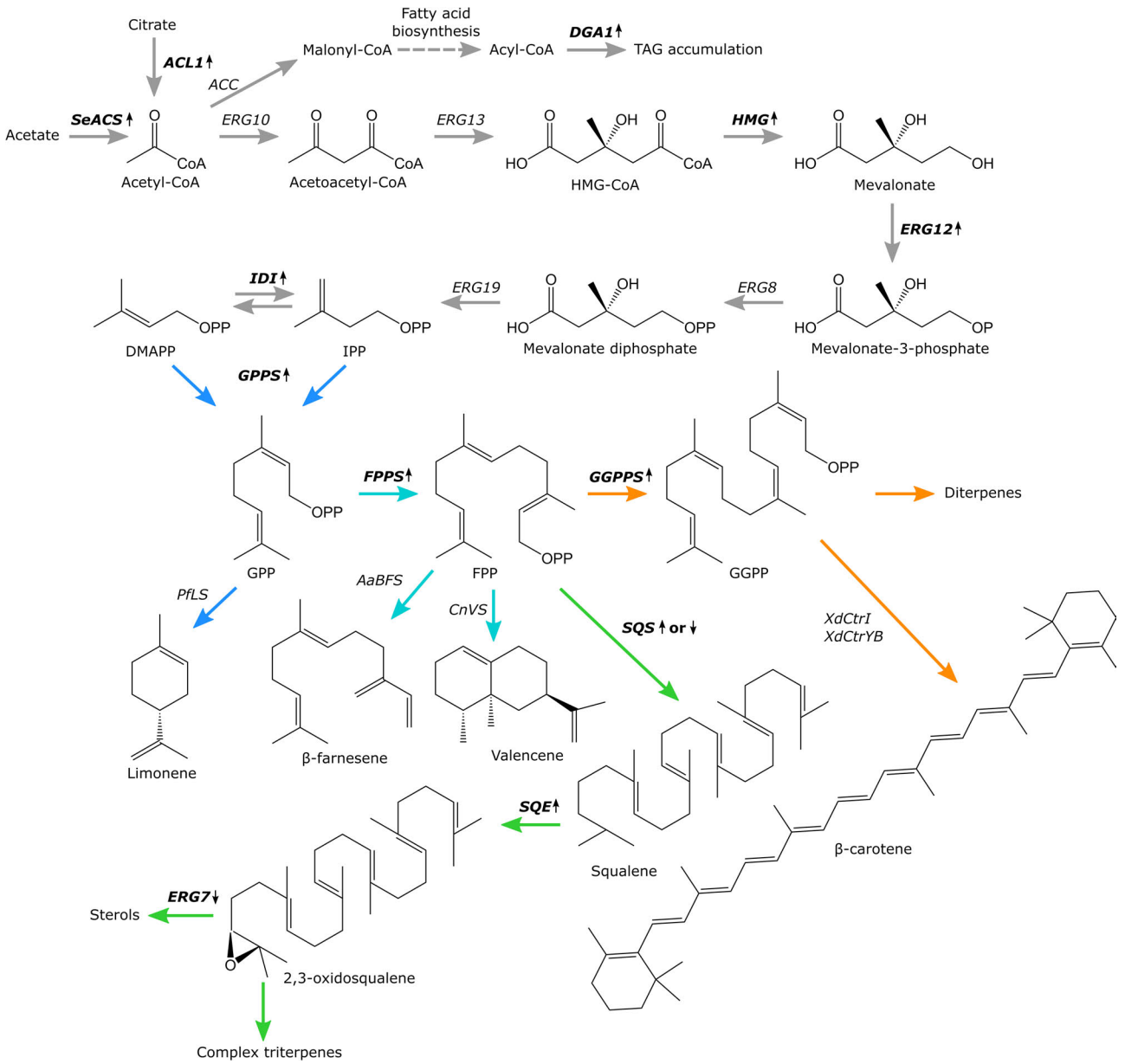

FIGURE 1 | Overview of the MVA-pathway and terpenes produced by engineered *Yarrowia lipolytica* platform strains. Biosynthetic enzymes targeted for upregulation or downregulation are bolded and marked with upward or downward pointing arrows, respectively. *ACL*, ATP citrate lyase 1; *SeACS*, *S. enterica* acetyl-CoA synthetase; *ACC*, acetyl-CoA carboxylase; *ERG10*, acetyl-CoA acetyltransferase; *ERG13*, 3-hydroxy-3-methylglutaryl-CoA synthase; *HMG*, 3-hydroxy-3-methylglutaryl-CoA reductase; *ERG12*, mevalonate kinase; *ERG8*, phosphomevalonate kinase; *ERG19*, mevalonate diphosphate decarboxylase; *IDI*, isopentyl diphosphate isomerase; *GPPS*, geranyl diphosphate synthase; *FPPS* (*ERG20*), farnesyl diphosphate synthase; *GGPPS*, geranylgeranyl diphosphate synthase; *SQS*, squalene synthase; *SQE*, squalene epoxidase; *ERG7*, lanosterol synthase; *PfLS*, *P. frutescens* limonene synthase; *AaBFS*, *A. annua* β-farnesene synthase; *CnVS*, *C. nootkatensis* valencene synthase; *XdCrtI*, *X. dendrorhous phytoene desaturase*; *XdCrtYB*, *X. dendrorhous* bi-functional phytoene synthase/lycopene cyclase. Metabolic branchways are marked with colored arrows, monoterpene biosynthesis, blue. Sesquiterpene biosynthesis, turquoise. Triterpene biosynthesis, green. Diterpene and carotenoid biosynthesis, orange.

Xanthophyllomyces dendrorhous phytoene desaturase (*XdCrtI*) (Accession: ATB19150.1), *X. dendrorhous* bi-functional phytoene synthase/lycopene cyclase (*XdCrtYB*) (Accession: Q7Z859.1) with an A190T substitution, and *Salmonella enterica* acetyl-CoA synthetase (*SeACS*) (Accession: WP_000083882.1) with a L641P substitution as described in Huang et al. (2018) were ordered as GeneArt String DNA fragments from Thermo Fischer Scientific. The codon-optimized nucleotide sequences can be found the **Supplementary Material**.

ERG20 was mutated into $ERG20^{F88C}$ based on an alignment of *Y. lipolytica* Erg20p (Accession number: XP_503599.1) and *S. cerevisiae* Erg20p (Accession number: CAA89462.1) amino

sequences (**Supplementary Figure 1**). The mutated residue was selected based on a previous report (Ignea et al., 2015). The alignment was made using Benchling software and was visualized with MView 1.63 (Benchling, 2020 Cloud-Based Informatics Platform for Life Sciences R&D | Benchling; Brown et al., 1998). In addition, *ERG20* was mutated into $ERG20^{F88W-N119W}$ based on a previous report (Cao et al., 2017). The amino acid substitutions were constructed with PCR mutagenesis and the primers are listed in **Supplementary Table 4**.

Yeast Transformation

The yeast strains used in this study are listed in **Supplementary Table 1**. A lithium-acetate based transformation protocol as described previously was used for yeast strain engineering and integration vectors were linearized with *Not*I-enzyme before transformation (Holkenbrink et al., 2018). Correct integration was verified with colony PCR using vector-specific primers and primers complementary to the genomic region adjacent to the integration site.

Yeast Cultivation

Yeast strains were inoculated into 2.5 mL YPD in 24-well plates with air-penetrable lid (EnzyScreen, Netherlands) and grown for 16–24 h at 30°C and 300 rpm agitation at 5 cm orbit cast. Then for limonene, β-farnesene, and valencene, the required volume for a starting 600 nm optical density (OD) of 0.1 was transferred to 2 mL of YP with 80 g/L glucose in glass tubes and a dodecane overlay of 200 μL was added. For squalene, 2,3-oxidosqualene, and β-carotene, the required volume for a starting 600 nm optical density (OD) of 0.1 was transferred to 2.5 mL of YP with 80 g/L glucose in a 24-deepwell plate. The inoculated media was incubated for 72 h at 30°C with 300 rpm agitation. All cultivations were performed in biological triplicates. OD and cell dry weight was measured by the end of cultivation.

Metabolite Analysis

For limonene, β-farnesene, and valencene, the cell culture broth was centrifuged and the dodecane phase was harvested for analysis. The dodecane samples were diluted in cyclohexane with either patchoulol or myrcene as an internal standard for valencene and β-farnesene, or limonene, respectively. β-carotene, was extracted as previously described (Kildegaard et al., 2017). For squalene and 2,3-oxidosqualene, 1 mL of culture broth was transferred into a 2 mL microtube, centrifuged and the supernatant was discarded. 500 μL of 0.5–0.75 mm acid-washed glass beads and 1 mL of acetonitrile were added to each sample. The samples were then incubated at 95°C at 650 rpm shaking for 1 h in a Thermo-Shaker TS-100 (biosan). Subsequently, the cells were broken with a Precellys®24 homogenizer (Bertin Corp.) four times at 5500 rpm for 20 s with samples being kept on ice in between rounds of breaking. Lastly, the samples were centrifuged, and the supernatant was collected for analysis.

Gas chromatographic (GC) analysis for valencene, limonene, and β-farnesene was conducted using Thermo Scientific GC Trace 1300 equipment with a flame ionization detector (FID) and equipped with a fused-silica capillary column (BPX5, 30 m × 0.25 mm ID, 0.25 μm, SGE Analytical Science). Helium at a constant flow rate of 1.0 mL/min was used as the carrier gas. The GC oven temperature started at 50°C for 1.5 min and then increased to 170°C at 30°C/min and hold for 1.5 min. Then from 170 to 300°C at 15°C/min and hold for 4.5 min, finalizing the chromatographic run at 20.2 min. The injector and detector ports were both kept at 300°C and the injector operated in a split mode of 20:1. Concentrations of beta-carotene, squalene, and 2,3-oxidosqualene were measured using a Dionex Ultimate 3000 HPLC with a Supelco Discovery HS F5-3 HPLC column (150 × 2.1 mm, 3 μm particle size) and a DAD-3000 Diode Array Detector at 450 and 210 nm, respectively. The mobile phase consisted of A: 10 mM ammonium formate and B: acetonitrile. The flow rate was 0.7 mL/min and the column was kept at 30°C. The mobile phase was introduced as 25% B and held at this composition for 2 min. The gradient was then ramped to 90% B to 4 min and this gradient held to 10.5 min and followed by a linear gradient to 25% B at 11.25 min. The column was equilibrated with 25% B until 13.5 min. Samples were held at 5°C during the analysis and 1 μL sample volume injected. Data analysis was performed using Chromeleon 7.2.9 and the analyte quantification was performed using peak area ratios of authentic standards. Quantities of limonene for ST9249, ST9395, and squalene for ST6512 were extrapolated from the standard curve regression.

RESULTS

Design of *Y. lipolytica* Platform Strains for Terpenoid Production

To design the platform strains, we compiled a list of studies for terpenoid production in *Y. lipolytica* (**Table 1**). While some studies generated highly modified strains by, for example, overexpressing the entire MVA-pathway, it may not be clear from the experimental design, which exact modifications had resulted in improvement of terpenoid titers. Therefore, we selected metabolic engineering strategies that had been clearly demonstrated to result in improved terpenoid production. These strategies formed the basis of the platform strains. Two key strategies were implemented for all platform strains: improvement of the precursor acetyl-CoA pool and up-regulation of the MVA-pathway to improve the accumulation of IPP/DMAPP (**Figure 1**). Increasing the acetyl-CoA pool was done by overexpression of the native ATP citrate lyase 1 (*ACL*) and the *Salmonella enterica* acetyl-CoA synthetase (*SeACS*), as this was shown to increase squalene titers in *Y. lipolytica* in combination with overexpression of the native 3-hydroxy-3-methylglutaryl-CoA reductase (*HMG*) (Huang et al., 2018). In *Y. lipolytica*, Aclp generates acetyl-CoA and oxaloacetate from citrate, whereas SeAcsp produces acetyl-CoA from acetate and CoA. To increase MVA-pathway flux, several genes involved in this pathway were overexpressed. The formation of mevalonic acid from 3-hydroxy-3-methylglutaryl-CoA is catalyzed by Hmgp and this is considered a key limiting step in the MVA-pathway (Ashour et al., 2010). Overexpression of *HMG* has been shown to boost the production of α-farnesene, linalool and limonene in *Y. lipolytica* (Cao et al., 2016, 2017; Yang et al., 2016). Although truncated versions of Hmgp have been used in *S. cerevisiae*, studies indicate that the non-truncated version is superior for terpenoid production in *Y. lipolytica* (Cao et al., 2016;

TABLE 1 | Metabolic engineering of *Yarrowia lipolytica* for terpenoid biosynthesis.

Compound	Carbon Source	Parental Strain	Relevant modifications related to terpenoid biosynthesis	Titer	References
Monoterpenoids					
Limonene	Glucose	Po1g	↑***HMG*** (↑***CILS*** or ↑*MsLS*)	D-limonene: 11.7 mg/L L-limonene: 11.1 mg/L (bioreactor)	Pang et al., 2019
	Glycerol Citrate	Po1f	↑*ArtLS* ↑*SltNDPS1* ↑***HMG1*** ↑***ERG12***	165.3 mg/L (bioreactor)	Cheng et al., 2019
	Glucose Pyruvic acid	Po1f	↑*ArtLS* ↑*SltNDPS1* ↑***HMG1*** ↑***ERG12***	23.6 mg/L (shake flask)	Cao et al., 2016
	Glucose	ATCC 20460	↑***HMG1*** ↑***ERG12*** ↑***ACL1*** ↑***SeACS*** ↑***IDI*** ↑***ERG20$^{F88W-N119W}$*** ↓***SQS*** ↑***PfLS***	35.9 mg/L (glass tube)	This study
Linalool	Citrate Pyruvate	Po1f	↑*AaLIS* ↑***ERG20$^{F88W-N119W}$*** ↑***HMG*** ↑***IDI***	6.96 mg/L (shake flask)	Cao et al., 2017
Sesquiterpenoids					
α-farnesene	Glucose Fructose	Po1h	↑*SctHMG* ↑***IDI*** ↑*MdFS-L-ERG20*	259.98 mg/L (bioreactor)	Yang et al., 2016
	Glucose	Po1f	↑*BdHMG* ↑*ERG13* ↑*MdFS-L-ERG20* ↑***ERG12*** ↑***IDI*** ↑*ERG8*,19 ↑***GPPS***	25.55 g/L (bioreactor)	Liu et al., 2019
β-farnesene	Glucose	ATCC 20460	↑***HMG1*** ↑***ERG12*** ↑***ACL1*** ↑***SeACS*** ↑***IDI*** ↑***ERG20*** ↑***AaBFS***	955 mg/L (glass tube)	This study
β-ionone	Glucose	Po1f	↑*carB* ↑*carRP* ↑*PhCCD1* ↑***GGPPS*** ↑*tHMG* ↑***ERG****8,10,****12****,13,19,20*Δ*pox3,5* ↑***IDI*** ↑*bbPK* ↑*bsPTA*	0.98 g/L (bioreactor)	Lu et al., 2020
	Glucose	Po1f	↑*carB* ↑*carRP* ↑*OfCCD1* ↑*SsNphT7* ↑*HpIDI* ↑***ERG****8,10,****12****,13,19* ↑*tHMG1* ↑***GPPS*** ↑*ERG20-GGPPS*	380 mg/L (bioreactor)	Czajka et al., 2018
α-santalene	Glucose	ATCC 201249	↑*ClSTS* ↑*ERG8* ↑***HMG***	27.92 mg/L (bioreactor)	Jia et al., 2019
Nootkatone valencene	Glucose	ATCC 201249	↑***CnVS*** ↑*CnCYP706M1-AtATR1* ↑*tHMG* ↑***ERG20***	Nootkatone: 978.2 μg/L Valencene: 22.8 mg/L (shake flask)	Guo et al., 2018
Valencene	Glucose	ATCC 20460	↑***HMG1*** ↑***ERG12*** ↑***ACL1*** ↑***SeACS*** ↑***IDI*** ↑***ERG20*** ↓***SQS*** ↑***CnVS***	113.9 mg/L (glass tube)	This study
Amorphadiene	Glucose	Po1g	↑*AaADS* ↑***HMG1*** ↑***ERG12***	171.5 mg/L (shake flask)	Marsafari and Xu, 2020
Triterpenoids					
Campesterol	Sunflower seed oil	ATCC 201249	Δ*ERG5* ↑*XlDHCR7*	453 mg/L (bioreactor)	Du et al., 2016
	Sunflower seed oil	ATCC 201249	Δ*ERG5* ↑*DrDHCR7* ↑*POX2*	942 mg/L (bioreactor)	Zhang et al., 2017b
Ginsenoside K	Glucose	ATCC 201249	↑*tHMG* ↑***ERG20*** ↑***SQS*** ↑*PgDS* ↑*PgPPDS* ↑*AtATR1* ↑*PgUGT1*	161.8 mg/L (bioreactor)	Li et al., 2019
Oleanolic Acid	Glucose	ATCC 201249	↑*tHMG* ↑***ERG20*** ↑***SQS*** ↑*GgBAS* ↑*MtCYP716A12-L-AtATR1*	540.7 mg/L (bioreactor)	Li et al., 2020
Betulinic acid	Glycerol	ATCC 201249	↑*tHMG1* ↑***SQS*** ↑*AtLUP1* ↑*MtCYP716A12* ↑*AtATR1*	26.53 mg/L (shake flask)	Sun et al., 2019
	Glucose	ATCC 201249	↑*RcLUS* ↑*BPLO* ↑*LjCPR* ↑***SQS*** ↑***SQE*** ↑***HMG1*** ↑*MFE1*	204.89 mg/L (shake flask)	Jin et al., 2019
Squalene	Glucose Citrate	Po1f	↑***HMG1*** ↑***ACL1*** ↑***SeACS***	10 mg/gDCW (shake flask)	Huang et al., 2018
	Glucose	ATCC MYA2613	↑*carB* ↑*carRP* ↑***ERG****8,10,****12****,13,19,****20*** ↑*tHMG* ↑***IDI*** Δ*gut2* Δ*pox3,4,5,6*	531.6 mg/L	Gao et al., 2017
	Glucose	ATCC 20460	↑***HMG1*** ↑***ERG12*** ↓***ERG7*** ↑***ACL1*** ↑***SeACS*** ↑***IDI*** ↑***ERG20*** ↑***SQS***	402.4 mg/L (deepwell plate)	This study
2,3-oxidosqualene	Glucose	ATCC 20460	↑***HMG1*** ↑***ERG12*** ↓***ERG7*** ↑***ACL1*** ↑***SeACS*** ↑***IDI*** ↑***ERG20*** ↑***SQS*** ↑***SQE***	22 mg/L (deepwell plate)	This study
Protopanaxadiol	Xylose	ATCC 201249	↑*SsXYL1* ↑*SsXYL2* ↑*XKS* ↑*PgDS* ↑*PgPPDS-L-AtATR1* ↑*tHMG* ↑***ERG20*** ↑***SQS*** ↑*TKL* ↑*TAL* ↑*TX* Δ*pox1,2,3*	300.63 mg/L (bioreactor)	Wu et al., 2019

(Continued)

TABLE 1 | Continued

Compound	Carbon Source	Parental Strain	Relevant modifications related to terpenoid biosynthesis	Titer	References
Carotenoids					
Lycopene	Glucose	H222	↑*PaCrtB* ↑*PaCrtI* ↑***GGPPS*** ↑***HMG1*** Δ*pox1–6* Δ*gut2*	16 mg/gDCW (bioreactor)	Matthäus et al., 2014
	Glucose	Po1f	↑***HMG*** ↑*PaCrtE* ↑*PaCrtB* ↑*PaCrtI* ↑*ERG19*	21.1 mg/gDCW (bioreactor)	Schwartz et al., 2017
β-Carotene	Glucose	ATCC MYA2613	↑*carB* ↑*carRP* ↑***ERG****8,10,****12****, 13,19,****20*** ↑***GGPPS*** ↑*tHMG* ↑***IDI*** Δ*pox3,4,5,6*	4 g/L (bioreactor)	Gao et al., 2017
	Glucose	Po1f	↑*carB* ↑*carRP* ↑***GGPPS*** ↑***HMG*** ↑*ERG13* Δ*pox2,3*	4.5 g/L (bioreactor)	Zhang et al., 2020
	Glucose	ATCC 20460	↑*carB* ↑*carRP* ↑***HMG*** ↑***GGPPS*** ↑*DGA2* ↑*GPD1*Δ*pox1–6* Δ*tgl4*	6.5 g/L (bioreactor)	Larroude et al., 2018
	Glucose	ATCC 20460	↑***HMG1*** ↑***ERG12*** ↑***ACL1*** ↑***SeACS*** ↑***IDI*** ↑GGPPS↓***SQS*** ↑***XdcrtYB*** ↑***XdcrtI***	164 mg/L (deepwell plate)	This study
Astaxanthin	Glucose	GB20	↑***XdcrtYB*** ↑***XdcrtI*** ↑***HMG*** ↓***SQS*** ↑*XdcrtE* ↑*PscrtW* ↑*PacrtZ*	54.6 mg/L (microtiter plate)	Kildegaard et al., 2017
	Glucose	GB20	↑***XdcrtYB*** ↑***XdcrtI*** ↑***HMG*** (↑SQS ↑XdcrtE ↑SsGGP*PS* ↑*HpBKT* ↑*HpCrtZ*	285 mg/L (bioreactor)	Tramontin et al., 2019

Genes modified in this study are bolded in the table. ***AaADS****, Artemisia annua amorphadiene synthase;* ***AaBFS****, A. annua* β*-farnesene synthase;* ***AaLIS****, Actinidia arguta linalool synthase;* ***ACL1****, ATP citrate lyase 1;* ***ArtLS****, Agastache rugosa limonene synthase;* ***AtATR1****, Arabidopsis thaliana NADPH-cytochrome P450 reductase 1;* ***AtLUP1****, A. thaliana lupeol synthase;* ***BbPK****, Bifidobacterium bifidum phosphoketolase;* ***BdHMG****, Bordetella petrii HMG;* ***BpLO****, Betula platyphylla lupeol C-28 oxidase;* ***BsPTA****, Bacillus subtilis phosphotransacetylase;* ***carB****, Mucor circinelloides phytoene dehydrogenase;* ***carRP****, M. circinelloides phytoene synthase/lycopene cyclase;* ***CnCYP706M1-AtATR1****, fusion of Callitropsis nootkatensis cytochrome P450 and AtATR1;* ***CnVS****, C. nootkatensis valencene synthase;* ***CILS****, Citrus limon d-limonene synthase;* ***CISTS****, Clausena lansium* α*-santalene synthase;* ***DGA2****, diacylglycerol acyltransferase 2;* ***DrDHCR1****, Danio rerio 7-dehydrocholesterol reductase;* ***ERG5****, C22-sterol desaturase;* ***ERG7****, lanosterol synthase;* ***ERG8****, phosphomevalonate kinase gene;* ***ERG10****, acetyl-CoA C-acetyltransferase;* ***ERG12****, mevalonate kinase;* ***ERG13****, Hydroxymethylglutaryl-CoA synthase;* ***ERG19****, mevalonate diphosphate decarboxylase encoding gene;* ***ERG20****, farnesyl diphosphate synthase;* ***ERG20***$^{F88W-N119W}$*, geranyl diphosphate synthase;* ***ERG20-GGPPS****, fusion of ERG20 and* ***GGPPS****, geranylgeranyl diphosphate synthase;* ***GgBAS****, Glycyrrhiza glabra* β*-amyrin synthase;* ***GPD****, glyceraldehyde-3-phosphate dehydrogenase;* ***GPPS****, geranyl diphosphate synthase;* ***HMG****, Hydroxymethylglutaryl-CoA reductase;* ***HpBKT****, Haematococcus pluvialis* β*-carotene ketolase;* ***HpIPI****, Haematococcus pluvialis isopentyl diphosphate isomerase;* ***HpCrtZ****, H. pluvialis* β*-carotene hydroxylase;* ***IDI****, isopentyl diphosphate isomerase;* ***LjCPR****, Lotus japonicus cytochrome P450 reductase;* ***MdFS-L-ERG20****, Malus domestica* α*-farnesene synthase linked to ERG20;* ***MFE1****, multifunctional* β*-oxidation enzyme 1;* ***MsLS****, Mentha spicata l-limonene synthase;* ***MtCYP716A12-L-AtATR1****, Medicago truncatula cytochrome P450 fused to AtATR1;* ***OfCCD1****, Osmanthus fragrans carotenoid cleavage dioxygenase 1;* ***PaCrtB****, Pantoea ananatis phytoene synthase;* ***PaCrtE****, P. ananatis geranylgeranyl diphosphate syntase;* ***PaCrtI****, P. ananatis phytoene desaturase;* ***PacrtZ****, P. ananatis* β*-carotene hydroxylase;* ***PfLS****, P. frutescens limonene synthase;* ***PgDS****, Panax ginseng dammarenediol II synthase;* ***PgPPDS****, P. ginseng cytochrome P450 enzyme;* ***PgPPDS-L-AtATR1****, PgPPDS linked to AtATR1;* ***PgUGT1****, P. ginseng UDP-glycosyltransferase;* ***PhCCD1****, Petunia hybrida carotenoid cleavage dioxygenase;* ***POX****, peroxisome acyl-CoA oxidase;* ***PscrtW****, Paracoccus sp. N81106* β*-carotene ketolase;* ***RcLUS****, Ricinus communis lupeol synthase;* ***SctHMG****, Saccharomyces cerevisiae truncated HMG,* ***SeACS****, S. enterica Acetyl-CoA synthetase;* ***SQE****, squalene epoxidase;* ***SQS****, squalene synthase;* ***SlNDPS1****, Solanum lycopersicum neryl diphosphate synthase 1;* ***SsGGPPS****, Synechococcus sp. GGPPS;* ***SsNphT7****, Streptomyces sp. Acetoacetyl CoA synthase;* ***SsXYL1****, Scheffersomyces stipitis xylose reductase XR;* ***SsXYL2****, S. stipitis xylose reductase XDH;* ***TAL****, transaldolase;* ***TGL****, triacylglycerol lipase;* ***TKL****, transketolase;* ***TX****, xylose transporter;* ***XdcrtE****, X. dendrorhous geranylgeranyl diphosphate synthase;* ***XdcrtI****, X. dendrorhous phytoene desaturase;* ***XdcrtYB****, Xanthophyllomyces dendrorhous bi-functional phytoene synthase/lycopene cyclase;* ***XKS****, xylulose kinase;* ***XlDHCR7****, Xenopus laevis 7-dehydrocholesterol reductase.*

Kildegaard et al., 2017; Bröker et al., 2018; Han et al., 2018). For example, the production of β-carotene was enhanced to a greater degree by *HMG* compared to *tHMG* both when solely expressed or in combination with the geranylgeranyl diphosphate synthase (*GGPPS*) (Kildegaard et al., 2017). Indeed, non-truncated *HMG* has also been used for production of several other terpenoids in *Y. lipolytica* such as betulinic acid (**Table 1**; Jin et al., 2019). Furthermore, overexpression of the mevalonate kinase (*ERG12*) in combination with *HMG* was shown to increase limonene titers in *Y. lipolytica* (Cao et al., 2016). Lastly, overexpression of the isopentyl diphosphate isomerase (*IDI*) that catalyzes the isomerization of IPP and DMAPP together with *HMG* has been shown to increase the production of linalool and α-farnesene in *Y. lipolytica* (Yang et al., 2016; Cao et al., 2017). Therefore, overexpression of *HMG*, *ERG12*, and *IDI* was selected to form the basis of the terpenoid platform strains. To further tailor the platform strains toward the production of either mono-, sesqui-, tri- or diterpenoids and carotenoids, strategies were implemented to direct IPP/DMAPP toward the appropriate phosphorylated isoprene unit and prevent the flux of this substrate toward undesired products. Monoterpenoids are derived from the GPP which is formed by the condensation of DMAPP and IPP (Ignea et al., 2014). Mutating the phenylalanine residue in position 96 and the asparagine residue in position 127 to tryptophan of *S. cerevisiae* Erg20p changed its function to a geranyl diphosphate synthase (Ignea et al., 2014). A *Y. lipolytica* Erg20p version with identical mutations in the positionally similar residues (*ERG20*$^{F88W-N119W}$) was used for linalool production in *Y. lipolytica* (Cao et al., 2017). Therefore, the mutated *Y. lipolytica* variant was selected to direct the flux of IPP/DMAPP toward monoterpenoid production. Both sesquiterpenoids and triterpenoids use FPP as the starting substrate, with FPP being dephosphorylated and typically re-arranged to form sesquiterpene backbones, while two units of FPP dimerize to form squalene, which is a precursor for many triterpenoids and sterols. Therefore, the native farnesyl diphosphate synthase (*ERG20*) was overexpressed in the sesqui- and triterpenoid platform strains, which also had been used to increase nootkatone

production in *Y. lipolytica* (Guo et al., 2018). Furthermore, since complex, cyclical triterpenoids often derive from 2,3-oxidosqualene, the squalene synthase (*SQS*) and squalene epoxidase (*SQE*) were overexpressed in the triterpenoid platform strain to increase 2,3-oxidosqualene formation. The substrate for diterpenoids and carotenoids is GGPP. Therefore, either the geranylgeranyl diphosphate synthase (*GGPPS*) or a mutated version of the native Erg20p, where the phenylalanine residue in position 96 was changed to tryptophan ($ERG20^{F88C}$), were overexpressed to generate two different diterpene/carotenoid platform strains (**Supplementary Figure 1**). A similar mutation in the *S. cerevisiae* Erg20p was demonstrated to change its function to a geranylgeranyl diphosphate synthase and improve diterpene production in *S. cerevisiae* (Ignea et al., 2015). To prevent carbon loss to undesired products, we sought to downregulate squalene formation in the mono-, sesqui-, diterpenoid and carotenoid platform strains by exchanging the native squalene synthase promoter (*pERG9*) with the relatively weak lanosterol 14-α-demethylase promoter (*pERG11*). Squalene is essential for sterol production which necessitates downregulation rather than deletion of *SQS* and the former strategy had previously been shown to increase β-carotene production in *Y. lipolytica* (Kildegaard et al., 2017). For the triterpene platform strain, the native lanosterol synthase promoter (*pERG7*) was truncated to decrease the flux of 2,3-oxidosqualene toward sterol synthesis. Both truncations leaving either a 100 or 50 remaining base pairs (bp) of the 3′ end of *pERG7* were constructed. By implementing these four strategies, platform strains for either mono-, sesqui-, tri-, or diterpene/carotenoids were constructed.

Evaluation of the Metabolic Engineering Strategies Using β-Farnesene as the Test Case

The selected metabolic engineering strategies were evaluated using sesquiterpene β-farnesene as the test compound. The strategies were then combined to generate platform strains without heterologous terpenoid pathways. β-farnesene is an acyclic sesquiterpene with potential applications as a biofuel precursor (George et al., 2015). Furthermore, β-farnesene has been produced at high titers in *S. cerevisiae*, which makes it an excellent compound for testing metabolic engineering strategies (Meadows et al., 2016). Therefore, the β-farnesene synthase from *Artemisia annua* (*AaBFS*) was integrated into the *Y. lipolytica* genome under expression of the *pTEFintron* promoter. This test-strain solely expressing *AaBFS* produced 212.7 ± 5.6 mg/L β-farnesene (**Figure 2**). Subsequently, the strategies for improvement of sesquiterpene production were implemented to discern their effect on β-farnesene production. The strategies were performed consecutively on each newly generated strain to demonstrate the cumulative effect of the modifications. First, the native *Y. lipolytica* genes *HMG* and *ERG12* were overexpressed in the β-farnesene producing strain, which increased β-farnesene titers to 631 ± 46.1 mg/L, an approximately 3-fold increase compared to the strain solely expressing *AaBFS*. Subsequently, overexpression of *IDI* and *ERG20* resulted in 729 ± 13.8 mg/L β-farnesene. Thirdly, the genes *ACL* and *SeACS* were expressed, which raised the titer to 955 ± 45.1 mg/L, a 4.5-fold increase compared to the sole expression of *AaBFS*. Lastly, the native squalene promoter was replaced with the weak promoter *pERG11* (*pERG11_SQS*). However, promoter replacement reduced the β-farnesene titer to 757 ± 14.5 mg/L.

Monoterpene Platform Strain

A platform strain for monoterpene production was constructed by expression of *HMG*, *ERG12*, *ACL*, *SeACS*, *IDI*, $ERG20^{F88W-N119W}$, and swapping the native squalene promoter (*pERG11_SQS*). To test the potential of the monoterpene platform strain, either a limonene synthase from *Perilla frutescens* (*PfLS*) or *Citrus limon* (*ClLS*) was expressed in the platform strain and the base strain. Limonene is a cyclic monoterpene used extensively as a flavor and fragrance ingredient due to its citrus-like characteristics (Cao et al., 2016). No limonene was detected for the base strain expressing *ClLS* (**Figure 3A**). The monoterpene platform strain expressing *ClLS* produced 0.1 ± 0.2 mg/L limonene. The base strain expressing *PfLS* produced 0.36 ± 0.04 mg/L limonene, while the monoterpene platform strain expressing *PfLS* produced 35.9 ± 1.1 mg/L limonene. This represents an almost 100-fold increase in limonene titer compared to the base strain.

Sesquiterpene Platform Strain

In parallel with the β-farnesene producing test-strain, a sesquiterpene platform strain was generated with the same modifications except for the integration and expression of *AaBFS*. This sesquiterpene platform strain was tested by expression of a valencene synthase from *Callitropsis nootkatensis* (*CnVS*) generating strain ST9204. Valencene is a cyclic sesquiterpene with a citrus-like aroma used for flavoring or fragrances (Beekwilder et al., 2014). For comparison, *CnVS* was expressed in a strain without any improvements generating strain ST9396. The sesquiterpene platform strain ST9204 produced 113.9 ± 6.6 mg/L valencene, while ST9396 produced 13.5 ± 2.8 mg/L (**Figure 3B**). This corresponds to an 8.4-fold increase in titer and demonstrates the utility of the sesquiterpene platform strain.

Triterpene Platform Strain

Squalene is a sought-after compound as a food and cosmetics additive, while many complex triterpenoids have pharmaceutical properties (Xu et al., 2016; Hill and Connolly, 2017). Therefore, platform strains for the production of squalene and complex triterpenoids were constructed. This was achieved by consecutively modifying the base strain (ST6512) through several rounds of engineering. Since squalene is naturally produced by *Y. lipolytica*, we could test the production in each intermediate strain constructed toward the final squalene and triterpene platform strain. First, *HMG* and *ERG12* were expressed which resulted in the production of 300.7 ± 29.1 mg/L squalene (**Figure 4**). Secondly, the native lanosterol promoter was truncated to leave either 100 bp or 50 bp of the promoter directly upstream of the lanosterol synthase gene (*pERG7_100bp* or *pERG7_50bp*, respectively) generating ST9009

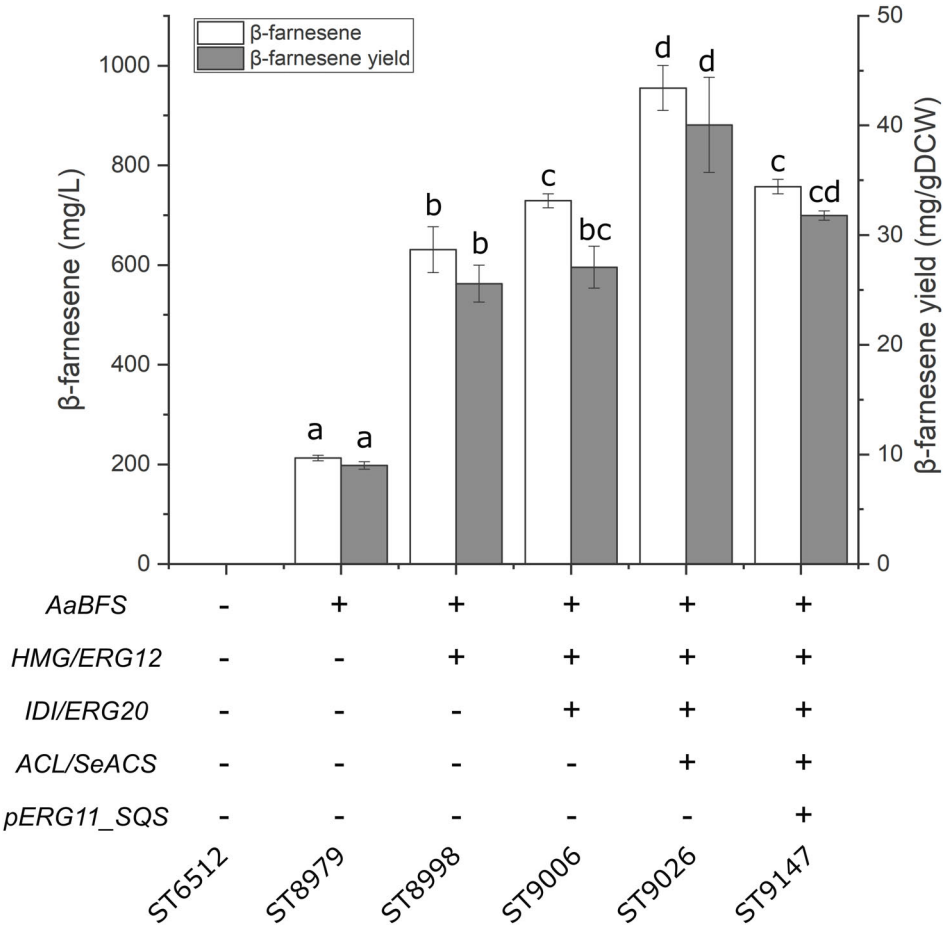

FIGURE 2 | β-farnesene production by the sesquiterpene platform strain. The cumulative effect of engineering strategies for β-farnesene production. *AaBFS*, *A. annua* β-farnesene synthase; *HMG*, HMG-reductase; *ERG12*, mevalonate kinase; *IDI*, isopentyl diphosphate isomerase; *ERG20*, farnesyl diphosphate synthase; *ACL*, ATP citrate lyase 1; *SeACS*, *S. enterica* acetyl-CoA synthetase; *pERG11_SQS*, substitution of the native squalene synthase promoter with the *pERG11*-promoter. Standard deviations from the values of three biological replicates are represented by error bars. Statistical significance (students *t*-test, two-tailed, $p < 0.05$) is denoted by the letters a, b, c, and d.

and ST9010, respectively. The lanosterol synthase catalyzes the committed step toward sterols from 2,3-oxidosqualene and limiting this step could potentially increase the pool of 2,3-oxidosqualene and squalene. Building on ST9010, *ACL* and *SeACS* were expressed and subsequently, *IDI* and *ERG20* were overexpressed. Further overexpression of the native squalene synthase (*SQS*) resulted in squalene platform strain which produced 402.4 ± 90 mg/L squalene. When instead *SQE* and *SQS* were co-overexpressed generating the complex triterpenoid platform strain (ST9106), only 262.7 ± 5.2 mg/L squalene were produced, while levels of 22 ± 5.9 mg/L 2,3-oxidosqualene was detected. Indeed, 2,3-oxidosqualene was measured for all the squalene producing strains but could only be detected in the complex triterpenoid platform strain. Overexpression of the native diacylglycerol O-acyltransferase (*DGA1*) together in the squalene platform strain resulted in 320 ± 16.2 mg/L squalene, less than when only expressing *SQS*. Overexpression of the native *DGA1* in combination with a truncated version of *HMG* in *S. cerevisiae* increased squalene titers, probably due to an increased lipid content providing storage for squalene accumulation (Wei et al., 2018). However, overexpression of *DGA1* in *Y. lipolytica* did not benefit squalene production in the context of this study, likely due to the diversion of acetyl-CoA to lipid biogenesis (**Figure 1**).

Diterpene and Carotenoid Platform Strain

To engineer a platform strain for the production of diterpenoids and carotenoids, the genes *HMG*, *ERG12*, *ACL*, *SeACS*, and *IDI* were overexpressed, while the native squalene promoter was swapped with the relatively weak promoter *pERG11* to reduce the flux toward squalene (*pERG11_SQS*). Additionally, either *GGPPS* or $ERG20^{F88C}$ was overexpressed to generate the diterpenoid/carotenoid platform strains ST9150 and ST9203, respectively. To test the potential of these platform strains, the genes encoding phytoene desaturase (*XdCtrl*) and bi-functional phytoene synthase/lycopene cyclase (*XdCtrYB*) from

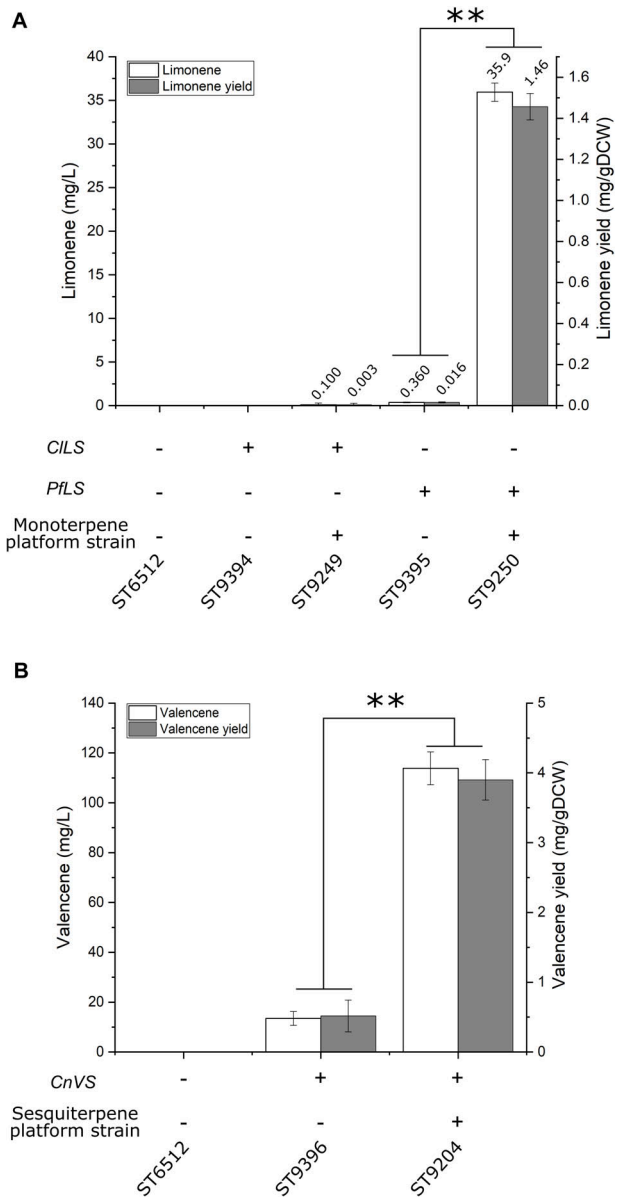

FIGURE 3 | Limonene and valencene production by platform strains. **(A)** Limonene production in base and monoterpene platform strain. *CILS*, *C. lemon* limonene synthase; *PfLS*, *P. frutescens* limonene synthase. The monoterpene platform strain contains the following gene overexpressions of *HMG*, *ERG12*, *ACL*, *SeACS*, *IDI*, $ERG20^{F88W-N119W}$, and swapping the native squalene promoter (*pERG11_SQS*). **(B)** Valencene production in base and sesquiterpene platform strain. *CnVS*, *C. nootkatensis* valencene synthase. The sesquiterpene platform strain contains the same modifications as the monoterpene platform strain, with the exception of *ERG20* instead of $ERG20^{F88W-N119W}$. Standard deviations from the values of three biological replicates are represented by error bars. Double asterisks marks significant change (student's *t*-test, two-tailed, $p < 0.001$).

X. dendrorhous for the production of β-carotene were expressed in both strains, generating ST9251 and ST9253, respectively. ST9251 produced 158 ± 24.1 mg/L β-carotene, while ST9253 produced 164 ± 37.6 mg/L β-carotene (**Figure 5**).

DISCUSSION

This study displays the capability of the oleaginous yeast *Y. lipolytica* for terpenoid production by the construction of tailored terpene platform strains. Each platform strain was designed for increased production of either mono-, sesqui-, tri-, or diterpenoids and carotenoids, and production potential was tested with terpenoids from the appropriate class. The effects of four different metabolic engineering strategies for sesquiterpenoid production were investigated in a strain expressing *AaBFS* for β-farnesene. Overexpression of *HMG* and *ERG12* had previously been shown to increase limonene production 112-fold to 23.56 mg/L in *Y. lipolytica* (Cao et al., 2016). The strategy of *HMG*-overexpression is very commonly used for terpenoid production in *Y. lipolytica*, with both truncated and non-truncated versions, and variants from other species being utilized, while the *ERG12* gene often is overexpressed together with the whole MVA-pathway (**Table 1**). Indeed, overexpression *ERG12* and *HMG* increased β-farnesene production approximately 3-fold, from 212.7 ± 5.6 mg/L to 631 ± 46.1 mg/L, demonstrating that this strategy works well for β-farnesene production. By further overexpression of *ERG20*, *IDI*, *SeACS*, and *ACL1* the titer of 955 ± 45.1 mg/L β-farnesene was reached. Improvement of acetyl-CoA by overexpression of *SeACS* and *ACL1* had a favorable effect on β-farnesene production which is consistent with previous reports demonstrating a similar effect for squalene production in *Y. lipolytica* (Huang et al., 2018). However, recent studies have found that strategies that increase β-oxidation such as overexpression of multifunctional β-oxidation enzyme 1 (*MFE1*) or implementing alternative routes for acetyl-CoA biogenesis by expression of phosphoketolases (*PK*) and phosphotransacetylases (*PTA*), the non-glycolytic oxidation pathway, can also increase terpenoid titers (**Table 1**; Jin et al., 2019; Lu et al., 2020). It would be highly interesting for future research to compare these strategies for terpenoid production in a systematic manner. β-farnesene has been produced at titers of 130 g/L by highly modified *S. cerevisiae* in 200,000-liter bioreactors and therefore is an excellent terpene to demonstrate the effect of metabolic engineering strategies (Meadows et al., 2016). While β-farnesene has not been produced previously in *Y. lipolytica*, the isomer α-farnesene has been produced by engineered *Y. lipolytica* at 25.55 g/L in 1-liter bioreactors (Liu et al., 2019). Interestingly, switching the endogenous squalene promoter with the weak *pERG11* promoter did not benefit β-farnesene production, although the same strategy was shown to boost β-carotene production in *Y. lipolytica* (Kildegaard et al., 2017). This could be caused the combination of reduced cellular sterol-content and high β-farnesene levels that may alter the lipid membrane properties and induce toxicity. It has been demonstrated that several low-molecular-weight terpenoids like limonene, geraniol, and pinene can be toxic to *S. cerevisiae* (Uribe et al., 1985; Liu et al., 2013; Zhao et al., 2016). Indeed, pinene was shown to potentially increase lipid membrane fluidity, while limonene could adversely affect the yeast cell wall (Brennan et al., 2013). *Candida albicans* cells exposed to high doses of linalool or

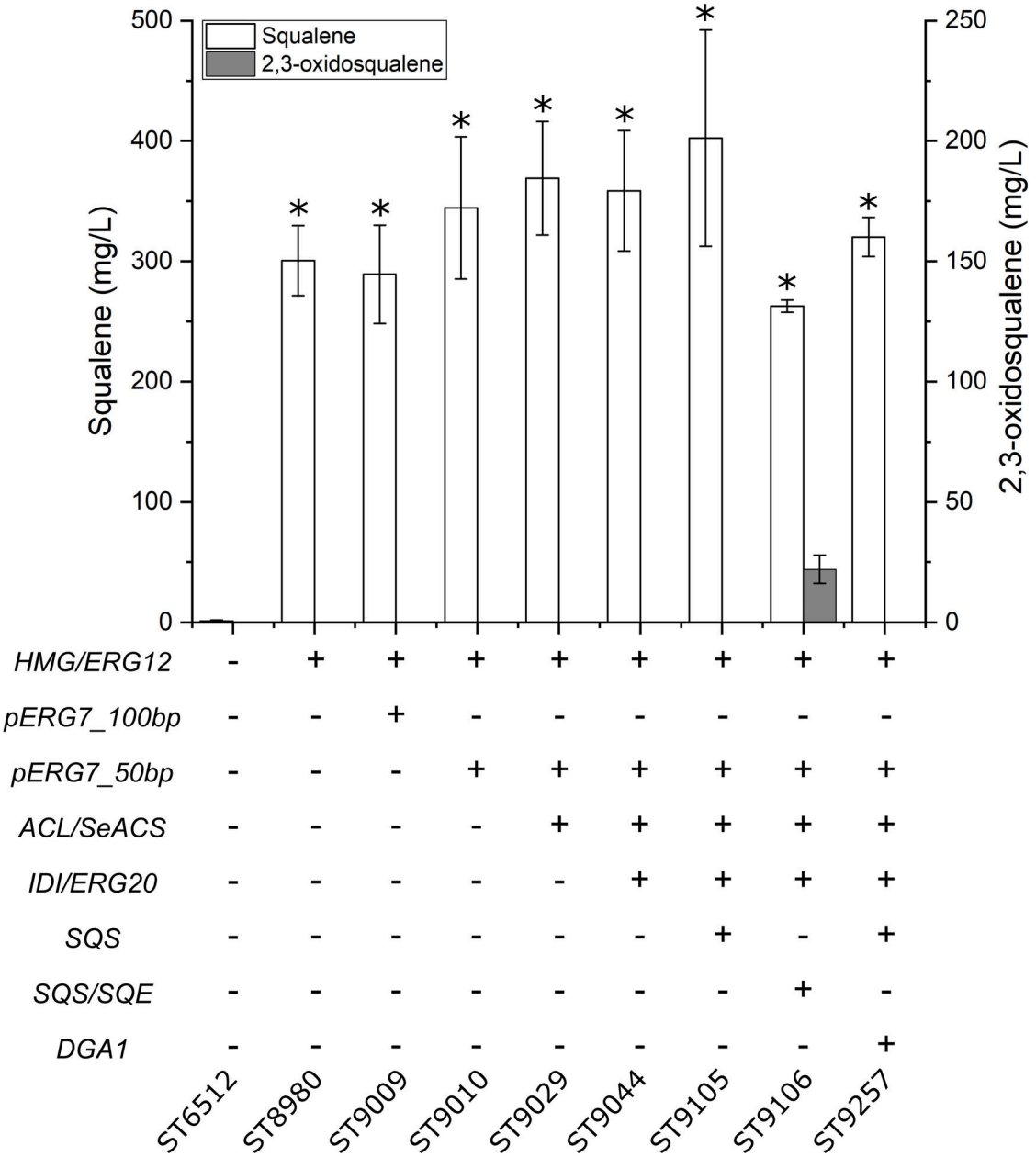

FIGURE 4 | Squalene and 2,3-oxidosqualene production by the triterpene platform strain. HMG, HMG-reductase; *ERG12*, mevalonate kinase; *pERG7_100bp* and *pERG7_50bp*, truncation of the native lanosterol synthase promoter to 100 or 50 bp, respectively, immediately upstream of the *ERG7*-gene; *ACL*, ATP citrate lyase 1; *SeACS*, *S. enterica* acetyl-CoA synthetase; *IDI*, isopentyl diphosphate isomerase; *ERG20*, farnesyl diphosphate synthase; *SQS*, squalene synthase; *SQE*, squalene epoxidase; *DGA1*, diacylglycerol O-acyltransferase 1. Standard deviations from the values of three biological replicates are represented by error bars. Asterisk marks statistical significant changes compared to ST6512 (student's *t*-test, two-tailed, $p < 0.05$).

its derivative linalyl acetate displayed apoptotic phenotypes and highly fluidized membranes leading to cell death (Khan et al., 2014; Blaskó et al., 2017). Two-phase cultivation with an organic phase has been shown to alleviate the toxicity of small terpenoids against *S. cerevisiae* (Brennan et al., 2012). Indeed, a dodecane phase can be used to reduce cell toxicity and to accumulate the produced compounds (Tippmann et al., 2016). It is therefore likely that the utilization of a dodecane phase for the accumulation of limonene, valencene, and β-farnesene also helped to limit adverse effects in *Y. lipolytica* in this study. The sesquiterpene valencene is the precursor of nootkatone, a compound used for cosmetics and fragrances, with insect repellant properties (Leonhardt and Berger, 2014). By simply integrating *CnVS* in the optimized sesquiterpene platform strain, 113.9 ± 6.6 mg/L valencene was produced, an approximately 8.4-fold increase

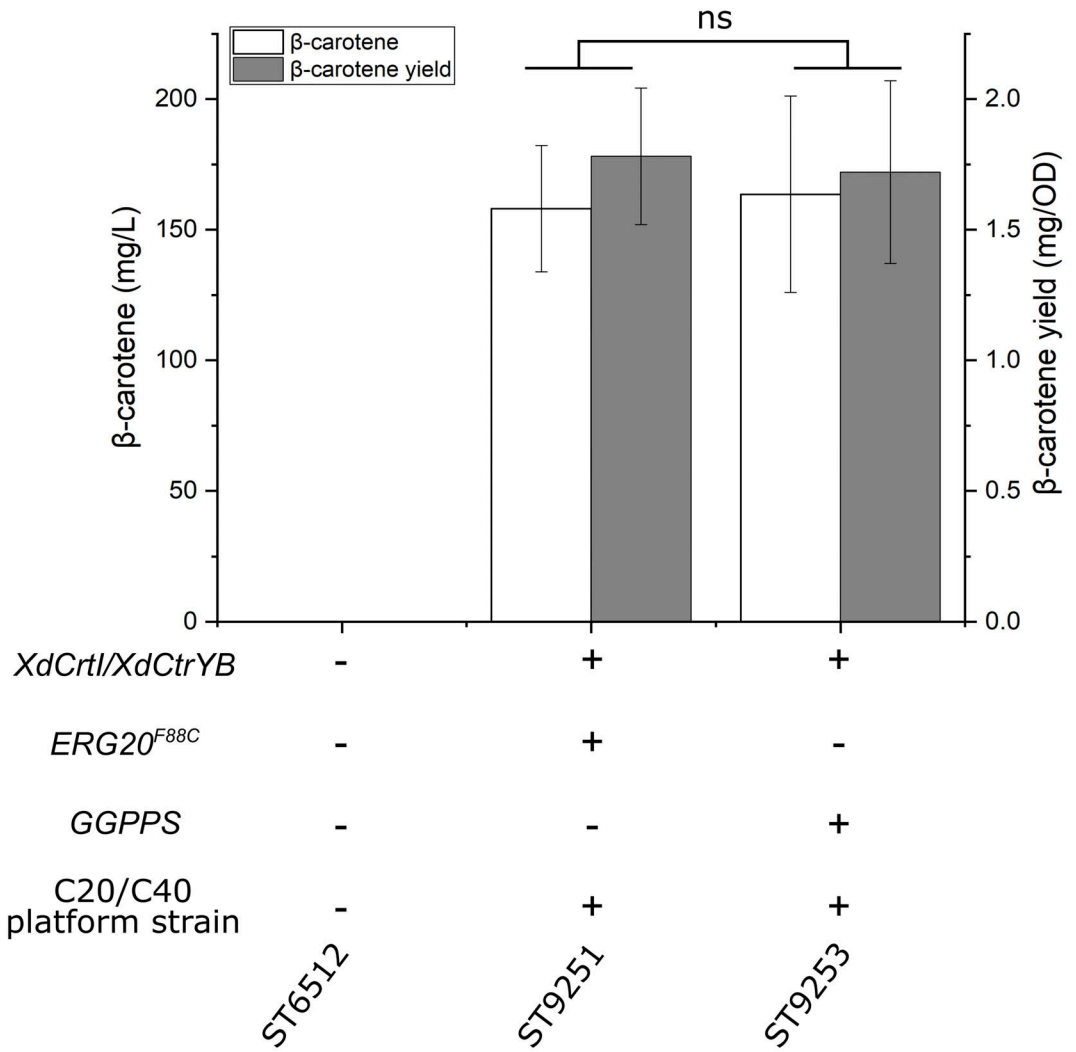

FIGURE 5 | β-carotene production by the diterpene/carotenoid platform strains. *XdCrtI*, *X. dendrorhous phytoene desaturase*; *XdCrtYB*, *X. dendrorhous* bi-functional phytoene synthase/lycopene cyclase; *ERG20*^{F88C}, mutated version with geranylgeranyl diphosphate synthase activity; *GGPPS*, geranylgeranyl diphosphate synthase. The diterpene/carotenoid (C20/C40) platform strain contains the following gene overexpressions *HMG*, *ERG12*, *ACL*, *SeACS*, and *IDI*, while the native squalene promoter was swapped (*pERG11_SQS*). Average values and standard deviations for each strain are based on two individual clones with three biological replicates each. Statistical non-significance is marked with ns (student's *t*-test, two-tailed, $p > 0.05$).

over the base strain. This example clearly illustrates the usefulness of pre-engineered strains for achieving high terpene titers quickly and without post-optimization of the strain. By comparison, previous valence production as precursor for nootkatone in engineered *Y. lipolytica* resulted in 22.8 mg/L valencene and 978.2 μg/L nootkatone during shake flask cultivation (Guo et al., 2018). The sesquiterpene platform strain is a powerful platform for the production of terpenes like valencene and could be engineered to produce more complex sesquiterpenoids. Limonene has been produced at 23.56 mg/L and 1.36 mg/gDCW in shake flasks by the *Y. lipolytica* strain Pof1-LN-051 expressing a limonene synthase from Korean mint *Agastache rugosa* (Cao et al., 2016). In a subsequent report, an additional limonene synthase copy was expressed in Pof1-LN-051, where after cultivation in 1.5 L bioreactors resulted in 165.3 mg/L, which is the highest reported limonene titer for *Y. lipolytica* (Cheng et al., 2019). By comparison, the expression of *PfLS* in the monoterpenoid platform strain resulted in 35.9 ± 1.1 mg/L and 1.46 ± 0.064 mg/gDCW limonene in small-scale cultivation. Therefore, the monoterpene platform strain clearly holds a great potential for limonene production, which potentially could be improved substantially by multi-copy integration of *PfLS* and scale-up into bioreactors. By integrating *HMG*, *ERG12*, *ERG20*, *IDI, SQS,* and truncating the native lanosterol promoter, a strain for squalene production was constructed. This strain was able to produce 402.4 ± 90 mg/L squalene by small-scale cultivation. Other reports of squalene production in highly modified *Y. lipolytica* show titers up to 531.6 mg/L by a strain with at least twelve modifications relevant to squalene production, including overexpression of the

entire MVA-pathway and knockouts of peroxisomal β-oxidation (*pox*) genes which could affect acetyl-CoA balance (**Table 1**; Gao et al., 2017). By comparison the squalene platform strain from this study contained only seven gene overexpression and one gene downregulation. Therefore, further engineering and scale-up could potentially improve the production of squalene described herein. Overexpression of *SQE* in combination with the modifications described for the squalene production strain resulted in 22 ± 5.9 mg/L 2,3-oxidosqualene. This platform strain can potentially be used for the production of complex triterpenoids. Since *SQE* was expressed under the *pGPD*-promoter, expressing additional copies of *SQE*, potentially under the relatively stronger *pTEFintron*-promoter, could raise 2,3-oxidosqualene levels further (Holkenbrink et al., 2018). The production of β-carotene for the carotenoid platform strains, 158 ± 24.1 mg/L or 164 ± 37.6 mg/L for ST9251 or ST9253, respectively, are lower than in previous reports (Kildegaard et al., 2017; Larroude et al., 2018). To achieve 6.5 g/L β-carotene, three copies of the pathway enzymes (*carB* and *CarRP*) and *GGPPS* were integrated in a W29-derived strain engineered for high lipogenesis (Larroude et al., 2018). Therefore, further engineering of the downstream biosynthetic pathway may be necessary when using the platform strains.

CONCLUSION

Tailored platform strains for the production of mono-, sesqui-, tri-, or diterpenes and carotenoids were constructed, and their potential was tested by the production of limonene, β-farnesene and valencene, squalene and 2,3-oxidosqualene, and β-carotene, respectively. These improved platform strains were metabolically engineered for improved terpenoid production and their use could result in almost 100-fold improvement production for some terpenes compared to base strains. These platform strains can potentially be improved even further by engineering and scale-up into bioreactors.

STRAIN AVAILABILITY STATEMENT

The platform strains and representative terpenoid producing strains from this study can be requested from Euroscarf. The Euroscarf accession numbers are given in parenthesis. ST9202, monoterpene platform strain (Y41400). ST9250, monoterpene platform strain with *PfLS* (Y41401). ST9395, base strain with *PfLS* (Y41402). ST9149, sesquiterpene platform strain (Y41403). ST9204, sesquiterpene platform strain with *CnVS* (Y41404). ST9396, base strain with *CnVS* (Y41405). ST9105, squalene production strain (Y41406). ST9106, triterpene platform strain (Y41407). ST6512, base strain (Y41408). ST9203, diterpene/carotenoid platform strain with $ERG20^{F88C}$ (Y41409). ST9150, diterpene/carotenoid platform strain with GGPPS (Y41410). The β-farnesene test-strains ST8979, ST8998, ST9006, ST9026, and ST9147 (Y41411-15).

DATA AVAILABILITY STATEMENT

The platform strains and representative strains for terpenoid production can be requested from Euroscarf or the authors.

AUTHOR CONTRIBUTIONS

JA, KK, and IB designed the experiments. MC, SJ, and JA carried out the experiments. MK provided critical assistance in developing GC-FID and HP-LC methods. JA analyzed the data. JA and IB wrote the manuscript. All authors contributed to the article and approved the submitted version.

FUNDING

The research was funded by The Novo Nordisk Foundation (Grant agreements NNF15OC0016592 and NNF10CC1016517). IB and KK acknowledge the financial support from the European Union's Horizon 2020 Research and Innovation Programs (European Research Council, YEAST-TRANS project no. 757384 and OLEFINE project no. 760798).

ACKNOWLEDGMENTS

The authors thank the ARS Culture Collection, NCAUR, United States, for providing the W29 *Y. lipolytica* strain Y-63764 and Volker Zickerman for providing the *Y. lipolytica* strain GB20 (Angerer et al., 2014).

SUPPLEMENTARY MATERIAL

The Supplementary Material for this article can be found online at: https://www.frontiersin.org/articles/10.3389/fbioe.2020.00945/full#supplementary-material

REFERENCES

Angerer, H., Radermacher, M., Ma kowska, M., Steger, M., Zwicker, K., Heide, H., et al. (2014). The LYR protein subunit NB4M/NDUFA6 of mitochondrial complex I anchors an acyl carrier protein and is essential for catalytic activity. *Proc. Natl. Acad. Sci. U.S.A.* 111, 5207–5212. doi: 10.1073/pnas.1322438111

Ashour, M., Wink, M., and Gershenzon, J. (2010). "Biochemistry of terpenoids: monoterpenes, sesquiterpenes and diterpenes," in *Biochemistry of Plant Secondary Metabolism*, ed. M. Wink (Oxford: Wiley-Blackwell), 258–303. doi: 10.1002/9781444320503.ch5

Beekwilder, J., van Houwelingen, A., Cankar, K., van Dijk, A. D. J., de Jong, R. M., Stoopen, G., et al. (2014). Valencene synthase from the heartwood of Nootka cypress (*Callitropsis nootkatensis*) for biotechnological production of valencene. *Plant Biotechnol. J.* 12, 174–182. doi: 10.1111/pbi.12124

Benchling (2020). *Cloud-Based Informatics Platform for Life Sciences R&D | Benchling*. Available online at: https://www.benchling.com/ (accessed March 9, 2020).

Blaskó, Á, Gazdag, Z., Gróf, P., Máté, G., Sárosi, S., Krisch, J., et al. (2017). Effects of clary sage oil and its main components, linalool and linalyl acetate, on the plasma membrane of *Candida albicans*: an in vivo EPR study. *Apoptosis* 22, 175–187. doi: 10.1007/s10495-016-1321-7

Brennan, T. C. R., Krömer, J. O., and Nielsen, L. K. (2013). Physiological and Transcriptional Responses of *Saccharomyces cerevisiae* to d-Limonene show changes to the cell wall but not to the plasma membrane. *Appl. Environ. Microbiol.* 79, 3590–3600. doi: 10.1128/AEM.00463-13

Brennan, T. C. R., Turner, C. D., Krömer, J. O., and Nielsen, L. K. (2012). Alleviating monoterpene toxicity using a two-phase extractive fermentation for the bioproduction of jet fuel mixtures in *Saccharomyces cerevisiae*. *Biotechnol. Bioeng.* 109, 2513–2522. doi: 10.1002/bit.24536

Bröker, J. N., Müller, B., van Deenen, N., Prüfer, D., and Schulze Gronover, C. (2018). Upregulating the mevalonate pathway and repressing sterol synthesis in *Saccharomyces cerevisiae* enhances the production of triterpenes. *Appl. Microbiol. Biotechnol.* 102, 6923–6934. doi: 10.1007/s00253-018-9154-7

Brown, N. P., Leroy, C., and Sander, C. (1998). MView: a web-compatible database search or multiple alignment viewer. *Bioinformatics* 14, 380–381. doi: 10.1093/bioinformatics/14.4.380

Cao, X., Lv, Y. B., Chen, J., Imanaka, T., Wei, L. J., and Hua, Q. (2016). Metabolic engineering of oleaginous yeast *Yarrowia lipolytica* for limonene overproduction. *Biotechnol. Biofuels* 9, 1–11. doi: 10.1186/s13068-016-0626-7

Cao, X., Wei, L. J., Lin, J. Y., and Hua, Q. (2017). Enhancing linalool production by engineering oleaginous yeast *Yarrowia lipolytica*. *Bioresour. Technol.* 245, 1641–1644. doi: 10.1016/j.biortech.2017.06.105

Cheng, B.-Q., Wei, L.-J., Lv, Y.-B., Chen, J., and Hua, Q. (2019). Elevating limonene production in oleaginous Yeast *Yarrowia lipolytica* via genetic engineering of limonene biosynthesis pathway and optimization of medium composition. *Biotechnol. Bioprocess Eng.* 24, 500–506. doi: 10.1007/s12257-018-0497-9

Christen, S., and Sauer, U. (2011). Intracellular characterization of aerobic glucose metabolism in seven yeast species by 13C flux analysis and metabolomics. *FEMS Yeast Res.* 11, 263–272. doi: 10.1111/j.1567-1364.2010.00713.x

Cravens, A., Payne, J., and Smolke, C. D. (2019). Synthetic biology strategies for microbial biosynthesis of plant natural products. *Nat. Commun.* 10, 1–12. doi: 10.1038/s41467-019-09848-w

Czajka, J. J., Nathenson, J. A., Benites, V. T., Baidoo, E. E. K., Cheng, Q., Wang, Y., et al. (2018). Engineering the oleaginous yeast *Yarrowia lipolytica* to produce the aroma compound β-ionone. *Microb. Cell Fact.* 17, 1–13. doi: 10.1186/s12934-018-0984-x

Du, H. X., Xiao, W. H., Wang, Y., Zhou, X., Zhang, Y., Liu, D., et al. (2016). Engineering *Yarrowia lipolytica* for campesterol overproduction. *PLoS One* 11:e0146773. doi: 10.1371/journal.pone.0146773

Dujon, B., Sherman, D., Fischer, G., Durrens, P., Casaregola, S., Lafontaine, I., et al. (2004). Genome evolution in yeasts. *Nature* 430, 35–44. doi: 10.1038/nature02579

Evolva (2020). *Our Valencene the Natural Choice for Flavour and Fragrance Applications*. Available online at: https://evolva.com/evevalencene/ (accessed March 9, 2020).

Fernandes, S. R., Barreiros, L., Oliveira, R. F., Cruz, A., Prudêncio, C., Oliveira, A. I., et al. (2019). Chemistry, bioactivities, extraction and analysis of azadirachtin: state-of-the-art. *Fitoterapia* 134, 141–150. doi: 10.1016/j.fitote.2019.02.006

Gao, S., Tong, Y., Zhu, L., Ge, M., Zhang, Y., Chen, D., et al. (2017). Iterative integration of multiple-copy pathway genes in *Yarrowia lipolytica* for heterologous β-carotene production. *Metab. Eng.* 41, 192–201. doi: 10.1016/j.ymben.2017.04.004

George, K. W., Alonso-Gutierrez, J., Keasling, J. D., and Lee, T. S. (2015). "Isoprenoid drugs, biofuels, and Chemicals—Artemisinin, farnesene, and beyond," in *Advances in Biochemical Engineering/Biotechnology*, eds J. Schrader and J. Bohlmann (Cham: Springer), 355–389. doi: 10.1007/10_2014_288

Groenewald, M., Boekhout, T., Neuvéglise, C., Gaillardin, C., Van Dijck, P. W. M., and Wyss, M. (2014). *Yarrowia lipolytica*: safety assessment of an oleaginous yeast with a great industrial potential. *Crit. Rev. Microbiol.* 40, 187–206. doi: 10.3109/1040841X.2013.770386

Guo, X., Sun, J., Li, D., and Lu, W. (2018). Heterologous biosynthesis of (+)-nootkatone in unconventional yeast *Yarrowia lipolytica*. *Biochem. Eng. J.* 137, 125–131. doi: 10.1016/j.bej.2018.05.023

Han, J. Y., Seo, S. H., Song, J. M., Lee, H., and Choi, E. S. (2018). High-level recombinant production of squalene using selected *Saccharomyces cerevisiae* strains. *J. Ind. Microbiol. Biotechnol.* 45, 239–251. doi: 10.1007/s10295-018-2018-4

Hill, R. A., and Connolly, J. D. (2017). Triterpenoids. *Nat. Prod. Rep.* 34, 90–122. doi: 10.1039/C6NP00094K

Holkenbrink, C., Dam, M. I., Kildegaard, K. R., Beder, J., Dahlin, J., Doménech Belda, D., et al. (2018). EasyCloneYALI: CRISPR/Cas9-based synthetic toolbox for engineering of the yeast *Yarrowia lipolytica*. *Biotechnol. J.* 13:1700543. doi: 10.1002/biot.201700543

Huang, Y.-Y., Jian, X.-X., Lv, Y.-B., Nian, K.-Q., Gao, Q., Chen, J., et al. (2018). Enhanced squalene biosynthesis in *Yarrowia lipolytica* based on metabolically engineered acetyl-CoA metabolism. *J. Biotechnol.* 281, 106–114. doi: 10.1016/j.jbiotec.2018.07.001

Ignea, C., Pontini, M., Maffei, M. E., Makris, A. M., and Kampranis, S. C. (2014). Engineering monoterpene production in yeast using a synthetic dominant negative geranyl diphosphate synthase. *ACS Synth. Biol.* 3, 298–306. doi: 10.1021/sb400115e

Ignea, C., Trikka, F. A., Nikolaidis, A. K., Georgantea, P., Ioannou, E., Loupassaki, S., et al. (2015). Efficient diterpene production in yeast by engineering Erg20p into a geranylgeranyl diphosphate synthase. *Metab. Eng.* 27, 65–75. doi: 10.1016/j.ymben.2014.10.008

Jia, D., Xu, S., Sun, J., Zhang, C., Li, D., and Lu, W. (2019). *Yarrowia lipolytica* construction for heterologous synthesis of α-santalene and fermentation optimization. *Appl. Microbiol. Biotechnol.* 103, 3511–3520. doi: 10.1007/s00253-019-09735-w

Jin, C.-C., Zhang, J.-L., Song, H., and Cao, Y.-X. (2019). Boosting the biosynthesis of betulinic acid and related triterpenoids in *Yarrowia lipolytica* via multimodular metabolic engineering. *Microb. Cell Fact.* 18:77. doi: 10.1186/s12934-019-1127-8

Janocha, S., Schmitz, D., and Bernhardt, R. (2015). Terpene hydroxylation with microbial cytochrome P450 monooxygenases. *Adv. Biochem. Eng. Biotechnol.* 148, 215–250. doi: 10.1007/10_2014_296

Khan, A., Ahmad, A., Khan, L. A., and Manzoor, N. (2014). *Ocimum sanctum* (L.) essential oil and its lead molecules induce apoptosis in Candida albicans. *Res. Microbiol.* 165, 411–419. doi: 10.1016/j.resmic.2014.05.031

Kildegaard, K. R., Adiego-Pérez, B., Doménech Belda, D., Khangura, J. K., Holkenbrink, C., and Borodina, I. (2017). Engineering of *Yarrowia lipolytica* for production of astaxanthin. *Synth. Syst. Biotechnol.* 2, 287–294. doi: 10.1016/j.synbio.2017.10.002

Larroude, M., Celinska, E., Back, A., Thomas, S., Nicaud, J. M., and Ledesma-Amaro, R. (2018). A synthetic biology approach to transform *Yarrowia lipolytica* into a competitive biotechnological producer of β-carotene. *Biotechnol. Bioeng.* 115, 464–472. doi: 10.1002/bit.26473

Leonhardt, R.-H., and Berger R. G. (2014). "Nootkatone," in *Biotechnology of Isoprenoids*, Vol. 148, *Advances in Biochemical Engineering/Biotechnology*, eds J. Schrader and J. Bohlmann (Berlin: Springer). doi: 10.1007/10_2014_279

Li, D., Wu, Y., Wei, P., Gao, X., Li, M., Zhang, C., et al. (2020). Metabolic engineering of *Yarrowia lipolytica* for heterologous oleanolic acid production. *Chem. Eng. Sci.* 218:115529. doi: 10.1016/j.ces.2020.115529

Li, D., Wu, Y., Zhang, C., Sun, J., Zhou, Z., and Lu, W. (2019). Production of triterpene ginsenoside compound K in the non-conventional yeast *Yarrowia lipolytica*. *J. Agric. Food Chem.* 67, 2581–2588. doi: 10.1021/acs.jafc.9b00009

Liu, J., Zhu, Y., Du, G., Zhou, J., and Chen, J. (2013). Response of *Saccharomyces cerevisiae* to D-limonene-induced oxidative stress. *Appl. Microbiol. Biotechnol.* 97, 6467–6475. doi: 10.1007/s00253-013-4931-9

Liu, Y., Jiang, X., Cui, Z., Wang, Z., Qi, Q., and Hou, J. (2019). Engineering the oleaginous yeast *Yarrowia lipolytica* for production of α-farnesene. *Biotechnol. Biofuels* 12:296. doi: 10.1186/s13068-019-1636-z

Lu, Y., Yang, Q., Lin, Z., and Yang, X. (2020). A modular pathway engineering strategy for the high-level production of β-ionone in *Yarrowia lipolytica*. *Microb. Cell Fact.* 19:49. doi: 10.1186/s12934-020-01309-0

Marella, E. R., Dahlin, J., Dam, M. I., ter Horst, J., Christensen, H. B., Sudarsan, S., et al. (2019). A single-host fermentation process for the production of flavor lactones from non-hydroxylated fatty acids. *Metab. Eng* S1096-7176:30254–X. doi: 10.1016/j.ymben.2019.08.009

Marsafari, M., and Xu, P. (2020). Debottlenecking mevalonate pathway for antimalarial drug precursor amorphadiene biosynthesis in *Yarrowia lipolytica*. *Metab. Eng. Commun.* 10:e00121. doi: 10.1016/j.mec.2019.e00121

Matthäus, F., Ketelhot, M., Gatter, M., and Barth, G. (2014). Production of lycopene in the non-carotenoid-producing yeast *Yarrowia lipolytica*. *Appl. Environ. Microbiol.* 80, 1660–1669. doi: 10.1128/AEM.03167-13

Meadows, A. L., Hawkins, K. M., Tsegaye, Y., Antipov, E., Kim, Y., Raetz, L., et al. (2016). Rewriting yeast central carbon metabolism for industrial isoprenoid production. *Nature* 537, 694–697. doi: 10.1038/nature19769

Moser, S., and Pichler, H. (2019). Identifying and engineering the ideal microbial terpenoid production host. *Appl. Microbiol. Biotechnol.* 103, 5501–5516. doi: 10.1007/s00253-019-09892-y

Pang, Y., Zhao, Y., Li, S., Zhao, Y., Li, J., Hu, Z., et al. (2019). Engineering the oleaginous yeast *Yarrowia lipolytica* to produce limonene from waste cooking oil. *Biotechnol. Biofuels* 12, 1–18. doi: 10.1186/s13068-019-1580-y

Schwartz, C., Frogue, K., Misa, J., and Wheeldon, I. (2017). Host and pathway engineering for enhanced lycopene biosynthesis in *Yarrowia lipolytica*. *Front. Microbiol.* 8:2233. doi: 10.3389/fmicb.2017.02233

Sun, J., Zhang, C., Nan, W., Li, D., Ke, D., and Lu, W. (2019). Glycerol improves heterologous biosynthesis of betulinic acid in engineered *Yarrowia lipolytica*. *Chem. Eng. Sci.* 196, 82–90. doi: 10.1016/j.ces.2018.10.052

Tetali, S. D. (2018). Terpenes and isoprenoids: a wealth of compounds for global use. *Planta* 249, 1–8. doi: 10.1007/s00425-018-3056-x

Tippmann, S., Nielsen, J., and Khoomrung, S. (2016). Improved quantification of farnesene during microbial production from *Saccharomyces cerevisiae* in two-liquid-phase fermentations. *Talanta* 146, 100–106. doi: 10.1016/j.talanta.2015.08.031

Tramontin, L. R. R., Kildegaard, K. R., Sudarsan, S., and Borodina, I. (2019). Enhancement of astaxanthin biosynthesis in oleaginous yeast *Yarrowia lipolytica* via microalgal pathway. *Microorganisms* 7:472. doi: 10.3390/microorganisms7100472

Turck, D., Castenmiller, J., de Henauw, S., Hirsch-Ernst, K., Kearney, J., Maciuk, A., et al. (2019). Safety of *Yarrowia lipolytica* yeast biomass as a novel food pursuant to Regulation (EU) 2015/2283. *EFSA J.* 17:e05594. doi: 10.2903/j.efsa.2019.5594

Uribe, S., Ramirez, J., and Pena, A. (1985). Effects of β-Pinene on yeast membrane functions. *J. Bacteriol* 161, 1195–1200. doi: 10.1128/jb.161.3.1195-1200.1985

Wei, L. J., Kwak, S., Liu, J. J., Lane, S., Hua, Q., Kweon, D. H., et al. (2018). Improved squalene production through increasing lipid contents in *Saccharomyces cerevisiae*. *Biotechnol. Bioeng.* 115, 1793–1800. doi: 10.1002/bit.26595

Wu, Y., Xu, S., Gao, X., Li, M., Li, D., and Lu, W. (2019). Enhanced protopanaxadiol production from xylose by engineered *Yarrowia lipolytica*. *Microb. Cell Fact.* 18, 1–12. doi: 10.1186/s12934-019-1136-7

Xu, W., Ma, X., and Wang, Y. (2016). Production of squalene by microbes: an update. *World J. Microbiol. Biotechnol.* 32:195. doi: 10.1007/s11274-016-2155-8

Yang, X., Nambou, K., Wei, L., and Hua, Q. (2016). Heterologous production of α-farnesene in metabolically engineered strains of *Yarrowia lipolytica*. *Bioresour. Technol.* 216, 1040–1048. doi: 10.1016/j.biortech.2016.06.028

Zhang, X.-K., Wang, D.-N., Chen, J., Liu, Z.-J., Wei, L.-J., and Hua, Q. (2020). Metabolic engineering of β-carotene biosynthesis in *Yarrowia lipolytica*. *Biotechnol. Lett.* 42, 945–956. doi: 10.1007/s10529-020-02844-x

Zhang, Y., Nielsen, J., and Liu, Z. (2017a). Engineering yeast metabolism for production of terpenoids for use as perfume ingredients, pharmaceuticals and biofuels. *FEMS Yeast Res.* 17, 1–11. doi: 10.1093/femsyr/fox080

Zhang, Y., Wang, Y., Yao, M., Liu, H., Zhou, X., Xiao, W., et al. (2017b). Improved campesterol production in engineered *Yarrowia lipolytica* strains. *Biotechnol. Lett.* 39, 1033–1039. doi: 10.1007/s10529-017-2331-4

Zhao, J., Bao, X., Li, C., Shen, Y., and Hou, J. (2016). Improving monoterpene geraniol production through geranyl diphosphate synthesis regulation in *Saccharomyces cerevisiae*. *Appl. Microbiol. Biotechnol.* 100, 4561–4571. doi: 10.1007/s00253-016-7375-1

Zyad, A., Tilaoui, M., Jaafari, A., Oukerrou, M. A., and Mouse, H. A. (2018). More insights into the pharmacological effects of artemisinin. *Phyther. Res.* 32, 216–229. doi: 10.1002/ptr.5958

Conflict of Interest: The authors declare that the research was conducted in the absence of any commercial or financial relationships that could be construed as a potential conflict of interest.

frontiers in Bioengineering and Biotechnology

ORIGINAL RESEARCH
published: 30 September 2020
doi: 10.3389/fbioe.2020.578793

Engineering *Saccharomyces cerevisiae* for the Overproduction of β-Ionone and Its Precursor β-Carotene

Javiera López[1†], Diego Bustos[2†], Conrado Camilo[1], Natalia Arenas[2], Pedro A. Saa[2] and Eduardo Agosin[1,2]*

[1] Centro de Aromas y Sabores, DICTUC S.A., Santiago, Chile, [2] Department of Chemical and Bioprocess Engineering, School of Engineering, Pontificia Universidad Católica de Chile, Santiago, Chile

β-ionone is a commercially attractive industrial fragrance produced naturally from the cleavage of the pigment β-carotene in plants. While the production of this ionone is typically performed using chemical synthesis, environmentally friendly and consumer-oriented biotechnological production is gaining increasing attention. A convenient cell factory to address this demand is the yeast *Saccharomyces cerevisiae*. However, current β-ionone titers and yields are insufficient for commercial bioproduction. In this work, we optimized *S. cerevisiae* for the accumulation of high amounts of β-carotene and its subsequent conversion to β-ionone. For this task, we integrated systematically the heterologous carotenogenic genes (CrtE, CrtYB and CrtI) from *Xanthophyllomyces dendrorhous* using markerless genome editing CRISPR/Cas9 technology; and evaluated the transcriptional unit architecture (bidirectional or tandem), integration site, and impact of gene dosage, first on β-carotene accumulation, and later, on β-ionone production. A single-copy insertion of the carotenogenic genes in high expression *loci* of the wild-type yeast CEN.Pk2 strain yielded 4 mg/gDCW of total carotenoids, regardless of the transcriptional unit architecture employed. Subsequent fine-tuning of the carotenogenic gene expression enabled reaching 16 mg/gDCW of total carotenoids, which was further increased to 32 mg/gDCW by alleviating the known pathway bottleneck catalyzed by the hydroxymethylglutaryl-CoA reductase (HMGR1). The latter yield represents the highest total carotenoid concentration reported to date in *S. cerevisiae* for a constitutive expression system. For β-ionone synthesis, single and multiple copies of the carotene cleavage dioxygenase 1 (CCD1) gene from *Petunia hybrida* (*Ph*CCD1) fused with a membrane destination peptide were expressed in the highest β-carotene-producing strains, reaching up to 33 mg/L of β-ionone in the culture medium after 72-h cultivation in shake flasks. Finally, interrogation of a contextualized genome-scale metabolic model of the producer strains pointed to *Ph*CCD1 unspecific cleavage activity as a potentially limiting factor reducing β-ionone production. Overall, the results of this work constitute a step toward the industrial production of this ionone and, more broadly, they demonstrate that biotechnological production of apocarotenoids is technically feasible.

Keywords: *Saccharomyces cerevisiae*, ionone, apocarotenoid biosynthesis, metabolic engineering, synthetic biology

OPEN ACCESS

Edited by:
Rodrigo Ledesma-Amaro, Imperial College London, United Kingdom

Reviewed by:
Kyle J. Lauersen, King Abdullah University of Science and Technology, Saudi Arabia
Dae-Hee Lee, Korea Research Institute of Bioscience and Biotechnology (KRIBB), South Korea

***Correspondence:**
Eduardo Agosin
agosin@ing.puc.cl

[†] These authors have contributed equally to this work

Specialty section:
This article was submitted to Synthetic Biology, a section of the journal Frontiers in Bioengineering and Biotechnology

Received: *01 July 2020*
Accepted: *08 September 2020*
Published: *30 September 2020*

Citation:
López J, Bustos D, Camilo C, Arenas N, Saa PA and Agosin E (2020) Engineering Saccharomyces cerevisiae for the Overproduction of β-Ionone and Its Precursor β-Carotene. Front. Bioeng. Biotechnol. 8:578793. doi: 10.3389/fbioe.2020.578793

INTRODUCTION

Isoprenoids are the largest and most diverse group of natural compounds found in nature. Many members of this family have attractive commercial applications in both the flavor and fragrance industries, finding place in cosmetics, perfumes and food formulations. An interesting subfamily of these compounds are plants apocarotenoids, highly valued by the food industry. These multifaceted compounds – produced by the enzymatic cleavage of carotenoids –encompass pigments, aromas and scent compounds, amongst others, with yet unknown functions.

One of the most interesting apocarotenoids are those of the family of ionones. Particularly, β-ionone – a highly valued ionone for its woody-violet aroma – is produced by the cleavage of the C40-compound β-carotene by the *carotenoid cleavage dioxygenase 1* (CCD1). This enzyme can symmetrically cleave the 9,10 (9',10') double bonds of multiple carotenoid substrates to produce a C14 dialdehyde and two C13 ionones (Vogel et al., 2008). Both molecules, β-carotene and β-ionone, have been heterologously produced by different microorganisms. In the case of β-carotene, a number of studies have reported heterologous β-carotene production by recombinant *Saccharomyces cerevisiae* strains in shake flasks (Yamano et al., 1994; Verwaal et al., 2007; Li et al., 2013; Zhao et al., 2015; Li et al., 2017), and bench-scale batch fermentations (Reyes et al., 2014; Olson et al., 2016; López et al., 2019), reaching up to 18 mg/gDCW in test tubes and 25 mg/gDCW in batch fermenters (Olson et al., 2016). All the above studies employed constitutive expression systems. On the other hand, Xie et al. (2015a) achieved 20.8 mg/gDCW in high-cell density fermentations after engineering an inducible expression system in recombinant yeast cells with a sequential control strategy (Xie et al., 2015b).

In the case of β-ionone, one of the first platforms used for its production was *S. cerevisiae,* reaching titers in the range of 0.2 to 5 mg/L (Beekwilder et al., 2014; López et al., 2015). More recent attempts by Werner et al. (2019) in two-phase fermentations in shake flasks, reported 180 mg/L of β-ionone – in the organic phase – using a β-carotene hyperproducer strain (Reyes et al., 2014), the highest titer reached to date in this yeast. Nevertheless, this strain has a poor performance under industrial fermentation conditions (López et al., 2019). Production in other microorganisms has also been attempted. For example, in *Escherichia coli*, titers of 32 mg/L in shake flasks and 500 mg/L in bioreactors have been reported (Zhang et al., 2018); while in the oleaginous yeast *Yarrowia lipolytica* its accumulation reached up to 60 mg/L and 380 mg/L of β-ionone in the same scales, respectively (Czajka et al., 2018).

Due to the low concentrations of carotenoids in plants [in the order of mg/100 g of fresh weight, Vogel et al. (2010)], it is expected that CCDs enzymes were not evolved to process high concentrations of their substrates (Chen et al., 2019). This is probably one of the reasons why in heterologous hosts, like *E. coli* and *S. cerevisiae*, CCD activity is suggested as the limiting production step (Czajka et al., 2018; Werner et al., 2019). The structure of CCD enzymes shows a conserved, seven-bladed β-propeller with a central tunnel, where a Fe^{2+} is located (Harrison and Bugg, 2014; Werner et al., 2019). A second conserved structural feature of these enzymes is located above the β-propeller, corresponding to a dome formed by loops and α-helices. This dome is a hydrophobic patch covering the enzyme's surface, which interacts with the hydrophobic side of biological membranes (Sui et al., 2013). Efforts in the optimization of the catalytic efficiency of these enzymes by protein engineering have been mildly successful due to the high conservation degree of their structural features (Floss and Walter, 2009). For example, Ye et al. (2018) improved β-ionone production in *E. coli* by optimizing the localization of the catalytic enzymes, e.g., CCD1, according to the availability of the corresponding substrate, e.g., β-carotene. More recently, *S. cerevisiae* strains expressing constructs of *Ph*CCD1 fused with membrane destination peptides showed β-ionone yields up to 4-fold higher than the strain carrying the native enzyme (Werner et al., 2019).

The industrial bioproduction of β-ionone is still commercially infeasible due to the currently poor yields, productivities and titers. Metabolic engineering of the microbial host is critical to ensure reaching economically viable production targets. A widely used approach to achieve high titers of secondary metabolites in biofactories involves the expression of heterologous genes using high-copy number plasmids. This strategy is, however, inefficient in most cases, as it typically requires the use of selective media, causes genomic instability, and can impose a high metabolic burden to the cell (Ryan et al., 2014). Conversely, genomic integration of expression cassettes is a more convenient strategy, since the resulting recombinant strains are generally more stable, and their gene expression more controllable (Jensen et al., 2014; Amen and Kaganovich, 2017). Nevertheless, the limited number of selection markers, integration sites and genetic arrangements, constrain the strain design as they restrict the allowable gene dosage (copy number) for the construction. The development of CRISPR/Cas9 technology in yeast has minimized the need of selection markers and, most importantly, it has proven to be highly effective for *S. cerevisiae* transformation, owed to its high homologous recombination capability in response to double strand breakage (DSB) (Jessop-Fabre et al., 2016). Moreover, this technology enables simultaneous integration of several expression cassettes, thereby accelerating strain construction and optimization (Ryan et al., 2014).

In this work, we constructed several *S. cerevisiae* strains using the CRISPR/Cas9 technology, capable of accumulating increasing concentrations of β-ionone, and its precursor, β-carotene. To this task, we first integrated the heterologous genes leading to β-carotene production into specific high-expression sites flanked by genetic elements that are essential for growth of the wild-type *S. cerevisiae* strain CEN.PK2-1c (Mikkelsen et al., 2012). These genes coded for the following enzymes: geranylgeranyl diphosphate synthase (CrtE), bifunctional phytoene synthase/lycopene cyclase (CrtYB), and phytoene desaturase (CrtI) (**Figure 1**). Integration of heterologous genes in these sites enabled robust expression of multi-gene constructs in few known *loci*, thereby avoiding genetic instability issues. The effect of both, the genetic constructs architecture and gene dosage, was then evaluated for generating high β-carotene producers. The most promising producers were later selected

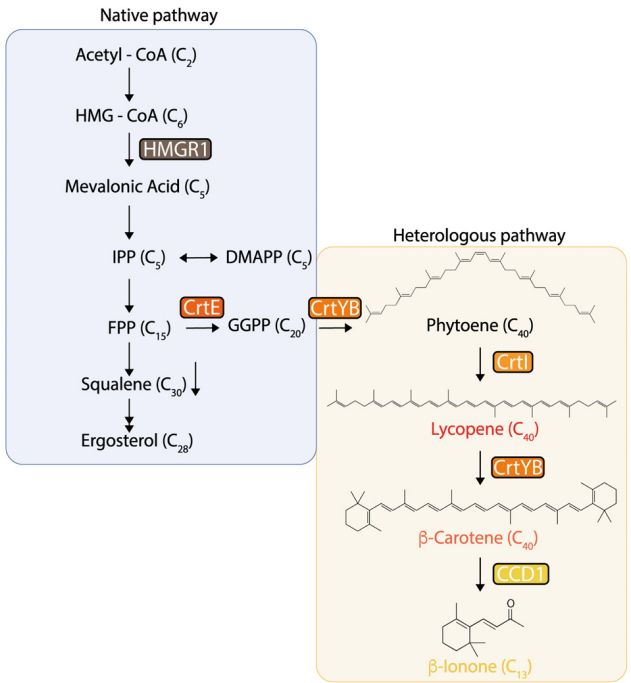

FIGURE 1 | Native and heterologous pathways for β-carotene and β-ionone production in *Saccharomyces cerevisiae*. In these pathways, the *tHMG1* gene (encoding a truncated HMG-CoA reductase), and the heterologous genes *crtE* (encoding geranylgeranyl diphosphate synthase), *crtYB* (encoding phytoene synthase/lycopene cyclase), *crtI* (encoding phytoene desaturase), and *PhCCD1* (encoding carotenoid cleavage dioxygenase from *P. hybrida*) were constitutively integrated into the yeast's genome in different locations, configurations, and dosage.

and transformed with an engineered CCD1 gene from *Petunia hybrida* (fyn-*Ph*CCD1) for β-ionone overproduction (Werner et al., 2019). Incremental increase of the gene dosage of fyn-*Ph*CCD1 up to a certain level enabled reaching the highest β-ionone titer reported to date in *S. cerevisiae* shake-flask cultures. Finally, a contextualized genome-scale stoichiometric model of the producer strains unveiled the potential high impact of *Ph*CCD1 inefficient activity for high β-ionone production.

RESULTS AND DISCUSSION

Design and Evaluation of Different Transcriptional Unit Architectures and Integration Sites for Carotenoids Production

To efficiently produce β-carotene in *S. cerevisiae*, we first evaluated the impact of the arrangement of the carotenogenic (heterologous) genes and the chromosomal integration *loci*, on the final production yield. For this purpose, we constructed several carotenogenic strains expressing the genes CrtE, CrtYB and CrtI from the yeast *X. dendrorhous* (**Table 1A**), under three constitutive strong yeast promoters (TEF1, PGK1 and TDH3).

Optimal co-expression of two or more of these genes was evaluated by building two differentially oriented transcriptional units: Head-to-Head (termed bidirectional hereafter); and Head-to-Tail, (termed tandem hereafter). The CrtE and CrtYB genes were expressed following these two arrangements using the strong constitutive promoters TEF1 and PGK1, respectively, included in the bidirectional promoter plasmid library developed by Partow et al. (2010). The third CrtI gene was expressed under the TDH3 promoter and integrated in a different *locus*, completing the β-carotene biosynthetic pathway (**Figure 2A**). The two resulting strains β-Car1.1 (bidirectional) and β-Car1.2 (tandem) were cultured in shake flasks, reaching similar total carotenoids titers of 4 mg/gDCW and 3.8 mg/gDCW, respectively (**Figure 2C**). These results indicated that carotenoid production was unaffected by gene orientation, suggesting that their transcription did not interfere with each other. It is worthy to mention that we did not evaluate a convergent (Tail-to-Tail orientation) construct, since Carquet et al. (2015) reported that transcriptional units with two genes in this orientation dramatically reduced gene expression (mRNA) compared to the tandem arrangement, possibly as a consequence of transcription interference (TI) at the terminator sites.

Following the above results, we constructed a tandem cassette with the three carotenogenic genes. Adding a third gene to the transcriptional unit has the advantage of simultaneously expressing the heterologous pathway using only one integration site in the yeast genome. Comparison of the β-Car1.1 and β-Car2.1 - both in tandem configuration - revealed that the pXI-5 *locus* was mostly unaffected by the size of the DNA construct (from 5 kb with two genes to 7.7 kb with three genes), at least until this length (**Figure 2C**), since this new strain also reached 3.8 mg/gDCW of total carotenoids at 72 h.

The second variable analyzed was the location (i.e., the integration site) of the carotenogenic genes. Several, well-defined chromosomal integration sites, e.g., URA3, LEU2 and HO sites, have been widely employed in *S. cerevisiae* for the expression of heterologous genes (Flagfeldt et al., 2009; Westfall et al., 2012). Mikkelsen et al. (2012) identified eleven strong integration sites, strategically positioned between essential genes, which enable the construction of genetically stable strains with minimal risk of gene loss by recombination. However, the authors reported that these sites differed in their expression strength, adding another design variable for the construction of production strains. Consequently, we evaluated the expression capacity of six different *loci* (β-Car2.1 to β-Car2.6 strains), using cloning-compatible USER integrating plasmids with the three carotenogenic genes (CrtE/CrtYB/CrtI) displayed in tandem (**Figure 2B**). In order to avoid recombination between the different DNA parts, we employed three different promoters and two terminators - t_{CYC} and t_{ADH1}. Moreover, we noted that after several rounds of cell cultures, the color of the pigmented strains remained constant, pointing to the generation of genetically stable recombinant strains (**Figure 2D**).

The β-carotene yields of the βCar2.1 to βCar2.6 resulting strains, expressing the carotenogenic pathway in either one of the two *loci* used before (XI-3 or XI-5 integration sites), or in other four additional sites (X-2, XI-1, XI-2, and X-4) were compared (**Figure 2C**). According to the integration site of the tandem, total carotenoid yields ranged between 2.6 and 4.1 mg/gDCW after 72 h cultivation, a 60% difference between the integration sites with the highest (pXI-5) and the lowest (pXI-2) expression. Therefore, our results confirmed XI-5 and XI-3 *loci* as the strongest integration sites, in agreement with Mikkelsen et al. (2012). Although we only evaluated 6 of the 11 high expression sites reported by these authors, the former are sufficient for our construction purposes as they enable engineering up to 18 genes using three-gene tandem cassettes. Moreover, this number could be eventually increased, since it is possible to engineer up to 7 genes in just one marker less construct using CRISPR/Cas9 (Shi et al., 2016).

Gene Dosage Tuning Significantly Impacts β-Carotene Accumulation

To further increase β-carotene yield, we integrated an extra copy of the three heterologous genes (tandem cassette) into the strain β-Car2.1, obtaining the β-Car3 strain (**Figure 3A** and **Table 1**). This strain produced up to 12 mg/gDCW of total carotenoids after 72 h cultivation in shake flasks, a 3-fold increase compared to the parental strain. No significant effect on cell growth (**Figure 3B** and **Supplementary Table S3**) was observed. While the increase in gene dosage improved the total carotenoids yield, an analysis of the carotenogenic profile revealed a higher lycopene content than the parental β-Car2 strain, which produced mainly β-carotene (**Figure 3C**). Indeed, in the β-Car3 strain, more than half of the total carotenoid content is lycopene, which still can be converted to β-carotene by the CrtYB enzyme.

Fine-tuning of the heterologous gene expression is likely the most difficult step during strain optimization, as the latter not only has to produce high amounts of the desired compound, but also avoid side reactions and toxicity. In our particular case, elevated lycopene concentrations impair normal yeast growth (López et al., 2015) and, therefore, the CrtI gene dosage – coding for the enzyme responsible of producing lycopene - has to be carefully tuned. Hence, we amplified only the first two genes from the tandem construct, CrtE and CrtYB, and then integrated them in the pX-2 site of the β-Car3 strain to promote phytoene production and lycopene consumption (**Figure 3A**). The resulting strain, β-Car4.b, produced a final yield of 16 mg/gDCW of total carotenoids after 72 h growth in shake flasks (**Figure 3B**). Moreover, the carotenoid profile showed an increased ratio of β-carotene to lycopene, although the strain still maintained a significant amount of residual lycopene. Notably, incorporation of the CrtI gene in this construct (see β-Car4.a in **Figure 3A**) was not beneficial for β-carotene

TABLE 1 | List of strains constructed in this study.

(A) β-Carotene production

Strain	Parental strain	Genotype	Integration site (Chr-Site)
CEN.PK2-1c	-	Mata ura3-52 trp1-289 leu2-3, 112 his3D	-
β-Car1.1/β-Car1.2	CEN.PK2-1c	P_{TEF1}-***CrtE***-T_{ADH1}/P_{PGK1}-***CrtYB***-T_{CYC}	XI-5
		P_{TDH3}-***CrtI***-T_{CYC}	XI-3
β-Car2.1	CEN.PK2-1c	P_{TEF1}-***CrtE***-T_{ADH1}/P_{PGK1}-***CrtYB***-T_{CYC}/P_{TDH3}-***CrtI***-T_{CYC}	XI-5
β-Car2.2	CEN.PK2-1c	P_{TEF1}-***CrtE***-T_{ADH1}/P_{PGK1}-***CrtYB***-T_{CYC}/P_{TDH3}-***CrtI***-T_{CYC}	XI-3
β-Car2.3	CEN.PK2-1c	P_{TEF1}-***CrtE***-T_{ADH1}/P_{PGK1}-***CrtYB***-T_{CYC}/P_{TDH3}-***CrtI***-T_{CYC}	X-2
β-Car2.4	CEN.PK2-1c	P_{TEF1}-***CrtE***-T_{ADH1}/P_{PGK1}-***CrtYB***-T_{CYC}/P_{TDH3}-***CrtI***-T_{CYC}	X-4
β-Car2.5	CEN.PK2-1c	P_{TEF1}-***CrtE***-T_{ADH1}/P_{PGK1}-***CrtYB***-T_{CYC}/P_{TDH3}-***CrtI***-T_{CYC}	XI-1
β-Car2.6	CEN.PK2-1c	P_{TEF1}-***CrtE***-T_{ADH1}/P_{PGK1}-***CrtYB***-T_{CYC}/P_{TDH3}-***CrtI***-T_{CYC}	XI-2
β-Car3	β-Car2.1	P_{TEF1}-***CrtE***-T_{ADH1}/P_{PGK1}-***CrtYB***-T_{CYC}/P_{TDH3}-***CrtI***-T_{CYC}	XI-3
β-Car4.a	β-Car3	P_{TEF1}-***CrtE***-T_{ADH1}/P_{PGK1}-***CrtYB***-T_{CYC}/P_{TDH3}-***CrtI***-T_{CYC}	X-2
β-Car4.b	β-Car3	P_{TEF1}-***CrtE***-T_{ADH1}/P_{PGK1}-***CrtYB***-T_{CYC}	X-2
β-Car5	β-Car4.b	P_{TEF1}-$\boldsymbol{tHMG1_{Sc}}$-T_{ADH1}/P_{PGK1}-$\boldsymbol{tHMG1_{Xd}}$-T_{CYC}	XI-1

(B) β-Ionone production

Strain	Parental Strain	Genotype	Integration Site (Chr-Site)
β-iono2.1	β-Car2.1	P_{PGK1}-$\boldsymbol{CCD1_{Ph}}$-T_{CYC}	XI-2
β-iono3.1	β-Car3	P_{PGK1}-$\boldsymbol{CCD1_{Ph}}$-T_{CYC}	XI-2
β-iono4.1	β-Car4.b	P_{PGK1}-$\boldsymbol{CCD1_{Ph}}$-T_{CYC}	XI-2
β-iono4.2	β-iono4.1	P_{PGK1}-$\boldsymbol{CCD1_{Ph}}$-T_{CYC}	X-4
β-iono5.1	β-Car5	P_{PGK1}-$\boldsymbol{CCD1_{Ph}}$-T_{CYC}	XI-2
β-iono5.2	β-iono5.1	P_{PGK1}-$\boldsymbol{CCD1_{Ph}}$-T_{CYC}	X-4
β-iono5.3	β-iono5.2	P_{PGK1}-$\boldsymbol{CCD1_{Ph}}$-T_{CYC}	XI-1

The bold font represent the name of genes.

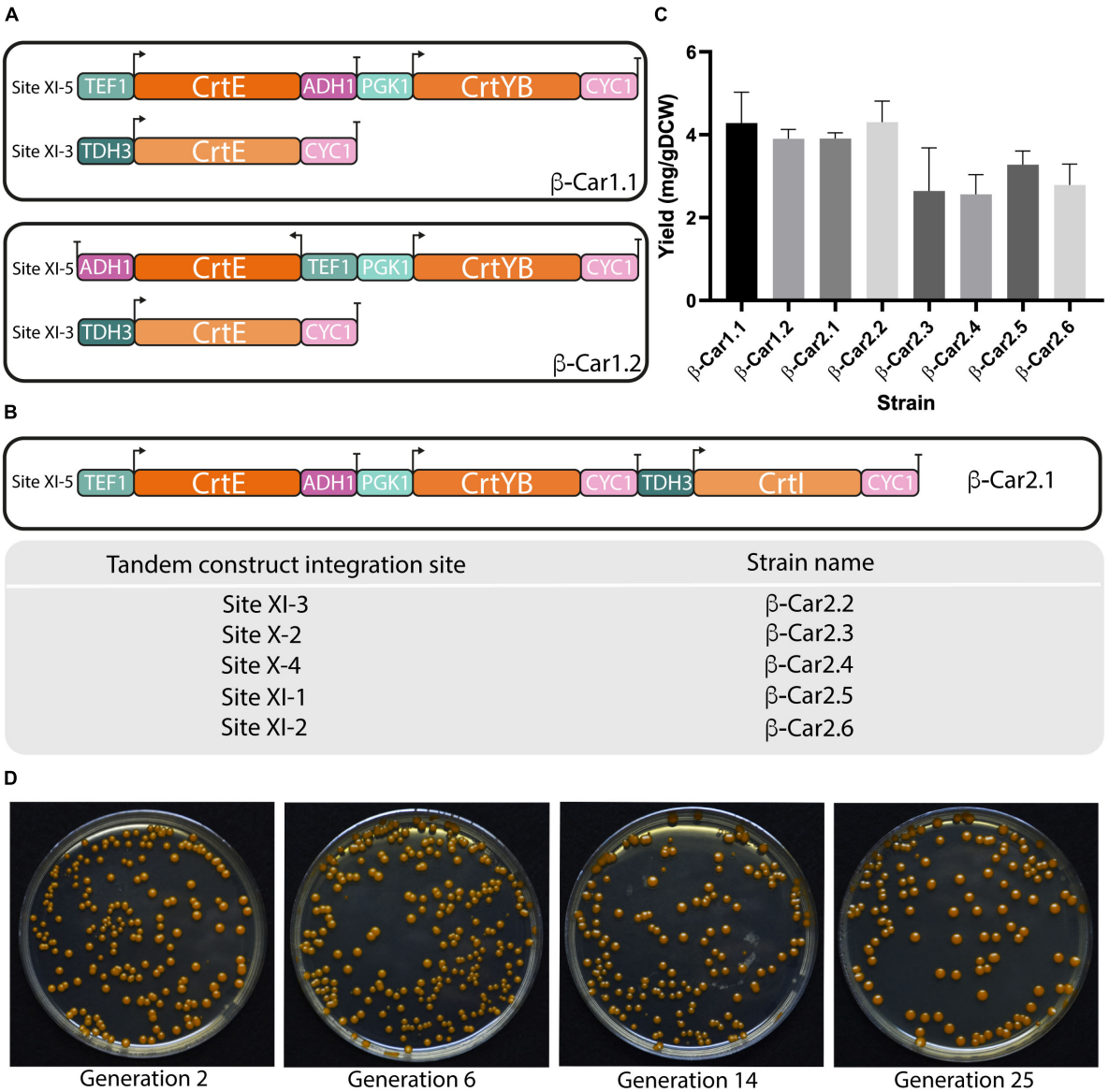

FIGURE 2 | Design and evaluation of different transcriptional unit architectures and integration sites for carotenoids production in *S. cerevisiae*. General scheme of the different transcriptional architectures **(A)** and integration sites **(B)** evaluated for carotenoids production in yeast. **(C)** Total carotenoids yields achieved in shake flask cultivations after 72 h by strains with a single copy of the carotenogenic genes in different arrangements. The data represent the average and standard deviation of three independently grown cultures. **(D)** Color pigmentation of transformants remained stable throughout cultivations.

synthesis; furthermore, it lowered final biomass concentration (**Supplementary Table S3**).

Finally, to further improve the carbon flux toward β-carotene, we integrated two extra copies of the truncated version of the HMG-CoA reductase gene (tHMGR1), one from *S. cerevisiae* and the other from *X. dendrorhous*, to avoid gene loss by recombination. The addition of several copies of this gene has been widely employed to increase the flux through the mevalonate (MVA) pathway in microbial cell factories, after this enzyme was identified as the major rate-limiting step of the pathway (Shimada et al., 1998; Wang and Keasling, 2002; Kampranis and Makris, 2012). The expression of these two genes in the β-Car4.b strain yielded the β-Car5 strain, which produced 32 mg/gDCW of total carotenoids (2-fold increase) (**Figure 3B**), with a higher ratio of β-carotene to lycopene (**Figure 3C**).

The Extent of β-Carotene Accumulation Determines β-Ionone Final Titer

To evaluate β-ionone production under different β-carotene production conditions, we integrated a previously engineered CCD1 gene from *Petunia hybrida* (called fyn-*Ph*CCD1 hereafter) (Werner et al., 2019) into the different carotenogenic strains. Since the initial carotene producing strains (β-Car1.1-2 and

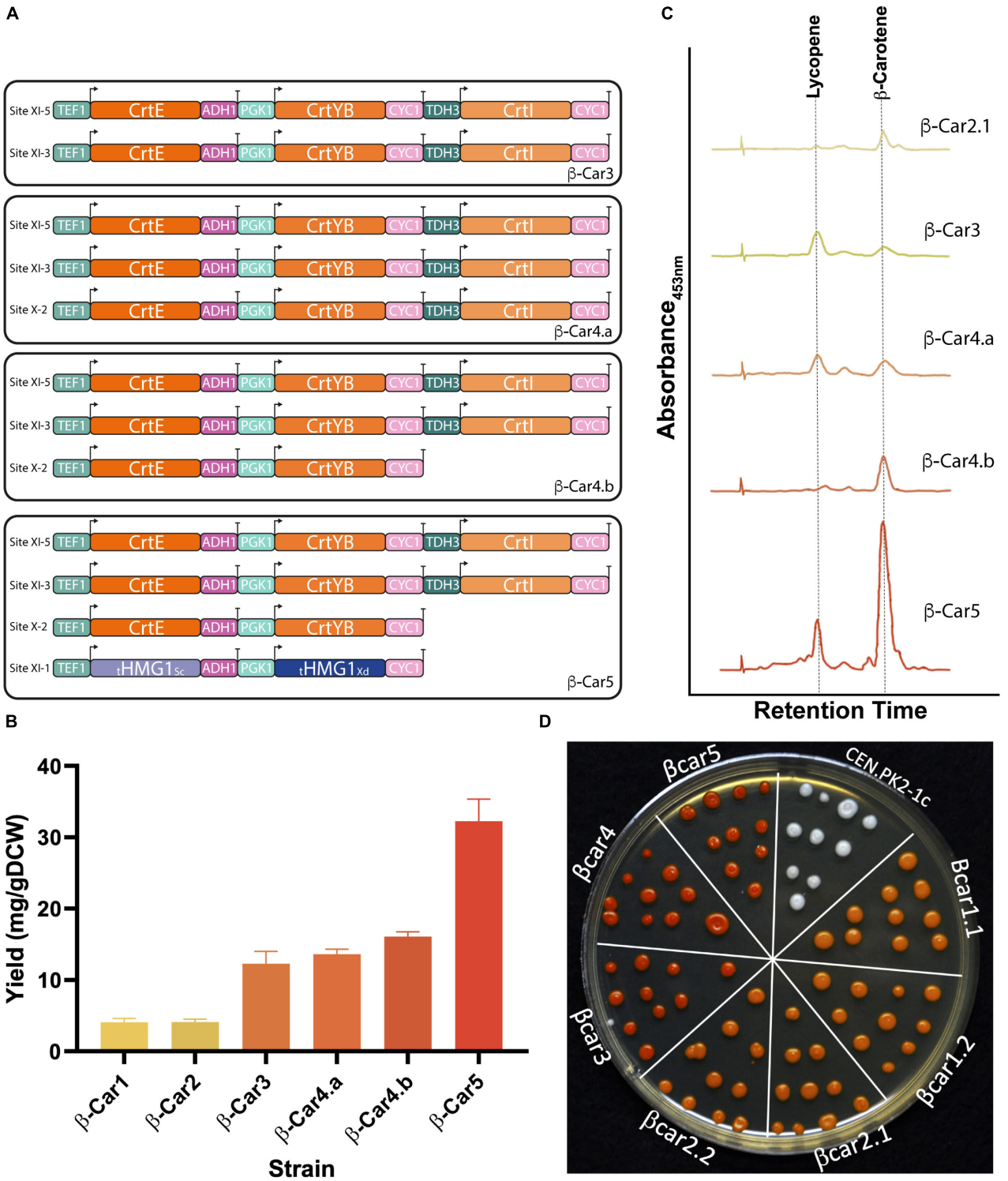

FIGURE 3 | Tuning gene dosage for high accumulation of total carotenoids and β-carotene. **(A)** Evaluation of transcriptional units with different gene dosage. **(B)** Total carotenoid yields reached by strains with different dosage of carotenogenic genes after 72 h of cultivation in shake flasks. This strategy produced an 8-fold increase from the initial yield (from 4 mg/g DCW of β-Car1, to 32 mg/g DCW of β-Car5). The presented data represents the average and standard deviation of three independent cultures. **(C)** Carotenogenic profiles measured by HPLC after 72 h of cultivation (profiles are in the same scale). **(D)** Representative colonies of the constructed strains. Cells were plated after 24 h in YPD culture and the picture was taken 48 h later.

β-Car2.1-6) displayed similar carotenoid yields, only the β-Car2.1 strain was transformed with the fyn-*Ph*CCD1 gene. Four new strains were constructed in a similar fashion, namely: β-iono2.1, β-iono3.1, β-iono4.1 and β-iono5.1, derived, respectively, from strains β-Car2.1, β-Car3, β-Car4.b, and β-Car5 (**Figure 4A**, refer to **Table 1** for details).

Overall, the more β-carotene the strain accumulates, the higher the β-ionone titer (**Figures 3B**, **4C**). For instance, the strain with the lowest total carotenoid accumulation (4 mg/gDCW in β-Car2.1) produced only 1.8 mg/L β-ionone after integration of fyn-*Ph*CCD1, whereas the strain with the highest carotenoid yield (32 mg/gDCW in β-Car5) reached 18.2 mg/L. The latter represents a 10-fold increase in the final β-ionone titer under the same culture conditions. The potential for further β-ionone production was also evaluated by measuring the residual content of carotenoids at the end of the cultivation (**Figure 4B**). The highest β-ionone (and β-carotene) producers – β-iono4.1 and β-iono5.1 – also exhibited the highest residual carotenoid content, 14.2 mg/gDCW and 26.7 mg/gDCW, respectively. Thus, there remains ample room for increasing β-ionone biosynthesis in β-iono5.1 strain, considering that approx. 18% of the total β-carotene was actually digested by the fyn-*Ph*CCD1 enzyme, according to our preliminary estimations. Finally, it is noteworthy that remnant carotenoids in these strains was mostly β-carotene, with no detectable traces of lycopene (**Supplementary Figure S1**).

Incrementing the Gene Dosage of fyn-*Ph*CCD1 Boosts β-Ionone Production in β-Carotene Hyperproducing Strains

To further increase β-ionone production, we integrated an additional copy of the fyn-*Ph*CCD1 gene in the β-iono5.1 strain, resulting the β-iono5.2 strain. The same strategy was performed in the β-iono4.1 (resulting in the β-iono4.2 strain), displaying similar results as in the case of the β-iono5.2 strain (**Supplementary Figure S2**). The β-iono5.2 strain reached a higher β-ionone titer of 26.3 mg/L compared to β-iono5.1 (18.2 mg/L, **Figure 4A**). Given that there are still significant amounts of accumulated total carotenoids, a third copy of the fyn-*Ph*CCD1 gene was integrated into the β-iono5.2 strain. The resulting β-iono5.3 strain achieved more than 33 mg/L of β-ionone, a 19-fold improvement over the initial strain (β-iono2), and the highest β-ionone-producing *S. cerevisiae* strain reported to date (**Figure 4A**). The increased production of β-ionone by the β-iono5 strains resulting from increasing the fyn-*Ph*CCD1 gene copy number can be clearly evidenced in the chromatograms for each of the latter strains (**Figure 4C**) and the aspect of the culture broth (**Figure 4D**).

Our final *S. cerevisiae* production platform achieved a similar titer than previous reports for *E. coli* in shake flask cultures (up to 32.4 mg/L of β-ionone, Zhang et al., 2018). In the latter study, the authors used high copy number plasmids – arranged in modular fashion - to increase the carbon flux through a heterologous MVA pathway, thereby increasing the flux toward β-ionone. Notably, the employed plasmids can reach up to 10 copies per cell, which exceeds the number of gene copies presented here. In order to lessen the metabolic burden imposed by the high copy plasmids and achieve high β-ionone concentrations, an inducible expression system was implemented that enabled decoupling production from growth (Zhang et al., 2018). However, such plasmids can suffer from genomic instability issues (Ryan et al., 2014) or lack of reproducibility in industrial fermentations (Rugbjerg and Sommer, 2019). In contrast, our strategy – though more conservative – is particularly robust and suited for cases where production is balanced and metabolic toxicity is not an issue. Importantly, if necessary, our platform can be readily adapted for inducible expression to decouple production from growth, and/or to down-regulate competing pathways.

Finally, we noted that both, the increase in β-ionone production and the decrease in total carotenoids accumulation, followed a nearly linear trend, which highlights that fyn-*Ph*CCD1 is likely capacity-limited, i.e., maximum catalytic rate (V_{max}) has been reached. However, the amount of β-carotene cleaved experimentally by fyn-*Ph*CCD1 does not correspond to the optimal stoichiometric amounts of produced β-ionone, i.e., 1 mol of β-carotene produces 2 mol of β-ionone. In order to gain further insights about the fate of β-carotene in β-iono strains, a genome-scale metabolic model was constructed and interrogated.

Genome-Scale Stoichiometric Analysis Suggests fyn-*Ph*CCD1 Has Highly Unspecific Cleavage Activity During β-Ionone Production

In order to better understand β-ionone production in yeast, we tailored an existing Genome-Scale Metabolic Model (GSMM) of *S. cerevisiae* for predicting the (apo)carotenoids yields for each producing strain. To this task, the curated *i*MM904 GSMM (Mo et al., 2009) was constrained for accurately representing aerobic growth with glucose as carbon source, as well as the production of the measured carotenoids. The details of the contextualization method can be found in the Methods section.

Before examining the carotenoid production profile, we evaluated the prediction power of the contextualized GSMM (**Figures 5A,B**). To this task, the GSMM was constrained to reproduce the observed biomass, β-ionone, and β-carotene yields for the different production strains (**Figures 4A,B**), and the specific growth and carbon dioxide rates reported for *S. cerevisiae* strains growing aerobically on glucose (Van Hoek et al., 1998). Using this data, the optimal (minimum) specific glucose uptake rate was computed for all the strains, and its value compared with the available experimental data (Van Hoek et al., 1998). This exercise amounts to optimize the biomass yield on glucose. Results showed excellent agreement between predictions and experimental measurements with a maximum relative error of approx. 10% (β-iono2.1 strain, **Figure 5A**), and an average deviation of approx. 3.3% (**Figure 5A**). Given these promising results, we next computed the degree of carbon recovery predicted by the GSMM using this reduced set of measurements. We note that calculation of this quantity is critical to properly interpret subsequent results about the (apo)carotenogenic production flux profile, as a low degree of closure (<80%) precludes drawing meaningful conclusions.

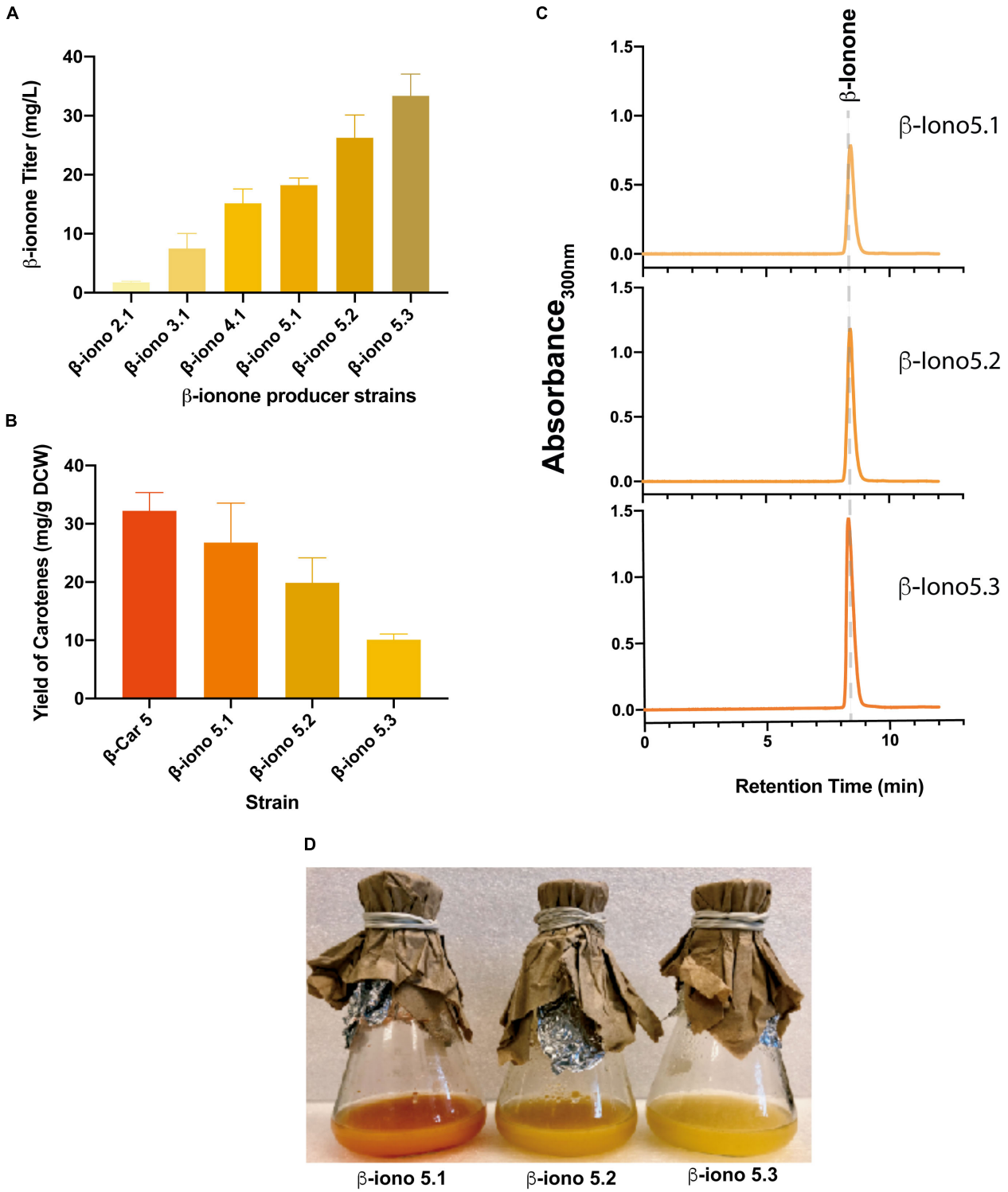

FIGURE 4 | Integration of engineered CCD1 and evaluation of the gene dosage for the production of β-ionone. **(A)** β-ionone titer correlates with higher β-carotene accumulation of the parental recombinant strains. Similarly, the increase in the gene dosage of fyn-PhCCD1 improves β-ionone titers in the same manner. **(B)** The higher the β-ionone accumulation, the lower the amount of residual carotenoids. **(C)** Chromatograms of the β-iono5 strains show increasing β-ionone titters as the fyn-*Ph*CCD1 gene copy number increases. **(D)** Shake flasks cultures of strains with increasing fyn-*Ph*CCD1 gene dosage evidence overall higher β-ionone production as the dark orange color associated to carotenoid accumulation fades.

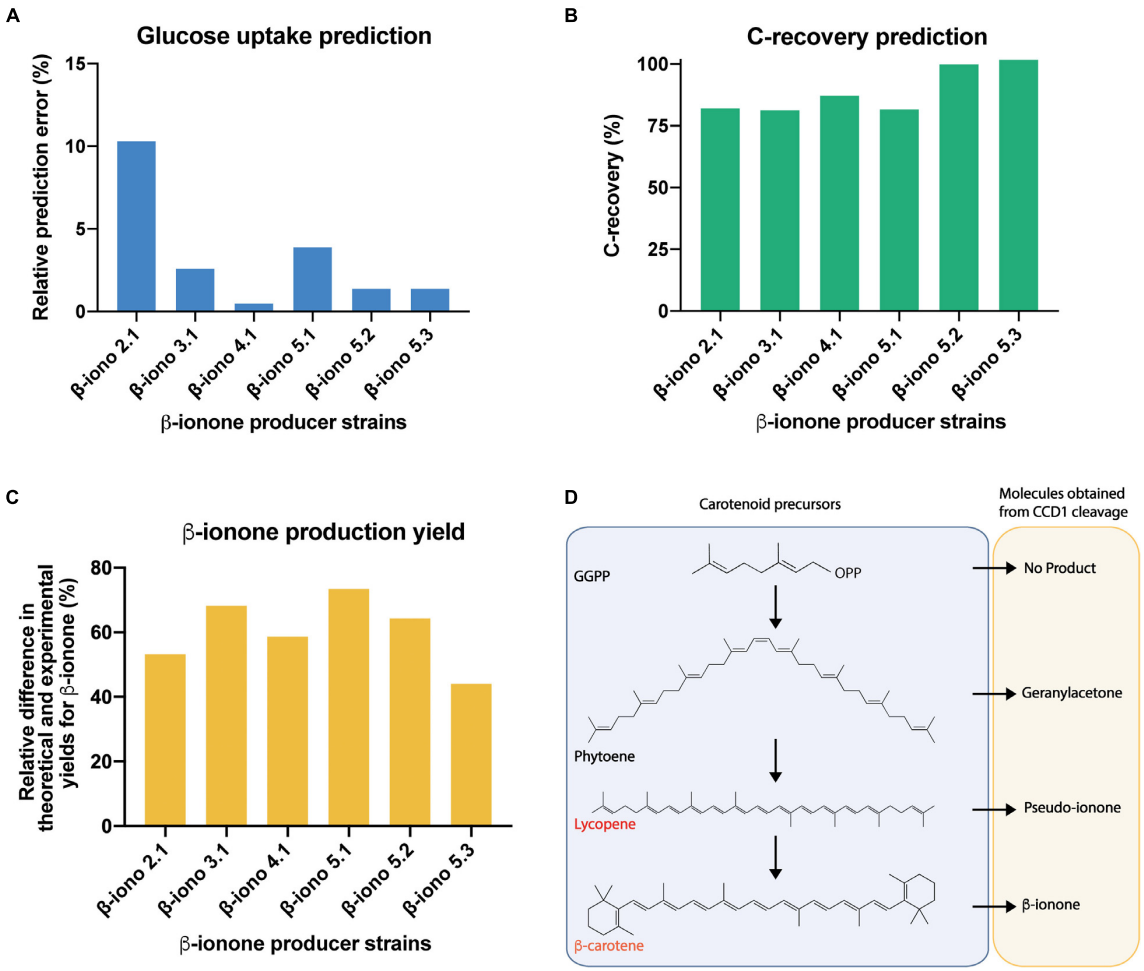

FIGURE 5 | Genome-scale stoichiometric analysis shows high degree of carbon balance closure in β-iono mutant strains and points to unspecific cleavage activity of *Ph*CCD1 for the reduced β-ionone yields observed. Evaluation of the prediction fidelity of the GSMM for optimal specific glucose uptake under culture conditions **(A)** and carbon recovery for all producer strains **(B)**. **(C)** Relative difference in the maximum predicted and experimental yield of β-ionone under conditions of high carbon balance closure. **(D)** Proposed apocarotenoids generated by the cleavage of the CCD1 enzyme on different carotenoids.

Notably, in spite of the limited amount of information, the contextualized GSMM was able to account for most of the consumed carbon by β-iono2.1, β-iono3.1, β-iono4.1, and β-iono5.1 (> 80% and up to 87% in β-iono4.1, **Figure 5B**), and in the case of the highest producers - β-iono5.2 and β-iono5.3 -, it was almost able to close the carbon balance (approx. 100% closure, **Figure 5B**).

The previous results indicated that the GSMM has a high prediction fidelity and, more importantly, it can be safely employed as a prospecting tool for gaining insights about the carbon redistribution in the β-ionone production pathway. In particular, it is of interest to determine how much of the β-carotene is cleaved and consumed by fyn-*Ph*CCD1 for producing β-ionone, relative to other possible (apo)carotenoid products. Indeed, this class of enzymes can act on multiple carotenoid substrates (e.g., ζ-carotene, γ-carotene, lycopene, β-carotene, among others) and produce several apocarotenogenesis products (e.g., geranylacetone, pseudoionone, β-ionone, among others) (Vogel et al., 2008) (see **Figure 5D**). Therefore, we used the contextualized GSMM to estimate the maximum production yield of β-ionone under the assumption that β-carotene is only being diverted to β-ionone and accumulated in the amounts observed experimentally. To this task, we calculated maximum β-carotene production under the experimental conditions, but without the requirement of β-ionone production. The difference between the theoretical and experimental β-carotene accumulation then represents the carbon that could have been allocated for achieving the maximum β-ionone yield. Lastly, we employed this quantity to constrain the carbon flux toward β-carotene formation and maximized the β-ionone yield. If all the carbon that could be allocated toward β-ionone coincides with the experimental production values, then the fyn-*Ph*CCD1 enzyme is producing β-ionone in the optimal stoichiometric amounts. This is, however, not the case for any of the β-iono strains (**Figure 5C**). Departures from the optimal β-carotene cleavage by fyn-*Ph*CCD1 range from 44% up

to 73.4%, which suggests a significant limitation in this enzyme. In fact, in the optimal scenario, fyn-*Ph*CCD1 produces the C14 compound derived from the double cleavage of β-carotene in a molar ratio ranging from 0.15 (β-iono5.1) to 0.32 (β-iono5.3) per mol of β-ionone, which is far from the optimal stoichiometric ratio of 1:2 (refer to **Supplementary File Presentation 1**). As the carbon mass balance must close, this necessarily implies that the fyn-*Ph*CCD1 is either cleaving the β-carotene at only one site and/or acting on other upstream substrates. Further experimental efforts should be then focused on measuring fyn-*Ph*CCD1 side reactions products to experimentally validate this hypothesis.

The engineered CCD1 employed in this work has indeed increased accessibility of other known lipophilic substrates for this enzyme (Werner et al., 2019), which offers support for the model suggestions. To tackle this limitation, site-directed mutagenesis may be applied to improve the selectivity and activity of *Ph*CCD1, thereby avoiding undesirable side-products, such as pseudo-ionone or geranyl acetate, and favoring ionone production. However, given the high similarity between the possible reactants and the highly conserved active site of this enzyme (Werner et al., 2019), it is likely that this strategy will be plagued with obstacles. Another plausible alternative is the fusion of key enzymes. Spatial proximity and the adequate disposition of the enzymes inside of a metabolic pathway is critical for the efficient conversion of intermediates into the final product. For instance, the CCD1 could be fused to the lycopene cyclase domain of the CrtYB, avoiding the access to other intermediates. A recent report of heterologous production of β-carotene in *S. cerevisiae* has shown promise for the optimization of carotenoids in yeast (Rabeharindranto et al., 2019).

CONCLUSION

In this work, we developed several recombinant *S. cerevisiae* strains, capable of producing increasing amounts of the apocarotenoid β-ionone and its precursor, β-carotene. To this task, we employed a systematic approach where different variables involved in the constitutive expression of recombinant genes were optimized, namely: the architecture of the heterologous transcription units, the location of the integration site, and the dosage of key genes needed for β-ionone synthesis. Our results demonstrated that high β-ionone production can be attained by implementing rational metabolic engineering strategies. Systematic assessment of the above variables led to the construction of recombinant strains capable of producing 32 mg/gDCW of total carotenoids (β-Car5), and 33 mg/L of β-ionone (β-iono5.3). While this study presents the highest β-ionone titers reported so far in *S. cerevisiae* using shake flasks cultures, there is still room for improvement. Achieving a balanced gene expression for optimal production of the heterologous pathway is critical for reaching even higher yields. Subsequent studies should be focused at fine-tuning the expression of relevant genes by directly measuring transcriptional/protein data and metabolic production performance. Another possible strategy for improving this system is the implementation of an inducible system, where the expressions of (apo)carotenogenic and competitive pathways (e.g., sterol pathway) are decoupled is a promising approach. Finally, our experimental and modeling results confirmed that β-ionone production in yeasts is limited by the CCD1 efficiency in high-accumulating β-carotene strains. Further protein engineering efforts are thus needed to increase the overall efficiency of heterologous β-ionone conversion. Fusion enzymes and enzyme redirection could be attractive strategies to tackle this obstacle.

MATERIALS AND METHODS

Genes and Plasmids

The genes used in this study were amplified by PCR from genomic DNA of *X. dendrorhous* (CrtYB, CrtE, CrtI and tHMGR1) and *S. cerevisiae* (tHMGR1). The gene coding for *fyn*-CCD1 of *P. hybrida* was kindly facilitated by Dr. Werner, where the peptide fyn and a linker were fused to the N-terminal of the full length *Ph*CDD1 gene (Werner et al., 2019). The TDH3 promoter was amplified by PCR from the episomal plasmid p426GDP.

Yeast integrating expression vectors were constructed using the Gibson Assembly method (Gibson et al., 2009) using the plasmid library developed by Mikkelsen et al. (2012). Genes and backbone vectors were PCR-amplified by Phusion High-Fidelity DNA polymerase (Thermo Scientific, Waltham, MA, United States), following the manufacturer's instructions. The resulting PCR products were purified using the Wizard SV Gel and PCR Clean-Up System kit (Madison, Wisconsin, United States). Purified DNA fragments were then mixed with 1.33x Gibson master mix (isothermal buffer, T5 exonuclease 1 U/μL, Phusion DNA polymerase 2 U/μL, and Taq DNA ligase 40 U/μL) in 10 μL of final volume and incubated for 60 min at 50°C. The reaction products were transformed in *E. coli* Top10 cells (Thermo Fisher Scientific, United States). The assembled plasmids were purified using E.Z.N.A plasmid mini Kit (Omega Bio-tek, United States) and verified by sequencing (Macrogen Inc., South Korea). Primers used for all amplifications are in **Supplementary Table S1**.

Depending on the transcriptional unit architecture, different construction workflows were employed. The bidirectional, head to head (HH), plasmid XI-5 HH YB/E was constructed as follows; pXI-5 plasmid was amplified to assemble in first place the CrtYB gene under the PGK1 promoter and CYC1 terminator. This plasmid was named XI-5 CrtYB. Then, XI-5 CrtYB was amplified to assemble the CrtE gene under TEF1 promoter and ADH1 terminator. The tandem architecture, head to tail (HT), of this last plasmid was constructed by the amplification of the transcriptional unit containing the CrtE gene, arranged in the same direction than the CrtYB gene. This plasmid was designated XI-5 HT YB/E. On the other hand, the XI-3 CrtI plasmid was built in two steps. Firstly, the TDH3 promoter was assembled into the pXI-3 plasmid, which was designated XI-3 TDH3. Then, the CrtI coding gene was inserted into the XI-3 TDH3 plasmid.

Finally, for the construction of XI-5 HT tHSc/tHXd and HT YB/E/I plasmids, the XI-5 HT YB/E was used as backbone. For XI-5 HT tHSc/tHXd, the XI-5 HT YB/E plasmid was used to assemble the coding gene tHMG1R of *X. dendrorhous* (under PGK1 promoter). This plasmid was named XI-5 HT tHXd/E. The latter was then amplified for inserting the coding gene tHMG1R from *S. cerevisiae* (under TEF1 promoter). For the construction of the HT YB/E/I plasmid, the XI-5 HT YB/E plasmid was opened by PCR and the transcriptional unit XI-3 CrtI amplified and assembled into the open plasmid XI-5 HT YB/E. The XI-3 CCD1 plasmid was constructed by replacing the CrtI gene of the XI-3 CrtI plasmid by the PhCCD1 gene. For the construction of the HT tHSc/tHXd/CCD1 plasmid, transcription units of the CrtYB and CrtE genes HT YB/E/I was replaced by the tHSc/tHXd construct from the XI-5 HT tHSc/tHXd plasmid. This yielded the HT tHSc/tHXd/I plasmid. In this plasmid, the CrtI gene was replaced with the *Ph*CCD1 gene from XI-3 CCD1 plasmid.

Yeast Strains Construction

The CEN.PK2-1c parental strain (MATa, *ura3-52 trp1-289 leu2-3, 112his3*Δ) was used in this study. The constructed strains are listed in **Table 1**. These strains were built using CRISPR/Cas9 method, following the protocol from Tom Ellis lab, which is freely available on the Benchling webpage[1]. The plasmids used in this study are available on Addgene, whereas the gRNAs were obtained from the USER library (**Supplementary Table S2**).

The β-Car strains were transformed following the same protocol, but using different integration constructs and primers, depending on the transcriptional architecture. In the following, the β-Car1 protocol is described for illustration. The protocol details for remaining β-Car strains can be found in **Supplementary Table S1**. The β-Car1 strain was built by the amplification of the XI-5 HH YB/E vector with the primers p1/p2 to be integrated on the pXI-5 locus of the CEN.PK strain. All the DNA fragments obtained by PCR had 40 bp homology to ensure integration into the genome. PCR protocols and product purification were executed as described before for plasmid construction. The transformants were selected using SC-URA plates (1.8 g/L yeast nitrogen base, 5 g/L ammonium sulfate, 0.8 g/L CSM-Ura mixture, 20 g/L of glucose, and 20 g/L of Bacto-agar). Only colored colonies were isolated and grown on YPD plates (1% yeast extract, 2% peptone, 2% glucose, and 1% Bacto-agar). One of the transformants was transformed with the XI-3 CrtI vector, which was amplified using primers p3/p4, to be integrated into the pXI-3 locus. The transformants were selected on SC-LEU (1.8 g/L yeast nitrogen base, 5 g/L ammonium sulfate, 0.8 g/L CSM-Leu mixture, 20 g/L of glucose, and 20 g/L of Bacto-agar). The correct integration into the pXI-3 locus was verified using primers for XI3F/XI3R. The positives colonies were grown on YPD plates.

Initial β-iono strains (2, 3, 4b, and 5) were generated by transformation of the corresponding β-Car strains. To this task, the XI-3 CCD1 plasmid was amplified using primers p9/p10 and integrated into the pXI-2 locus. The transformants were selected on SC-URA plates and positive colonies were grown on YPD plates. Correct cassette integration was verified by PCR using primers XI2F/XI2R. β-iono4.1 and β-iono5.1 strains were constructed by transformation of the β-Car4 and β-Car5 strains with the XI-3 CCD1 plasmid amplified using primers p11/p12 and integrated into the pX-4 locus. Transformants were selected on SC-LEU plates and positives colonies were grown on YPD plates. As before, PCR was performed to verify correct integration into the locus using primers X4F/X4R. Finally, the β-Iono5.1 strain was transformed with HT tHSc/tHxd/CCD1, which replaced the construct HT tHSc/tHXd on locus pXI-1. This yielded the β-iono5.2 strain, which was selected for positive transformants on SC-HIS (1.8 g/L yeast nitrogen base, 5 g/L ammonium sulfate, 0.8 g/L CSM-His mixture, 20 g/L of glucose, and 20 g/L of Bacto-agar). Again, correct integration was verified by PCR using primers CCD1F/XI1R.

Growth Conditions

Single colonies were inoculated in 3 mL pre-cultures in YPD medium (1% yeast extract, 2% peptone and 2% glucose). β-carotene-producing strains were grown in 250-mL shake flask cultures at 30°C and 170 rpm in a horizontal shaker with 20 mL of YPD medium. In the case of β-ionone producing strains, cultures were grown with 18 mL of YPD medium and a dodecane phase (10%v/v). All shake flask cultures were inoculated from pre-cultures to an initial OD_{600} of 0.1 (0.04 gDCW/L).

β-Ionone Quantification

Cultures were centrifuged for 10 min at 6000 rpm on 50-mL tubes. The organic phase was collected in 500-μL glass vials for subsequent analysis. β-ionone quantification was performed by HPLC LaChrom (Merk-Hitachi) coupled to a diode array detector, using a C30 YMC Carotenoid column (5 μm, 150 × 10 mm) (YMC, Japan). A mobile phase of 2-propanol with a 1 mL/min flow under isocratic condition was employed for elution. β-ionone was detected at 330 nm and 8.39 min retention time. Concentrations of β-ionone were estimated using a calibration curve with external standards with 12 to 378 mg/L linear range (refer to **Supplementary Figure S3** for more details).

Total Carotenoids Extraction and Profile Analysis

Carotenoid extraction was carried out after 72 h of cultivation. 250 μL of culture were centrifuged for 1 min at 13,000 rpm, the supernatant was discarded, and cell pellets broken with 500 μL of 0.5-mm glass beads with 1 mL dodecane in a homogenizer (Benchmark Scientific, NJ, United States) using 5 cycles of 90 s at 3,500 rpm. The cell-beads mixture was then centrifuged at 13,000 rpm for 2 min, and total carotenoids in the dodecane phase were quantified by spectrophotometry (Thermo Fisher, Waltham, MA, United States) at 453 nm. Total carotenoid concentration was estimated using a calibration curve of pure β-carotene (Carotenature, Switzerland), with 1 to 6 mg/L linear range. Samples above this range were diluted appropriately.

For determination of the carotene profile, the previous protocol was executed, but instead of dodecane, cells were broken

[1]https://benchling.com/pub/ellis-crispr-tools

using 1 mL of acetone. Carotenoids were then separated by RP-HPLC using a reverse phase RP18 column (5 μm, 4.6 × 125 mm) (Merck, Darmstadt, Germany). A mixture of acetonitrile:methanol:isopropyl (85:10:5 v/v) was employed as mobile phase with a 0.5 mL/min flow under isocratic conditions. The elusion spectrum was recovered using a diode array detector.

Genome-Scale Stoichiometric Analysis

To probe β-ionone production in yeast, an existing Genome-Scale Metabolic Model (GSMM) of *S. cerevisiae* was contextualized for predicting the different (apo)carotenoids production of the engineered strains. To this task, the curated *i*MM904 GSMM (Mo et al., 2009) was constrained following recent guidelines for accurately describing aerobic growth with glucose as sole carbon source in yeasts (Pereira et al., 2016; Torres et al., 2019). Stoichiometric calculations were performed using constrained-based methods from COBRA Toolbox v3.0 (Heirendt et al., 2019) within the MATLAB 2017a environment (The MathWorks, Natick, MA). The model and employed scripts are available in the **Supplementary File Presentation 1**.

DATA AVAILABILITY STATEMENT

All datasets presented in this study are included in the article/**Supplementary Material**.

AUTHOR CONTRIBUTIONS

JL and DB constructed the strains and performed shake flask cultures. CC developed the methods for the quantification of carotenoids and apocarotenoids and analyzed the results. JL, DB, and NA constructed the plasmid library used in this study. PAS developed the genome-scale metabolic model used for the apocarotenoid analysis. JL, DB, and PAS participated in the design, coordination of the study, and draft of the manuscript. EA supervised the whole research and revised the manuscript. All authors read and approved the final manuscript.

FUNDING

This work was funded by Fondecyt grant no. 1170745.

ACKNOWLEDGMENTS

We are grateful to Gabriela Diaz and Vasni Zavaleta for their skillful technical contributions to this work.

SUPPLEMENTARY MATERIAL

The Supplementary Material for this article can be found online at: https://www.frontiersin.org/articles/10.3389/fbioe.2020.578793/full#supplementary-material

REFERENCES

Amen, T., and Kaganovich, D. (2017). Integrative modules for efficient genome engineering in yeast. *Microbial. Cell* (Graz, Austria) 4, 182–190. doi: 10.15698/mic2017.06.576

Beekwilder, J., Van Rossum, H. M., Koopman, F., Sonntag, F., Buchhaupt, M., Schrader, J., et al. (2014). Polycistronic expression of a β-carotene biosynthetic pathway in *Saccharomyces cerevisiae* coupled to β-ionone production. *J. Biotechnol.* 192(Pt B), 383–392.

Carquet, M., Pompon, D., and Truan, G. (2015). Transcription interference and ORF nature strongly affect promoter strength in a reconstituted metabolic pathway. *Front. Bioeng. Biotechnol.* 3:21. doi: 10.3389/fbioe.2015.00021

Chen, X., Shukal, S., and Zhang, C. (2019). Integrating enzyme and metabolic engineering tools for enhanced α-Ionone production. *J. Agricul. Food Chem.* 67, 13451–13459.

Czajka, J. J., Nathenson, J. A., Benites, V. T., Baidoo, E. E. K., Cheng, Q., Wang, Y., et al. (2018). Engineering the oleaginous yeast *Yarrowia lipolytica* to produce the aroma compound β-ionone. *Microbial. Cell Fact.* 17:136.

Flagfeldt, D. B., Siewers, V., Huang, L., and Nielsen, J. (2009). Characterization of chromosomal integration sites for heterologous gene expression in *Saccharomyces cerevisiae*. *Yeast* 26, 545–551.

Floss, D. S., and Walter, M. H. (2009). Role of carotenoid cleavage dioxygenase 1 (CCD1) in apocarotenoid biogenesis revisited. *Plant Signal. Behav.* 4, 172–175.

Gibson, D. G., Young, L., Chuang, R.-Y., Venter, J. C., Hutchison Iii, C. A., and Smith, H. O. (2009). Enzymatic assembly of DNA molecules up to several hundred kilobases. *Nat. Methods* 6, 343–345.

Harrison, P. J., and Bugg, T. D. (2014). Enzymology of the carotenoid cleavage dioxygenases: reaction mechanisms, inhibition and biochemical roles. *Arch. Biochem. Biophys.* 544, 105–111.

Heirendt, L., Arreckx, S., Pfau, T., Mendoza, S. N., Richelle, A., Heinken, A., et al. (2019). Creation and analysis of biochemical constraint-based models using the COBRA Toolbox v.3.0. *Nat. Protocols* 14, 639–702.

Jensen, N. B., Strucko, T., Kildegaard, K. R., David, F., Maury, J., Mortensen, U. H., et al. (2014). EasyClone: method for iterative chromosomal integration of multiple genes in *Saccharomyces cerevisiae*. *FEMS Yeast Res.* 14, 238–248.

Jessop-Fabre, M. M., Jakoèiûnas, T., Stovicek, V., Dai, Z., Jensen, M. K., Keasling, J. D., et al. (2016). EasyClone-MarkerFree: a vector toolkit for marker-less integration of genes into Saccharomyces cerevisiae via CRISPR-Cas9. *Biotechnol. J.* 11, 1110–1117.

Kampranis, S. C., and Makris, A. M. (2012). Developing a yeast cell factory for the production of terpenoids. *Comput. Struct. Biotechnol. J.* 3:e201210006.

Li, J., Shen, J., Sun, Z., Li, J., Li, C., Li, X., et al. (2017). Discovery of several novel targets that enhance β-Carotene production in *Saccharomyces cerevisiae*. *Front. Microbiol.* 8:1116. doi: 10.3389/fmicb.2017.01116

Li, Q., Sun, Z., Li, J., and Zhang, Y. (2013). Enhancing beta-carotene production in *Saccharomyces cerevisiae* by metabolic engineering. *FEMS Microbiol. Lett.* 345, 94–101.

López, J., Cataldo, V. F., Peña, M., Saa, P. A., Saitua, F., Ibaceta, M., et al. (2019). Build your bioprocess on a solid strain—β-Carotene production in recombinant *Saccharomyces cerevisiae*. *Front. Bioeng. Biotechnol.* 7:171. doi: 10.3389/fbioe.2019.00171

López, J., Essus, K., Kim, I.-K., Pereira, R., Herzog, J., Siewers, V., et al. (2015). Production of β-ionone by combined expression of carotenogenic and plant CCD1 genes in *Saccharomyces cerevisiae*. *Microbial. Cell Fact.* 14:84.

Mikkelsen, M. D., Buron, L. D., Salomonsen, B., Olsen, C. E., Hansen, B. G., Mortensen, U. H., et al. (2012). Microbial production of indolylglucosinolate through engineering of a multi-gene pathway in a versatile yeast expression platform. *Metab Eng.* 14, 104–111.

Mo, M. L., Palsson, B. O., and Herrgard, M. J. (2009). Connecting extracellular metabolomic measurements to intracellular flux states in yeast. *Bmc Systems Biol.* 3:37. doi: 10.1186/1752-0509-3-37

Olson, M. L., Johnson, J., Carswell, W. F., Reyes, L. H., Senger, R. S., and Kao, K. C. (2016). Characterization of an evolved carotenoids hyper-producer

of *Saccharomyces cerevisiae* through bioreactor parameter optimization and Raman spectroscopy. *J. Ind. Microbiol. Biotechnol.* 43, 1355–1363.

Partow, S., Siewers, V., Bjørn, S., Nielsen, J., and Maury, J. (2010). Characterization of different promoters for designing a new expression vector in *Saccharomyces cerevisiae*. *Yeast* 27, 955–964.

Pereira, R., Nielsen, J., and Rocha, I. (2016). Improving the flux distributions simulated with genome-scale metabolic models of *Saccharomyces cerevisiae*. *Metab Eng. Commun.* 3, 153–163.

Rabeharindranto, H., Castaño-Cerezo, S., Lautier, T., Garcia-Alles, L. F., Treitz, C., Tholey, A., et al. (2019). Enzyme-fusion strategies for redirecting and improving carotenoid synthesis in S. *cerevisiae*. *Metab. Eng. Commun.* 8:e00086.

Reyes, L. H., Gomez, J. M., and Kao, K. C. (2014). Improving carotenoids production in yeast via adaptive laboratory evolution. *Metab. Eng.* 21, 26–33.

Rugbjerg, P., and Sommer, M. O. A. (2019). Overcoming genetic heterogeneity in industrial fermentations. *Nat. Biotechnol.* 37, 869–876.

Ryan, O. W., Skerker, J. M., Maurer, M. J., Li, X., Tsai, J. C., Poddar, S., et al. (2014). Selection of chromosomal DNA libraries using a multiplex CRISPR system. *eLife* 3:e03703.

Shi, S., Liang, Y., Zhang, M. M., Ang, E. L., and Zhao, H. (2016). A highly efficient single-step, markerless strategy for multi-copy chromosomal integration of large biochemical pathways in *Saccharomyces cerevisiae*. *Metab. Eng.* 33, 19–27.

Shimada, H., Kondo, K., Fraser, P. D., Miura, Y., Saito, T., and Misawa, N. (1998). Increased carotenoid production by the food yeast candida utilis through metabolic engineering of the isoprenoid pathway. *Appl. Environ. Microbiol.* 64, 2676–2680.

Sui, X., Kiser, P. D., Lintig, J., and Palczewski, K. (2013). Structural basis of carotenoid cleavage: from bacteria to mammals. *Arch. Biochem. Biophys.* 539, 203–213. doi: 10.1016/j.abb.2013.06.012

Torres, P., Saa, P. A., Albiol, J., Ferrer, P., and Agosin, E. (2019). Contextualized genome-scale model unveils high-order metabolic effects of the specific growth rate and oxygenation level in recombinant Pichia pastoris. *Metab. Eng. Commun.* 9:e00103. doi: 10.1016/j.mec.2019.e00103

Van Hoek, P., Van Dijken, J. P., and Pronk, J. T. (1998). Effect of specific growth rate on fermentative capacity of baker's yeast. *Appl. Environ. Microbiol.* 64, 4226–4233. doi: 10.1128/AEM.64.11.4226-4233.1998

Verwaal, R., Wang, J., Meijnen, J.-P., Visser, H., Sandmann, G., Van Den Berg, J. A., et al. (2007). High-Level production of beta-carotene in *Saccharomyces cerevisiae* by Successive Transformation with carotenogenic genes from Xanthophyllomyces dendrorhous. *Appl. Environ. Microbiol.* 73:4342–4350. doi: 10.1128/AEM.02759-06

Vogel, J. T., Tan, B.-C., Mccarty, D. R., and Klee, H. J. (2008). the carotenoid cleavage dioxygenase 1 enzyme has broad substrate specificity, cleaving multiple carotenoids at two different bond positions. *J. Biol. Chem.* 283, 11364–11373. doi: 10.1074/jbc.M710106200

Vogel, J. T., Tieman, D. M., Sims, C. A., Odabasi, A. Z., Clark, D. G., and Klee, H. J. (2010). Carotenoid content impacts flavor acceptability in tomato (*Solanum lycopersicum*). *J. Sci. Food Agricul.* 90, 2233–2240.

Wang, G. Y., and Keasling, J. D. (2002). Amplification of HMG-CoA reductase production enhances carotenoid accumulation in *Neurospora crassa*. *Metab. Eng.* 4, 193–201. doi: 10.1006/mben.2002.0225

Werner, N., Ramirez-Sarmiento, C. A., and Agosin, E. (2019). Protein engineering of carotenoid cleavage dioxygenases to optimize β-ionone biosynthesis in yeast cell factories. *Food Chem.* 299:125089. doi: 10.1016/j.foodchem.2019.125089

Westfall, P. J., Pitera, D. J., Lenihan, J. R., Eng, D., Woolard, F. X., Regentin, R., et al. (2012). Production of amorphadiene in yeast, and its conversion to dihydroartemisinic acid, precursor to the antimalarial agent artemisinin. *Proc. Natl. Acad. Sci.U.S.A.* 109, E111–E118.

Xie, W., Lv, X., Ye, L., Zhou, P., and Yu, H. (2015a). Construction of lycopene-overproducing *Saccharomyces cerevisiae* by combining directed evolution and metabolic engineering. *Metab. Eng.* 30, 69–78. doi: 10.1016/j.ymben.2015.04.009

Xie, W., Ye, L., Lv, X., Xu, H., and Yu, H. (2015b). Sequential control of biosynthetic pathways for balanced utilization of metabolic intermediates in *Saccharomyces cerevisiae*. *Metab. Eng.* 28, 8–18.

Yamano, S., Ishii, T., Nakagawa, M., Ikenaga, H., and Misawa, N. (1994). Metabolic engineering for production of β-carotene and lycopene in *Saccharomyces cerevisiae*. *Biosci. Biotechnol. Biochem.* 58, 1112–1114.

Ye, L., Zhu, X., Wu, T., Wang, W., Zhao, D., Bi, C., et al. (2018). Optimizing the localization of astaxanthin enzymes for improved productivity. *Biotechnol. Biofuels* 11:278.

Zhang, C., Chen, X., Lindley, N. D., and Too, H. P. (2018). A "plug-n-play" modular metabolic system for the production of apocarotenoids. *Biotechnol. Bioeng.* 115, 174–183. doi: 10.1002/bit.26462

Zhao, X., Shi, F., and Zhan, W. (2015). Overexpression of ZWF1 and POS5 improves carotenoid biosynthesis in recombinant *Saccharomyces cerevisiae*. *Lett. Appl. Microbiol.* 61, 354–360. doi: 10.1111/lam.12463

Conflict of Interest: JL was employed by the company DICTUC S.A. EA is an advisor for DICTUC S.A.

The remaining authors declare that the research was conducted in the absence of any commercial or financial relationships that could be construed as a potential conflict of interest.

frontiers in Bioengineering and Biotechnology

ORIGINAL RESEARCH
published: 06 October 2020
doi: 10.3389/fbioe.2020.585935

Engineering an Alcohol-Forming Fatty Acyl-CoA Reductase for Aldehyde and Hydrocarbon Biosynthesis in *Saccharomyces cerevisiae*

Jee Loon Foo[1,2†], Bahareh Haji Rasouliha[1,2†], Adelia Vicanatalita Susanto[1,2], Susanna Su Jan Leong[1,2,3] and Matthew Wook Chang[1,2]*

[1] Department of Biochemistry, Yong Loo Lin School of Medicine, National University of Singapore, Singapore, Singapore, [2] NUS Synthetic Biology for Clinical and Technological Innovation (SynCTI), National University of Singapore, Singapore, Singapore, [3] Singapore Institute of Technology, Singapore, Singapore

OPEN ACCESS

Edited by:
Rodrigo Ledesma-Amaro, Imperial College London, United Kingdom

Reviewed by:
Guokun Wang, Technical University of Denmark, Denmark
Zihe Liu, Beijing University of Chemical Technology, China

***Correspondence:**
Matthew Wook Chang
bchcmw@nus.edu.sg

† These authors have contributed equally to this work

Specialty section:
This article was submitted to Synthetic Biology, a section of the journal Frontiers in Bioengineering and Biotechnology

Received: 22 July 2020
Accepted: 08 September 2020
Published: 06 October 2020

Citation:
Foo JL, Rasouliha BH, Susanto AV, Leong SSJ and Chang MW (2020) Engineering an Alcohol-Forming Fatty Acyl-CoA Reductase for Aldehyde and Hydrocarbon Biosynthesis in Saccharomyces cerevisiae. Front. Bioeng. Biotechnol. 8:585935. doi: 10.3389/fbioe.2020.585935

Aldehydes are a class of highly versatile chemicals that can undergo a wide range of chemical reactions and are in high demand as starting materials for chemical manufacturing. Biologically, fatty aldehydes can be produced from fatty acyl-CoA by the action of fatty acyl-CoA reductases. The aldehydes produced can be further converted enzymatically to other valuable derivatives. Thus, metabolic engineering of microorganisms for biosynthesizing aldehydes and their derivatives could provide an economical and sustainable platform for key aldehyde precursor production and subsequent conversion to various value-added chemicals. *Saccharomyces cerevisiae* is an excellent host for this purpose because it is a robust organism that has been used extensively for industrial biochemical production. However, fatty acyl-CoA-dependent aldehyde-forming enzymes expressed in *S. cerevisiae* thus far have extremely low activities, hence limiting direct utilization of fatty acyl-CoA as substrate for aldehyde biosynthesis. Toward overcoming this challenge, we successfully engineered an alcohol-forming fatty acyl-CoA reductase for aldehyde production through rational design. We further improved aldehyde production through strain engineering by deleting competing pathways and increasing substrate availability. Subsequently, we demonstrated alkane and alkene production as one of the many possible applications of the aldehyde-producing strain. Overall, by protein engineering of a fatty acyl-CoA reductase to alter its activity and metabolic engineering of *S. cerevisiae*, we generated strains with the highest reported cytosolic aliphatic aldehyde and alkane/alkene production to date in *S. cerevisiae* from fatty acyl-CoA.

Keywords: synthetic biology, metabolic engineering, protein engineering, *de novo* biosynthesis, biofuels, aldehydes

INTRODUCTION

Fatty aldehydes are a class of compounds with a wide range of applications, such as fragrances and flavorings (Kohlpaintner et al., 2013). Importantly, due to the reactivity of the carbonyl functional group, they are versatile chemicals that can undergo a wide range of reactions, including oxidation, reduction, addition, imination, and amination (Murray, 2019). Therefore, fatty aldehydes can be converted to a gamut of compounds and are important precursors in the chemical manufacturing industry (Kohlpaintner et al., 2013; Murray, 2019). Conventionally, fatty aldehydes and their derivatives are synthesized chemically from fossil resources, which require harsh conditions and expensive and/or toxic catalysts (Kohlpaintner et al., 2013). Alternatively, fatty aldehydes can be biosynthesized under ambient conditions from fatty acids or their acyl-CoA forms via enzymatic reactions in biological systems (Reiser and Somerville, 1997; Koeduka et al., 2002; Schirmer et al., 2010; Akhtar et al., 2013). The aldehydes could also serve as precursors to concurrently produce their derivatives *in vivo* via other metabolic pathways (Schirmer et al., 2010; Jin et al., 2016; Ladkau et al., 2016). Thus, metabolic engineering of microorganisms for biosynthesizing fatty aldehydes could provide a platform for sustainable and economical production of aldehydes from renewable resources. By introducing synthetic metabolic pathways, the aldehydes formed could also serve as substrates for conversion to a variety of valuable chemicals.

Initial successes in microbial fatty aldehyde bioproduction were achieved in *Escherichia coli* by employing fatty acyl-CoA reductase (FACR) or fatty acyl-(acyl-carrier-protein) (ACP) reductase (FAAR) to transform endogenous fatty acyl-CoAs and/or fatty acyl-A CPs to aldehydes (Reiser and Somerville, 1997; Schirmer et al., 2010). The aldehyde-producing microbes were applied in the context of biofuel production, as aliphatic and olefinic aldehydes can be transformed by aldehyde deformylating oxygenases (ADOs) or aldehyde decarbonylases (ADs) into alkanes and alkenes (ALKs) (Schirmer et al., 2010; Marsh and Waugh, 2013), which are ideal biofuel candidates since they are major components in fossil fuels and have high energy density. Subsequently, there was much interest in employing similar fatty acyl-CoA-dependent pathways for fatty aldehyde and ALK production in the model yeast *Saccharomyces cerevisiae* because it is a robust industrial host able to withstand harsh fermentation conditions and does not succumb to phage contamination (Hong and Nielsen, 2012; Foo et al., 2017). However, due to the poor activity of the aldehyde-forming FAARs and FACRs when used in the yeast strain (Buijs et al., 2014; Zhou et al., 2016b), fatty aldehyde production levels in *S. cerevisiae* were extremely low, leading to mediocre ALK production titers compared with those achieved in *E. coli* (Choi and Lee, 2013). Consequently, free fatty acid (FFA)-dependent pathways were preferred for fatty aldehyde and ALK production in *S. cerevisiae* because carboxylic acid reductase (CAR) and fatty acid α-dioxygenase (DOX) show higher activity in *S. cerevisiae* and produced more aldehydes as substrates for conversion to ALKs (Zhou et al., 2016b; Foo et al., 2017).

In this work, we sought to generate a catalytically efficient aldehyde-forming FACR to re-establish the feasibility of *de novo* fatty acyl-CoA-dependent ALK biosynthesis pathway in *S. cerevisiae* due to the merits of utilizing fatty acyl-CoAs as substrates. First, fatty acyl-CoA is readily available in *S. cerevisiae* for utilization in fatty acyl-CoA-dependent pathways without the need to overexpress thioesterases and delete fatty acyl-CoA synthetases to accumulate FFAs, which are required when implementing FFA-dependent pathways (Runguphan and Keasling, 2014). Second, the coenzyme A moiety is hydrophilic and possesses both acidic and basic functional groups. Therefore, fatty acyl-CoAs are much more soluble over a wider range of pH to serve as substrates than FFAs (Forneris and Mattevi, 2008), which are soluble only at high pH. Third, fatty acyl-CoAs are intracellular, while FFAs upon formation can diffuse or be transported out of the cells, often resulting in under-utilization of FFAs and resource wastage due to challenges in transporting extracellular FFAs back into the cells (Teixeira et al., 2017). Although no catalytically efficient aldehyde-forming FACR has been identified for application in *S. cerevisiae*, high levels of fatty alcohols have been produced in *S. cerevisiae* using heterologous alcohol-forming FACRs (Runguphan and Keasling, 2014; Feng et al., 2015; Zhou et al., 2016a). Hence, we aim to repurpose alcohol-forming FACR for aldehyde production by protein engineering.

Alcohol-forming FACRs possess two reductase functions: one for reduction of fatty acyl-CoAs to aldehydes and another for subsequent reduction of aldehydes to alcohols. Although many of these FACRs have only one active site for both reductase functions (Hellenbrand et al., 2011), an alcohol-forming FACR from *Marinobacter aquaeolei* VT8, maFACR, was predicted to have two distinct domains, each putatively performing one reductase function (Willis et al., 2011; **Figure 1A**). Moreover, functional expression of maFACR in *S. cerevisiae* has been reported for fatty alcohol production (d'Espaux et al., 2017). Therefore, maFACR is a good candidate for rational engineering into an aldehyde-forming FACR by inactivating the domain that reduces aldehyde to alcohol (**Figure 1B**). Herein, we described identification of the catalytic residues of maFACR and verification of the two domains' functions. Subsequently, maFACR was engineered into an aldehyde-forming FACR by inactivating the aldehyde reductase domain through mutation of the corresponding catalytic residues. *In vivo* production of aldehyde in *S. cerevisiae* was demonstrated using the engineered maFACR, and the production host was optimized to improve the aldehyde titer by increasing fatty acyl-CoA availability and deleting competing pathways. To exemplify application of the engineered maFACR for pathway construction in *S. cerevisiae*, the engineered maFACR was co-expressed with a cyanobacterial ADO (cADO) to achieve *de novo* production of ALK (**Figure 1C**). Upon optimization of the culture condition and expression system, we attained the highest reported cytosolic production of fatty aldehyde and ALK from fatty acyl-CoA in *S. cerevisiae* reported to date.

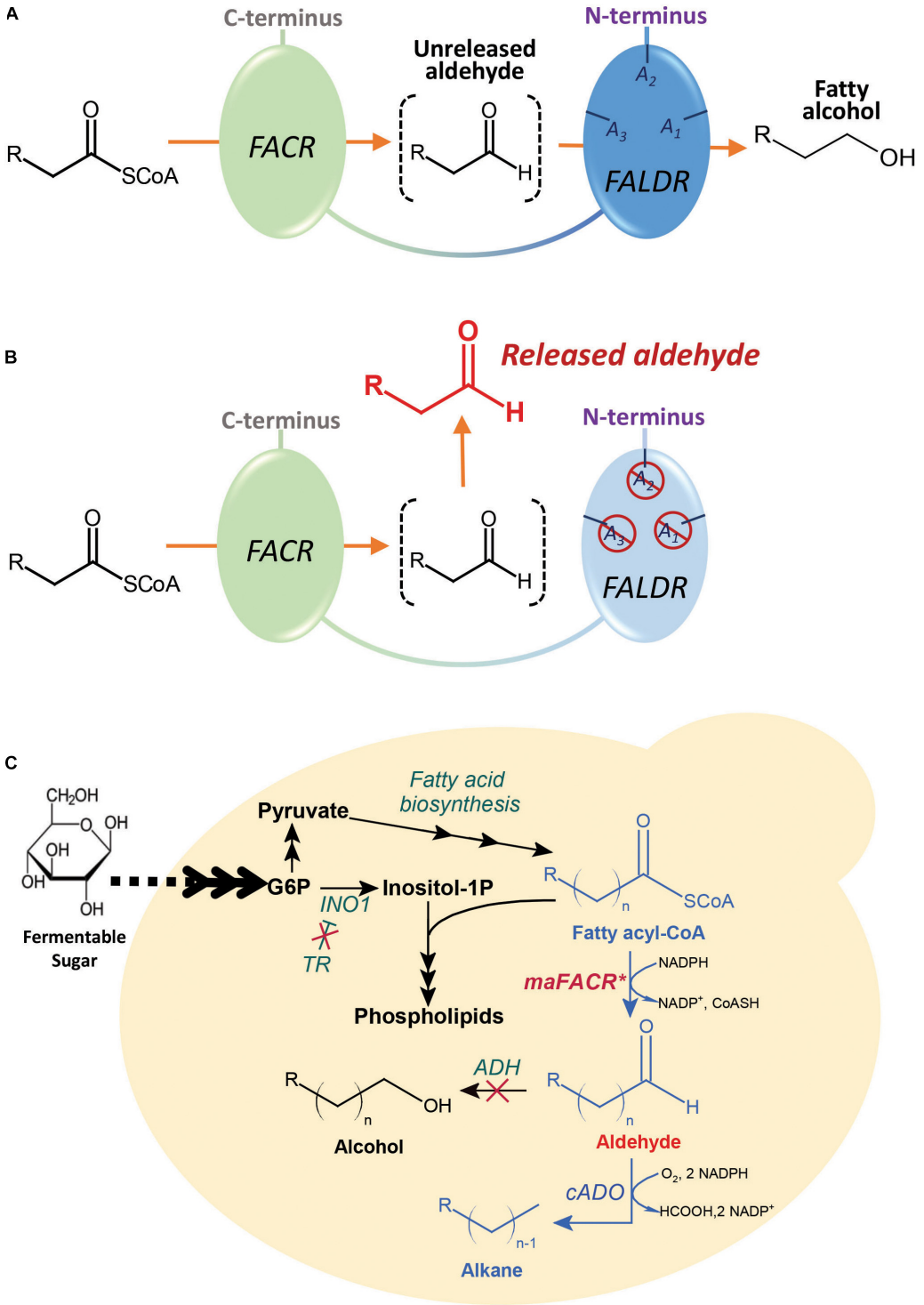

FIGURE 1 | Schematic illustration of the maFACR engineering strategy and metabolic pathway for the fatty acyl-CoA-dependent production of alkanes and alkenes (ALKs) in engineered *Saccharomyces cerevisiae*. **(A)** maFACR converts fatty acyl-CoA to alcohol without releasing the aldehyde intermediate. It putatively has two distinct domains: a fatty acyl-CoA reductase (FACR) domain for reducing fatty acyl-CoA to aldehyde and a fatty aldehyde reductase (FALDR) domain to reduce aldehyde to fatty alcohol. The FALDR domain has catalytic residues A1, A2, and A3, which are found in this work to be Ser126, Tyr152, and Lys156, respectively. **(B)** Mutating the FALDR catalytic residues A1, A2, and A3 with the S126D, Y152F, and K156A modifications, respectively, inactivates the domain, thus allowing the release of aldehyde from the enzyme. **(C)** The engineered aldehyde-forming maFACR* is employed for conversion of endogenous fatty acyl-CoAs to aldehydes in *S. cerevisiae* and subsequent production of ALKs by deformylation of the aldehydes with cADO. To improve aldehyde titer, a transcription regulator (TR) was deleted to increase fatty acyl-CoA production, and ADHs were inactivated to diminish reduction of aldehydes to alcohols. *INO1*, inositol-3-phosphate synthase.

MATERIALS AND METHODS

Strains, Oligonucleotides, Chemicals, and Culture Media

Saccharomyces cerevisiae BY4741 [American Type Culture Collection (ATCC)] was used to construct the yeast strains in this study. *Escherichia coli* TOP10 (Invitrogen) and Rosetta 2(DE3) (Novagen) were used for plasmid propagation, and protein expression and purification, respectively. Yeast extract, peptone, and tryptone were procured from BD Biosciences (Singapore). Molecular biology reagents were purchased from New England Biolabs (Singapore). Plasmids were isolated using QIAprep Spin Miniprep Kit (Qiagen). PCR purification and DNA gel extraction were performed with Wizard SV Gel and PCR Clean-Up System (Promega). The genes for maFACR [National Center for Biotechnology Information (NCBI) Protein ID: WP_011785966.1] from *Marinobacter aquaeolei* VT8 and cADO from *Synechococcus* elongatus PCC 7942 (NCBI Protein ID: WP_011378104.1) were obtained through gene synthesis (Genscript, China) and provided as plasmids pUC57-maFACR and pUC57-cADO, respectively. The sequences were codon-optimized for expression in *S. cerevisiae* and had the Kozak sequence AAAA added before the start codon of the genes. All other chemicals were purchased from Sigma Aldrich (Singapore) unless otherwise stated. All plasmids and yeast strains used in this study are listed in **Supplementary Table S1**. Oligonucleotides were synthesized by Integrated DNA Technologies (Singapore) and listed in **Supplementary Table S2**. All genes were verified by sequencing (1st BASE, Singapore) after cloning. Codon-optimized gene sequences are listed in **Supplementary Table S6**.

E. coli was cultivated in lysogeny broth (LB; 1% tryptone, 0.5% yeast extract, and 1% NaCl) and supplemented with ampicillin (100 mg/L) and/or chloramphenicol (30 mg/L) when required. YPD medium (1% yeast extract, 2% peptone, and 2% glucose) was used for non-selective cultivation of *S. cerevisiae*. Yeast transformants with URA3 and/or LEU2 selection markers were cultivated in yeast minimal medium consisting of yeast nitrogen base (YNB, 6.7 g/L) supplemented with the appropriate synthetic complete amino acid dropout mixture (YNB-URA, YNB-LEU, or YNB-URA-LEU), and glucose and/or galactose at required concentrations as carbon source. Solid growth media were similarly prepared with addition of 2% agar to the recipe described.

Sequence Alignment of maFACR

Eight proteins were randomly selected from the MupV_like_SDR_e and SDR_c families using the NCBI database (Sayers et al., 2020), and their amino acid sequences were aligned to that of maFACR using ClustalX2 (Larkin et al., 2007).

Protein Structure Homology Modeling and Analysis of maFACR

The amino acid sequence of maFACR was uploaded to the Robetta server (Kim et al., 2004). Pymol (Schrodinger, 2010) was used to align the five predicted structures and generate their rendered images.

DNA Transformation and Strain Construction

Yeast competent cells were prepared, and DNAs were transformed using the LiOAc/PEG method (Gietz and Schiestl, 2007). *ADH1*–7 and *SFA1* were deleted from BY4741 using gene disruption cassettes as described in literature (Yu et al., 2016). Generation of BYΔ6 derivatives with multi-gene deletion was mediated by an adapted CRISPR/Cas9 system (Jakociunas et al., 2015) using protocols detailed in **Supplementary Material.**

Plasmid Construction

Plasmid pmaFACR

maFACR was digested from pUC57-maFACR with *Hin*dIII/*Xho*I and cloned into pYES2/CT (Thermo Fisher, Singapore) to obtain pmaFACR.

Generation of maFACR Variants

Single-site mutants of maFACR were generated by QuikChange protocol (Agilent) using pmaFACR as template and complementary primer pairs, as indicated in **Supplementary Table S2**. Multi-site mutants were created by sequential mutation using the same protocol. maFACR with truncated N-terminal domain was generated by amplifying maFACR with the primer pair Nter-F/Nter-R. Similarly, the C-terminal domain was truncated from maFACR by amplifying maFACR with the primers Cter-F/Cter-R. The truncated maFACR genes were digested with *Hin*dIII/*Xho*I and ligated to pYES2/CT to create the single-domain forms of maFACR. The names of the variants and the respective mutations/truncations are denoted in **Table 1**.

Plasmid pMAL-maFACR and the Corresponding Plasmids for the Mutants

maFACR and the site-mutated variants were amplified with the primers maFACR-MAL-F/maFACR-MAL-R using the corresponding pYES2/CT-based plasmids as templates. The sequences encoding the N- and C-terminal domains of maFACR were subcloned by amplifying the respective genes from the corresponding pYES2/CT-based plasmids with the primer pairs maFACR-MAL-F/Nter-MAL-R and Cter-MAL-F/maFACR-MAL-R, respectively. The amplified genes were digested with *Ase*I/*Eco*RI and ligated with pMAL-c5x (New England Biolabs, Singapore) digested with *Nde*I/*Eco*RI.

Plasmids pUdTT and pUdAT

pUdTT and pUdAT were constructed by replacing the P_{TEF1}–P_{GAL1} promoter cassette in pUdGT (Foo et al., 2017) with P_{TEF1}–P_{TPI1} and P_{TEF1}–P_{ADH2}, respectively. P_{TEF1} was amplified with the primer pairs pESC-pmt-TEF1-F/pESC-pmt-TEF1-R using pUdGT as template. P_{TPI1} and P_{ADH2} were amplified using the primer pairs pESC-pmt-TPI1-F/pESC-pmt-TPI1-R and pESC-pmt-ADH2-F/pESC-pmt-ADH2-R, respectively, and purified genomic DNA of BY4741 as template. The P_{TEF1}–P_{TPI1} promoter cassette was generated by splicing P_{TEF1} and P_{TPI1} PCR fragments through overlap extension PCR using the primers pESC-pmt-TEF1-R and pESC-pmt-TPI1-R. The P_{TEF1}–P_{ADH2} promoter cassette was created similarly using the P_{ADH2} instead

TABLE 1 | *In vitro* assay of FACR and FALDR activities in maFACR variants.

maFACR variant[a]	FACR specific activity[b]		FALDR specific activity[c]	
	(nmol NTB min^{-1} mg^{-1} protein)	(nmol NTB min^{-1} $nmol^{-1}$ protein)	(nmol NADP+ min^{-1} mg^{-1} protein)	(nmol NADP+ min^{-1} $nmol^{-1}$ protein)
$maFACR_{WT}$	63.2 ± 1.5	7.3 ± 0.2	7789.3 ± 43.8	905.3 ± 5.1
$maFACR_{S126D}$	60.9 ± 8.5	7.1 ± 1.0	ND	ND
$maFACR_{K156A}$	73.2 ± 2.3	8.5 ± 0.3	ND	ND
$maFACR_{Y152F}$	64.1 ± 0.9	7.4 ± 0.1	ND	ND
$maFACR_{SYK}$	70.2 ± 0.8	8.2 ± 0.1	ND	ND
$maFACR_{Cter}$	3.0 ± 0.2	0.23 ± 0.02	ND	ND
$maFACR_{S515A}$	ND	ND	2,594.0 ± 285.0	301.5 ± 33.1
$maFACR_{K527A}$	ND	ND	2,689.0 ± 73.1	312.5 ± 8.5
$maFACR_{Y532F}$	ND	ND	2,440.6 ± 263.1	283.7 ± 30.6
$maFACR_{Nter}$	ND	ND	12,875.0 ± 291.2	1,104.2 ± 25.0

[a] *$maFACR_{WT}$ is the wild-type enzyme. $maFACR_{SYK}$ has the mutations S126D, Y152F, and K156A. $maFACR_{Nter}$ and $maFACR_{Cter}$ are the N- and C-terminal domains, respectively. Otherwise, $maFACR_X$ refers to a single-site mutant, whereby the mutation X is S126D, Y152F, K156A, S515A, Y527F, or K532A.* [b] *Palmitoyl-CoA was the substrate used.* [c] *Decanal was the substrate used.ND, not detected; FACR, acyl-CoA reductase; FALDR, fatty aldehyde reductase.*

of P_{TPI1} PCR fragment and pESC-pmt-ADH2-R instead of pESC-pmt-TPI1-R for overlap extension PCR. The P_{TEF1}–P_{GAL1} and P_{TEF1}–P_{ADH2} cassettes were digested with *Bam*HI/*Eco*RI and cloned into pUdGT to replace the P_{TEF1}–P_{GAL1} segment, thus generating pUdTT and pUdAT, respectively.

Plasmids pUdGT-cADO, pUdTT-cADO, and pUdAT-cADO

cADO gene was digested from pUdGT-DOX-cADO (Foo et al., 2017) with *Bam*HI/*Xho*I and ligated into pUdGT, pUdTT, and pUdAT to obtain pUdGT-cADO, pUdTT-cADO, and pUdAT-cADO, respectively.

Plasmid pGT-ALK, pTT-ALK, and pAT-ALK

$maFACR_{SYK}$ was amplified with the primer pair pESC-maFACR-F/pESC-maFACR-R from pmaFACR. The amplicon was digested with *Eco*RI/*Sac*I and ligated into pUdGT-cADO, pUdTT-cADO, and pUdAT-cADO to generate pGT-ALK, pTT-ALK, and pAT-ALK, respectively (**Supplementary Figure S1**).

Protein Expression and Purification

maFACR and its mutants were expressed and purified by adaptation of the protocols in literature (Willis et al., 2011). *E. coli* Rosetta 2(DE3) harboring pMAL-maFACR was cultivated in 5 ml of LB with ampicillin and chloramphenicol (LBAC) overnight with shaking at 37°C. These starter cultures were diluted to OD_{600} ∼ 0.05 in 500 ml of fresh LBAC and grown to OD_{600} ∼ 0.5 with shaking at 37°C before the cells were induced with 200 μM of isopropyl-β-thiogalactopyranoside. The induced cells were grown at 16°C for 16 h with shaking at 225 rpm and harvested by centrifugation (4,000 × *g*, 5 min at 4°C). The cells were resuspended in 30 ml of chilled lysis buffer (20 mM of Tris–HCl, pH 7.0, 200 mM of NaCl, 1.0 mM of EDTA, and 10% glycerol) and passed thrice through a high pressure homogenizer (Avestin Emulsiflex C3, Germany) at 10,000 psi for lysis. The lysate was centrifuged (15,000 × *g*, 20 min at 4°C), and the soluble fraction was filtered through 0.45-μm filter. The filtrate was incubated with amylose beads (UcallM Biotechnology, China) for 30 min, and the mixture was loaded onto an Econo-Pac chromatography column (Bio-Rad, Singapore). The beads were washed 3 × 10 ml of binding buffer (20 mM of Tris–HCl, pH 7.0, 200 mM of NaCl, and 1.0 mM of EDTA) and 3 × 10 ml of equilibration buffer (20 mM of Tris–HCl, pH 7.0, and 50 mM of NaCl). The bound protein was eluted with 3 × 2 ml of elution buffer (20 mM of Tris–HCl, pH 7.0, 50 mM of NaCl, and 10 mM of maltose). All other maFACR mutants were similarly purified. The eluted proteins were buffer-exchanged with 3 × 15 ml of equilibration buffer in 100 kDa (for full-length maFACRs) or 50 kDa (for $maFACR_{Cter}$ and $maFACR_{Nter}$) cutoff ultrafiltration concentrator (Sartorius Vivaspin Turbo 15, Singapore) and concentrated to 0.5 ml. The extinction coefficients of the proteins were calculated by ProtParam in ExPASy (Gasteiger et al., 2003), and the concentration of the proteins was determined based on their absorption at 280 nm.

In vitro Specific Activity Assays and Aldehyde Production Analysis

In vitro NADPH and 5,5'-dithiobis-(2-nitrobenzoic acid) (DTNB) specific activity assays were adapted from protocols in literature (Willis et al., 2011). A 4 × enzyme solution was prepared by diluting a maFACR variant in an assay buffer consisting of 80 mM of Tris–HCl (pH 7.0), 200 mM of NaCl, and 2 mg/ml bovine serum albumin (BSA). A 4 × palmitoyl-CoA substrate solution was prepared by diluting a 5 mM aqueous stock solution to 20 μM in deionized water. A 4 × decanal substrate solution was prepared by dissolving the aldehyde to 10 mM in dimethyl sulfoxide (DMSO) and diluting to 240 μM in deionized water. A 4 × DTNB solution was prepared by dissolving the reagent to 10 mg/ml in DMSO and diluting to 0.4 mg/ml in deionized water. A 4 × NADPH solution was prepared by dissolving the co-factor to 2 mg/ml in 1 mM of Tris–HCl, pH 7.0, and diluting to 0.6 mg/ml in deionized

water. The FACR specific activity assays were performed by mixing 50 μl of the 4 × enzyme, palmitoyl-CoA, NADPH, and DTNB solutions in a 96-well plate and monitored at 340 nm on a Synergy HT multi-mode microplate reader (Biotek Instruments, Inc.). The fatty aldehyde reductase (FALDR) specific activity assays were similarly performed by replacing the palmitoyl-CoA and DTNB solutions with decanal and deionized water, respectively, and were monitored at 412 nm. Thus, the reaction mixtures contained 20 mM of Tris–HCl, pH 7.0, 200 mM of NaCl, 2 mg/ml of BSA, 0.5 mg/ml of NADPH, 60 μM of decanal or 5 μM of palmitoyl-CoA substrate, and 0.1 mg/ml of DTNB (for DTNB assay only). The final concentrations of the maFACR variants in the FACR and FALDR assays were 5.0 and 1.3 μM, respectively. All assays were performed in duplicates.

For *in vitro* aldehyde production analysis of $maFAR_{SYK}$, 4 × substrate solutions of various chain lengths of fatty acyl-CoAs were prepared by diluting 5 mM of aqueous stock solutions to 100 μM in deionized water; 100 μl of reactions was prepared as described for the FACR assays, except that DTNB solution was replaced with deionized water. The reactions were incubated at 25°C for 18 h and extracted with 100 μl of ethyl acetate. The organic extracts were analyzed by gas chromatography–mass spectrometry (GCMS) as described in literature (Foo et al., 2017).

De novo Biochemical Production and Analysis

All cultures were cultivated at 30°C with shaking at 225 rpm. Overnight starter cultures were prepared by growing the production strains in YNB-URA with 2.0% glucose (YD-U), and the cells were washed before being diluted to OD_{600} ∼ 0.4 in the respective media for biochemical production. For aldehyde production, the strains harboring pmaFACR or the various maFACR mutants were cultivated in 25 ml of YNB-URA with 0.2% glucose and 1.8% galactose. After 48 h of cultivation, the cells were harvested by centrifugation (3 min, 4,000 × *g*). For ALK production with pGT-ALK or pTT-ALK, strains transformed with the plasmids were cultivated in 50 ml of YDG-U (with varying concentrations of glucose and galactose) or YD-U, respectively. At specific time points, 10 ml of the cultures was harvested by centrifugation (3 min, 4,000 × *g*).

ALK production from BYΔ6OYGA with pAT-ALK by batch feeding with glucose was performed by starting the cell cultivation in 50 ml of YNB-URA with 0.8% glucose. After 24 h of growth and every subsequent 12 h between 24 and 72 h, 0.2% glucose was supplemented by addition of 0.5 ml of 20% glucose (total 2.0% glucose when corrected to 50 ml). Single feeding was performed similarly except that cell cultivation commenced in YD-U and 0.5 ml of sterile deionized water was added at each time point instead of 20% glucose. After 96 h of cultivation, 10 ml of the cultures was harvested by centrifugation (3 min, 4,000 × *g*). The harvested cells were processed and analyzed by GCMS as described in literature (Foo et al., 2017). All experiments were performed in biological duplicates.

RESULTS

Identification of Domains and Catalytic Residues in maFACR

In order to engineer the alcohol-forming maFACR for aldehyde production, we sought to first analyze the protein sequence of maFACR to identify its domains and catalytic residues. A search using BLAST identified two distinct domains corresponding to short dehydrogenase/reductase (SDR) families, i.e., MupV_like_SDR_e family at the N-terminus and SDR_c family at the C-terminus. As reported by Willis et al. (2011), residues 370–660 at the C-terminus show high homology (74% similar and 53% identical) to residues 9–295 of an aldehyde-forming FACR from *Acinetobacter baylyi* (formerly *Acinetobacter calcoaceticus*). Therefore, the C-terminal domain possibly contributes to the FACR activity of maFACR for aldehyde biosynthesis from fatty acyl-CoA. By inference, since maFACR is an alcohol-forming FACR, it is hypothesized that the N-terminal domain functions as an aldehyde reductase to convert the aldehyde intermediate to alcohol, although this domain has only low homology to a known FALDR (Willis et al., 2011).

Enzymes from SDR families are characterized by a serine/threonine–tyrosine–lysine catalytic triad (King et al., 2007). By aligning the maFACR sequence to that of proteins from the MupV_like_SDR_e and SDR_c families, Ser126, Tyr152, and Lys156 were identified as the catalytic residues of the N-terminal domain, while Ser515, Tyr527, and Lys532 were located as the catalytic residues of the C-terminal domain (**Figures 2A,B**). These are consistent with the orientation of the catalytic residues in the protein structures predicted by the Robetta server (**Figures 2C,D** and **Supplementary Figure S2**). In order to determine the enzymatic functions of the domains and verify the identities of the catalytic residues, we created variants of maFACR for *in vitro* assays. Specifically, the N- and C-terminal domains (i.e., $maFACR_{Nter}$ and $maFACR_{Cter}$, respectively) were expressed separately as residues 1–380 and 340–661, respectively, and the identified catalytic residues were inactivated with the following mutations: S126D, Y152F, and K156A in the N-terminal domain, and S515A, Y527F, and K532A in the C-terminal domain.

Verification of Domain Functions and Catalytic Residues by *in vitro* Assay of maFACR Variants

In vitro assay of the FACR and FALDR activities of the maFACR variants was performed using palmitoyl-CoA and decanal, respectively, as substrates, because they were found to be the best substrates of maFACR (Willis et al., 2011). FACR activities of the maFACR variants were evaluated colorimetrically by using DTNB to measure the rate of CoASH liberated when fatty acyl-CoAs were converted to aldehydes. FALDR activities of the mutant enzymes were determined spectrometrically by monitoring the rate of NADPH depletion during reduction of aldehydes to alcohols. FACR and FALDR activities of wild-type maFACR were similar to those reported in literature (Willis et al., 2011; **Table 1**). Interestingly, the N-terminal domain

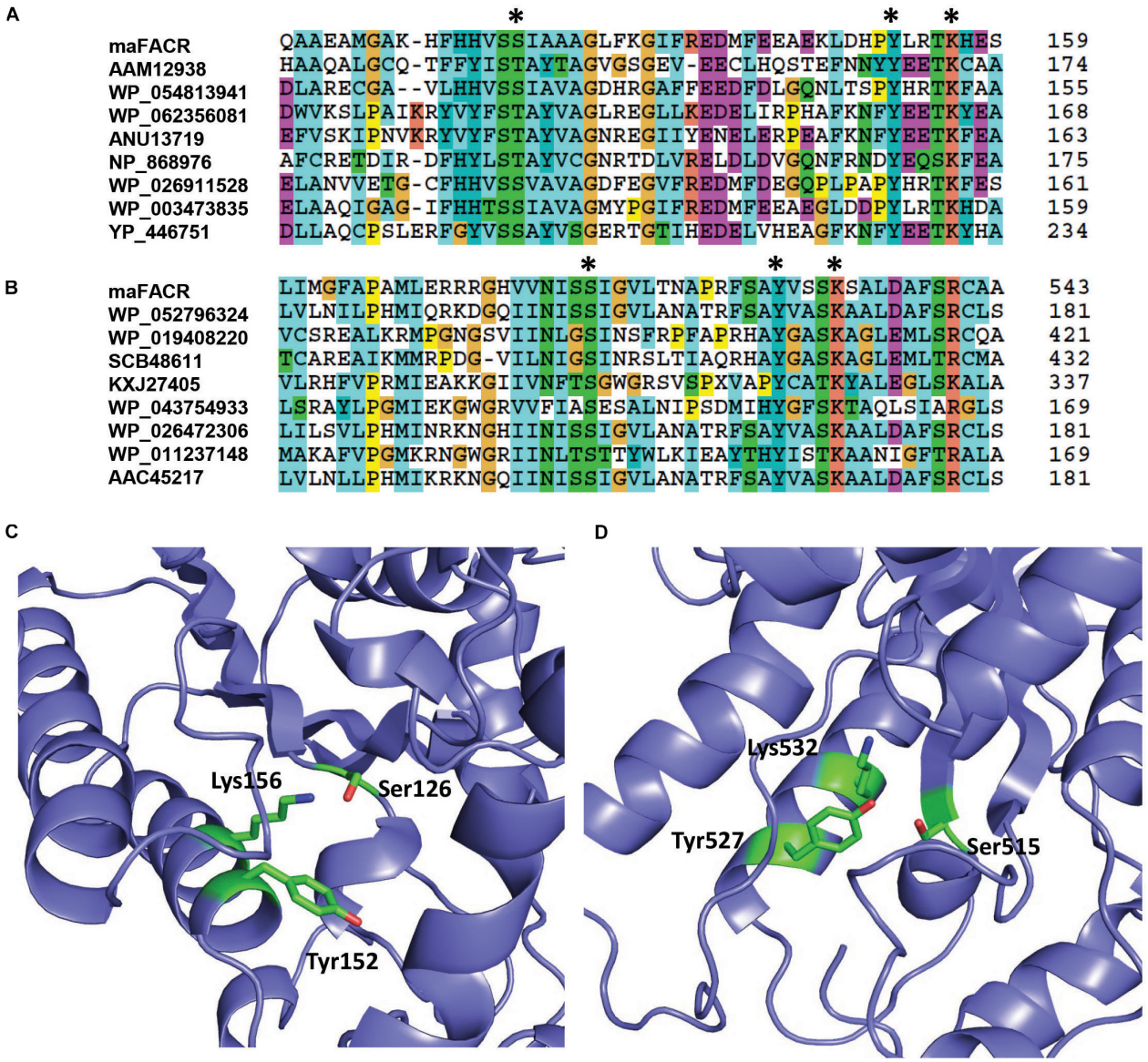

FIGURE 2 | Identification of catalytic residues in maFACR. Alignments of the amino acid sequence of maFACR with proteins from the MupV_like_SDR_e and SDR_c families are shown in **(A,B)** to identify the catalytic residues (marked *) in the N- and C-terminal domains, respectively. The number on the right for each respective protein indicates the amino acid number of the last residue shown. The identified catalytic residues (in green) of the N- and C-terminal domains in a predicted structure of maFACR are shown in **(C,D)**, respectively.

maFACR$_{Nter}$ showed 22.0% higher FALDR activity than wild-type maFACR (**Table 1**). In contrast, the C-terminal domain maFACR$_{Cter}$ exhibited only 3.2% FACR activity as compared with the wild-type enzyme (**Table 1**). As predicted, no FALDR and FACR activities were detected from the C- and N-terminal domains, respectively. It is unclear why, relative to wild-type maFACR, maFACR$_{Nter}$ has higher FALDR activity while maFACR$_{Cter}$ has lower FACR activity, but it is known that protein truncation can alter structural flexibility, substrate accessibility, and quaternary structure of enzymes, which could all affect the activity (Gorfe et al., 2009; Yu et al., 2017; Latip et al., 2018). Nonetheless, these results strongly validate the hypothesis that the C-terminal domain is an FACR while the N-terminal domain functions as an FALDR.

To ascertain the catalytic residues, single-site S126D, Y152F, K156A, S515A, Y527F, and K532A mutants were assayed to establish their effects on the FACR and FALDR activities (**Table 1**). As expected, the mutations S126D, Y152F, and K156A in the N-terminal domain fully inactivated the FALDR activity of maFACR, while the FACR activity remained. Likewise, the FACR activity was abolished by the S515A, Y527F, and K532A mutations in the C-terminal domain, while the FALDR activity was still present, albeit lowered. These results verify that Ser126, Tyr152, and Lys156 are the catalytic residues for

the FALDR activity in the N-terminal domain and that Ser515, Tyr527, and Lys532 are the catalytic residues for the FACR activity in the C-terminal domain. Furthermore, the triple-site S126D/Y152F/K156A mutant (maFACR$_{SYK}$) converted C8–C18 fatty acyl-CoAs *in vitro* to aldehydes without detectable alcohols (**Supplementary Figure S3**), consistent with the broad fatty acyl-CoA substrate range of the wild-type maFACR reported (Willis et al., 2011). The absence of alcohol production by the triple-site mutant further indicates that the C-terminal domain has no FALDR activity and demonstrates the successful engineering of the alcohol-forming maFACR to one that produces aldehydes.

In vivo Production of Fatty Aldehydes From Fatty Acyl-CoA With maFACR Variants and Engineered *Saccharomyces cerevisiae* Strains

The wild-type maFACR and its aldehyde-forming variants were overexpressed in *Saccharomyces cerevisiae* for *in vivo* production of fatty aldehyde from endogenous fatty acyl-CoA. The maFACRs were all functionally expressed, as evidenced by the production of aldehydes and/or alcohols (**Figure 3** and **Supplementary Figure S4**). As expected, the wild-type maFACR produced only alcohols and no detectable aldehydes (Willis et al., 2011). *S. cerevisiae* strains expressing the maFACR variants all produced aldehydes as well as alcohols, which were likely due to reduction of aldehydes by endogenous alcohol dehydrogenases (ADHs) (de Smidt et al., 2008), since we have demonstrated *in vitro* that the C-terminal domain of maFACR$_{SYK}$ has no FALDR activity (**Supplementary Figure S3**). Nevertheless, compared with the wild-type maFACR, the amount of alcohols formed by the maFACR variants was markedly reduced due to the loss of FALDR activity from the enzyme (**Figure 3A**).

maFACRs with single-site S126D, Y152F, or K156A mutation produced similar amounts of total fatty aldehydes (1,432, 1,344, and 1,356 μg/L, respectively) (**Figure 3B**). The major aldehydes formed were hexadecanal (503–535 μg/L) and octadecanal (765–868 μg/L), along with small amounts of 9-octadecenal (31–42 μg/L) and 9–hexadecenal (13–14 μg/L). Shorter aldehydes were not detected, but the presence of 1-tetradecanol suggests that tetradecanal was produced but reduced by endogenous ADHs. Although it is straightforward to simply use the C-terminal FACR domain for aldehyde production, maFACR$_{Cter}$ produced the lowest amount of aldehydes (287 μg/L) among the maFACR variants, which is consistent with the *in vitro* results (**Table 1**). Therefore, the maFACRs with mutated catalytic residues were preferred for *in vivo* aldehyde production. Henceforth, the triple-site S126D/Y152F/K156A mutant maFACR$_{SYK}$, which performed similarly to the single-site mutants in terms of aldehyde and alcohol biosynthesis, was used in subsequent experiments for aldehyde production.

In order to further improve aldehyde production, we attempted to first diminish aldehyde reduction to alcohols by deleting ADH genes. Eight widely studied ADHs, *ADH1*–*7*, and *SFA1* (de Smidt et al., 2008), were deleted to generate single-gene deletion strains for investigating the effects of the ADH deficiencies on aldehyde and alcohol production with maFACR$_{SYK}$. Expression of maFACR$_{SYK}$ in strains without *ADH1*, *ADH2*, or *ADH3* resulted in complete growth inhibition; thus, aldehyde and alcohol production could not be quantified. All other ADH deletion strains produced less alcohols than the wild-type strain (**Figure 4A**). Notably, total alcohol production was reduced most by *ADH6*Δ, from 2,118 μg/L in BY4741 to 1,314 μg/L in strain BYΔ6 (37.9% reduction). Being a medium-chain ADH (Larroy et al., 2002), *ADH6*Δ has greater effects on diminishing formation of shorter fatty alcohols, lowering levels of 1-tetradecanol, 9-hexadecen-1-ol, and 1-hexadecanol by 79.2, 63.2, and 41.0% while reducing production of 9-octadecenol and 1-octadecanol by 37.9 and 13.5%, respectively (**Figure 4B**). Despite the reduction in alcohol production, none

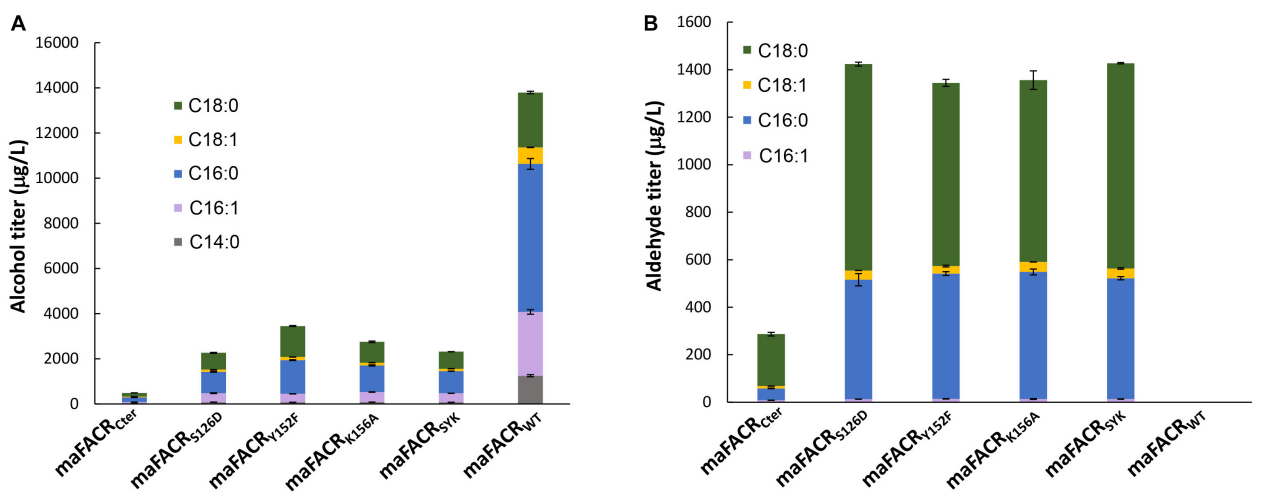

FIGURE 3 | Fatty aldehyde and alcohol production by maFACR variants in *Saccharomyces cerevisiae*. Fatty aldehyde and alcohol production titers from *S. cerevisiae* expressing variants of maFACR are shown in **(A,B)**, respectively. Wild-type maFACR did not produce detectable fatty aldehyde. Data are shown as the mean ± SD of biological duplicates.

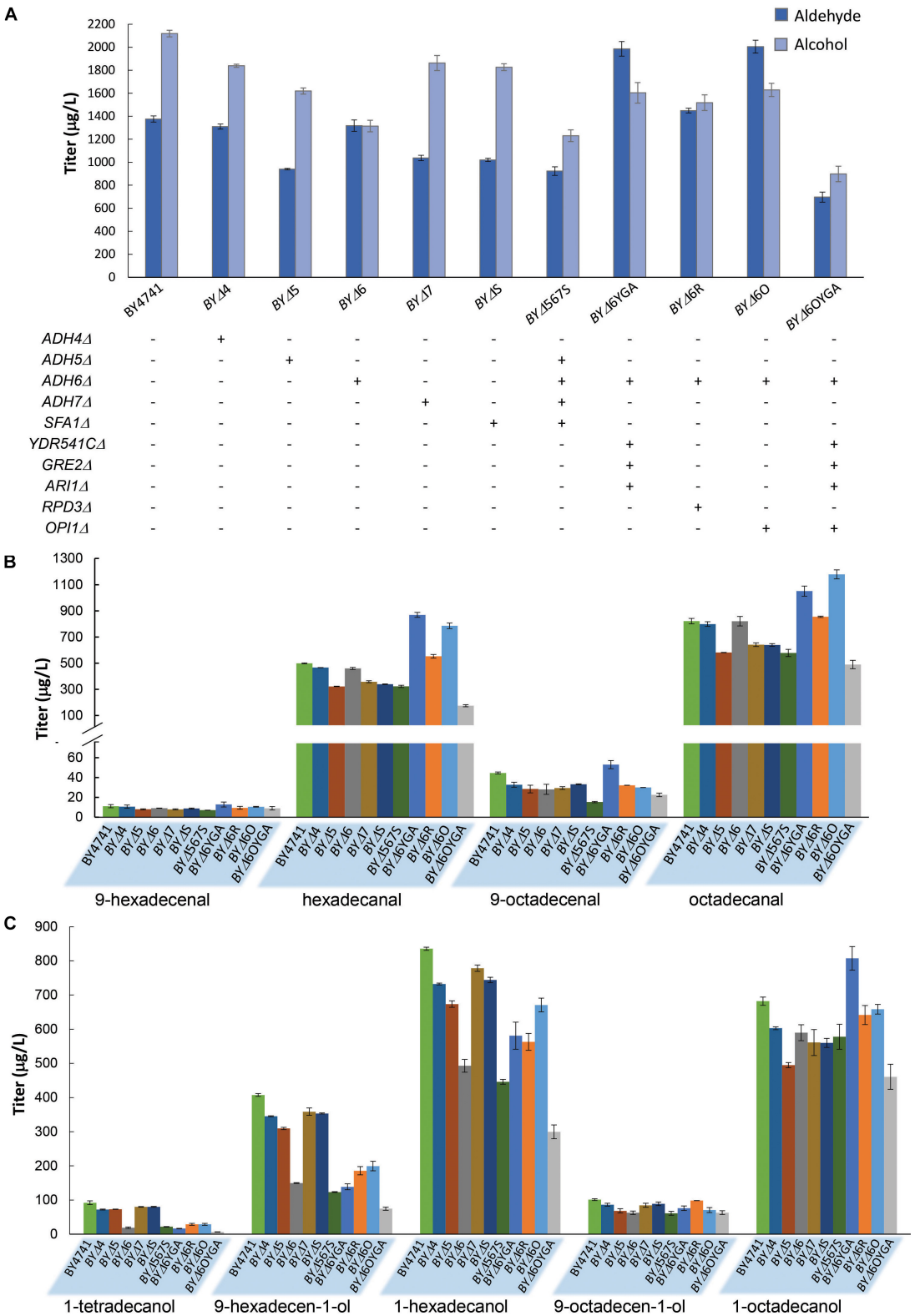

FIGURE 4 | Fatty aldehyde and alcohol production from *Saccharomyces cerevisiae* mutants expressing maFACR$_{SYK}$. **(A)** maFACR was expressed in *S. cerevisiae* mutants with various gene inactivation and the total fatty aldehyde and alcohol titers are shown. "+" and "-" denote the presence and absence of the indicated gene inactivation in the corresponding strain. **(B,C)** Show the compositions of fatty aldehydes and alcohols, respectively, in the various yeast mutants. Data are shown as the mean ± SD of biological duplicates.

of the deletions increased aldehyde production, although the *ADH4*Δ and *ADH6*Δ strains (i.e., BYΔ4 and BYΔ6, respectively) produced similar amounts of total aldehydes (1,310 and 1,318 μg/L, respectively) as compared with the parent strain (1,376 μg/L) (**Figures 4A,C**). Deletion of *ADH5*, *ADH7*, and *SFA1* lowered aldehyde production by at least 24%. In an attempt to further reduce formation of alcohols to accumulate aldehydes, particularly those shorter than C16, we further inactivated three ADHs that were reported to have a broad substrate range and activity on medium chain-length fatty aldehydes, i.e., *YDR541C*, *GRE2*, and *ARI1* (Liu and Moon, 2009; Moon and Liu, 2012, 2015), from the BYΔ6 strain. The 4-ADH-deficient strain, BYΔ6YGA, increased aldehyde production by 50.7% than did BYΔ6, reaching a titer of 1,986 μg/L (**Figure 4A**). Notably, although the amount of alcohols formed was increased to 1,603 μg/L, it was evidently lower than the level of aldehydes produced, essentially directing metabolic flux more toward the desired aldehydes than the alcohol side products.

Subsequently, we attempted to enhance aldehyde production by elevating substrate availability. Deletion of the transcription repressors *OPI1* and *RPD3* has been shown to increase fatty acyl-CoA biosynthesis for enhancing product titers in pathways that utilize fatty acyl-CoA as substrate (Teo et al., 2015). Hence, we disrupted *OPI1* and *RPD3* from the BYΔ6 strain (resulting in strains BYΔ6O and BYΔ6R, respectively) and overexpressed $maFACR_{SYK}$ to determine the transcription repressor candidate that will benefit aldehyde production upon deletion. Both *OPI1*- and *RPD3*-disrupted strains increased aldehyde production, but deletion of *OPI1* conferred greater improvement, enhancing the aldehyde titer by 52.1% over the BYΔ6 strain (45.7% as compared with BY4741) to reach 2,005 μg/L (**Figure 4A**). Surprisingly, although BYΔ6O and BYΔ6YGA were the best aldehyde producers, combining the gene deletions to create strain BYΔ6OYGA was deleterious to aldehyde production, achieving a titer of only 697 μg/L. This is likely due to marked growth inhibition upon expressing $maFACR_{SYK}$ in BYΔ6OYGA (**Supplementary Figure S5**). Nevertheless, we have demonstrated successful application of our engineered aldehyde-forming FACR for aldehyde production in *S. cerevisiae* and systematic host engineering for optimizing aldehyde titer.

Application of $maFAR_{SYK}$ for *de novo* Alkene Production From Fatty Acyl-CoA in *Saccharomyces cerevisiae*

After establishing the capability of $maFACR_{SYK}$ for aldehyde production in *S. cerevisiae*, we aimed to demonstrate the application of this enzyme for downstream production of biochemicals. By employing the aldehyde-forming $maFACR_{SYK}$ and co-expressing a cADO from *Synechococcus elongatus* (Schirmer et al., 2010), we converted the saturated and unsaturated aldehydes formed to the biofuel candidates alkanes and alkenes, respectively, essentially achieving *de novo* production of ALKs from fermentable sugar (**Figure 5** and **Supplementary Figure S6A**). We initially co-expressed both cADO with $maFACR_{SYK}$ constitutively (under P_{TEF1} and P_{TPI1}, respectively) with the pTT-ALK plasmid in BY4741 but were only able to produce 242 μg/L of ALKs (**Supplementary Table S7**). To improve the ALK titer, we utilized the plasmid pGT-ALK to express $maFACR_{SYK}$ under the galactose-inducible P_{GAL1} promoter instead, as we have demonstrated previously that controlled expression of the aldehyde-forming enzyme is beneficial for alkane production (Foo et al., 2017). By transforming pGT-ALK into BY4741, 489 μg/L of ALKs was produced in medium containing 0.2% glucose and 1.8% galactose after 96 h (**Figure 5A**, Condition I). Since the BYΔ6O and BYΔ6YGA host strains produced the highest amount of aldehydes, we attempted to improve ALK production in these strains. Indeed, ALK production was increased by 44.3% to 706 μg/L in BYΔ6YGA after 96 h. However, BYΔ6O/pGT-ALK exhibited a lag in growth and ALK production, reaching only 426 μg/L in titer after 96 h. Unexpectedly, although aldehyde production was not the highest in BYΔ6OYGA and BYΔ6OYGA/pGT-ALK exhibited growth inhibition, maximum ALK production reached 770 μg/L in BYΔ6OYGA, which is 9.2 and 57.5% higher than in BYΔ6YGA/pGT-ALK and BY4741/pGT-ALK, respectively. Interestingly, the improvement in maximum ALK titer in BYΔ6YGA/pGT-ALK over BY4741/pGT-ALK is mainly due to increased ALKs of longer chain lengths (63.1 and 116.0% increase in heptadecane and 8-heptadecene vs. 9.0 and 48.2% increase in pentadecane and 7-pentadecene, respectively, and 6.4% decrease in tridecane) (**Figures 5B–F**, Condition I). In contrast, the improved ALK production in BYΔ6OYGA/pGT-ALK is attributed to higher levels of shorter chain-length ALKs (11.6, 74.4, and 133.0% increase in tridecane, pentadecane, and 7-pentadecene vs. 41.5 and 50.5% increase in heptadecane and 8-heptadecene, respectively) (**Figures 5B–F**, Condition I).

To improve ALK production, we varied the proportion of glucose and galactose in the medium to improve cell growth and vary the induction of $maFACR_{SYK}$ expression by galactose. Keeping total sugar concentration at 2.0%, glucose concentration was increased to formulate media with glucose/galactose ratio of 1.0%:1.0% and 1.5%:0.5%. Compared with cultivation in medium with 0.2% glucose, growth and ALK production of all strains improved when glucose concentration was increased to 1.0% (**Figure 5A**, Condition II and **Supplementary Figure S6B**). The greatest fold improvement in ALK production was found in BY4741/pGT-ALK, increasing the titer by 3.5-fold to achieve 1,496 μg/L. BYΔ6OYGA/pGT-ALK is still the highest producer, reaching a maximum ALK titer of 1,540 μg/L. Although the titers of BY4741/pGT-ALK and BYΔ6OYGA/pGT-ALK were almost identical, the chain-length profile of the strains was noticeably different, with BYΔ6OYGA/pGT-ALK again showing ability to produce more C13 and C15 ALKs than the other strains (**Figures 5B–F**, Condition II). Specifically, tridecane, pentadecane, and 7-pentadecene peak titers of BYΔ6OYGA/pGT-ALK were 52.0, 58.3, and 31.0% higher than BY4741/pGT-ALK, but heptadecane and 8-heptadecene peak titers of BYΔ6OYGA/pGT-ALK were 7.9 and 7.7% lower than BY4741/pGT-ALK, respectively. Further, increasing glucose concentration to 1.5% led to decrease in ALK production (**Figure 5A**, Condition III), possibly due to excessive repression of $maFACR_{SYK}$ expression under the P_{GAL1} promoter.

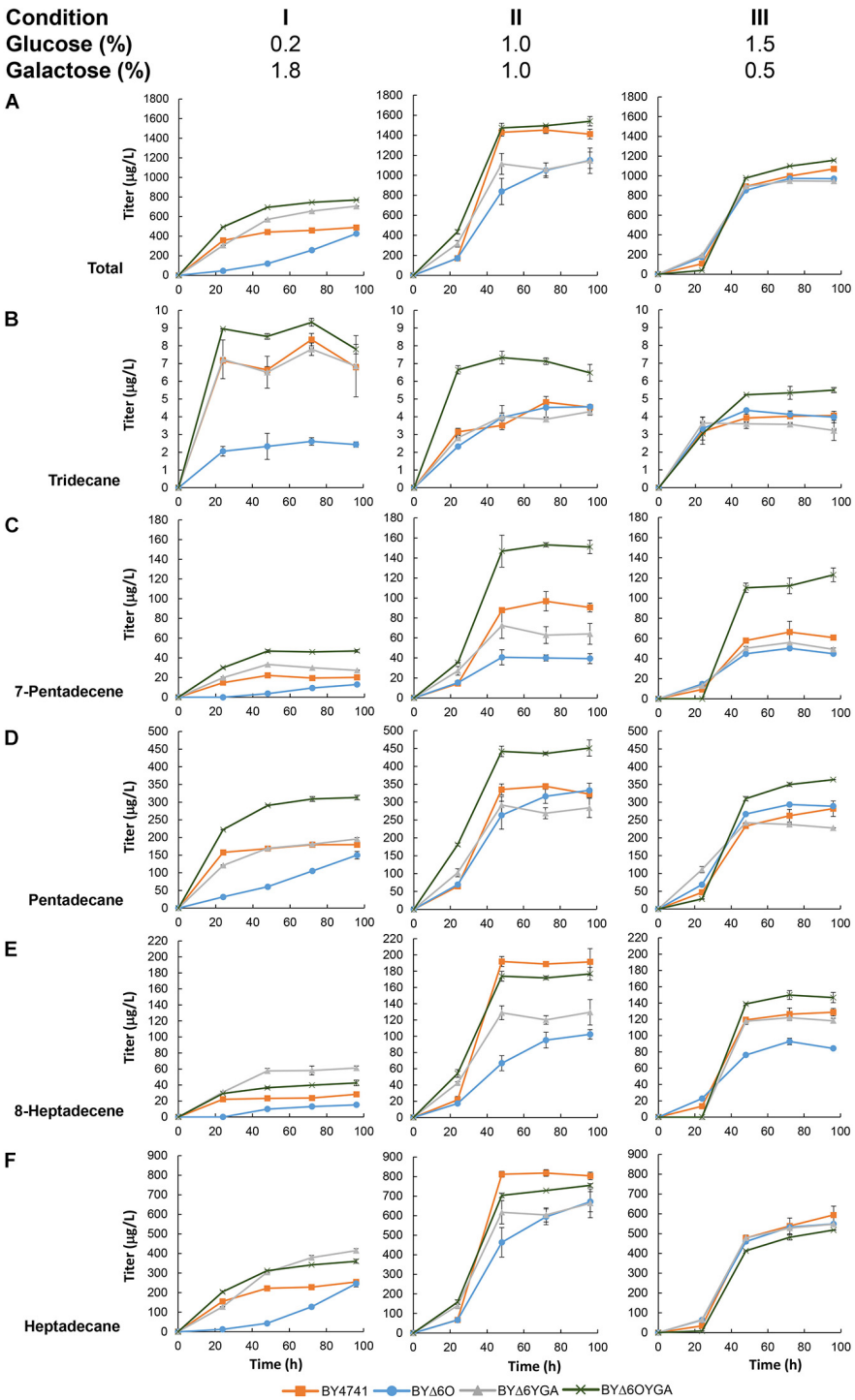

FIGURE 5 | *De novo* alkane and alkene (ALK) production via a fatty acyl-CoA-dependent pathway in various *Saccharomyces cerevisiae* mutants. Time profiles of the ALK titers from different glucose/galactose ratio in BY4741, BYΔ6O, BYΔ6YGA, and BYΔ6OYGA harboring a fatty acyl-CoA-dependent ALK biosynthesis pathway are shown. Total titers **(A)** as well as the titers of individual ALK components, i.e., **(B)** tridecane, **(C)** 7-pentadecene, **(D)** pentadecane, **(E)** 8-heptadecene, and **(F)** heptadecane are presented. Data are shown as the mean ± SD of biological duplicates.

Thus far, the ALK production pathway that we have constructed using pGT-ALK relies on galactose for induction of maFACR$_{SYK}$ expression. However, galactose is much more expensive than glucose and is not economical, particularly for large-scale cultures. As we have shown that constitutive expression of maFACR$_{SYK}$ from pTT-ALK is deleterious to ALK

production, we therefore replaced the P_{GAL1} promoter with the growth-phase-dependent P_{ADH2} promoter to construct another plasmid, pAT-ALK. Using P_{ADH2}, $maFACR_{SYK}$ expression is strongly repressed in the presence of glucose and will be expressed upon glucose depletion (Lee and DaSilva, 2005), thus effecting controlled expression of $maFACR_{SYK}$ without the need for additional inducer. Hence, with pAT-ALK, we can implement the ALK biosynthesis pathway in *S. cerevisiae* using a medium with only glucose as the carbon source, which is a system that is more economical and industrially relevant than if galactose is required. The plasmid was transformed into our best host strain for ALK production, BYΔ6OYGA, and the resulting strain was cultivated in medium with 2.0% glucose supplied by single feeding or batch feeding for producing ALKs. In the single-feeding experiments, 2.0% glucose was provided at the start of the cultivation, and this produced 856.7 μg/L ALKs after 96 h (**Figure 6**). By supplying the 2.0% glucose through batch feeding, i.e., starting with 0.8% glucose and supplementing with 0.2% glucose every 12 h between 24 and 72 h, the final ALK titer was increased by 54.2% to 1,321 μg/L. The improved ALK titer using batch feeding of glucose might be due to reduced repression of $maFACR_{SYK}$ expression since glucose concentration was kept lower throughout the cultivation compared with single feeding. This could have increased the availability of aldehyde for conversion to ALKs. Interestingly, the OD_{600} of the cultures after 96 h was higher when glucose was provided by batch feeding (OD_{600} = 14.5) than single feeding (OD_{600} = 10.1), suggesting that the Crabtree effect could have been reduced by batch feeding, which resulted in increased biomass and ALK production (Halka et al., 2018). Although the ALK titer achieved with BYΔ6OYGA/pAT-ALK by continuous glucose feeding was slightly lower (85.8%) than the highest ALK titer produced in BYΔ6OYGA/pGT-ALK under galactose-dependent condition (1,540 μg/L, **Figure 5A**, Condition II), it may be improved by optimizing the glucose concentration and feeding strategy during the fed-batch cultivation. Overall, we have demonstrated downstream application of our engineered $maFACR_{SYK}$ for production of ALKs and enhanced the ALK biosynthesis by optimizing the culture composition and choice of promoters.

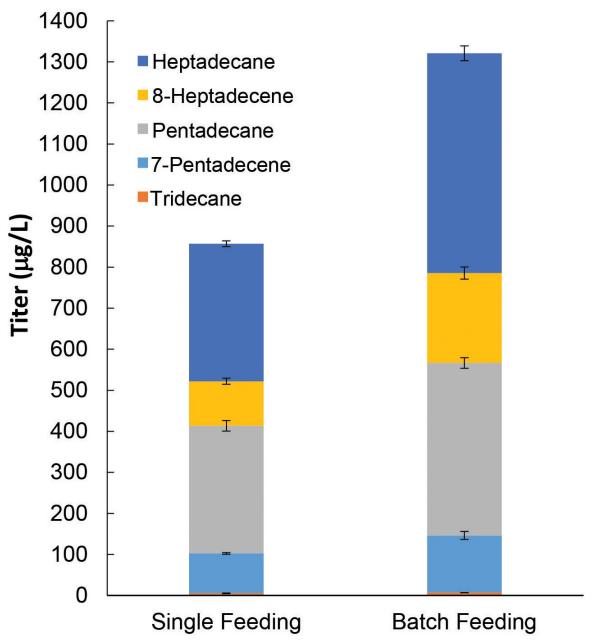

FIGURE 6 | *De novo* alkane and alkene (ALK) production from fatty acyl-CoA via an inducer-independent biosynthetic pathway in *Saccharomyces cerevisiae*. By expressing $maFACR_{SYK}$ under the growth phase-dependent P_{ADH2} promoter, an inducer-independent ALK biosynthesis pathway with controlled expression of $maFACR_{SYK}$ was implemented. In the single feeding experiment, 2% glucose was fed at the start of the cultivation. In the batch feeding experiment, 2% glucose was fed in batches over the course of the cultivation. Data are shown as the mean ± SD of biological duplicates.

DISCUSSION

Aldehyde-forming bacterial enzymes have been employed with success for producing aldehydes in *Escherichia coli*, particularly the FACR from *Acinetobacter baylyi* and FAAR from *Synechococcus elongatus* (Schirmer et al., 2010; Lehtinen et al., 2018). However, there has been limited success in converting fatty acyl-CoAs into aldehydes in *Saccharomyces cerevisiae* due to the low activity of the aldehyde-forming FAARs and FACRs when employed in the yeast strain (**Supplementary Figure S7**; Buijs et al., 2014; Zhou et al., 2016b). In contrast, alcohol-forming bacterial, mammalian, and avian FACRs have been functionally expressed in *S. cerevisiae* for high-level fatty alcohol production (Runguphan and Keasling, 2014; Feng et al., 2015; d'Espaux et al., 2017). Analysis of the mammalian and avian FACRs shows only one distinct active site for reduction of both fatty acyl-CoA and aldehyde (Hellenbrand et al., 2011); thus, these enzymes are difficult to engineer rationally to eliminate solely the FALDR activity. On the other hand, maFACR has two distinct domains that appear to correspond to FACR and FALDR domains. Therefore, we selected this enzyme for rational engineering because the FALDR activity can be inactivated independent of the FACR activity. Indeed, we successfully repurposed in this work the alcohol-forming maFACR into one that is aldehyde-forming, thus demonstrating the importance of protein engineering for synthetic biology and metabolic engineering applications (Foo et al., 2012).

Through *in vivo* enzymatic assay, we have verified the catalytic roles of the two domains of maFACR and identified the catalytic residues involved. The reduction of fatty acyl-CoA to fatty alcohol by maFACR was proposed to proceed via a reaction mechanism where a two-step reduction occurred within one active site or two highly cooperative active sites through a hemithioacetal intermediate covalently bound to maFACR (Willis et al., 2011). Our results indicate that two active sites are involved, whereby fatty acyl-CoA is reduced to aldehyde in the C-terminal domain and further reduced to alcohol in the N-terminal domain. Additionally, structures proposed by homology modeling of maFACR with the Robetta server do not show any cysteine near the catalytic residues (**Supplementary Figure S8**). Thus, an enzyme-bound thiohemiacetal intermediate

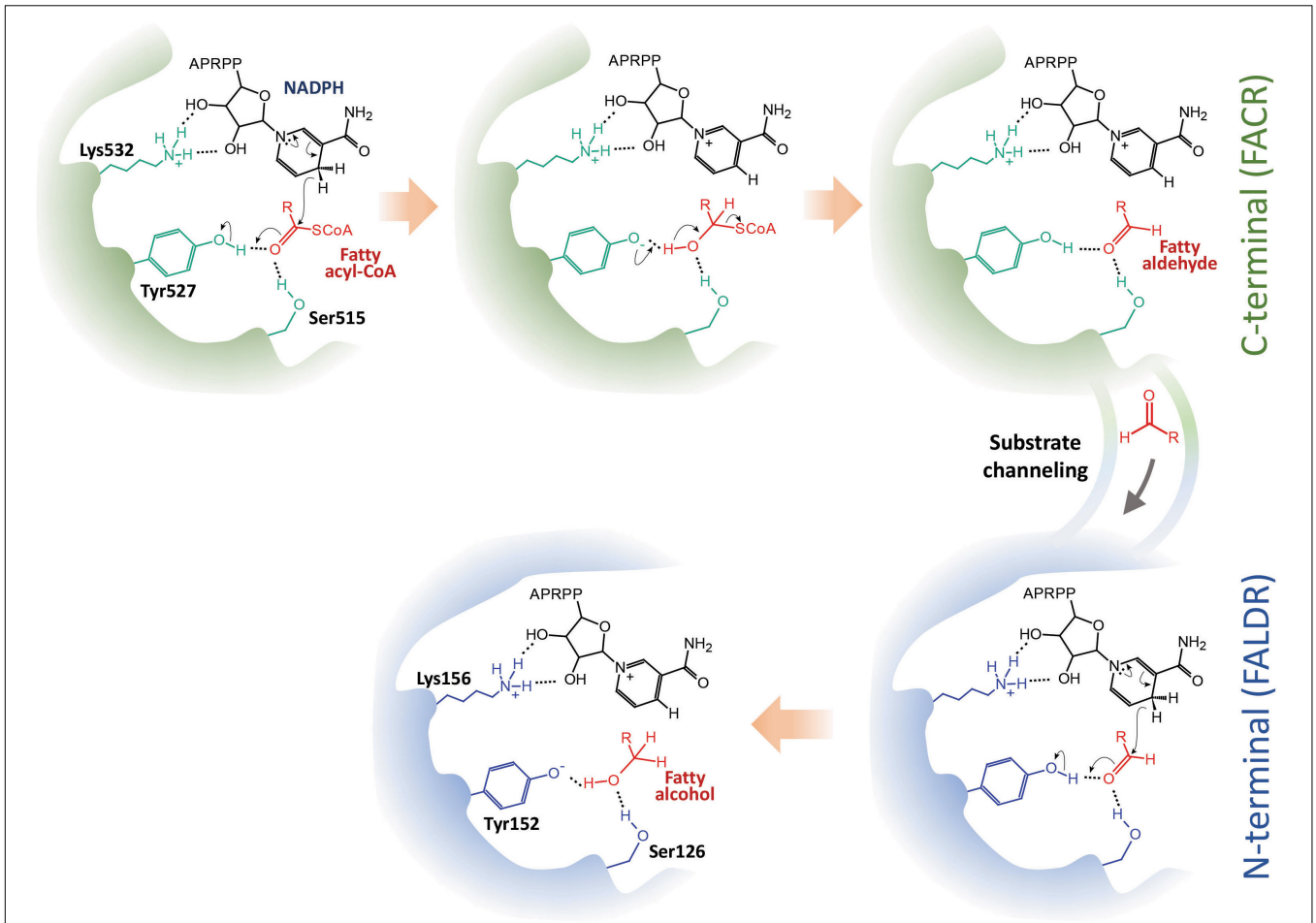

FIGURE 7 | Proposed reaction mechanism of maFACR. We propose a mechanism whereby fatty acyl-CoA is reduced in the C-terminal fatty acyl-CoA reductase (FACR) domain (in green) to aldehyde, which is transferred to the N-terminal fatty aldehyde reductase (FALDR) domain (in blue) for further reduction to fatty alcohol. Ser515 and Tyr527 in the FACR domain first activate the carboxyl group of the fatty acyl-CoA by hydrogen bonding. NADPH, which interacts with Lys532 via hydrogen bonding, donates a hydride to reduce the fatty acyl-CoA to a hemithioacetal upon proton donation by Try527. Subsequent elimination of CoASH forms a fatty aldehyde, which is channeled to the N-terminal. Similarly, Ser126 and Tyr152 activate the carbonyl group of the fatty aldehyde to facilitate reduction by a hydride donated by an NADPH bound to Lys156. Upon accepting a proton from Tyr152, a fatty alcohol is formed. APRPP, adenosine-2-phosphate ribose pyrophosphate moiety of NAPDH.

appears to be unlikely. Since the two domains of maFACR belong to SDR families, we propose that each domain employs the general SDR catalytic mechanism involving the Ser-Tyr-Lys triad for substrate binding, hydride transfer, and co-factor binding (**Figure 7**; Nobutada et al., 2001). It is unclear how the aldehyde intermediate is transferred from the FACR domain to the FALDR domain without releasing the aldehyde from the enzyme, but efficient substrate channeling between domains/protomers has been well-documented in enzymes (Huang et al., 2001). The crystal structure of maFACR will be required to determine the exact mechanism for aldehyde transfer between the domains.

We employed the engineered maFACR$_{SYK}$ for *in vivo* aldehyde production in *S. cerevisiae* BY4741 and was already able to produce 1,376 μg/L aldehyde without strain optimization. This contrasts with previous reports that deletion of the aldehyde dehydrogenase *HFD1* was critical for aldehyde production in *S. cerevisiae* by preventing oxidation of aldehydes to fatty acids (Buijs et al., 2014; Zhou et al., 2016a). Interestingly, deleting this gene from *ADH6*Δ was deleterious to aldehyde titer, drastically reducing the total aldehyde formed by 97.5–33 μg/L (**Supplementary Table S8**). This could be due to differences in strain background, as *HFD1*Δ in BY4741 also led to reduced titer when DOX from rice was used for aldehyde production (Foo et al., 2017). Thus, *HFD1* deletion was not investigated further. Nevertheless, we successfully improved BY4741 to increase aldehyde and reduce alcohol production by deleting several alcohol dehydrogenases and upregulating fatty acyl-CoA biosynthesis.

Although our efforts in this work have enhanced aldehyde biosynthesis in *S. cerevisiae*, there is still much room for improvement. To further increase aldehyde production, directed evolution of maFACR$_{SYK}$ and other alcohol-producing FACRs may be explored to generate mutants with higher aldehyde-producing ability. Notably, TaFACR and MmFACR from owl

and mouse, respectively, were shown to produce much more fatty alcohols than maFACR (d'Espaux et al., 2017), suggesting that these avian and mammalian FACRs have higher activities in converting fatty acyl-CoAs to aldehyde intermediates. However, as aforementioned, avian and mammalian FACRs may share the same active site for reduction of both fatty acyl-CoAs and aldehydes (Hellenbrand et al., 2011) and thus could not be easily engineered rationally like maFACR to eliminate the FALDR activity. Nevertheless, if directed evolution of TaFACR and MmFACR can significantly increase the affinity for fatty acyl-CoA over aldehyde, highly active aldehyde-forming variants can potentially be generated. Furthermore, despite deletion of several transcription regulators and ADHs, the improvement in aldehyde accumulation is still limited. One possible reason is the presence of several aldehyde dehydrogenases (ALDHs) in *S. cerevisiae* other than *HFD1*. Deletion of the five other major ALDHs (*ALD2–6*) (Navarro-Avino et al., 1999) may be evaluated to determine if enzymatic oxidation could be reduced to aid aldehyde accumulation. Expression of efflux pumps and the use of solvent overlay may also be investigated to transfer the aldehydes out of the cells to drive the flux toward aldehyde production by minimizing *in vivo* enzymatic conversion of aldehyde to by-products (Zhang et al., 2016; Zhou et al., 2016a; Perez-Garcia and Wendisch, 2018). The use of efflux pumps and solvent overlay has been successfully employed to improve biochemical production and hence may also be applicable for improving the accumulation of aldehydes (Zhang et al., 2016; Zhou et al., 2016a).

For ALK production, BYΔ6OYGA is the best host strain, although BYΔ6O and BYΔ6YGA are better host strains for producing aldehydes, suggesting a synergy between the deletion of *OPI1* along with the four ADHs that benefits the deformylation of aldehydes to ALKs, particularly those of shorter chain lengths. The reason is unclear, although it is possible that *OPI1* deletion increased the availability of fatty acyl-CoA, and deletion of the four medium-chain ADHs reduced competition from the ADHs with the cADO for the shorter chain-length aldehyde substrates, thus increasing the titer and skewing the ALK

TABLE 2 | Comparison of reported ALK production titers in yeast.

Host	ALK pathway enzymes	Remarks	ALK titer (mg/L)[a]	References
Saccharomyces cerevisiae	Engineered FACR and cADO	Wild-type *S. cerevisiae*	**1.496**	This work
	Engineered FACR and cADO	Four ADHs were deleted. Fatty acyl-CoA biosynthesis was upregulated by deleting *OPI1*.	**1.54**	
S. cerevisiae	Cyanobacterial FAAR and cADO	*HFD1* aldehyde dehydrogenase gene was deleted.	**0.14**	Zhou et al., 2016b
	CAR and cADO	*POX1* was deleted to inactivate beta-oxidation. *HFD1* and *ADH5* were deleted to inactivate competing pathways.	0.8	
S. cerevisiae	Cyanobacterial FAAR and cADO	Cytosolic ALK pathway in wild-type *S. cerevisiae*.	**0.035**	Zhou et al., 2016a
	CAR and cADO	Cytosolic ALK pathway in wild-type *S. cerevisiae*.	0.06	
	CAR and cADO	Cytosolic ALK pathway. *POX1* was deleted to inactivate beta-oxidation. *HFD1*, *ADH5*, and *SFA1* were deleted to inactivate competing pathways.	0.7	
	CAR and cADO	Peroxisomal ALK pathway. *POX1* was deleted to inactivate beta-oxidation. *HFD1* was deleted to inactivate competing pathway.	1.2	
	CAR and cADO	Peroxisomal ALK pathway. *POX1* was deleted to inactivate beta-oxidation. *HFD1* was deleted to inactivate competing pathway. Peroxisome biogenesis was increased by deleting *PEX31–32* and overexpressing *PEX34*.	3.55	
S. cerevisiae	DOX and cADO	*FAA1* and *FAA4* were deleted to accumulate FFAs.	0.074	Foo et al., 2017
Yarrowia lipolytica	Bacterial FACR and cADO	Cytosolic ALK pathway in an oleaginous yeast host.	**3.2**	Xu et al., 2016
	Bacterial FACR and cADO	The ALK pathway was targeted to the endoplasmic reticulum of the oleaginous yeast.	**16.8**	
	CAR and cADO	Cytosolic ALK pathway in an oleaginous yeast host.	23.3	
S. cerevisiae	Fatty acid decarboxylase, UndA	The host was engineered to produce medium-chain fatty acids and inactivate the beta-oxidation pathway. The highest titer was achieved with 20 g/L of glucose.	3.35	Zhu et al., 2017
S. cerevisiae	Fatty acid decarboxylase, OleT	*FAA1* and *FAA4* were deleted to accumulate FFAs. *HEM3* was overexpressed to increase the heme co-factor. *CCP1* was deleted to accumulate H_2O_2. The highest titer was achieved upon gene expression tuning and bioreactor process optimization.	3.7	Chen et al., 2015

ALK, alkane and alkene; FACR, fatty acyl-CoA reductase; FAAR, fatty acyl-(acyl-carrier-protein) reductase; cADO, cyanobacterial aldehyde deformylating oxygenase; FFA, free fatty acid.[a]*Titers of fatty acyl-CoA-dependent ALK pathway are shown in bold. Otherwise, the titers were from FFA-dependent ALK pathways.*

production profile toward shorter chain length. It is also noted that *YDR541C*, *GRE2*, and *ARI1* are NADPH-dependent ADHs (Liu and Moon, 2009; Choi et al., 2010; Moon and Liu, 2015). Therefore, their absence may improve availability of NADPH to cADO, which requires two molecules of NADPH for each deformylation reaction, hence accelerating the deformylation step. Further experiments will be required to elucidate the roles of the deletions in BYΔ6OYGA that promote ALK production. Nonetheless, we have achieved ALK titer up to 1,540 μg/L, which is to our knowledge the highest cytosolic ALK production to date in *S. cerevisiae* from fatty acyl-CoA. Even without genetic modification of the parent strain BY4741, our ALK production pathway using our engineered maFACR attained 1,496 μg/L ALK, which is already approximately 40- and 10-fold higher than the ALK titers reported in wild-type (Zhou et al., 2016a) and engineered *S. cerevisiae* strains (Zhou et al., 2016b), respectively, using cytosolic fatty acyl-CoA-based pathways with a low-activity aldehyde-forming FAAR (**Table 2**). In recent works on ALK production in *S. cerevisiae*, FFA-based pathways using CAR or DOX were favored for forming aldehydes toward ALK production due to the low activity of aldehyde-forming FACRs in *S. cerevisiae* (Zhou et al., 2016b; Foo et al., 2017). With our engineered maFACR$_{SYK}$, we have achieved ALK titers that are comparable with those attained via FFA-dependent pathways, including those based on fatty acid decarboxylases (Chen et al., 2015; Zhu et al., 2017; **Table 2**), thus re-establishing the viability of the fatty acyl-CoA-based ALK production pathway. By employing maFACR$_{SYK}$ in conjunction with novel strategies, such as organelle targeting of the ALK production pathway (Xu et al., 2016; Zhou et al., 2016a) and genetic circuit development (Lo et al., 2016; Xia et al., 2019), and expressing maFACR$_{SYK}$ in non-conventional oleaginous host strains, such as *Yarrowia lipolytica* (Xu et al., 2016), ALK production in yeast can potentially be further improved. However, the ALK titers obtained in yeast strains still pale in comparison with those achieved in *E. coli* (Choi and Lee, 2013). More studies are required to identify the bottlenecks of ALK production pathways in yeast, such as competing pathways, co-factor availability, and low activity of cADO. As advances in synthetic biology and synthetic genomics for *S. cerevisiae* gain momentum (Chen et al., 2018; Foo and Chang, 2018), new tools are increasingly available for improving characteristics of yeast to maximize the potential of yeast as a production host for fatty aldehydes and their derivatives.

CONCLUSION

In this work, we successfully engineered an alcohol-forming FACR into one that produces aldehyde and validated the functions of the two domains in the enzyme as well as the catalytic residues. By expressing the engineered maFACR$_{SYK}$ in *Saccharomyces cerevisiae* and strain optimization through gene deletion to increase substrate availability and inactivate competing pathways, 2,005 μg/L of fatty aldehyde was produced. To our knowledge, this is the highest reported fatty aldehyde titer produced from fatty acyl-CoA in *S. cerevisiae*. Subsequently, we demonstrated the utilization of our engineered maFACR$_{SYK}$ for downstream application, namely, ALK production, in this work. In combination with culture optimization, we attained ALK titer of 1,540 μg/L and skewed the ALK production profile toward shorter chain length. The ALK titer is the highest achieved to date via cytosolic ALK production in *S. cerevisiae* from fatty acyl-CoA. We believe that our engineered maFACR$_{SYK}$ and yeast strains re-established the feasibility of aldehyde production from fatty acyl-CoA in *S. cerevisiae* for potential applications in biosynthesizing ALKs and other valuable aldehyde-derived compounds.

DATA AVAILABILITY STATEMENT

All datasets presented in this study are included in the article/**Supplementary Material.**

AUTHOR CONTRIBUTIONS

JF, BR, and AS performed the experiments and analyzed the experimental data. MC, SL, and JF oversaw the project and provided guidance. JF, BR, and MC wrote, reviewed, and edited the manuscript. All authors have read and agreed to the published version of the manuscript.

FUNDING

This work was supported by the Synthetic Biology Initiative of the National University of Singapore (DPRT/943/09/14), the Singapore Ministry of Education (MOE/2014/T2/2/128), the Defense Threat Reduction Agency (DTRA, HDTRA1-13-1-0037), the Summit Research Program of the National University Health System (NUHSRO/2016/053/SRP/05), and the Synthetic Biology R&D Programme (SBP-P2, SBP-P7, SBP-P9) and Industry Alignment Fund-Industry Collaboration Project of the National Research Foundation of Singapore (ICP1600012).

SUPPLEMENTARY MATERIAL

The Supplementary Material for this article can be found online at: https://www.frontiersin.org/articles/10.3389/fbioe.2020.585935/full#supplementary-material

REFERENCES

Akhtar, M. K., Turner, N. J., and Jones, P. R. (2013). Carboxylic acid reductase is a versatile enzyme for the conversion of fatty acids into fuels and chemical commodities. *Proc. Natl. Acad. Sci. U.S.A.* 110, 87–92. doi: 10.1073/pnas.1216516110

Buijs, N. A., Zhou, Y. J., Siewers, V., and Nielsen, J. (2014). Long-chain alkane production by the yeast *Saccharomyces cerevisiae*. *Biotechnol. Bioeng.* 112, 1275–1279. doi: 10.1002/bit.25522

Chen, B., Lee, D. Y., and Chang, M. W. (2015). Combinatorial metabolic engineering of *Saccharomyces cerevisiae* for terminal alkene production. *Metab. Eng.* 31, 53–61. doi: 10.1016/j.ymben.2015.06.009

Chen, B., Lee, H. L., Heng, Y. C., Chua, N., Teo, W. S., Choi, W. J., et al. (2018). Synthetic biology toolkits and applications in *Saccharomyces cerevisiae*. *Biotechnol. Adv.* 36, 1870–1881. doi: 10.1016/j.biotechadv.2018.07.005

Choi, Y. H., Choi, H. J., Kim, D., Uhm, K. N., and Kim, H. K. (2010). Asymmetric synthesis of (S)-3-chloro-1-phenyl-1-propanol using *Saccharomyces cerevisiae* reductase with high enantioselectivity. *Appl. Microbiol. Biotechnol.* 87, 185–193. doi: 10.1007/s00253-010-2442-5

Choi, Y. J., and Lee, S. Y. (2013). Microbial production of short-chain alkanes. *Nature* 502, 571–574. doi: 10.1038/nature12536

de Smidt, O., Du Preez, J. C., and Albertyn, J. (2008). The alcohol dehydrogenases of *Saccharomyces cerevisiae*: a comprehensive review. *FEMS Yeast Res.* 8, 967–978. doi: 10.1111/j.1567-1364.2008.00387.x

d'Espaux, L., Ghosh, A., Runguphan, W., Wehrs, M., Xu, F., Konzock, O., et al. (2017). Engineering high-level production of fatty alcohols by *Saccharomyces cerevisiae* from lignocellulosic feedstocks. *Metab. Eng.* 42, 115–125. doi: 10.1016/j.ymben.2017.06.004

Feng, X., Lian, J., and Zhao, H. (2015). Metabolic engineering of *Saccharomyces cerevisiae* to improve 1-hexadecanol production. *Metab. Eng.* 27, 10–19. doi: 10.1016/j.ymben.2014.10.001

Foo, J. L., and Chang, M. W. (2018). Synthetic yeast genome reveals its versatility. *Nature* 557, 647–648. doi: 10.1038/d41586-018-05164-3

Foo, J. L., Ching, C. B., Chang, M. W., and Leong, S. S. J. (2012). The imminent role of protein engineering in synthetic biology. *Biotechnol. Adv.* 30, 541–549. doi: 10.1016/j.biotechadv.2011.09.008

Foo, J. L., Susanto, A. V., Keasling, J. D., Leong, S. S., and Chang, M. W. (2017). Whole-cell biocatalytic and de novo production of alkanes from free fatty acids in *Saccharomyces cerevisiae*. *Biotechnol. Bioeng.* 114, 232–237. doi: 10.1002/bit.25920

Forneris, F., and Mattevi, A. (2008). Enzymes without borders: mobilizing substrates, delivering products. *Science* 321, 213–216. doi: 10.1126/science.1151118

Gasteiger, E., Gattiker, A., Hoogland, C., Ivanyi, I., Appel, R. D., and Bairoch, A. (2003). ExPASy: The proteomics server for in-depth protein knowledge and analysis. *Nucleic Acids Res.* 31, 3784–3788. doi: 10.1093/nar/gkg563

Gietz, R. D., and Schiestl, R. H. (2007). High-efficiency yeast transformation using the LiAc/SS carrier DNA/PEG method. *Nat. Protoc.* 2, 31–34. doi: 10.1038/nprot.2007.13

Gorfe, A. A., Lu, B., Yu, Z., and Mccammon, J. A. (2009). Enzymatic activity versus structural dynamics: the case of acetylcholinesterase tetramer. *Biophys. J.* 97, 897–905. doi: 10.1016/j.bpj.2009.05.033

Halka, L. M., Nowacki, C., Kleinschmidt, A., Koenen, K., and Wichmann, R. (2018). Glucose limited feed strategy leads to increased production of fusicocca-2,10(14)-diene by *Saccharomyces cerevisiae*. *AMB Express* 8:132. doi: 10.1186/s13568-018-0662-8

Hellenbrand, J., Biester, E. M., Gruber, J., Hamberg, M., and Frentzen, M. (2011). Fatty acyl-CoA reductases of birds. *BMC Biochem.* 12:64. doi: 10.1186/1471-2091-12-64

Hong, K. K., and Nielsen, J. (2012). Metabolic engineering of *Saccharomyces cerevisiae*: a key cell factory platform for future biorefineries. *Cell. Mol. Life Sci.* 69, 2671–2690. doi: 10.1007/s00018-012-0945-1

Huang, X., Holden, H. M., and Raushel, F. M. (2001). Channeling of substrates and intermediates in enzyme-catalyzed reactions. *Annu. Rev. Biochem.* 70, 149–180. doi: 10.1146/annurev.biochem.70.1.149

Jakociunas, T., Bonde, I., Herrgard, M., Harrison, S. J., Kristensen, M., Pedersen, L. E., et al. (2015). Multiplex metabolic pathway engineering using CRISPR/Cas9 in *Saccharomyces cerevisiae*. *Metab. Eng.* 28, 213–222. doi: 10.1016/j.ymben.2015.01.008

Jin, Z., Wong, A., Foo, J. L., Ng, J., Cao, Y. X., Chang, M. W., et al. (2016). Engineering *Saccharomyces cerevisiae* to produce odd chain-length fatty alcohols. *Biotechnol. Bioeng.* 113, 842–851. doi: 10.1002/bit.25856

Kim, D. E., Chivian, D., and Baker, D. (2004). Protein structure prediction and analysis using the Robetta server. *Nucleic Acids Res.* 32, W526–W531. doi: 10.1093/nar/gkh468

King, J. D., Harmer, N. J., Preston, A., Palmer, C. M., Rejzek, M., Field, R. A., et al. (2007). Predicting protein function from structure–the roles of short-chain dehydrogenase/reductase enzymes in Bordetella O-antigen biosynthesis. *J. Mol. Biol.* 374, 749–763. doi: 10.1016/j.jmb.2007.09.055

Koeduka, T., Matsui, K., Akakabe, Y., and Kajiwara, T. (2002). Catalytic properties of rice alpha-oxygenase. A comparison with mammalian prostaglandin H synthases. *J. Biol. Chem.* 277, 22648–22655. doi: 10.1074/jbc.M110420200

Kohlpaintner, C., Schulte, M., Falbe, J., Lappe, P., Weber, J., and Frey, G. D. (2013). *Aldehydes, Aliphatic: Ullmann's Encyclopedia of Industrial Chemistry*. Hoboken, NJ: Wiley. doi: 10.1002/14356007.a01_321.pub3

Ladkau, N., Assmann, M., Schrewe, M., Julsing, M. K., Schmid, A., and Buhler, B. (2016). Efficient production of the Nylon 12 monomer omega-aminododecanoic acid methyl ester from renewable dodecanoic acid methyl ester with engineered *Escherichia coli*. *Metab. Eng.* 36, 1–9. doi: 10.1016/j.ymben.2016.02.011

Larkin, M. A., Blackshields, G., Brown, N. P., Chenna, R., Mcgettigan, P. A., Mcwilliam, H., et al. (2007). Clustal W and Clustal X version 2.0. *Bioinformatics* 23, 2947–2948. doi: 10.1093/bioinformatics/btm404

Larroy, C., Fernandez, M. R., Gonzalez, E., Pares, X., and Biosca, J. A. (2002). Characterization of the *Saccharomyces cerevisiae* YMR318C (ADH6) gene product as a broad specificity NADPH-dependent alcohol dehydrogenase: relevance in aldehyde reduction. *Biochem. J.* 361, 163–172. doi: 10.1042/0264-6021:3610163

Latip, W., Raja Abd Rahman, R. N. Z., Leow, A. T. C., Mohd Shariff, F., Kamarudin, N. H. A., and Mohamad Ali, M. S. (2018). The effect of N-terminal domain removal towards the biochemical and structural features of a thermotolerant lipase from an antarctic *Pseudomonas* sp. Strain *AMS*3. *Int. J. Mol. Sci.* 19:560. doi: 10.3390/ijms19020560

Lee, K. M., and DaSilva, N. A. (2005). Evaluation of the *Saccharomyces cerevisiae* ADH2 promoter for protein synthesis. *Yeast* 22, 431–440. doi: 10.1002/yea.1221

Lehtinen, T., Efimova, E., Santala, S., and Santala, V. (2018). Improved fatty aldehyde and wax ester production by overexpression of fatty acyl-CoA reductases. *Microb. Cell Fact* 17:19. doi: 10.1186/s12934-018-0869-z

Liu, Z. L., and Moon, J. (2009). A novel NADPH-dependent aldehyde reductase gene from *Saccharomyces cerevisiae* NRRL Y-12632 involved in the detoxification of aldehyde inhibitors derived from lignocellulosic biomass conversion. *Gene* 446, 1–10. doi: 10.1016/j.gene.2009.06.018

Lo, T. M., Chng, S. H., Teo, W. S., Cho, H. S., and Chang, M. W. (2016). A two-layer gene circuit for decoupling cell growth from metabolite production. *Cell Syst.* 3, 133–143. doi: 10.1016/j.cels.2016.07.012

Marsh, E. N., and Waugh, M. W. (2013). Aldehyde decarbonylases: enigmatic enzymes of hydrocarbon biosynthesis. *ACS Catal.* 3:cs400637t.

Moon, J., and Liu, Z. L. (2012). Engineered NADH-dependent GRE2 from *Saccharomyces cerevisiae* by directed enzyme evolution enhances HMF reduction using additional cofactor NADPH. *Enzyme Microb. Technol.* 50, 115–120. doi: 10.1016/j.enzmictec.2011.10.007

Moon, J., and Liu, Z. L. (2015). Direct enzyme assay evidence confirms aldehyde reductase function of Ydr541cp and Ygl039wp from *Saccharomyces cerevisiae*. *Yeast* 32, 399–407. doi: 10.1002/yea.3067

Murray, B. A. (2019). Reactions of aldehydes and ketones and their derivatives. *Organ. React. Mech.* 2015, 1–71. doi: 10.1002/0470858583.ch1

Navarro-Avino, J. P., Prasad, R., Miralles, V. J., Benito, R. M., and Serrano, R. (1999). A proposal for nomenclature of aldehyde dehydrogenases in *Saccharomyces cerevisiae* and characterization of the stress-inducible ALD2 and ALD3 genes. *Yeast* 15, 829–842. doi: 10.1002/(sici)1097-0061(199907)15:10a<829::aid-yea423>3.0.co;2-9

Nobutada, T., Takamasa, N., Kazuo, T. N., and Akira, H. (2001). SDR structure, mechanism of action, and substrate recognition. *Curr. Organ. Chem.* 5, 89–111. doi: 10.2174/1385272013375751

Perez-Garcia, F., and Wendisch, V. F. (2018). Transport and metabolic engineering of the cell factory *Corynebacterium glutamicum*. *FEMS Microbiol. Lett.* 365:fny166. doi: 10.1093/femsle/fny166

Reiser, S., and Somerville, C. (1997). Isolation of mutants of Acinetobacter calcoaceticus deficient in wax ester synthesis and complementation of one mutation with a gene encoding a fatty acyl coenzyme A reductase. *J. Bacteriol.* 179, 2969–2975. doi: 10.1128/jb.179.9.2969-2975.1997

Runguphan, W., and Keasling, J. D. (2014). Metabolic engineering of *Saccharomyces cerevisiae* for production of fatty acid-derived biofuels and chemicals. *Metab. Eng.* 21, 103–113. doi: 10.1016/j.ymben.2013.07.003

Sayers, E. W., Beck, J., Brister, J. R., Bolton, E. E., Canese, K., Comeau, D. C., et al. (2020). Database resources of the national center for biotechnology information. *Nucleic Acids Res.* 48, D9–D16. doi: 10.1093/nar/gkz899

Schirmer, A., Rude, M. A., Li, X., Popova, E., and Del Cardayre, S. B. (2010). Microbial biosynthesis of alkanes. *Science* 329, 559–562. doi: 10.1126/science.1187936

Schrodinger, L. L. C. (2010). The PyMOL Molecular Graphics System, Version 1.3r1.

Teixeira, P. G., Ferreira, R., Zhou, Y. J., Siewers, V., and Nielsen, J. (2017). Dynamic regulation of fatty acid pools for improved production of fatty alcohols in *Saccharomyces cerevisiae*. *Microb. Cell Fact.* 16:45. doi: 10.1186/s12934-017-0663-3

Teo, W. S., Ling, H., Yu, A. Q., and Chang, M. W. (2015). Metabolic engineering of *Saccharomyces cerevisiae* for production of fatty acid short- and branched-chain alkyl esters biodiesel. *Biotechnol. Biofuels* 8:177. doi: 10.1186/s13068-015-0361-5

Willis, R. M., Wahlen, B. D., Seefeldt, L. C., and Barney, B. M. (2011). Characterization of a fatty acyl-CoA reductase from *Marinobacter aquaeolei* VT8: a bacterial enzyme catalyzing the reduction of fatty acyl-CoA to fatty alcohol. *Biochemistry* 50, 10550–10558. doi: 10.1021/bi2008646

Xia, P. F., Ling, H., Foo, J. L., and Chang, M. W. (2019). Synthetic genetic circuits for programmable biological functionalities. *Biotechnol. Adv.* 37:107393. doi: 10.1016/j.biotechadv.2019.04.015

Xu, P., Qiao, K., Ahn, W. S., and Stephanopoulos, G. (2016). Engineering *Yarrowia lipolytica* as a platform for synthesis of drop-in transportation fuels and oleochemicals. *Proc. Natl. Acad. Sci. U.S.A.* 113, 10848–10853. doi: 10.1073/pnas.1607295113

Yu, A. Q., Juwono, N. K., Foo, J. L., Leong, S. S., and Chang, M. W. (2016). Metabolic engineering of *Saccharomyces cerevisiae* for the overproduction of short branched-chain fatty acids. *Metab. Eng.* 34, 36–43. doi: 10.1016/j.ymben.2015.12.005

Yu, Y., Liu, Z., Yang, M., Chen, M., Wei, Z., Shi, L., et al. (2017). Characterization of full-length and truncated recombinant kappa-carrageenase expressed in *Pichia pastoris*. *Front. Microbiol.* 8:1544. doi: 10.3389/fmicb.2017.01544

Zhang, C., Chen, X., Stephanopoulos, G., and Too, H. P. (2016). Efflux transporter engineering markedly improves amorphadiene production in *Escherichia coli*. *Biotechnol. Bioeng.* 113, 1755–1763. doi: 10.1002/bit.25943

Zhou, Y. J., Buijs, N. A., Zhu, Z., Gomez, D. O., Boonsombuti, A., Siewers, V., et al. (2016a). Harnessing yeast peroxisomes for biosynthesis of fatty-acid-derived biofuels and chemicals with relieved side-pathway competition. *J. Am. Chem. Soc.* 138, 15368–15377. doi: 10.1021/jacs.6b07394

Zhou, Y. J., Buijs, N. A., Zhu, Z., Qin, J., Siewers, V., and Nielsen, J. (2016b). Production of fatty acid-derived oleochemicals and biofuels by synthetic yeast cell factories. *Nat. Commun.* 7:11709. doi: 10.1038/ncomms11709

Zhu, Z., Zhou, Y. J., Kang, M. K., Krivoruchko, A., Buijs, N. A., and Nielsen, J. (2017). Enabling the synthesis of medium chain alkanes and 1-alkenes in yeast. *Metab. Eng.* 44, 81–88. doi: 10.1016/j.ymben.2017.09.007

Conflict of Interest: The authors declare that the research was conducted in the absence of any commercial or financial relationships that could be construed as a potential conflict of interest.

frontiers in Bioengineering and Biotechnology

ORIGINAL RESEARCH
published: 22 October 2020
doi: 10.3389/fbioe.2020.00954

Engineering the Yeast *Yarrowia lipolytica* for Production of Polylactic Acid Homopolymer

Sophie Lajus[1], Simon Dusséaux[1], Jonathan Verbeke[2], Coraline Rigouin[1], Zhongpeng Guo[1], Maria Fatarova[1], Floriant Bellvert[1], Vinciane Borsenberger[1], Mélusine Bressy[1], Jean-Marc Nicaud[2], Alain Marty[1,3] and Florence Bordes[1]**

[1] TBI, CNRS, INRAE, INSA, Université de Toulouse, Toulouse, France, [2] INRAE, AgroParisTech, Université Paris-Saclay, Micalis Institute, Jouy-en-Josas, France, [3] Carbios, Biopôle Clermont Limagne, Saint-Beauzire, France

Polylactic acid is a plastic polymer widely used in different applications from printing filaments for 3D printer to mulching films in agriculture, packaging materials, etc. Here, we report the production of poly-D-lactic acid (PDLA) in an engineered yeast strain of *Yarrowia lipolytica*. Firstly, the pathway for lactic acid consumption in this yeast was identified and interrupted. Then, the heterologous pathway for PDLA production, which contains a propionyl-CoA transferase (PCT) converting lactic acid into lactyl-CoA, and an evolved polyhydroxyalkanoic acid (PHA) synthase polymerizing lactyl-CoA, was introduced into the engineered strain. Among the different PCT proteins that were expressed in *Y. lipolytica*, the *Clostridium propionicum* PCT exhibited the highest efficiency in conversion of D-lactic acid to D-lactyl-CoA. We further evaluated the lactyl-CoA and PDLA productions by expressing this PCT and a variant of *Pseudomonas aeruginosa* PHA synthase at different subcellular localizations. The best PDLA production was obtained by expressing the PCT in the cytosol and the variant of PHA synthase in peroxisome. PDLA homopolymer accumulation in the cell reached 26 mg/g-DCW, and the molecular weights of the polymer (Mw = 50.5 × 10^3 g/mol and Mn = 12.5 × 10^3 g/mol) were among the highest reported for an *in vivo* production.

Keywords: *Yarrowia lipolytica*, polylactic acid, cellular compartments, PHA synthase, CoA analysis

OPEN ACCESS

Edited by:
Mark Blenner, Clemson University, United States

Reviewed by:
Jingwen Zhou, Jiangnan University, China
Guokun Wang, Technical University of Denmark, Denmark

****Correspondence:***
Alain Marty
alain.marty@carbios.fr
Florence Bordes
Florence.bordes@insa-toulouse.fr

Specialty section:
This article was submitted to Synthetic Biology, a section of the journal Frontiers in Bioengineering and Biotechnology

Received: *14 April 2020*
Accepted: *23 July 2020*
Published: *22 October 2020*

Citation:
Lajus S, Dusséaux S, Verbeke J, Rigouin C, Guo Z, Fatarova M, Bellvert F, Borsenberger V, Bressy M, Nicaud J-M, Marty A and Bordes F (2020) Engineering the Yeast Yarrowia lipolytica for Production of Polylactic Acid Homopolymer. Front. Bioeng. Biotechnol. 8:954. doi: 10.3389/fbioe.2020.00954

INTRODUCTION

Today, most plastics are made from petroleum products and are highly persistent in the environment. With the growing awareness of the society concerns in the environment, the depletion of fossil resources and the increase in energy cost, the need for the development of sustainable production systems for polymer materials is more pressing than ever.

Polylactic acid produced from lactic acid, is expected to become both an alternative to petroleum-based plastic and a very important bio-based polymer because of its biocompatible properties and biodegradability in industrial composting. PLA can be easily processed by extrusion,

Abbreviations: CoA, coenzyme A; LDH, lactate dehydrogenase; PCT, propionyl-CoA transferase; PDLA, poly-D-lactic acid; PHA, polyhydroxyalkanoic acid; PLA, polylactic acid; PLLA, poly-L-lactic acid.

injection, molding, blowing, dry-jet-wet spinning, etc., and allows a large range of applications, particularly for short-term uses (i.e., food packaging, bags, films, fibers, etc.) (Jamshidian et al., 2010). Due to their excellent biocompatibility and mechanical properties, PLA and its copolymers are becoming widely used in tissue engineering for function restoration of impaired tissues, in drug delivery systems, and in various medical implants (Jamshidian et al., 2010).

Lactic acid, the synthon of PLA, exists in two enantiomeric forms, D-lactic acid and L-lactic acid. Different types of polymers can be then synthetized from them, homopolymers, such as PLLA exclusively comprising L-lactic acid, PDLA only being made of D-lactic acid, and polymers consisting of both. Enantiomeric composition of the polymer modulates PLA mechanical properties, especially crystallinity percentage, glass transition and melting temperatures (Ingrao et al., 2015). Homopolymers are crystalline and exhibit a T_m around 180°C. The crystallinity and T_m of PLA polymers usually decrease as enantiopurity of the lactate units lowers. Interestingly, mixing PLLA and PDLA at a 1:1 ratio improves the polymer characteristic as it results in crystalline stereo-complex PLA with T_m 50°C higher than the one of the homopolymers (Masutani and Kimura, 2014).

To date, PLA is a widely used biobased polymer exclusively produced from the polymerization of lactic acid *via* a chemical process; for which the ring-opening polymerization of lactide (cyclic dimer of lactic acid) is the most effective method of synthesis in the industry. The polymerization process in itself raises environmental, economic and health concerns as it requires a high-energy input with extreme temperature and pressure conditions, and the use of metal catalyst that often produces harmful residues. Moreover, although lactic acid produced by bacterial fermentation from renewable resources can be used, further purification and concentration steps are needed to obtain a starting materials compatible with the subsequent chemical polymerization, thus increasing the chemical footprint of the whole process.

Developing a fully biological process thus offers an attractive perspective especially for environmental concerns. In the last decade, alternative biological *in vivo* processes have been developed to produce PDLA or co-polymer containing D-lactic acid (Taguchi et al., 2008; Jung et al., 2010; Yang et al., 2010, 2011; Jung and Lee, 2011). This eco-friendly process is composed of two enzymatic steps, first activation of D-lactic acid in D-lactyl-CoA catalyzed by a PCT, and then polymerization of the resulting D-lactyl-CoA by a PHA synthase (**Supplementary Figure S1**). The CoA activation of lactic acid is not naturally found in biological processes and no occurrence of this reaction has ever been described in the KEGG database. However, literature reports that PCT from some organisms are able to accept lactic acid as well as propionic acid as substrate (Yang et al., 2010; Lindenkamp et al., 2013). The second step, polymerization, takes advantage of the promiscuous activity of PHA synthase that naturally synthetizes polymers of hydroxy-fatty acids but that is also able to polymerize lactyl-CoA into PLA (instead of hydroxy-acyl-CoA into PHA). Taguchi et al. (2008) have engineered the *Pseudomonas* sp. 61-3 PHA synthase to polymerize together lactyl-CoA and 3HB-CoA (for 3-hydroxybutyrate) and demonstrated that *Escherichia coli* expressing the engineered PHA synthases produced poly-3HB-*co*-LA copolymer containing 6 mol% of lactic acid. Further improvement of the incorporation of lactic acid (up to 20 to 49 mol%) were achieved by co-expressing the evolved PHA synthases with the *C. propionicum* PCT (Yang et al., 2010). Interestingly, PDLA homopolymer were also detected although its accumulation was quite poor (2 and 7% of DCW, for Dry Cell Weight) (Yang et al., 2010). Nevertheless, the higher the lactate proportion was in the polymer, the lower was the polymer titer. Further metabolic engineering of the resultant *E. coli* strains was necessary to improve the PDLA accumulation up to 11% DCW (Jung et al., 2010).

In this study, we use the aerobic yeast *Yarrowia lipolytica* to produce PLA. Metabolic engineering of this robust yeast has already been reported for different applications such as efficient recombinant protein expression [lipases, cellulases, etc. (Guo et al., 2017; Madzak, 2018; Celińska and Nicaud, 2019)], aroma compound production (for review, see Coelho et al., 2010) or valuable fatty acid production (Beopoulos et al., 2014; Ledesma-Amaro and Nicaud, 2016; Rigouin et al., 2017). Interestingly, this yeast has also been proven to be convenient for the production of polyhydroxyalkanoates (PHA) (Haddouche et al., 2010, 2011; Gao et al., 2015). A recent work showed that PHA accumulation can reach up to 25% DCW (Rigouin et al., 2019), which demonstrates the potential use of this yeast for polymer accumulation.

Here, we attempted to implement a pathway enabling the yeast *Y. lipolytica* to produce a homopolymer only composed of D-lactic acid (PDLA). The first step was to prevent the consumption of the substrate by identifying enzymes that are involved in lactic acid consumption in *Y. lipolytica*. Afterward, we optimized the first step of the pathway by evaluating the ability of PCT proteins from several microorganisms to produce D-lactyl-CoA in *Y. lipolytica* and then, we investigate the influence of subcellular localization of the PCT on the production of this intermediate molecule. At last, PDLA production was quantified by expressing the PHA synthase targeted to different organelles.

MATERIALS AND METHODS

Yeast Strains, Growth, and Culture Conditions for Strain Construction

All the plasmid constructions (**Table 1**) were made in the DH5 alpha strain (Promega, Madison, WI, United States). The *Y. lipolytica* strains used in this study were derived from the wild-type strain W29 (ATCC 20460) (see **Table 2**). The auxotrophic strain Po1d (Leu$^-$, Ura$^-$) has been described by Barth and Gaillardin (1996). Yl*CYB21* and Yl*DLD1* characterization was performed in the strain JMY2394 to facilitate both deletions and targeted integration at the zeta docking platform (*zeta*, *ku70*Δ) (Bordes et al., 2007; Verbeke et al., 2013). For clarity purpose, this strain will be named PK. PLA producing strains were derived from the strain JMY2159 (*MATA ura3-302 leu2-270 xpr2-322 pox1-6*Δ, *dga1*Δ, *lro1*Δ, *dga2*Δ, *fad2*Δ) (Beopoulos et al., 2014). The medium and growth conditions for *E. coli* were as described

TABLE 1 | *E. coli* strains and plasmids.

Strain (host strain)	Genotype or plasmid	References
DH5a	F80d*lac*ZDm15, *rec*A1, *end*A1, *gyr*A96, *thi*-1, *hsd*R17 (r_k-, m_k+), *sup*E44, *rel*A1, *deo*R, D(*lac*ZYA-*arg*F)U169	Promega
JME547	pUB-Cre1 (*Cre ARS68 Hyg in*)	Fickers et al. (2003)
JME803	JMP62 URA3ex pTEF	Beopoulos et al. (2012)
JME804	JMP62 LEU2ex pTEF	Beopoulos et al. (2014)
JME2075	TopoPUT-DLD1	This work
JME2253	TopoPLT-CYB21	This work
JMY2316	JMP62 LEU2ex TEF-YlDLD1	This work
JMY2318	JMP62 LEU2ex TEF-YlCYB21	This work
ThEc_040	JMP62 URA3ex TEF-PaPHA synthase opt E130D, S325T, S477R, Q481M perox	This work
ThEc_055	JMP62 URA3ex TEF-PaPHA synthase opt E130D, S325T, S477R, Q481M cyto	This work
ThEc_039	JMP62 URA3ex TEF-PaPHA synthase opt E130D, S325T, S477R, Q481M mito	This work
ThEc_054	JMP62 LEU2ex TEF-CpPCT opt V193A cyto	This work
ThEc_021	JMP62 URA3ex TEF-EnPCT opt cyto	This work
ThEc_043	JMP62 URA3ex TEF-EcPCT opt cyto	This work
ThEc_045	JMP62 URA3ex TEF-RePCT opt cyto	This work
ThEc_018	JMP62 URA2ex TEF-YlACS2 opt cyto	This work
ThEc_016	JMP62 LEU2ex TEF-Cp-PCT opt V193A perox	This work
ThEc_038	JMP62 LEU2ex TEF-Cp-PCT opt V193A mito	This work
ThEc_041	JMP62 LEU2ex 4UAS-TEF-Cp-PCT opt V193A cyto	This work

by Sambrook et al. (1989). Rich YPD medium (10 g/L yeast extract, 10 g/L peptone, 10 g/L glucose), minimal glucose medium (YNB containing 0.17% (w/v) yeast nitrogen base (without amino acids and ammonium sulfate, YNBww; Difco, Paris, France), 0.5% (*w/v*) NH_4Cl, 0.1% (*w/v*) yeast extract (BD Bioscience, Sparks, MD, United States) and 50 mM phosphate buffer, pH 6.8 and minimal medium supplemented with casamino acids (YNBcasa, YNB supplemented with casamino acids; Difco, Paris, France) or uracil (YNBura) were prepared as described previously (Mlickova et al., 2004). Growth of the indicated strain was compared to the growth of the control strain (CS cont) on YNB medium containing different carbon sources: 10 g/L glucose (initial pH 6.8), or 10 g/L DL-lactic acid (racemic mixture), or 5 g/L D-lactic acid or 5 g/L L-lactic acid (initial pH 3.5 for all lactic acid cultures). All liquid cultures were done under agitation in Erlenmeyer baffled flasks with a ratio 1/5 between volume of culture and volume of flask.

In silico Sequence Analysis

Gene and protein sequences were obtained from NCBI,[1] UniprotKB[2] and the yeast genomic database Génolevures.[3] Peptidic sequence alignments were realized by Clustal Omega at the EMBL-EBI server.[4] LDH characteristic protein domains were searched with Pfam server[5] (El-Gebali et al., 2019) that include an Interproscan analysis (Finn et al., 2017).

Target signal predictions were realized at the CBS predictions servers[6] and Mitoprot.[7]

General Genetic Techniques

Restriction enzymes were obtained from New England Biolabs (Evry, France). Genomic DNA from yeast transformants was obtained as described by Querol et al. (1992). An Applied Biosystem 2720 thermal cycler (Thermo Fisher Scientific, Courtaboeuf, France) with both *Taq* (Takara, Shiga, Japan) and *Pyrobest* (Takara, Shiga, Japan) DNA polymerase was used for PCR amplification. Amplified fragments were purified with the QIAgen Purification Kit (Qiagen, Hilden, Germany) and DNA fragments were recovered from agarose gels with the QIAquick Gel Extraction Kit (Qiagen). The yeast cells were transformed by the lithium acetate method (Barth and Gaillardin, 1996) or using Frozen-EZ Transformation kit (Zymo Research, Irvine, CA, United States).

Construction of Disrupted Strains Followed by Marker Excision

The deletion cassettes were generated by PCR amplification as described by Fickers et al. (2003). Briefly, the promoter (P) and terminator regions (T) were amplified from genomic DNA and fused by PCR with an I-*Sce*I restriction site at the junction. The PT resulting cassettes were then inserted into the PCR4RBlunt-TOPO vector (Life Technologies, Carlsbad, CA, United States) and the auxotrophic marker (either URA3ex or LEU2ex amplified by PCR) was then inserted into the vectors using I-*Sce*I restriction site to generate the corresponding (respectively PUT or PLT) vectors (**Table 1**). The PUT and PLT disruption cassettes were transformed into *Y. lipolytica*. Transformants were selected on appropriated selective media YNBcasa or YNBura, respectively, or YNB when transformants were prototroph. The corresponding ver1 and ver2 primers (**Supplementary Table S1**) were used to check gene disruption by PCR amplification of the genomic loci. Marker rescue was performed after transformation with the replicative plasmid pUB4-CreI as described by Fickers et al. (2003). The list of the primers for cassette design and strain verification is given in **Supplementary Table S1**.

Cloning and Expression of the Individual Genes of Interest Under Control of the TEF and HTEF Constitutive Promoters

Yl*DLD*1 and Yl*CYB*21 genes were respectively amplified from genomic DNA of *Y. lipolytica* with primer couples ylDLD1for/ylDLD1rev and ylCYB21for/ylCYB21rev (**Supplementary Table S1**). After digestion by *Bam*HI and

[1] www.ncbi.nlm.nih.gov

[2] http://www.uniprot.org/help/uniprotkb

[3] http://gryc.inra.fr/

[4] http://www.ebi.ac.uk/Tools/msa/clustalo/

[5] http://pfam.xfam.org/

[6] http://www.cbs.dtu.dk/services/

[7] https://ihg.gsf.de/ihg/mitoprot.html

TABLE 2 | *Y. lipolytica* strains.

Strain and used name	Parental strain	Genotype	References
Po1d	/	*MATA ura3-302 leu2-270 xpr2-322*	Barth and Gaillardin (1996)
JMY2394 (PK)	Po1d	*ku70Δ, zeta*	Verbeke et al. (2013)
PK control	Po1d	*ku70::URA3ex, zeta, LEU2ex*	Verbeke et al. (2013)
PK dld1Δ	PK	*dld1::URA3ex, LEU2ex*	This work
PK dld1Δ + TEF-DLD1	PK	*dld1Δ, pTEF-YlDLD1-LEU2ex, URA3ex*	This work
PK cyb21Δ	PK	*cyb21::LEU2ex, URA3ex*	This work
PK cyb21Δ + TEF-CYB21	PK	*cyb21Δ, pTEF-YlCYB21-LEU2ex, URA3ex*	This work
JMY2159	Po1d	*pox1-6Δ, dga1Δ, lro1Δ, dga2Δ, fad2Δ*	Beopoulos et al. (2014)
CS (for chassis strain)	JMY2159	*dld1Δ*	This work
CS cont	CS	*dld1Δ, URA3ex, LEU2ex*	This work
CS TEF-CpPCTc	CS	*dld1Δ, TEF-CpPCT opt V193A cyto-LEU2ex, URA3ex*	This work
CS TEF-CpPCTp	CS	*dld1Δ, TEF-CpPCT opt V193A pero-LEU2ex, URA3ex*	This work
CS TEF-CpPCTm	CS	*dld1Δ, TEF-CpPCT opt V193A mito-LEU2ex, URA3ex*	This work
CS HTEF-Cp PCTc	CS	*dld1Δ, HTEF-CpPCT opt V193A cyto-LEU2ex, URA3ex*	This work
CS TEF-EcPCTc	CS	*dld1Δ, TEF-EcPCT opt cyto-URA3ex, LEU2ex*	This work
CS TEF-RePCTc	CS	*dld1Δ, TEF-RePCT opt cyto-URA3ex, LEU2ex*	This work
CS TEF-EnPCTc	CS	*dld1Δ, TEF-EnPCT opt cyto-URA3ex, LEU2ex*	This work
CS TEF-YlACS2c	CS	*dld1Δ, TEF-YlACS2 opt cyto-URA3ex, LEU2ex*	This work
CS TEF-CpPCTc + TEF-PaPHAp	CS	*dld1Δ, TEF-CpPCT opt V193A cyto-LEU2ex, TEF-PaPHAC opt E130D, S325T, S477R, Q481M perox-URA3ex*	This work
CS TEF-CpPCTc + TEF-PaPHAm	CS	*dld1Δ, TEF-CpPCT opt V193A cyto-LEU2ex, TEF-PaPHAC opt E130D, S325T, S477R, Q481M mito-URA3ex*	This work
CS TEF-CpPCTc + TEF-PaPHAc	CS	*dld1Δ, TEF-CpPCT opt V193A cyto-LEU2ex, TEF-PaPHAC opt E130D, S325T, S477R, Q481M cyto-URA3ex*	This work
CS HTEF-CpPCTc + TEF-PaPHAp	CS	*dld1Δ, HTEF-CpPCT opt V193A cyto-LEU2ex, TEF-PaPHAC opt E130D, S325T, S477R, Q481M perox-URA3ex*	This work
CS HTEF-CpPCTc + HTEF-PaPHAp	CS	*dld1Δ, HTEF-CpPCT opt V193A cyto-LEU2ex, HTEF-PaPHAC opt E130D, S325T, S477R, Q481M perox-URA3ex*	This work

*Avr*II, the DNA fragments were inserted into the corresponding sites of the expression vector, deriving from JMP62 (Nicaud et al., 2002) under the control of TEF constitutive promoter (Müller et al., 1998).

The genes encoding CoA transferase from *E. coli* (EcPCT; GenBank accession number: AFJ29290.1), PCT from *Emiricella nidulans* FGSC A4 (EnPCT; GenBank accession number: EAA58342.1), PCT from *Ralstonia eutropha* H16 (RePCT; GenBank accession number: CAJ93797.1), variant V193A of PCT from *Clostridium propionicum* (CpPCT; GenBank accession number: CAB77207.1, Yang et al., 2010), and *ACS2*, encoding acetyl-CoA synthase from *Y. lipolytica* (YlACS2; accession number: XP_505057.1), were synthesized by GenScript (Hong Kong, China) with codon optimization based on the codon bias of *Y. lipolytica* (sequences in **Supplementary Information**), and cloned under the expression promoter TEF or hybrid promoter HTEF (Nicaud et al., 2002; Dulermo et al., 2017).

The plasmid allowing the expression of variants of PHA synthase from *Pseudomonas aeruginosa* corresponds to the JMP62-URA3-PHA plasmid (Haddouche et al., 2010) in which the POX promoter has been replaced by the TEF promoter by a *Cla*I-*Bam*HI cloning.

The variants of the PHA synthase were constructed by site directed mutagenesis using the QuikChange II Site-Directed Mutagenesis Kit (Agilent, Santa Clara, CA, United States), and primers are listed in **Supplementary Table S2**. All the sequences were checked by Sanger sequencing (Eurofins Genomics, Les Ulis, France).

After construction, all the plasmids were linearized by *Not*I and used to transform *Y. lipolytica*. Yeast transformants were selected by auxotrophy on the adequate minimal medium and the presence of the genes of interest was verified by PCR.

Proteins were targeted to different subcellular compartments using specific targeting signals. For peroxisome targeting, PTS1 tag, which corresponds to the last 14 amino acids of the *Y. lipolytica* isocitrate dehydrogenase (Uniprot accession number: P41555) was introduced at the C-terminal part of the protein of interest (Smith et al., 2000). For mitochondria targeting, MTS tag corresponds to the first 26 amino acids of the *Y. lipolytica* mitochondrial malic enzyme (Uniprot accession number: Q6C5F0) and was fused at the N-terminal part of the protein of interest.

Culture Conditions for PLA Production

Yeast cells were first grown on rich YPD medium at 28°C overnight. Cells were then harvested by centrifugation to remove medium and resuspended in minimal medium YNBcasa with 30 g/L glucose and 10 g/L of racemic lactic acid (L enantiomer used as carbon source and D enantiomer used as synthon for

PDLA production) with an initial OD_{600nm} around 0.5 measured with a DR 3900 spectrophotometer (Hach Lange, Loveland, CO, United States). The cultures were grown at 28°C, with an agitation of 100 rpm for 5 days. Cells were then harvested by centrifugation, washed twice with water, and the cell pellet was kept at −80°C until further analysis. Culture media were filtered through a 0.4 μm filter and kept at −20°C until analyzed.

Substrate Analysis

Glucose concentration was determined using a YSI 2900 analyzer (System C industrie, St Paul Trois Chateaux, France) or by high-performance liquid chromatography using Thermo Fisher Scientific system equipped with a RI detector and a Biorad column (Aminex HPX-87H column 300 × 7.8 mm, Marnes la Coquette, France) at 40°C using 5 mM H_2SO_4 as mobile phase at 0.4 mL/min.

Lactate concentration was determined by high-performance liquid chromatography in the same conditions described for glucose quantification. The enantiomeric composition of lactic acid was determined by high-performance liquid chromatography using Thermo Fisher Scientific system equipped with a UV detector at 254 nm and Chirex 3126 (D)-penicillamine 150 × 4.6 mm column (Phenomenex, Le Pecq, France) at 22°C using 2 mM $CuSO_4$, 15% methanol (v/v) as the mobile phase at 1 mL/min.

Microscopy

To observe PLA accumulation, cells were grown as described in section "Culture Conditions for PLA Production" and washed twice with water. Pellets were then resuspended in water and PLA accumulation was immediately visualized in the cells using BODIPY 493/503 dye (Thermo Fisher Scientific) diluted at 1 μg/mL and imaged using Eclipse Ni-E epifluorescence microscope (Nikon France S.A, Champigny sur Marne, France).

Lactyl-CoA Extraction and Determination

Yeast strains were grown in minimal medium YNBcasa with 30 g/L glucose and 10 g/L of racemic lactic acid. For PCT enantiospecificity analysis, instead of 10 g/L of racemic lactic acid solution, a mixture of 5 g/L of unlabeled L-lactic acid and 5 g/L of labeled D-lactic acid-3-^{13}C (Sigma–Aldrich, St. Quentin Fallavier, France) was used (named also (^{13}C)-D-lactic acid in this paper). At indicated time, cells were collected, separated from medium by fast filtration, and washed with 10-fold diluted medium. The filter was then placed in liquid nitrogen for rapid freezing and kept at −80°C before extraction. Then, the filter was placed in chilled extraction solution (80% methanol, 20% water with 125 mM formic acid) and subject to 3 cycles of 10 second vortex and 10 second sonication. Samples were collected, dried, and resuspended in analysis buffer (2% methanol, 98% water with 25 mM ammonium formate) by vortexing and sonication.

Yeast extracts were analyzed by UHPLC-FTMS (LTQ Orbitrap velos, Thermo Fisher Scientific) for lactyl-CoA quantification. Samples were kept at 4°C in the autosampler. A reversed phase C-18 column (Phenomenex Kinetex, 100 mm × 3 mm, particle size 1.7 μm, guard column SecurityGuard Ultra) was used for the separation (at 40°C) with a gradient of 50 mM ammonium formate adjusted to pH 8.10 with ammonium hydroxide (solvent A) and methanol (solvent B). The flow rate was set to 0.4 mL/min and the multi-step linear gradient was: 2% B at 0 min, 2% B at 2 min, 25% B at 23 min, 95% B at 23.1 min, 95% B at 28 min, 2% B at 28.1 min, 2% B at 36 min. The injection volume was 5 μL (full loop mode). Mass spectra were acquired with FTMS in positive mode with electrospray ionization at resolution R = 60,000 (at *m/z* 400) and recorded for the range of *m/z* 750-1500. Source temperature was 250°C, capillary temperature was 275°C, sheath gas at 50 AU, auxiliary gas at 10 AU, S lens level at 70%, and source voltage 4 kV. Qualitative and quantitative analyses were performed with Trace Finder software (Thermo Fisher Scientific). Identification and quantification of lactyl-CoA and lactyl-3-^{13}C-CoA were determined by extracting and integrating their exact mass (5 ppm) with Tracefinder® software (Thermo Fisher Scientific). The correction of the area of lactyl-3-^{13}C-CoA for naturally occurring isotopes from lactyl-CoA was performed with IsoCor® adapted for high resolution mass spectrometry (Millard et al., 2012; Heuillet et al., 2018).

PLA Extraction and Analysis

About 1.5 g of lyophilized cells were resuspended in 15 mL of 100 mM Tris, pH 8 added with 0.5 mg/mL zymolyase and incubated at 25°C overnight. Cell suspensions were frozen at −80°C and freeze dried until polymer extraction. Produced polymer was extracted using a Soxhlet apparatus with chloroform. To do so, about 1.5 g of dried cells were used and the chamber of the Soxhlet apparatus was filled 10 times with solvent, then solvent, and extracted materials were collected.

When necessary, PLA polymer was precipitated to remove residual fatty acids as described by Nomura et al. (2004). Briefly, PLA was precipitated by addition of ten volumes of cyclohexane to the solution of PLA in chloroform and collected by centrifugation.

Polymer composition was determined by NMR on a Bruker Avance II 500 spectrometer (Bruker Wissembourg, France). The cells extracts were thoroughly dried, prior to being diluted in $CDCl_3$ containing 1% TMS (internal standard), and transferred to 5 mm NMR tubes. NMR spectra were recorded at 298 K. Each NMR spectrum was acquired using an excitation flip angle of 30° at a radiofrequency field of 29.7 kHz, a relaxation delay of 10 s and 2 dummy scans. For each experiment, 16 scans were performed with a repetition delay of 6.5 s. PLA concentrations were determined by integration of the specific quadruplet signal at 5.19 ppm.

Molecular weight averages and dispersity of the polymer were determined by gel permeation chromatography (GPC) at 20°C using a Shimadzu system (Marne la Vallée, France) equipped with Wyatt detectors (MALLS, Dawn Heleos-II, 18 angles and refractometer, Optilab T-rEX, Toulouse, France) with two Agilent columns (PLGel 5um MIXED-C 300 × 7.5 mm). The elution solvent used was dichloromethane. Samples were resuspended in dichloromethane and filtered through a 0.4 μm filter. The weight averages and dispersity were calculated using dn/dc value determined for these conditions and equal to 0.0296.

Polylactic acid composition was analyzed according to Faisal et al. (2007). Briefly, PLA hydrolysis was conducted at 180°C and

100 bars, in distilled water for 50 min using ASE system (Thermo Scientific, Villebon-sur-Yvette, France). The hydrolysate was collected and analyzed as described in section "Substrate Analysis" for enantiomeric composition of lactic acid.

RESULTS

Lactate Uptake: *Y. lipolytica*'s Lactate Dehydrogenases

In silico Identification

To maximize the pool of substrate for PLA production, we investigated lactic acid catabolism in the yeast *Y. lipolytica*. Mansour et al. (2008) showed that this yeast is capable of consuming lactic acid but the proteins responsible for its consumption remained unknown. In *Saccharomyces cerevisiae*, two classes of enzyme are responsible for the conversion of lactic acid to pyruvate: LDH, that are encoded by DLD genes, and lactate cytochrome oxydoreductase (encoded by CYB2 gene) (Ookubo et al., 2008). Therefore, a BLAST research on *Y. lipolytica* genome was carried out on the basis of these two classes of enzymes, revealing 4 genes namely Yl*DLD1*, Yl*DLD2*, Yl*CYB21* and Yl*CYB22* (YALI0E03212, YALI0C06446, YALI0D12661, and YALI0E21307, respectively) encoding putative lactate degradation enzymes. Analysis of their protein sequences using Mitoprot website showed that YlDld1p and YlDld2p may contain a N-terminal mitochondrial target signal (respective scores of 0.9998 and 0.9962), suggesting that these LDH are targeted to mitochondria. The presence of peroxisomal target sequences PTS1 (SKL for YlCyb22p and VKL for YlCyb21p) on both Yl*Cyb* sequences suggested the peroxisome as their subcellular location. Pfam and Interproscan website analyses indicated that YlDld1p and YlDld2p present a FAD_binding_4 domain (PF01565 family), suggesting that they may exhibit specific activity toward D-lactic acid whereas YlCyb21p and YlCyb22p present a Cyt-b5 domain (PF00173 family), indicating that they may have specific activity for L-lactic acid.

Disruption and Complementation of the *Y. lipolytica* Lactate Degradation Enzymes

In order to elucidate the role of the identified enzymes, we first performed the deletions of those genes in the Po1d zeta *Ku70*Δ strain, designated as PK thereafter (Verbeke et al., 2013). This strain shows a better rate of homologous recombination, which facilitates downstream deletions. Transformants were tested for their ability to grow on different carbon sources: glucose, D- or L-lactic acid or a racemic mixture of the latter (**Figure 1**). All tested strains grew equally on glucose and Yl*CYB22* and Yl*DLD2* deletions did not affect the growth of strains on any lactic acid substrate, compared with the control strain, suggesting that these genes were not implicated in lactic acid metabolism (data not shown). On the contrary, deletion of Yl*CYB21* and Yl*DLD1* genes partially abolished the growth of the corresponding strains (PK c*yb21*Δ and PK *dld1*Δ) on a racemic mixture of L- and D-lactic acid (**Figure 1A**). Consistently, no consumption of L- or D-lactic acid was observed for those corresponding strains (**Figure 1B**). Of note, the growth of PK *dld1*Δ strain was highly impeded (**Figure 1A**), probably due to its limited L-lactic acid consumption (**Figure 1B**). However, as expected, this strain was not capable to consume D-lactic acid (**Figure 1B**).

To confirm the observed phenotypes, we overexpressed the deleted genes under the control of the constitutive promoter TEF in a rescue experiment. As shown in **Figures 1C,D**, the overexpression of Yl*DLD1* gene in PK *dld1*Δ strain completely restored the growth and D-lactic acid consumption. Similarly, overexpression of Yl*CYB21* gene in the deleted PK *cyb21*Δ strain restored the growth of the resulting strain on L-lactic acid (**Figures 1E,F**). Taken together, our results clearly illustrated that in *Y. lipolytica*, Yl*CYB21* and Yl*DLD1* genes encode for LDH, specific for L- and D-lactic acid, respectively.

Chassis Strain Construction

The JMY2159 strain (*MATA ura3-302 leu2-270 xpr2-322 pox1-6*Δ*, dga1*Δ*, lro1*Δ*, dga2*Δ*, fad2*Δ*)* (Beopoulos et al., 2014), constructed for another purpose, combines different modifications suitable for PDLA production: (1) the deletion of the six genes encoding the acyl-CoA dehydrogenase (*POX* genes) abolishes the fatty acid degradation in the peroxisome into 3-hydroxy-acyl-CoA, the natural substrate of PHA synthase: it will allow the production of a homopolymer of D-lactic acid; (2) the deletion of the 3 acyl-transferase genes (*DGA1*, *DGA2* and *LRO1*) prevents the formation of triacylglycerols and their accumulation in lipid bodies: it will allow visualization of PLA production using the lipophilic BODIPY fluorescent dye staining without interference of fluorescence associated with lipid bodies; (3) the Δ12 desaturase (*FAD2*) has also been removed from this strain but the deletion was not reverted since it does not interfere with PLA metabolic pathway. To perform our study, we further deleted Yl*DLD1* gene and, after prototrophy restoration of the strain, we obtained the chassis strain that was, as expected, unable to grow on D-lactic acid and presented the following genotype *MATA ura3-302 leu2-270 xpr2-322 pox1-6*Δ*, dga1*Δ*, lro1*Δ*, dga2*Δ*, fad2*Δ*, dld1*Δ. All the following constructions were performed in this chassis strain, subsequently named CS for clarity purposes (**Table 2**).

Lactyl-CoA Production Catalyzed by PCT

Expression of Different PCT Proteins

To be used as substrate by the PHA synthase, lactic acid has first to be activated into lactyl-CoA. We selected different PCT enzymes for this reaction: (1) PCT from *C. propionicum* (CpPCT) and PCT from *R. eutropha* (RePCT) that have been shown to be able to use lactic acid in addition to propionate as substrate (Yang et al., 2010; Lindenkamp et al., 2013), (2) a CoA transferase from *E. coli* (EcPCT) described to be active on short chain length substrates (Rangarajan et al., 2005), (3) a PCT from *E. nidulans* FGSC A4 (EnPCT) (Brock and Buckel, 2004), and (4) a potential acetyl-coenzyme A synthase from *Y. lipolytica* (YlACS2 encoded by YALI0F05962g), which presents 28% of identity with the PCT from *C. propionicum*. As a first approach, all these enzymes were expressed in the chassis strain

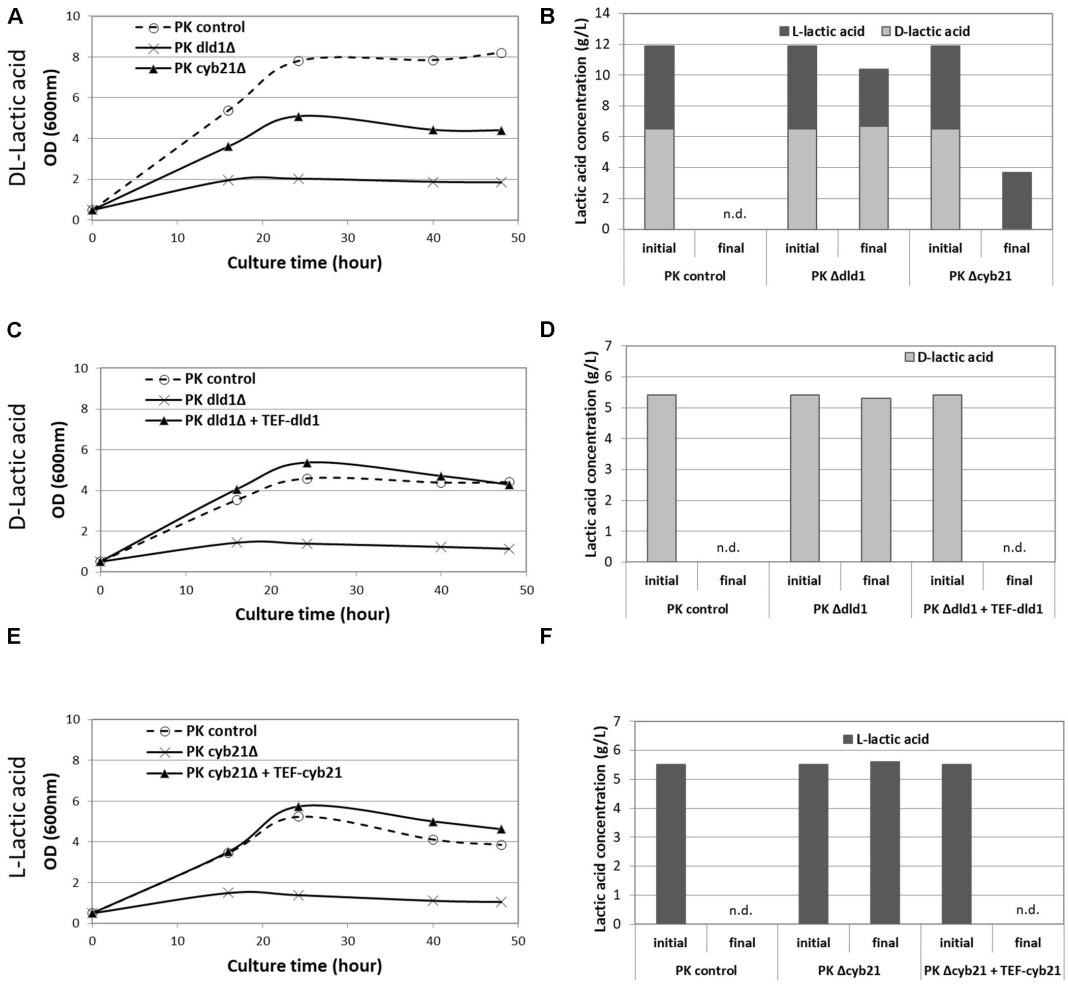

FIGURE 1 | Growth curves of strains with lactate dehydrogenase deletion and lactic acid consumption. Growth curves of PK control strain, PK dld1Δ and PK cyb21Δ strains with DL-lactic acid as carbon source **(A)**, and their lactic acid consumption **(B)**; PK control strain, PK dld1Δ and PK dld1Δ + TEF-DLD1 strains on D-lactic acid **(C)** and their D-lactic acid consumption **(D)**; PK control strain, PK cyb21Δ and PK cyb21Δ + TEF-CYB21 strains on L-lactic acid **(E)** and their L-lactic acid consumption **(F)**. Data presented are representative of at least three independent experiments. n.d., not detected.

under the control of the constitutive TEF promoter and without addition of any targeting signal, meaning that proteins were expected to be expressed in the cytosol. Throughout the text, cytoplasmic expression is indicated by a "c" at the end of the protein name.

To study the functionality of the above enzymes to produce lactyl-CoA and their putative enantio-specificity for lactic acid substrate, *Y. lipolytica* strains expressing individual CoA transferase protein were grown on minimum medium supplemented with glucose, L-lactic acid and (^{13}C)- D-lactic acid. The utilization of labeled (^{13}C)-D-lactic acid, allowed to distinguish by mass spectrometry labeled (^{13}C)-D-lactyl-CoA from unlabeled L-lactyl-CoA. After 24 h of cultivation, similar cellular levels of acetyl-CoA were detected for all strains (**Supplementary Figure S2**). As shown in **Figure 2**, only the expression of CpPCTc or RePCTc enzymes allowed the production of lactyl-CoA which is not detectable in CS control. Lactyl-CoA was not detectable in strains expressing EcPCT, EnPCT and YlACS2 (data not shown). Regarding the enantiospecificity, the strain expressing CpPCTc produced about 80% of labeled D-lactyl-CoA at 24 h and 95% after 100 h of culture, suggesting that this enzyme is specific for D-lactic acid (**Figure 2**). Surprisingly, for the strain expressing RePCTc, production of L-lactyl-CoA was detected after 24 h but no labeled D-lactyl-CoA was detected. However, after 100 h of cultivation, this strain also produced labeled D-lactyl-CoA, but the production was only about 25% of the production obtained by the strain expressing CpPCTc. Therefore, CpPCT was chosen for further engineering of *Y. lipolytica* for the production of PDLA.

Subcellular Localization of PCT Protein

In silico analysis suggested that YlDld1 protein is likely to be targeted to mitochondria, indicating that the metabolism of D-lactic acid may be favored in this specific compartment. In order to study the impact of PCT localization within

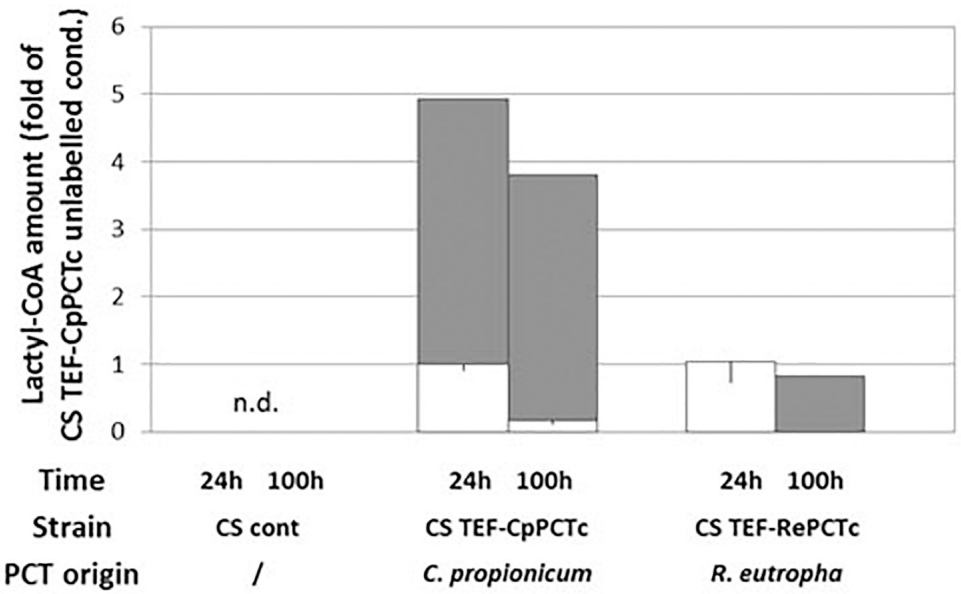

FIGURE 2 | Quantification of D- and L-lactyl-CoA produced in strain expressing PCT protein from different organisms. Strains were grown for 24 h and 100 h on minimum medium containing a mixture of 5 g/L of unlabeled L-lactic acid and 5 g/L of labeled D-lactic acid 3-^{13}C. After a normalization, results were expressed as fold of CS + TEF-CpPCTc strain unlabeled result at 24 h. White bars: unlabeled compound, gray bars: ^{13}C-labeled compound. For clarity purposes, only half error bars have been represented; to the bottom for unlabeled compound and to the top for labeled one. *N* = 3 independent experiments. n.d., not detected.

the cell on lactyl-CoA production, cytosolic expression (CpPCTc) was compared with mitochondrial (CpPCTm) or peroxisomal expression (CpPCTp), as production of PHA polymers has already been described in this compartment (Haddouche et al., 2010). We then measured lactyl-CoA production by these strains. As we showed that CpPCT was specific for D-lactic acid, cultures were performed using unlabeled D-lactic acid. After 24 h of cultivation, quantification of CoA compounds was performed. The analysis showed that acetyl-CoA amounts were equivalent in all the strains (**Supplementary Figure S3**). Nevertheless, the amount of lactyl-CoA was highly affected by the subcellular localization of the CpPCT. Indeed, lactyl-CoA was almost undetectable when CpPCT was targeted to the mitochondrial matrix (**Figure 3**). When CpPCT was addressed to the peroxisomes, lactyl-CoA production was dramatically decreased (about 10-fold) compared to cytosolic expression (**Figure 3**). Consequently, CpPCT was expressed as a cytosolic protein in the following experiments to optimize the first step of PDLA production.

PLA Production and Characterizations of the Polymer

Expression of PHA Synthase

The second step for PLA production is the polymerization of D-lactyl-CoA into PDLA by the PHA synthase (**Supplementary Figure S1**). The ability of the yeast *Y. lipolytica* to produce PHA polymers in peroxisomes has been demonstrated previously by targeting a PHA synthase from *P. aeruginosa* to this compartment (Haddouche et al., 2010, 2011; Gao et al., 2015; Rigouin et al., 2019). The ability of the PHA synthase from *Pseudomonas* species to produce polymer containing lactic acid was already demonstrated in bacteria (for example, see Taguchi et al., 2008). Taguchi et al. (2008) described many different variants of the PHA synthase with an improved ability to use short synthons, such as lactyl-CoA. In the present work, we co-expressed CpPCTc with either the *P. aeruginosa* wild-type PHA synthase or with the quadruple variant (E130D, S325T, S477R, and Q481M) which has been described to allow the production of PDLA in engineered bacteria (Jung et al., 2010). After 5 days of culture and extraction, PDLA was quantified by NMR analysis. Our results showed that expressing the wild-type PHA synthase did not lead to any PDLA polymer production neither expressed in the cytosol nor targeted to the peroxisome (data not shown). When expressing the *P. aeruginosa* quadruple PHA synthase variant either in the cytosol or in the mitochondria very low level of PDLA was detected (**Figure 4**). For both cytoplasmic and mitochondrial targeting, the low levels of PDLA accumulation might result from low activity in these compartments or low substrate concentration. However, when the PHA synthase variant was targeted into peroxisomes, PDLA was successfully accumulated (**Figure 4**). Later, PaPHAp will refer to the quadruple variant targeted into the peroxisomes.

To confirm this result, we followed PDLA accumulation by fluorescence microscopy using BODIPY dye (**Supplementary Figure S4**). Images clearly showed no PDLA accumulation in

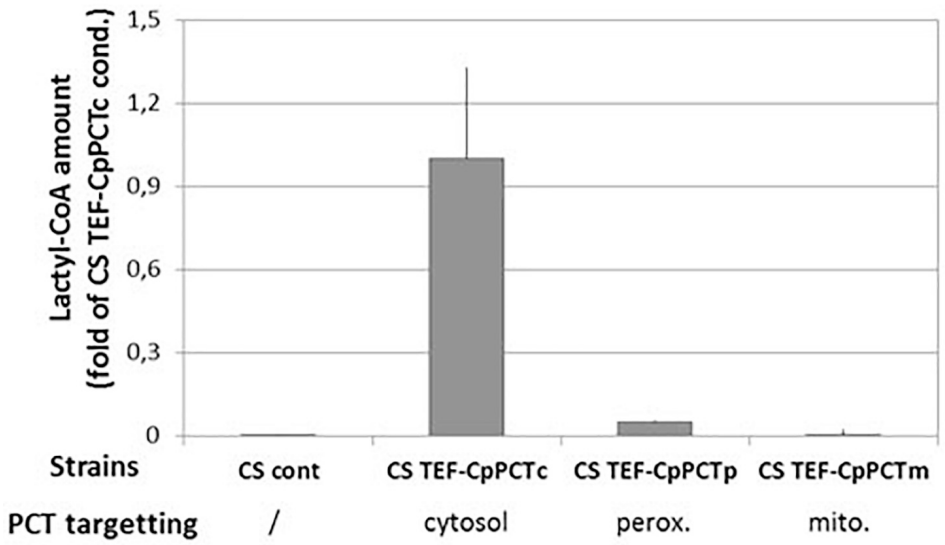

FIGURE 3 | Quantification of lactyl-CoA produced in strain expressing PCT protein from *C. propionicum* targeted to different subcellular compartments. Strains were grown for 24 h on minimum medium containing a mixture of 10 g/L of lactic acid. After a normalization, results were expressed as fold of CS TEF-CpPCTc strain result. For clarity purposes, only half error bars have been represented. *N* = 3 independent experiments.

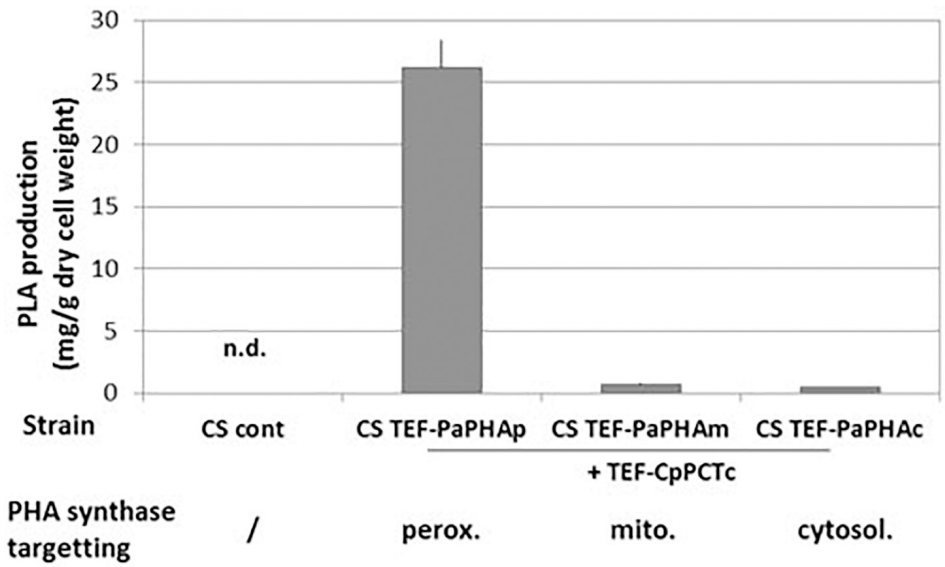

FIGURE 4 | PDLA quantification in strains expressing PHA polymerase targeted to different subcellular compartments. Strains expressing cytosolic PCT from *C. propionicum* and PHA synthase from *P. aeruginosa* targeted to indicated compartment were grown for 5 days on minimum medium containing a mixture of 10 g/L of lactic acid. After extraction, PLA quantification was measured by NMR using PLA specific peaks. *N* = 3 minimum independent experiments. n.d., not detected.

the CS strain. However, in the strain CS TEF-CpPCTc + TEF-PaPHAp, PDLA production was detected after 2 days and this production increased during the three following days. These results demonstrate that D-lactyl-CoA produced in the cytosol is likely transported into peroxisomes for an efficient polymerization by PHA synthase quadruple variant. After 5 days, the biomass reached 6.1 g/L and the accumulation of PLA reached 26.2 ± 2.3 mg/g DCW, corresponding to a titer of 158.5 mg/L. However, optimization of the production was not the purpose of this study and these data are only based on samples obtained after 5 days of culture in baffled flasks.

As shown in **Figure 5**, the ^{1}H-NMR spectra of the polymer produced with this strain displayed specific quadruplet of

PLA homopolymers (copolymers produce an unresolvable multiplet), but also signals of free fatty acids (**Figure 5A**). Furthermore, the double doublets (type AB) between 2.66 and 2.45 ppm, which are characteristic of 3-hydroxy-fatty acids were not observed in the spectra indicating that the PLA polymer was solely constituted of lactic acid units. After a step of purification by cyclohexane precipitation, ^{1}H-NMR of the purified PLA showed that fatty acids contaminants were successfully removed (**Figure 5B**). To further determine the lactic acid enantiomeric composition of the polymer, it was subjected to total hydrolysis (Faisal et al., 2007), and the hydrolysate was analyzed by HPLC using an enantiospecific lactic acid column. Only D-lactic acid could be detected (**Figure 6**). The combined analysis done by NMR and by HPLC give evidence that the polymer produced *in vivo* is an enantiopure PDLA homopolymer devoid of any 3-hydroxy-fatty acid. Additionally, the polymer size was determined using GPC and we found that PDLA molecular weights (Mw) reached 50.5×10^3 g/mol and dispersity of 4.05.

Optimization of PDLA Production

In order to determine the best production conditions, we assessed the impact of the substrate supply (D-lactic acid) on PDLA production in the CS TEF-CpPCTc + TEF-PaPHAp strain. For this purpose, cells were grown in minimum medium supplemented with glucose and L-lactic acid at 5 g/L with D-lactic acid concentration ranging from 0.5 g/L to 10 g/L. We observed that PDLA production increased when initial D-lactic acid concentration varied from 0.5 g/L to 5 g/L then reached a plateau (**Supplementary Figure S5**). D-Lactic acid was quantified in the medium at the end of the cultures and no culture was depleted in lactic acid (data not shown). It was worth noting that in all cases, D-lactic acid introduced was in excess in the media regarding PDLA production. These results demonstrate that when initial D-lactic acid concentration is equal to or above 5 g/L, the substrate supply is not bottlenecking the pathway.

To improve PDLA production, we increased PCT and PHA synthase expression level using a hybrid TEF promoter (HTEF) which has showed to increase protein expression (Dulermo et al., 2017). The promoter change did not affect

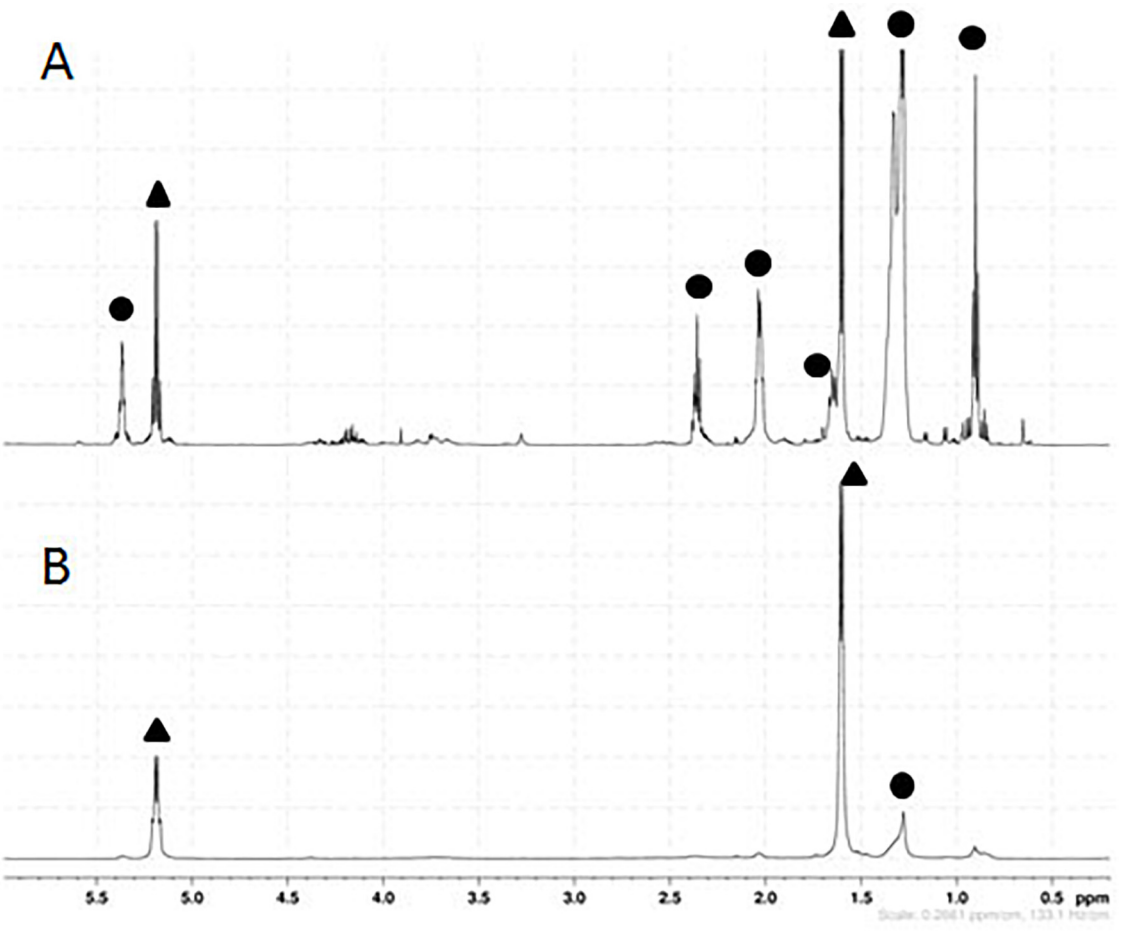

FIGURE 5 | Proton nuclear magnetic resonance (1H-NMR) spectra of PLA. PLA was extracted from lyophilized culture of CS TEF-CpPCTc + TEF-PaPHAp strain using chloroform soxhlet **(A)** and then purified **(B)**. Signals pertaining to PLA are designated by a black triangle, whilst signals belonging to free fatty acids from the cellular extraction are indicated by a black circle. These experiments are representative of three independent experiments.

acetyl-CoA level (CS HTEF-CpPCTc) but did increase two-fold the cellular lactyl-CoA content (**Figure 7** and **Supplementary Figure S6**).

As using HTEF promoter to control CpPCT expression has a positive impact on lactyl-CoA accumulation, new strains were constructed expressing CpPCTc under HTEF control and PHA synthase variant under either the control of the TEF or the HTEF promoter. A first PDLA quantification was determined by strains grown in the conditions optimized for PLA production. Interestingly, these preliminary results showed the improvement of PDLA production to 30.6 mg/g $_{DCW}$ for HTEF-CpCPTc + TEF-PaPHAp and up to 34.8 mg/g $_{DCW}$ for HTEF-CpCPTc + HTEF-PaPHAp corresponding to a 32% improvement in PDLA production (**Supplementary Figure S7**). However, using HTEF promoter to control CpCPTc (HTEF/TEF) or both genes (HTEF/HTEF), the Mw of the

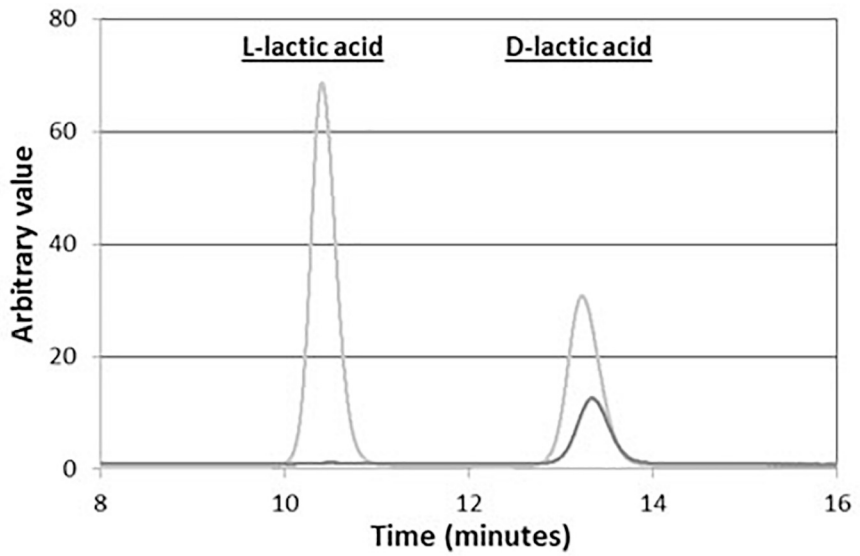

FIGURE 6 | Composition in lactic acid of PLA produced *in vivo* in CS TEF-CpPCTc + TEF-PaPHAp yeast strain after hydrolysis. PLA was extracted from CS + TEF-CpPCTc + TEF-PaPHAp strain after 5-day cultivation, then purified and hydrolyzed. The extracted solution was then analyzed by HPLC. This experiment is representative of three independent experiments.

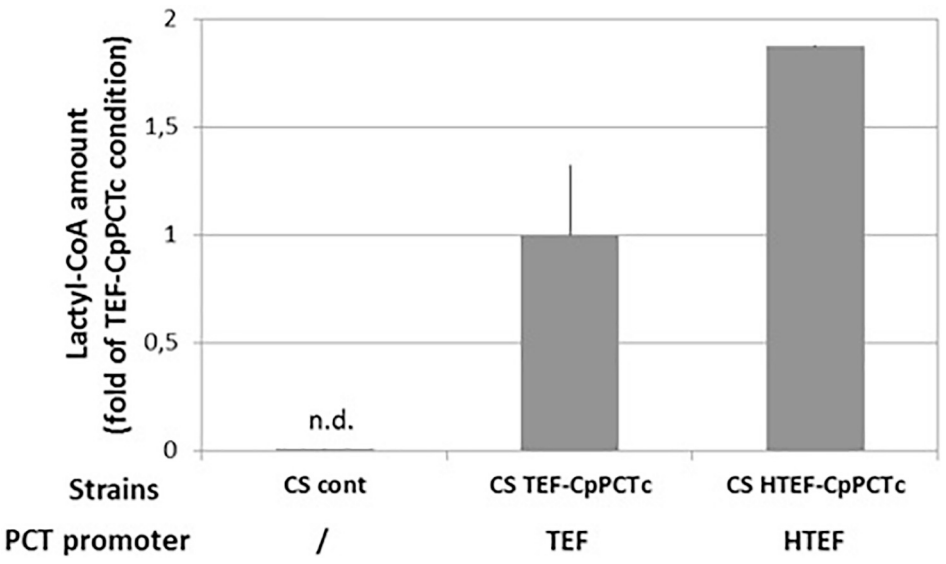

FIGURE 7 | Quantification of lactyl-CoA produced in strain expressing *C. propionicum* cytosolic PCT protein under the control of different promoters. Strains were grown for 24 h on minimum medium containing a mixture of 10 g/L of lactic acid. After a normalization, results were expressed as fold of CS TEF-CpPCTc strain result. For clarity purposes, only half error bars have been represented. *N* = 3 independent experiments.

polymers observed decreased (from 50.5×10^3 g/mol to 30.3 and 22.5×10^3 g/mol, respectively).

DISCUSSION

Although microbial PHA production has been extensively described in a variety of organisms that could accumulate impressive quantities of biopolymer (>80% DCW) (Choi et al., 2020), PLA biosynthesis has been only reported in *E. coli* strains so far. Despite the initial PLA accumulation in the engineered *E. coli* was very low (of only 0.5% DCW), further improvement of the accumulation yield of PLA to 11% DCW has been achieved after an extensive work of metabolic engineering (Jung et al., 2010). In this study, we report for the first time the production of PDLA in an eukaryotic organism, the yeast *Y. lipolytica* and a 2.6% DCW accumulation of PLA was obtained after limited modifications (the deletion of Yl*DLD1* responsible of the D-lactate consumption and the expression of the two enzymes of the PLA biosynthesis pathway).

More importantly, our results give valuable insights for PDLA production in compartmentalized eukaryotes. We investigated three cellular compartments (cytosol, mitochondria and peroxisomes) for the two steps of the PDLA production pathway. Mitochondria present the advantage of a high acetyl-CoA pool (Xua et al., 2016), which is essential as it is the co-substrate of the reaction for the CoA transferase activity of the PCT, whereas peroxisomes have already been proven to be a good environment for PHA production (Rigouin et al., 2019). It is interesting to note that the best PDLA production is obtained when the two enzymes of the pathway are located in different cellular compartments. Indeed, the production of the first intermediate, D-lactyl-CoA, is optimal when the PCT is expressed in the cytosol, and its polymerization in PDLA, only occurs when the PHA synthase is addressed to the peroxisomes. Our results clearly demonstrate that metabolic pathway efficiency can be highly modified using enzyme targeting strategies.

In our particular case, lactyl-CoA was not produced when the PCT was targeted to the mitochondria. This result suggests that either the physiological environment of this organelle may inactivate the enzyme, or that D-lactic acid may not be transported in the mitochondria in this condition. When the PCT is targeted to peroxisomes, a small production of lactyl-CoA has been detected, which indicates that the enzyme is active in that compartment to some extent. However, we could not exclude an incomplete transport of the PCT into the peroxisome via the PEX5 import pathway inducing some residual activity in the cytosol. Nevertheless, the lactyl-CoA production is much lower into the peroxisome than the one observed in the cytosol. One possible explanation could be that the deletion of the β-oxidation pathway (necessary for the production of a homopolymer deprived of any hydroxyalkanoates) severely reduced the acetyl-CoA pool and thus greatly limits the PCT activity in this compartment.

Interestingly, the highest PDLA production is achieved when the PHA synthase is targeted to peroxisomes. It suggests that the D-lactyl-CoA is efficiently transported to peroxisomes where it can be polymerized. This could be done by half-ABC peroxisomal CoA transporters likely Pxa1p or Pxa2p (Dulermo et al., 2015). We strongly suspect that the confined environment of the peroxisome helps to overcome the low affinity of the enzyme for D-lactyl-CoA by bringing the reaction partners closer and by increasing their local concentration. This is also supported by previous reports showing that dimerization of this enzyme is crucial for its activity (Wodzinska et al., 1996; Zhang et al., 2000; Chek et al., 2020). This spatial constraint of the peroxisome is also likely to help the PHA synthase to stay attached to the polymer to ensure the elongation reaction, thus explaining the high molecular weight of PLA obtained here. The inheritance of peroxisome during cell division is another advantage of the system (Chang et al., 2007). Indeed, commonly, these organelles are not made *de novo*, but are distributed equitably between daughter and mother cells, thus ensuring a low polydispersity for the polymer.

The engineered yeast strain yielded a polymer solely composed of lactic acid without any 3-hydroxy-fatty acid contamination. This purity results from (1) confinement of the polymerization in peroxisomes with the use of a strain devoid of the beta oxidation pathway, meaning the absence of 3-hydroxy-fatty acid production in this compartment and, (2) PHA synthase has no access to 3-hydroxy-fatty acid which may be produced from *de novo* fatty acid synthesis as this one occurs in cytosol. The use of a eukaryotic host that allows compartmentalization is thus a major advantage to obtain a polymer only composed of lactic acid.

Nowadays, the synthesis of PLA is based on a biosourced synthon polymerized by a chemical process. The development of microorganism able to polymerize lactic acid opens the way to establish a fully biological process for plastic synthesis. With a biological polymerization, the downstream purification steps of lactic acid needed for the chemical process could be drastically reduced as we demonstrate that neither enantiopure nor highly concentrated lactic acid is needed to produce a polymer of excellent enantiopurity, which is a crucial characteristic for the polymer properties. To go further, both the biological lactic acid production and lactic acid polymerization could be combined in a one–pot bioreactor either by co-culturing strains dedicated for each step or by integrating the two steps in one unique organism. Indeed, in *E. coli*, the highest accumulation was reported for strains metabolically engineered to produce lactate. Such a strategy presents the benefit to alleviate limitations related with the import of the synthon into the cells. It could thus be interesting to metabolically engineer a PDLA producing strain to produce its own D-lactic acid or, conversely, to engineer metabolic pathway for PDLA in an eukaryotic chassis capable of D-lactic acid production. In this context, D-lactic acid eukaryotic producer such as *S. cerevisiae*, *Pichia kudriavzevii* or *Rhizopus oryzae* (Sauer et al., 2010; Baek et al., 2016; Park et al., 2018) could be good candidates. However, biological polymer production raise the question of its extraction, as the purification of microbial biopolymers is

one of the major challenges to overcome for their industrial development (Kosseva and Rusbandi, 2018). In this field, the polymer extraction could benefit of the recent advances on lipid extraction developed in *Y. lipolytica* (Drévillon et al., 2018; Yook et al., 2019).

DATA AVAILABILITY STATEMENT

The raw data supporting the conclusions of this article will be made available by the authors, without undue reservation, to any qualified researcher.

AUTHOR CONTRIBUTIONS

JV realized the *in silico* sequence analysis. SL, SD, JV, and MB carried out strain constructions and monitoring of the culture. SL realized the polymer extractions and analysis by gel permeation chromatography. VB setup and performed the NMR analysis. MF and FBe set up the condition for CoA extraction and analysis by GC-MS. SL, SD, JV, MB, CR, and ZG performed the experiments. All participated to the analysis of the results. SL, FBo, AM, and J-MN contributed to the design of the study. FBo, AM, and J-MN supervised the study. SL wrote the first draft of the manuscript. All authors contributed to manuscript revision, read and approved the submitted version.

FUNDING

This project was co-funded by national funding and the Carbios company in the framework of contract OSEO ISI for the Strategic Industrial Innovation Project THANAPLAST – No. I 1206040W.

ACKNOWLEDGMENTS

Glucose analyses were achieved on TWB Biotransformation and culture process platform and on TWB Analytical platform (TWB, Toulouse, France). Lactic acid quantification and polymer molecular weight measurement were performed on TWB Analytical platform. RMN and lactyl-CoA quantification were achieved on MetaToul platform (INSA Toulouse, France).

SUPPLEMENTARY MATERIAL

The Supplementary Material for this article can be found online at: https://www.frontiersin.org/articles/10.3389/fbioe.2020.00954/full#supplementary-material

REFERENCES

Baek, S. H., Kwon, E. Y., Kim, Y. H., and Hahn, J. S. (2016). Metabolic engineering and adaptive evolution for efficient production of D-lactic acid in *Saccharomyces cerevisiae*. *Appl. Microbiol. Biotechnol.* 100, 2737–2748. doi: 10.1007/s00253-015-7174-0

Barth, G., and Gaillardin, C. (1996). "*Yarrowia lipolytica*," *in Nonconventional Yeasts in Biotechnology*. Berlin: Springer, 313–388. doi: 10.1007/978-3-642-79856-6_10

Beopoulos, A., Haddouche, R., Kabran, P., Dulermo, T., Chardot, T., and Nicaud, J. M. (2012). Identification and characterization of DGA2, an acyltransferase of the DGAT1 acyl-CoA:diacylglycerol acyltransferase family in the oleaginous yeast Yarrowia lipolytica. New insights into the storage lipid metabolism of oleaginous yeasts. *Appl. Microbiol. Biotechnol.* 93, 1523–1537. doi: 10.1007/s00253-011-3506-x

Beopoulos, A., Verbeke, J., Bordes, F., Guicherd, M., Bressy, M., Marty, A., et al. (2014). Metabolic engineering for ricinoleic acid production in the oleaginous yeast *Yarrowia lipolytica*. *Appl. Microbiol. Biotechnol.* 98, 251–262. doi: 10.1007/s00253-013-5295-x

Bordes, F., Fudalej, F., Dossat, V., Nicaud, J. M., and Marty, A. (2007). A new recombinant protein expression system for high-throughput screening in the yeast *Yarrowia lipolytica*. *J. Microbiol. Methods* 70, 493–502. doi: 10.1016/j.mimet.2007.06.008

Brock, M., and Buckel, W. (2004). On the mechanism of action of the antifungal agent propionate. Propionyl-CoA inhibits glucose metabolism in *Aspergillus nidulans*. *Eur. J. Biochem.* 271, 3227–3241. doi: 10.1111/j.1432-1033.2004.04255.x

Celińska, E., and Nicaud, J. M. (2019). Filamentous fungi-like secretory pathway strayed in a yeast system: peculiarities of *Yarrowia lipolytica* secretory pathway underlying its extraordinary performance. *Appl. Microbiol. Biotechnol.* 103, 39–52. doi: 10.1007/s00253-018-9450-2

Chang, J., Fagarasanu, A., and Rachubinski, R. A. (2007). Peroxisomal peripheral membrane protein YlInp1p is required for peroxisome inheritance and influences the dimorphic transition in the yeast *Yarrowia lipolytica*. *Eukaryot. Cell* 6, 1528–1537. doi: 10.1128/EC.00185-07

Chek, M. F., Kim, S.-Y., Mori, T., Tan, H. T., Sudesh, K., and Hakoshima, T. (2020). Asymmetric open-closed dimer mechanism of polyhydroxyalkanoate synthase PhaC. *iScience* 23:101084. doi: 10.1016/j.isci.2020.101084

Choi, S. Y., Rhie, M. N., Kim, H. T., Joo, J. C., Cho, I. J., Son, J., et al. (2020). Metabolic engineering for the synthesis of polyesters: a 100-year journey from polyhydroxyalkanoates to non-natural microbial polyesters. *Metab. Eng.* 58, 47–81. doi: 10.1016/j.ymben.2019.05.009

Coelho, M. A. Z., Amaral, P. F. F., and Belo, I. (2010). *Yarrowia lipolytica*: an industrial workhorse. *Appl. Microbiol. Microb. Biotechnol* 2, 930–944.

Drévillon, L., Koubaa, M., and Vorobiev, E. (2018). Lipid extraction from *Yarrowia lipolytica* biomass using high-pressure homogenization. *Biomass Bioenergy* 115, 143–150. doi: 10.1016/j.biombioe.2018.04.014

Dulermo, R., Brunel, F., Dulermo, T., Ledesma-Amaro, R., Vion, J., Trassaert, M., et al. (2017). Using a vector pool containing variable-strength promoters to optimize protein production in *Yarrowia lipolytica*. *Microb. Cell Fact.* 16:31. doi: 10.1186/s12934-017-0647-3

Dulermo, R., Gamboa-Meléndez, H., Ledesma-Amaro, R., Thévenieau, F., and Nicaud, J. M. (2015). Unraveling fatty acid transport and activation mechanisms in *Yarrowia lipolytica*. *Biochim. Biophys. Acta - Mol. Cell Biol. Lipids* 1851, 1202–1217. doi: 10.1016/j.bbalip.2015.04.004

El-Gebali, S., Mistry, J., Bateman, A., Eddy, S. R., Luciani, A., Potter, S. C., et al. (2019). The Pfam protein families database in 2019. *Nucleic Acids Res.* 47, D427–D432. doi: 10.1093/nar/gky995

Faisal, M., Saeki, T., Tsuji, H., Daimon, H., and Fujie, K. (2007). Depolymerization of Poly (L-lactic acid) under hydrothermal conditions. *Asian J. Chem.* 19, 1714–1722.

Fickers, P., Le Dall, M. T., Gaillardin, C., Thonart, P., and Nicaud, J. M. (2003). New disruption cassettes for rapid gene disruption and marker rescue in the yeast *Yarrowia lipolytica*. *J. Microbiol. Methods* 55, 727–737. doi: 10.1016/j.mimet.2003.07.003

Finn, R. D., Attwood, T. K., Babbitt, P. C., Bateman, A., Bork, P., Bridge, A. J., et al. (2017). InterPro in 2017-beyond protein family and domain annotations. *Nucleic Acids Res.* 45, D190–D199. doi: 10.1093/nar/gkw1107

Gao, C., Qi, Q., Madzak, C., and Lin, C. S. K. (2015). Exploring medium-chain-length polyhydroxyalkanoates production in the engineered yeast *Yarrowia lipolytica*. *J. Ind. Microbiol. Biotechnol.* 42, 1255–1262. doi: 10.1007/s10295-015-1649-y

Guo, Z. P., Duquesne, S., Bozonnet, S., Cioci, G., Nicaud, J. M., Marty, A., et al. (2017). Conferring cellulose-degrading ability to *Yarrowia lipolytica* to facilitate a consolidated bioprocessing approach. *Biotechnol. Biofuels* 10:132. doi: 10.1186/s13068-017-0819-8

Haddouche, R., Delessert, S., Sabirova, J., Neuvéglise, C., Poirier, Y., and Nicaud, J. M. (2010). Roles of multiple acyl-CoA oxidases in the routing of carbon flow towards β-oxidation and polyhydroxyalkanoate biosynthesis in *Yarrowia lipolytica*. *FEMS Yeast Res.* 10, 917–927. doi: 10.1111/j.1567-1364.2010.00670.x

Haddouche, R., Poirier, Y., Delessert, S., Sabirova, J., Pagot, Y., Neuvéglise, C., et al. (2011). Engineering polyhydroxyalkanoate content and monomer composition in the oleaginous yeast *Yarrowia lipolytica* by modifying the -oxidation multifunctional protein. *Appl. Microbiol. Biotechnol.* 91, 1327–1340. doi: 10.1007/s00253-011-3331-2

Heuillet, M., Bellvert, F., Cahoreau, E., Letisse, F., Millard, P., and Portais, J.-C. (2018). Methodology for the validation of isotopic analyses by mass spectrometry in stable-isotope labeling experiments. *Anal. Chem.* 90, 1852–1860. doi: 10.1021/acs.analchem.7b03886

Ingrao, C., Tricase, C., Cholewa-Wójcik, A., Kawecka, A., Rana, R., and Siracusa, V. (2015). Polylactic acid trays for fresh-food packaging: a carbon footprint assessment. *Sci. Total Environ.* 537, 385–398. doi: 10.1016/j.scitotenv.2015.08.023

Jamshidian, M., Tehrany, E. A., Imran, M., Jacquot, M., and Desobry, S. (2010). Poly-lactic acid: production, applications, nanocomposites, and release studies. *Compr. Rev. Food Sci. Food Saf.* 9, 552–571. doi: 10.1111/j.1541-4337.2010.00126.x

Jung, Y. K., Kim, T. Y., Park, S. J., and Lee, S. Y. (2010). Metabolic engineering of *Escherichia coli* for the production of polylactic acid and its copolymers. *Biotechnol. Bioeng.* 105, 161–171. doi: 10.1002/bit.22548

Jung, Y. K., and Lee, S. Y. (2011). Efficient production of polylactic acid and its copolymers by metabolically engineered *Escherichia coli*. *J. Biotechnol.* 151, 94–101. doi: 10.1016/j.jbiotec.2010.11.009

Kosseva, M. R., and Rusbandi, E. (2018). Trends in the biomanufacture of polyhydroxyalkanoates with focus on downstream processing. *Int. J. Biol. Macromol.* 107, 762–778. doi: 10.1016/j.ijbiomac.2017.09.054

Ledesma-Amaro, R., and Nicaud, J.-M. (2016). *Yarrowia lipolytica* as a biotechnological chassis to produce usual and unusual fatty acids. *Prog. Lipid Res.* 61, 40–50. doi: 10.1016/J.PLIPRES.2015.12.001

Lindenkamp, N., Schürmann, M., and Steinbüchel, A. (2013). A propionate CoA-transferase of ralstonia eutropha H16 with broad substrate specificity catalyzing the CoA thioester formation of various carboxylic acids. *Appl. Microbiol. Biotechnol.* 97, 7699–7709. doi: 10.1007/s00253-012-4624-9

Madzak, C. (2018). Engineering *Yarrowia* lipolytica for use in biotechnological applications: a review of major achievements and recent innovations. *Mol. Biotechnol.* 60, 621–635. doi: 10.1007/s12033-018-0093-4

Mansour, S., Beckerich, J. M., and Bonnarme, P. (2008). Lactate and Amino Acid Catabolism in the Cheese-Ripening Yeast *Yarrowia lipolytica*. *Appl. Environ. Microbiol.* 74, 6505–6512. doi: 10.1128/AEM.01519-08

Masutani, K., and Kimura, Y. (2014). PLA Synthesis and Polymerization. *R. Soc. Chem.* 2014, 1–36.doi: 10.1039/9781782624806-00001

Millard, P., Letisse, F., Sokol, S., and Portais, J.-C. (2012). IsoCor: correcting MS data in isotope labeling experiments. *Bioinformatics* 28, 1294–1296. doi: 10.1093/bioinformatics/bts127

Mlickova, K., Roux, E., Athenstaedt, K., d'Andrea, S., Daum, G., Chardot, T., et al. (2004). Lipid Accumulation, lipid body formation, and Acyl coenzyme a oxidases of the yeast *Yarrowia lipolytica*. *Appl. Environ. Microbiol.* 70, 3918–3924. doi: 10.1128/AEM.70.7.3918-3924.2004

Müller, S., Sandal, T., Kamp-Hansen, P., and Dalbøge, H. (1998). Comparison of expression systems in the yeasts *Saccharomyces cerevisiae*, *Hansenula polymorpha*, *Klyveromyces lactis*, *Schizosaccharomyces pombe* and *Yarrowia lipolytica*. Cloning of two novel promoters from *Yarrowia lipolytica*. *Yeast* 14, 1267–1283. doi: 10.1002/(sici)1097-0061(1998100)14:14<1267::aid-yea327>3.0.co;2-2

Nicaud, J.-M., Madzak, C., van den Broek, P., Gysler, C., Duboc, P., Niederberger, P., et al. (2002). Protein expression and secretion in the yeast *Yarrowia lipolytica*. *FEMS Yeast Res.* 2, 371–379.

Nomura, C. T., Taguchi, K., Taguchi, S., and Doi, Y. (2004). Coexpression of genetically engineered 3-ketoacyl-ACP synthase III (fabH) and polyhydroxyalkanoate synthase (phaC) genes leads to short-chain-length-medium-chain-length polyhydroxyalkanoate copolymer production from glucose in *Escherichia coli* JM109. *Appl. Environ. Microbiol.* 70, 999–1007. doi: 10.1128/AEM.70.2.999-1007.2004

Ookubo, A., Hirasawa, T., Yoshikawa, K., Nagahisa, K., Furusawa, C., and Shimiku, H. (2008). Improvement of L -lactate Production by CYB2 gene disruption in a recombinant *Saccharomyces cerevisiae* strain under low pH condition. *Biosci. Biotechnol. Biochem.* 72, 3063–3066. doi: 10.1271/bbb.80493

Park, H. J., Bae, J. H., Ko, H. J., Lee, S. H., Sung, B. H., Han, J. I., et al. (2018). Low-pH production of d-lactic acid using newly isolated acid tolerant yeast *Pichia kudriavzevii* NG7. *Biotechnol. Bioeng.* 115, 2232–2242. doi: 10.1002/bit.26745

Querol, A., Barrio, E., Huerta, T., and Ramón, D. (1992). Molecular monitoring of wine fermentations conducted by active dry yeast strains. *Appl. Environ. Microbiol.* 58, 2948–2953. doi: 10.1128/aem.58.9.2948-2953.1992

Rangarajan, E. S., Li, Y., Ajamian, E., Iannuzzi, P., Kernaghan, S. D., Fraser, M. E., et al. (2005). Crystallographic trapping of the glutamyl-CoA thioester intermediate of family I CoA transferases. *J. Biol. Chem.* 280, 42919–42928. doi: 10.1074/jbc.M510522200

Rigouin, C., Gueroult, M., Croux, C., Dubois, G., Borsenberger, V., Barbe, S., et al. (2017). Production of medium chain fatty acids by *Yarrowia lipolytica*: combining molecular design and TALEN to engineer the fatty acid synthase. *ACS Synth. Biol.* 6, 1870–1879. doi: 10.1021/acssynbio.7b00034

Rigouin, C., Lajus, S., Ocando, C., Borsenberger, V., Nicaud, J. M., Marty, A., et al. (2019). Production and characterization of two medium-chain-length polydroxyalkanoates by engineered strains of *Yarrowia lipolytica*. *Microb. Cell Fact.* 18:99. doi: 10.1186/s12934-019-1140-y

Sambrook, J., Fritsch, E. F., and Maniatis, T. (1989). *Molecular Cloning: A Laboratory Manual*. New York, NY:Cold Spring Horbor Laboratory Press.

Sauer, M., Porro, D., Mattanovich, D., and Branduardi, P. (2010). 16 years research on lactic acid production with yeast–ready for the market? *Biotechnol. Genet. Eng. Rev.* 27, 229–256. doi: 10.1080/02648725.2010.10648152

Smith, J. J., Brown, T. W., Eitzen, G. A., and Rachubinski, R. A. (2000). Regulation of peroxisome size and number by fatty acid beta-oxidation in the yeast *Yarrowia lipolytica*. *J. Biol. Chem.* 275, 20168–20178. doi: 10.1074/jbc.M909285199

Taguchi, S., Yamada, M., Matsumoto, K., Tajima, K., Satoh, Y., Munekata, M., et al. (2008). A microbial factory for lactate-based polyesters using a lactate-polymerizing enzyme. *Proc. Natl. Acad. Sci. U. S. A.* 105, 17323–17327. doi: 10.1073/pnas.0805653105

Verbeke, J., Beopoulos, A., and Nicaud, J.-M. (2013). Efficient homologous recombination with short length flanking fragments in Ku70 deficient *Yarrowia lipolytica* strains. *Biotechnol. Lett.* 35, 571–576. doi: 10.1007/s10529-012-1107-0

Wodzinska, J., Snell, K. D., Rhomberg, A., Sinskey, A. J., Biemann, K., and Stubbe, J. (1996). Polyhydroxybutyrate synthase: evidence for covalent catalysis. *J. Am. Chem. Soc.* 118, 6319–6320. doi: 10.1021/ja961108a

Xua, P., Qiao, K., Ahn, W. S., and Stephanopoulos, G. (2016). Engineering *Yarrowia lipolytica* as a platform for synthesis of drop-in transportation fuels

and oleochemicals. *Proc. Natl. Acad. Sci. U. S. A.* 113, 10848–10853. doi: 10.1073/pnas.1607295113

Yang, T. H., Jung, Y. K., Kang, H. O., Kim, T. W., Park, S. J., and Lee, S. Y. (2011). Tailor-made type II *Pseudomonas* PHA synthases and their use for the biosynthesis of polylactic acid and its copolymer in recombinant *Escherichia coli*. *Appl. Microbiol. Biotechnol.* 90, 603–614. doi: 10.1007/s00253-010-3077-2

Yang, T. H., Kim, T. W., Kang, H. O., Lee, S.-H., Lee, E. J., Lim, S.-C., et al. (2010). Biosynthesis of polylactic acid and its copolymers using evolved propionate CoA transferase and PHA synthase. *Biotechnol. Bioeng.* 105, 150–160. doi: 10.1002/bit.22547

Yook, S. D, Kim, J., Woo, H. M., Um, Y., and Lee, S. M. (2019). Efficient lipid extraction from the oleaginous yeast *Yarrowia lipolytica* using switchable solvents. *Renew. Energy* 132, 61–67. doi: 10.1016/j.renene.2018.07.129

Zhang, S., Yasuo, T., Lenz, R. W., and Goodwin, S. (2000). Kinetic and mechanistic characterization of the polyhydroxybutyrate synthase from *Ralstonia eutropha*. *Biomacromolecules* 1, 244–251. doi: 10.1021/bm005513c

Conflict of Interest: The authors declare that this project was co-funded by national funding and the Carbios company. The funder Carbios had the following involvement in the study: co-design and co-supervision of the study and contribution to manuscript redaction. AM is employed by the Carbios company. Some of the results are part of a patent corresponding to application number WO2017/10577 with SL, SD, JV, VB, J-MN, AM and FB as co-inventors.

The remaining authors declare that the research was conducted in the absence of any commercial or financial relationships that could be construed as a potential conflict of interest.

frontiers in Bioengineering and Biotechnology

REVIEW
published: 23 October 2020
doi: 10.3389/fbioe.2020.594126

Deploying Microbial Synthesis for Halogenating and Diversifying Medicinal Alkaloid Scaffolds

*Samuel A. Bradley, Jie Zhang and Michael K. Jensen**

Novo Nordisk Foundation Center for Biosustainability, Technical University of Denmark, Lyngby, Denmark

Plants produce some of the most potent therapeutics and have been used for thousands of years to treat human diseases. Today, many medicinal natural products are still extracted from source plants at scale as their complexity precludes total synthesis from bulk chemicals. However, extraction from plants can be an unreliable and low-yielding source for human therapeutics, making the supply chain for some of these life-saving medicines expensive and unstable. There has therefore been significant interest in refactoring these plant pathways in genetically tractable microbes, which grow more reliably and where the plant pathways can be more easily engineered to improve the titer, rate and yield of medicinal natural products. In addition, refactoring plant biosynthetic pathways in microbes also offers the possibility to explore new-to-nature chemistry more systematically, and thereby help expand the chemical space that can be probed for drugs as well as enable the study of pharmacological properties of such new-to-nature chemistry. This perspective will review the recent progress toward heterologous production of plant medicinal alkaloids in microbial systems. In particular, we focus on the refactoring of halogenated alkaloids in yeast, which has created an unprecedented opportunity for biosynthesis of previously inaccessible new-to-nature variants of the natural alkaloid scaffolds.

Keywords: alkaloids, yeast, halogenation, plants, new-to-nature

OPEN ACCESS

Edited by:
Farshad Darvishi,
Alzahra University, Iran

Reviewed by:
Gregory Guirimand,
Kobe University, Japan
Fumihiko Sato,
Kyoto University, Japan

****Correspondence:***
Michael K. Jensen
mije@biosustain.dtu.dk

Specialty section:
This article was submitted to Synthetic Biology, a section of the journal Frontiers in Bioengineering and Biotechnology

Received: *12 August 2020*
Accepted: *02 October 2020*
Published: *23 October 2020*

Citation:
Bradley SA, Zhang J and Jensen MK (2020) Deploying Microbial Synthesis for Halogenating and Diversifying Medicinal Alkaloid Scaffolds. Front. Bioeng. Biotechnol. 8:594126. doi: 10.3389/fbioe.2020.594126

INTRODUCTION

Plants express biosynthetic pathways capable of performing a fascinating plethora of complex chemistry (Wilson and Roberts, 2014; Kutchan et al., 2015; Wurtzel and Kutchan, 2016). Consequently, many of the biologically active compounds utilized commercially, particularly pharmaceuticals, agrochemicals, flavors and fragrances, are plant-derived natural products. Pharmaceutically important classes of plant natural products include the terpenes and terpenoids (Pichersky and Raguso, 2018; Zhou and Pichersky, 2020), polyketides (Ma et al., 2009), alkaloids (Springob and Kutchan, 2009), as well as other aromatic amino acids derivatives (Springob and Kutchan, 2009). Natural products display an impressive range and density of pharmaceutical activities, many of them are FDA-approved, and more than 50% of compounds recently introduced in drug discovery pipelines are natural products or derivatives thereof (Newman and Cragg, 2016). However, most bioactive compounds possess complex structures with multiple stereocenters and oxygenated functional groups which complicate, and even preclude, total synthesis as a means of production. For this reason extraction from natural plant resources remains indispensable for

sourcing bioactive compounds. For example, vincristine and vinblastine are alkaloids found in the Madagascar periwinkle (*Catharanthus roseus*) and listed by the WHO as essential medicines (World Health Organisation Model Lists of Essential Medicines, 2019). They are commercially produced by semi-synthesis, in which the biological precursors vindoline and catharanthine are extracted from *C. rosesus* and subsequently chemically coupled *in vitro* (Courdavault et al., 2020). Yet, due to the vagaries inherent to agriculture and natural habitats, the low *in planta* accumulation, and the complex mixture of chemically similar compounds found in *C. roseus*, vincristine supply for clinical usage can be unstable (Groot et al., 2018). Consequently, there is considerable interest in producing plant medicinal alkaloids, and other bioactive plant natural products, by refactoring the biosynthetic pathways in microorganisms, so-called microbial synthesis (Chang et al., 2007; Ajikumar et al., 2010; Brown et al., 2015; Fossati et al., 2015; Galanie et al., 2015; Qu et al., 2015; Li et al., 2018).

Supplying plant-derived therapeutics for human illnesses using microbial synthesis could create cheaper, greener and more reliable sources of these compounds as microbes (i) grow faster (hours for yeast as compared to months/years for plants), (ii) can be engineered to produce less complex mixtures of plant natural product, and (iii) can be cultivated using more standardized and easily scalable fermentation and downstream processing methods (Junker, 2004; Jungbauer, 2013; Buyel et al., 2015; Liu et al., 2016; Zydney, 2016; Wang et al., 2019a). Budding yeast (*Saccharomyces cerevisiae*) presents an attractive chassis for refactoring complex biosynthetic pathways of bioactive natural products, thanks to its eukaryotic cell architecture capable of supporting biosynthetic pathways that require significant endomembrane systems (e.g., P450 enzymes) or compartmentalization (Avalos et al., 2013; Zhou et al., 2016). Indeed, the seminal demonstration of artemisinic acid production in yeast (Ro et al., 2006; Paddon and Keasling, 2014) has inspired research into microbial biosynthesis of many more bioactive plant natural products. This is exemplified by the recent engineering of the native yeast mevalonate pathway to enable high flux toward geranyl pyrophosphate (GPP), and introduction of a heterologous hexanoyl-CoA biosynthetic pathway for the complete biosynthesis of cannabinoids (Luo et al., 2019). From tyrosine derivatives, biosynthesis of the common benzylisoquinoline alkaloid (BIA) precursor (S)-reticuline was a landmark achievement toward *de novo* biosynthesis of medicinal alkaloids, including hydrocodone, thebaine, stylopine, and noscapine (Galanie and Smolke, 2015; Hori et al., 2016; Li et al., 2018). Likewise, morphinan BIAs codeine and morphine have also been synthesized in yeast based on feeding substrates (R)-reticuline, salutaridine, and codeine (Fossati et al., 2015). In addition to BIAs, another major class of alkaloids are the monoterpene indole alkaloids (MIAs) derived from GPP and tryptophan (De Luca et al., 2014). Brown et al. (2015) demonstrated the *de novo* synthesis of strictosidine, the common precursor of all MIAs, in yeast through the successful refactoring of 12 heterologous enzymatic steps. Ehrenworth et al. (2015) engineered yeast to produce tetrahydrobiopterin for a mono-oxidation of tryptophan to 5-hydroxytryptophan and further onto 5-hydroxytryptamine (serotonin), which when coupled to exogenously fed secologanin enabled production of 10-hydroxystrictosidine. Further downstream of the MIA building blocks, Qu et al. (2015) demonstrated the seven-step conversion of tabersonine to the marketed anticancer precursor vindoline. In addition to BIAs and MIAs, the ergot alkaloid precursor chanoclavine-1 and the complex ergot alkaloid cycloclavine derived from tryptophan and the C5 isoprenoid unit dimethylallyl diphosphate (DMAPP) also exemplifies successful hijacking of native yeast metabolites for microbial alkaloid synthesis (Nielsen et al., 2014; Jakubczyk et al., 2015). Milne et al. (2020) recently reported the refactoring of the hallucinogenic alkaloid psilocybin biosynthetic pathway extending from an engineered shikimate pathway and coupled via tryptophan decarboxylase to yield the starting block tryptamine for four-step psilocybin biosynthesis. Beyond the refactoring of complete alkaloid biosynthetic pathways derived from natural mevalonate pathway C10 and C15 precursor units, GPP and FPP, respectively, Ignea et al. (2018) also refactored biosynthesis of 40 different C11 non-canonical terpene scaffolds, based on 2-methyl GPP production and engineered C11-specific monoterpene synthases. Lastly, tropane alkaloids derived from the arginine and polyamine metabolism biosynthesis, also should be mentioned to emphasize the versatility of yeast metabolism and cell architecture for microbial synthesis of bioactive alkaloids (Ping et al., 2019; Srinivasan and Smolke, 2019). While this review will focus on two major classes of alkaloids, BIAs and MIAs, it deserves to be mentioned that other branches of yeast's native metabolism have been harnessed for microbial biosynthesis of non-alkaloid bioactive natural products. This includes the production of methylxanthines from the S-adenosyl methionine (SAM) *de novo* purine synthesis pathways, and adenine nucleotide pools (McKeague et al., 2016), as well as phenylpropanoids resveratrol and breviscapin produced from the shikimate pathway (Becker et al., 2003; Liu et al., 2018). Together with an elaborate review of yeast metabolism for the production of broader classes of plant natural products, this has recently been excellently covered by Chen et al. (2020).

Beyond the rational refactoring of plant natural product pathways for microbial biosynthesis of natural alkaloids, synthetic biologists are taking inspiration from medicinal chemistry campaigns investigating small-molecule drug leads, with the objective of expanding the repertoire of medicinal plant alkaloids by including their unnatural derivatives. Bioactive natural products often proceed from lead to licensing without undergoing significant modification (Ganesan, 2008). However, there is evidence that the derivatives of plant alkaloids possess new or improved pharmaceutical activities (Leggans et al., 2013; Sears and Boger, 2015; Gautam et al., 2016; Li et al., 2018). This will be of interest for (i) finding drugs against therapeutic targets that are currently considered "undruggable," such as B-class GPCRs (Barker et al., 2013), and ii) finding improved variants against current targets—for example, 10-fluorovinblastine, 10-fluorovincristine (Sears and Boger, 2015),

and halogenated noscapine variants (DeBono et al., 2015) have demonstrated improved inhibition of tumor growth relative to the natural variants. Yet, the sparsity of derivatized natural products occurs because the same complexity that bedevils total synthesis of natural products also hinders systematic chemical modification. The high number of reactive oxygenic groups makes it difficult to chemically modify specific positions without also modifying others, creating a complex product mixture. Consequently, large collections of discrete natural product derivatives are not readily available for bioactivity screening (Dandapani and Marcaurelle, 2010). It has been often hypothesized that a biological approach could generate relatively pure lead compound derivatives by harnessing the intrinsically high substrate and product specificity of enzymes. Accordingly, a number of studies have investigated the natural promiscuity of the biosynthetic pathways for medicinal plants alkaloids by feeding building block analogs or expressing building-block modifying enzymes (McCoy et al., 2006; Yerkes et al., 2008; Runguphan et al., 2010; McDonald et al., 2019). However, the slow growth rate, relatively sparse molecular toolbox, and complex regulatory systems of plants have prevented systematic engineering of the pathway as a whole, and generally limited the biological exploration of chemical space to what is achievable with the natural promiscuity. Thus, while the refactoring of these pathways into microorganisms, as described above, holds great potential to yield valuable production workhorses for existing pharmaceuticals in the near future, microbial synthesis may furthermore facilitate the engineering of natural product pathways to open up entirely novel regions of chemical space that are currently inaccessible.

The recent acceleration of refactoring elements of plant metabolism in microorganisms, discussed above, is creating an unprecedented resource of plant alkaloid pathways in a context more amenable their engineering. Such engineering efforts can be used to improve the pathway turnover of complex intermediate derivatives, thereby allowing researchers to produce previously inaccessible classes of compounds that can be screened for therapeutic potential. It is therefore timely to bring together these refactoring efforts and the studies reporting parts that can be integrated into future cell factories optimized for producing alkaloid derivatives. While there is a near infinite number of possible natural product derivatives, this review will first focus on the introduction of halogens (fluorine, chlorine, bromine and iodine) into natural product scaffolds, using the MIA and BIA pathways as test cases (**Figures 1A–C**). Secondly, although no yeast cell factories optimized for producing halogenated MIAs and BIAs yet exist, a number of *in vitro* and *in planta* studies have characterized the turnover of halogenated intermediates and developed parts relevant to achieving this goal. These will be reviewed with respect to the pathway sections that have been refactored in yeast. Finally, how such strains would represent an unprecedented opportunity to develop semi-synthetic medicinal chemistry campaigns that probe entirely new regions of chemical space will be discussed (**Figure 1D**).

HALOGENATION IN NATURE AND PHARMACOLOGY

Halogens form group seven of the periodic table and the biologically relevant members are fluorine, chlorine, bromine and iodine. Although the prevalence of these elements in nature is becoming increasingly understood, they are not often found naturally in plant alkaloids (Runguphan et al., 2010). Conversely, halogens are highly prevalent in licensed pharmaceuticals, and often have beneficial effects on the ligand binding and their pharmacokinetic properties of human therapeutics (Fejzagić et al., 2019). This is due to a unique combination of chemical properties—bulkiness alters the sterics of ligand binding, the high electronegativity can alter the charge interactions of ligand binding, their specific orbital architectures support unique intermolecular interactions and their hydrophobicity can improve bioavailability (**Figure 2**). These properties and their effects on drugs have been recently reviewed (Fejzagić et al., 2019). As a consequence of these properties, organohalogens make up roughly 25% of licensed drugs (Xu et al., 2014) and 40% of all new drugs being tested (Fejzagić et al., 2019). Of these, 57% contain fluorine, 38% contain chlorine, whereas bromine and iodine make up just 5% between them (Xu et al., 2014; Fejzagić et al., 2019). In addition to directly altering pharmacokinetic properties of a compound, halogens can act as "chemical handles" for targeting further drug derivatization (Runguphan and O'Connor, 2013; Frese et al., 2016; Corr et al., 2017). They provide effective leaving groups that can allow synthetic chemists to more selectively alter the activated carbon without creating non-specific alterations at other points of the structure. This is significant when attempting to further modify complex natural products for drug use (**Figure 1D**) because their structural complexity makes specific substitution difficult to achieve, resulting in complex mixtures that can be costly to separate (Frese and Sewald, 2015; Schnepel and Sewald, 2017). Furthermore, FDA approval of novel compounds for therapeutic use is conditional on a pure compound being obtainable. Therefore, achieving regio-specific introduction of halogens into natural product scaffolds may also provide the key to building the natural product variant libraries that would allow the relatively unexplored derivative space surrounding natural products to be systematically probed for novel pharmaceutical activities.

However, despite considerable interest and a number of engineering studies targeting individual enzymes (Chen et al., 2006; McCoy et al., 2006; Yerkes et al., 2008; Glenn et al., 2011; Wang et al., 2019b), there has yet to be a systematic study aimed at optimizing pathway production of new-to-nature analogs of plant medicinal alkaloids. The complex chemistries of natural products that make halogenation so useful for targeting cross-coupling reactions (**Figure 1D**) also makes it extremely difficult to selectively halogenate the desired site in the first place (Chung and Vanderwal, 2016). Where it is possible chemically, this requires expensive catalysts (palladium) and elemental halogen, which is both toxic and energetically expensive to produce (Schnepel and Sewald, 2017; Fejzagić et al., 2019). The intrinsically high selectivity of enzymes therefore makes enzymatic halogenation a tempting alternative for achieving

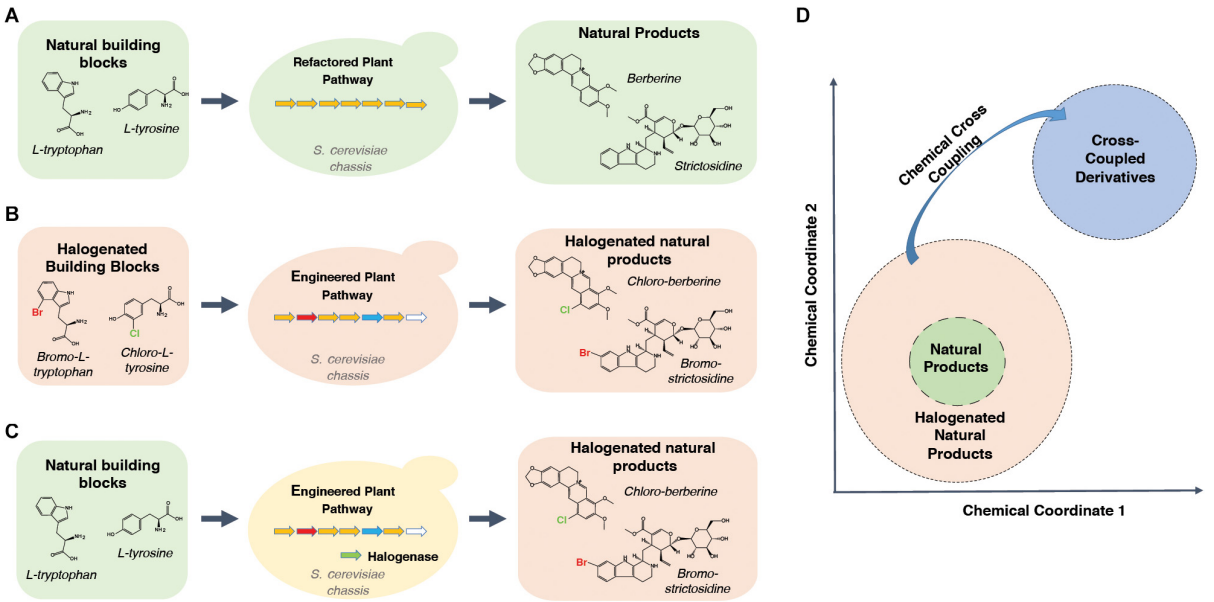

FIGURE 1 | Deploying synthetic biology to access novel regions of chemical space. **(A)** Readily available bulk feedstocks can be fed to yeast strains hosting refactored plant biosynthetic pathways. Natural products can then be extracted from fermentation broth. **(B)** Engineering of the plant biosynthetic pathway within the yeast chassis can allow or improve turnover of halogenated substrate analogs. Halogenated natural product scaffolds can be extracted from the fermentation broth. Promiscuous or engineered enzyme variants in engineered plant pathways are colored by red, blue and white arrows in the middle panel. **(C)** Introduction of halogenases can yield halogenated products from natural substrates. Promiscuous or engineered enzyme variants in engineered plant pathways are colored by red, blue and white arrows in the middle panel. Halogenase is depicted by a green arrow. **(D)** Schematic depicting the halogen derivatives surrounding natural product scaffolds in a hypothetical chemical space in which more similar compounds appear closer together. Halogens can facilitate targeted cross-coupling reactions that allow "hopping" to entirely new and chemically distinct regions of chemical space.

greener, cheaper, regio- and stereo-selective halogenation of natural products.

The potential for enzymatic halogenation emerged with the discovery of widespread halogenation in nature, which pointed toward a rich trove of halogenating enzymes operating under benign conditions (Gribble, 2003, 2018). Today, more than 6,000 naturally occurring organohalogens have been identified in a range of organisms across all three kingdoms of life, with functions including pheromones, hormones, antimicrobials, halogen recyclers, and structural proteins (Gribble, 2018). For the known organohalogens, chlorination, and bromination are the most common modifications although examples of iodination and fluorination are also reported (Gribble, 2003, 2018). Marine species and soil bacteria have provided the richest source of halogenated compounds due to the relative abundance of halogens in these habitats, particularly bromine in the ocean. A concerted effort to identify the enzymes responsible for incorporating inorganic halogen into metabolism has yielded a set of structurally and mechanistically diverse halogenases capable of catalyzing the formation of F-C, Cl-C, Br-C, and I-C bond formations (Schnepel and Sewald, 2017; Fejzagić et al., 2019).

Of the numerous halogenases, the flavin-dependent halogenases (FDHs) have been a focus for biotechnologists, due to their high substrate- and regio-specificity, and their ability to function independently of carrier proteins that bind the substrate. A subgroup of FDHs targeting the indole moiety of tryptophan are the most well studied group of FDHs, due to the prevalence of indole as a building block in both biology and synthetic chemistry (Frese and Sewald, 2015; Dhuguru and Skouta, 2020). Mechanistically, these tryptophan halogenases are similar to haem-dependent haloperoxidases and vanadium-dependent haloperoxidases in that they form a hypohalous acid (HOX) intermediate. However, unlike these other halogenases, the tryptophan FDHs do not release the HOX intermediate into solution. Instead, the HOX molecule moves through a 10 Å internal tunnel to the active site, where the halide is transferred, via a conserved lysine (Yeh et al., 2007; Flecks et al., 2008), to a specific carbon of the indole moiety of tryptophan (Karabencheva-Christova et al., 2017). Thus, this mechanism avoids the spurious halogenation associated with free HOX and achieves specific halogenation in a single step, compared to the 4–5 steps required for synthetic production of halogenated tryptophan. Indole moiety-targeting FDHs halogenating positions 5, 6 and 7 of the indole ring have been identified (Dong et al., 2005; Yeh et al., 2005; Zehner et al., 2005; Seibold et al., 2006; Fujimori et al., 2007; Heemstra and Walsh, 2008; Foulston and Bibb, 2010; Zeng and Zhan, 2011; Chang and Brady, 2013; Menon et al., 2016; Neubauer et al., 2018; Domergue et al., 2019; Ismail et al., 2019; Luhavaya et al., 2019; Lee et al., 2020; Lingkon and Bellizzi, 2020; **Table 1**) and, with the exception of a recently discovered brominase (Ismail et al., 2019), preferentially catalyze chlorination over bromination. Chlorination at position 4 has been observed but the responsible enzyme has not been identified

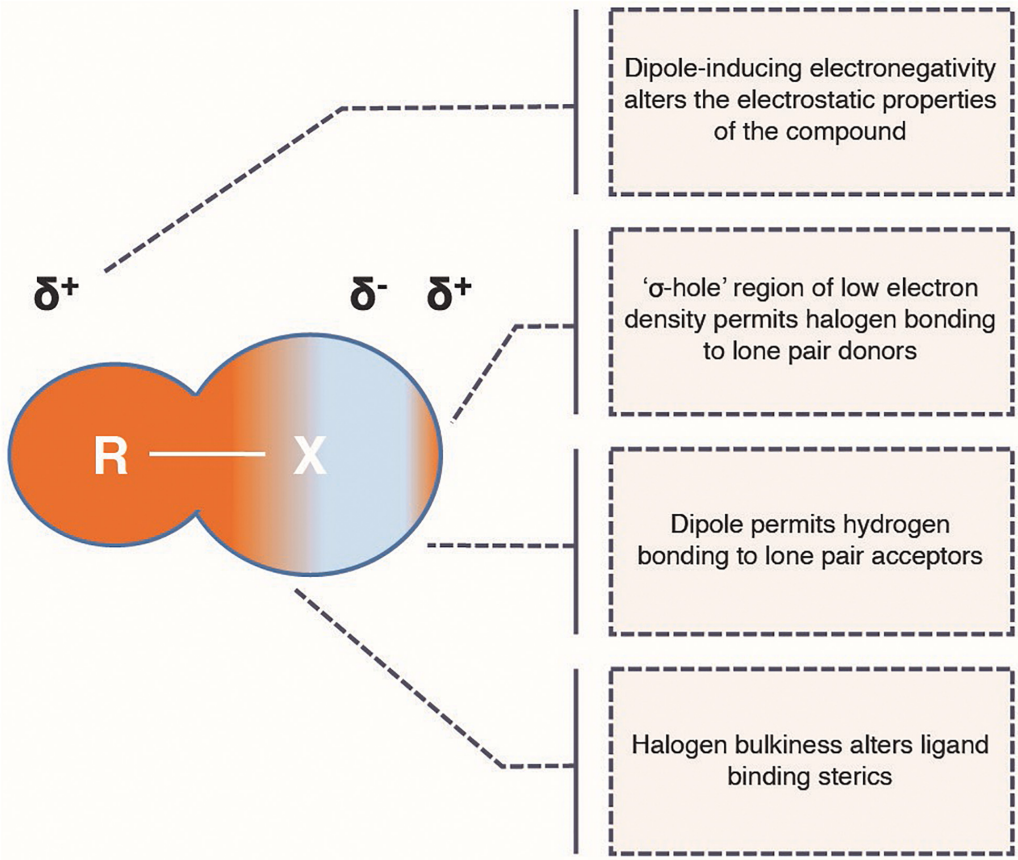

FIGURE 2 | Ligand binding properties of halogen atoms. A schematic outlining the physiochemical properties of a halogen atom (X = F, Cl, Br, or I) and its potential effects on the ligand binding properties of a pharmaceutical (R = halogen-bound atom of natural product scaffold). $\delta^{\pm}$ denote dipole partial charges.

(Payne et al., 2015). There are currently no known halogenases that will specifically fluorinate or iodinate tryptophan. Other common alkaloid building blocks also lack specific halogenases. However, more flavin-dependent halogenases continue to be discovered and characterized (Lingkon and Bellizzi, 2020).

Overall, there is a convincing body of evidence to suggest that halogenated derivatives of natural product scaffolds could be a rich source of improved or entirely novel pharmaceuticals. Furthermore, the site-specific introduction of halogens can facilitate production of a near-infinite number of other derivatives via cross-coupling reactions (**Figure 1D**). While achieving the site selective halogenation required for this has been historically difficult, the integration of halogenases or derivatized feedstocks into natural product biosynthetic pathways is beginning to open these exciting regions of chemical space.

EXPANDING NATURAL PRODUCT CHEMICAL SPACE THROUGH SYNTHETIC BIOLOGY

The well-documented effects of halogen atoms on the ligand binding and pharmacokinetic properties of pharmaceuticals present a tantalizing prospect of new or improved pharmaceuticals being created by introducing halogens into these classes of already bioactive compounds. This field remains in its infancy, but the number of studies reporting microbial synthesis of new-to-nature variants of medicinal plant alkaloids is growing. This section will review the progress made toward microbial synthesis of halogenated and other new-to-nature MIA and BIA variants, and describe protein engineering efforts predating microbial refactoring that can be integrated into emerging microbial strains. While this review will focus on MIAs and BIAs, the work performed to assess and engineer derivative turnover of these pathways provides an effective template that should be possible to emulate with other plant medicinal alkaloids (**Table 2**).

New-to-Nature Monoterpenoid Indole Alkaloids

MIA biosynthetic pathways have been popular testbeds, both *in vivo* and *in vitro*, for the biosynthesis of new-to-nature derivatives of plant medicinal alkaloids (**Figure 3A**). An early *in vivo* study, in which chemically synthesized tryptamines with substitutions on the indole ring were fed to *C. roseus* hairy root cultures or seedlings, observed production of fluorinated

TABLE 1 | Tryptophan and indole-targeting halogenases.

Name	GenBank accession number	Organism	Reported activities	References
Tryptophan and indole targeting halogenases				
PrnA	AAB97504.1	*Pseudomonas fluorescens BL915*	Trp-7 halogenase	Keller et al., 2000; Dong et al., 2005
RebH	CAC93722.1	*Lechevalieria aerocolonigenes ATCC 39243*	Trp-7 halogenase	Yeh et al., 2005
KtzQ	ABV56597.1	*Kutzneria sp. 744*	Trp-7 halogenase	Fujimori et al., 2007; Heemstra and Walsh, 2008
KtzR	ABV56598.1	*Kutzneria sp. 744*	Trp-6 halogenase	Fujimori et al., 2007; Heemstra and Walsh, 2008
ThaL	ABK79936.1	*Streptomyces albogriseolus*	Trp-6 halogenase	Seibold et al., 2006
SttH	ADW94630.1	*Streptomyces toxytricini*	Trp-6 halogenase	Zeng and Zhan, 2011
BorH	AGI62217.1	Uncultured bacterium	Trp-6 halogenase	Chang and Brady, 2013; Lingkon and Bellizzi, 2020
ThdH	AGF50179.1	*Streptomyces albogriseolus MJ286−76F7*	Trp-6 halogenase	Milbredt et al., 2014
ThHal	OEJ97865.1	*Streptomyces violaceusniger SPC6*	Trp-6 halogenase	Menon et al., 2016
Tar14	WP_081761942.1	*Saccharomonospora* sp. *CNQ490*	Trp-6 halogenase	Luhavaya et al., 2019
SatH	WP_078654696.1	*Streptomyces albus*	Trp-6 halogenase	Lee et al., 2020
PyrH	AAU95674.1	*Streptomyces rugosporus NRRL 21084*	Trp-5 halogenase	Zehner et al., 2005
*Xszen*FHal	WP_038240559.1	*Xenorhabdus szentirmaii*	Trp-5 and indole halogenase	Domergue et al., 2019
BrvH	EDX81295.1	*Brevundimonas* sp. *BAL3*	Indole halogenase	Neubauer et al., 2018
Xcc4156	6Y1W_A	*Xanthomonas campestris* pv. campestris B100	Indole halogenase	Ismail et al., 2019

A tabulated summary of the available FDHs targeting free tryptophan and/or indole.

serpentine and ajmalicine, two "late-stage" MIA compounds with demonstrated pharmaceutical activities (Mccoy and O'connor, 2006). Furthermore, the authors speculated that fluorinated analogs could be widely incorporated into MIAs with minimal engineering effort due to the small size of fluorine. In another seminal study, two tryptophan halogenases (RebH and PyrH) were expressed in *C. roseus* and *de novo* production of 12-chloro-19,20-dihydroakuamicine, 10-chloroajmalicine, 15-chlorotabersonine, and 12-bromo-19,20-Dihydroakuammicine was observed (Runguphan et al., 2010). Detection of multiple "late-stage" MIA variants indicates an encouraging level of native promiscuity. However, it was observed that production of MIAs required expression of a previously identified promiscuous STR mutant (Bernhardt et al., 2007) and, interestingly, that the halogenated substrates shifted the major MIA products, most likely due to promiscuity differences forcing substrate flux into different branches (Bernhardt et al., 2007). It was further noted that accumulation of chlorotryptophan occurred, suggesting that the native tryptophan decarboxylase does not well tolerate substrate derivatives. The group were able to circumnavigate this in a follow up study in which one of the halogenases was engineered to target tryptamine instead of tryptophan (Glenn et al., 2011). This strategy may also greatly simplify separation of halogenated and unhalogenated MIAs, which would not be possible by targeting tryptophan as complete halogenation of this proteogenic amino acid would be toxic.

Other studies have more systematically investigated individual enzymes *in vitro*. The promiscuity of strictosidine synthase for various analogs of tryptophan and secologanin has been studied (McCoy et al., 2006), and it has been found that substitutions on positions 4 and 7 of the indole ring of tryptamine and smaller substitutions in general are more well tolerated (McCoy et al., 2006). Another study found that strictosidine-β-glucosidase is promiscuous for a variety of indole ring substitutions and postulated that this is because the indole moiety faces outwards from the binding site (Yerkes et al., 2008).

In parallel to these studies, a number of engineering efforts to expand substrate and product promiscuity of MIA enzymes have been undertaken. This is significant because it means that many of individual parts are already defined and ready to be combinatorially tested in microbes. Engineering to improve MIA pathway turnover of substrate analogs was first reported more than 10 years ago with the rational engineering of strictosidine synthase, through introduction of point mutations, to accept analogs of secologanin with methyl ester and vinyl positions (Chen et al., 2006). Shortly following this, a V208A point mutation in the *R. serpentina* strictosidine synthase homolog was found to improve promiscuity for tryptamines with substitutions at positions 5 and 6 of the indole ring, which the wildtype enzyme does not readily accept (Loris et al., 2007). Following this, two further *C. roseus* strictosidine synthase homolog mutants (V214M and F232L) were designed to improve promiscuity for tryptamine derivatives, and the authors subsequently observed evidence of previously unobserved brominated MIAs (Bernhardt et al., 2007). Significantly, this study also noted that the expense of purchasing chemically synthesized brominated strictosidine analogs limited the scope of the study. This expense, contrasted with the utility of chlorine and bromine in targeting site-specific cross-coupling reactions and tryptophan's ubiquity as a synthetic building block, has driven significant interest in the more cost effective semi-synthesis or *de novo* biosynthesis of halogenated tryptophan using tryptophan halogenases (Smith et al., 2014; Frese and Sewald, 2015; Latham et al., 2018; Fejzagić et al., 2019;

TABLE 2 | Enzymatically produced alkaloids from halogenated substrates.

Halogen	Halogenated substrate	Derivatized compound(s) detected	Chassis	References
Monoterpene indole alkaloids				
Fluorine	4-, 5-, 6-, 7-fluoroindole	Tryptophan	*In vitro*	Smith et al., 2014
	4-fluorotryptophan	Tryptamine	*In vitro*	McDonald et al., 2019
	5-fluorotryptamine	Serpentine, ajmalicine, yohimbine, vindolidine, vindoline, catharanthine	*C. roseus*	Mccoy and O'connor, 2006
	5-fluorotryptamine	Strictosidine	*In vitro*	Loris et al., 2007
	5-fluorotryptamine	Ajmalicine, tabersonine, serpentine, catharanthine	*C. roseus*	Runguphan et al., 2009
	6-fluorotryptamine	Serpentine, ajmalicine, yohimbine, akuammicine, vindolidine, catharanthine,	*C. roseus*	Mccoy and O'connor, 2006
	6-fluorotryptamine	Strictosidine	*In vitro*	Loris et al., 2007
	4-fluorotryptamine	Strictosidine, strictosidine aglycone, canthemine	*In vitro*	McCoy et al., 2006
	5-, 6-, 7-fluorotryptamine	Strictosidine, strictosidine aglycone	*In vitro*	McCoy et al., 2006
	10-, 11-fluorostrictosidine	Strictosidine aglycone	*In vitro*	Yerkes et al., 2008
Chlorine	4-, 5-, 6-, 7-chloroindole	Tryptophan	*In vitro*	Smith et al., 2014
	4-, 5-, 6-, 7-, (5,6)-(di)chlorotryptophan	Tryptamine	*In vitro*	McDonald et al., 2019
	5-chloro-L-tryptophan	Tryptamine, strictosidine, tabersonine, ajmalicine, catharanthine	*C. roseus*	Runguphan et al., 2010
	7-chloro-L-tryptophan	Tryptamine, strictosidine, dihydroakuamicine,	*C. roseus*	Runguphan et al., 2010
	5-chlorotryptamine	Strictosidine	*C. roseus*	Bernhardt et al., 2007
	5-chlorotryptamine	Ajmalicine, catharanthine, tabersonine, strictosidine, cathenamine, serpentine, isositsirikine	*C. roseus*	Runguphan and O'Connor, 2009
	7-chlorotryptamine	Dihydroakuammicine	*C. roseus*	Runguphan and O'Connor, 2013
	6-chlorotryptophan	Tryptamine	*N. benthamiana*	Fräbel et al., 2016
	7-chlorotryptophan	Tryptamine	*N. benthamiana*	Fräbel et al., 2016
	6-chlorotryptamine	Dihydroakuamicine, akuammicine, tabersonine	*C. roseus*	Runguphan and O'Connor, 2013
Bromine	4-, 5-, 6-, 7-bromoindole	Tryptophan	*In vitro*	Smith et al., 2014
	4-, 5-, 6-, 7-bromotryptophan	Tryptamine	*In vitro*	McDonald et al., 2019
	7-bromo-L-tryptophan	Dihydroakuammicine	*C. roseus*	Runguphan et al., 2010
	5-bromotryptamine	Strictosidine, ajmalicine, yohimbine, akuammicine	*C. roseus*	Bernhardt et al., 2007
	5-bromotryptamine	Ajmalicine, strictosidine, serpentine, isositsirikine	*C. roseus*	Runguphan and O'Connor, 2009
	7-bromotryptamine	Dihydroakuammicine	*C. roseus*	Runguphan and O'Connor, 2013
Iodine	7-iodoindole	Tryptophan	*In vitro*	Smith et al., 2014
	5-, 7-iodotryptophan	Tryptamine	*In vitro*	McDonald et al., 2019
Benzylisoquinoline alkaloids				
Fluorine	2-(4-(trifluoromethoxy)phenyl)acetaldehyde, 2-(2-fluorophenyl)acetaldehyde, 2-(3-fluorophenyl)acetaldehyde, 2-(4-fluorophenyl)acetaldehyde	Norcoclaurine	*In vitro*	Ruff et al., 2012
	3-(4-trifluoromethylphenyl)-1-propylaldehyde	Norcoclaurine	*In vitro*	Nishihachijo et al., 2014
	4—fluorophenylacetaldehyde	Norcoclaurine	*In vitro*	Pesnot et al., 2012
	3-fluoro-L-tyrosine	L-DOPA, tyramine, dopamine, norcoclaurine	*In vitro*	Wang et al., 2019b
	3-fluoro-L-tyrosine	L-DOPA, dopamine, norcoclaurine, methylcoclaurine, reticuline	*S. cerevisiae*	Li et al., 2018
Chlorine	3-chloro-L-tyrosine	Dopamine	*In vitro*	Wang et al., 2019b
	3-chloro-L-tyrosine	L-DOPA, dopamine, norcoclaurine, methylcoclaurine, reticuline	*S. cerevisiae*	Li et al., 2018
Bromine	4—bromophenylacetaldehyde	Norcoclaurine	*In vitro*	Pesnot et al., 2012
	2-bromophenylacetaldehyde	Norcoclaurine	*In vitro*	Wang et al., 2019b
	para-bromo-*meta*-L-tyrosine	Dopamine	*In vitro*	Wang et al., 2019b

(Continued)

TABLE 2 | Continued

Name	GenBank accession number	Organism	Reported activities	References
Iodine	3-iodo-L-tyrosine	Dopamine	*In vitro*	Wang et al., 2019b
	3-iodo-L-tyrosine	L-DOPA, dopamine, norcoclaurine, methylcoclaurine, reticuline	*S. cerevisiae*	Li et al., 2018

A tabulated summary of studies reporting enzymatic synthesis, using wild type or engineered enzymes, of new-to-nature MIAs and BIAs from halogenated substrates. Information is provided on the nature of the halogenated substrate, the natural scaffold of which halogenated derivatives were detected, and chassis in which the conversions were established.

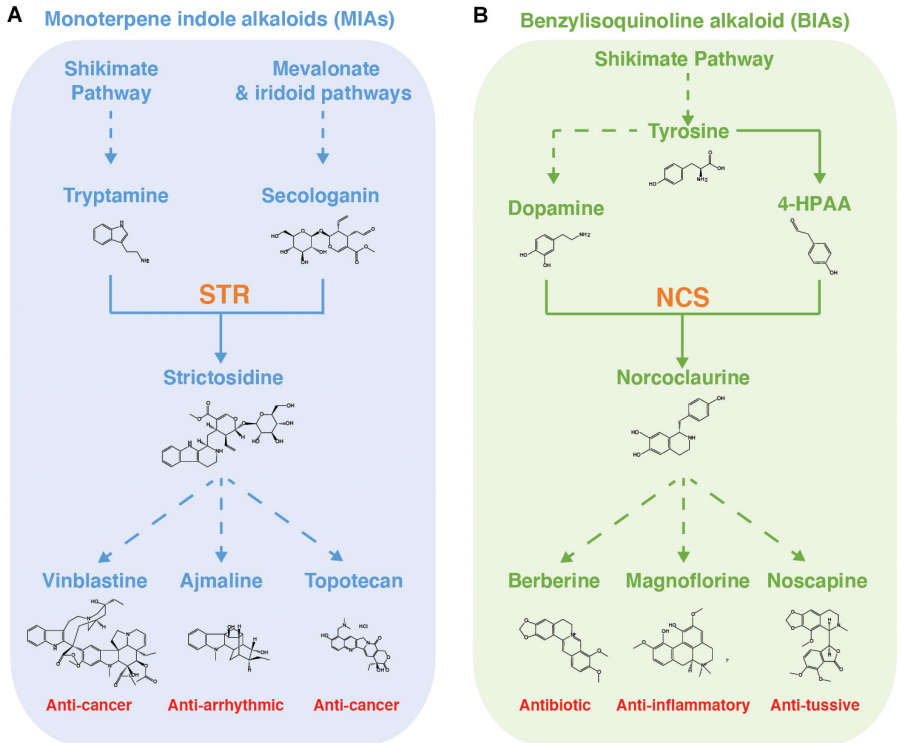

FIGURE 3 | MIA and BIA biosynthetic pathways in yeast. Summaries of the **(A)** monoterpene indole alkaloid biosynthetic pathway, as refactored in yeast, and **(B)** benzylisoquinoline alkaloid biosynthetic pathway, with example compounds and, in red, their pharmaceutical applications. STR, strictosidine synthase. NCS, norcoclaurine synthase. Solid arrow denotes single reaction. Dashed arrow denotes multiple reactions.

Table 1). Both of these approaches are viable for the more efficient production of halogenated variants of MIAs and MIA precursors. For example, a recently identified promiscuous tryptophan synthase is able to combine halogenated indole with serine to yield enantiopure samples of fluorinated, chlorinated, brominated and iodinated tryptophan (Smith et al., 2014). This enzyme could facilitate the introduction of halogens into the MIA pathway by feeding halogenated indole. Due to its lack of chirality, halogenated indole is significantly cheaper to synthesize than halogenated tryptophan and is therefore a far more attractive feedstock. This consideration of different feedstocks is particularly relevant for the introduction of fluorine into alkaloid scaffolds because only one, relatively poor, enzyme has been identified as being able to catalyze fluorination (O'Hagan and Deng, 2015). Alternatively, the introduction of bacterial tryptophan halogenases that target the indole ring of tryptophan can facilitate *de novo* production of chlorinated and brominated MIAs.

To improve the utility of promiscuous enzymes, studies have implemented rational enzyme engineering, directed evolution and synthetic biology to assess and improve substrate scope (Glenn et al., 2011; Payne et al., 2015; Shepherd et al., 2015; Neubauer et al., 2020), regio-specificity (Lang et al., 2011; Andorfer et al., 2016; Shepherd et al., 2016; Moritzer et al., 2019), stability (Payne et al., 2013; Poor et al., 2014; Minges et al., 2020) and activity (Andorfer et al., 2016, 2017; Kong et al., 2020) of FDH halogenases (**Table 3**). Of particular interest are a study deploying directed evolution to yield RebH variants targeting positions 5, 6, and 7 of tryptamine (Andorfer et al., 2016), which could help to avoid the tryptophan decarboxylase bottleneck, and a study in which the substrate specificity of RebH was evolved to target, albeit with lower activities, "late-stage" MIAs such as the yohimbines (Payne et al., 2015), which may allow promiscuity requirements to be eschewed entirely. These studies have relied on HPLC as a detection method, often limiting the size of the library that can be screened

TABLE 3 | Engineered Tryptophan FDHs.

Brief description	References
Halogenase engineering studies	
Tryptamine Position 7-targeting RebH mutant (Y455W).	Glenn et al., 2011
PrnA mutant (F103A) with switched activity from a position 7 to a position 5 tryptophan halogenase.	Lang et al., 2011
Improved functional RebH expression in *E. coli* through co-expression of the bacterial chaperones GroEL/GroES. Improved functional RebF expression through fusion with maltose binding protein.	Payne et al., 2013
Thermostable RebH mutant (S2P, M71V, K145M, E423D, E461G, S130L, N166S, Q494R).	Poor et al., 2014
Collection of RebH mutants that chlorinate substrates that are not accepted by the wild type enzyme (including tricyclic tryptoline, large indoles, and carbazoles).	Payne et al., 2015
RebH and PrnA mutants with expanded substrate scopes that include alternative aryl substrates.	Shepherd et al., 2015
SttH mutant (L460F/P461E/P462T) with switched activity from a position 6 to a position 5 tryptophan halogenase.	Shepherd et al., 2016
Three RebH mutants chlorinating tryptamine at positions 5 (I52H, L380F, F465C, N470S, Q494R, R509Q), 6 (I52M, S110P, S130L, N166S, L380F, S448P, Y455W, F465L, N470S, Q494R, R509Q), or 7 (N470S) with regiospecificity of at least 90%.	Andorfer et al., 2016
Bifunctional fusion enzyme consisting of a reductase (RebF) and a halogenase (RebH) showed improved yields of 7-chloro-tryptophan *in vivo*.	Andorfer et al., 2017
ThaL mutant (V52I, V82I, S360T, G469S, and S470N) with switched activity from a position 6 to a position 7 tryptophan halogenase.	Moritzer et al., 2019
Thermostable ThaL mutant (S359G, K374L, I393V) with improved activity at 25 C.	Minges et al., 2020
Bifunctional fusion enzyme consisting of a reductase (Fre) and a halogenase (XanH) showed slightly elevated halogenase activity *in vitro* compared to the two-component system.	Kong et al., 2020

A tabulated summary of key studies reporting engineered halogenases that can be integrated into future MIA cell factories. With the exception of XanH, halogenases that do not target indole or tryptophan have been excluded.

(Schnepel and Sewald, 2017). The recent development of novel, transcription factor-based biosensors returning a fluorescent output in response to 5- or 6-bromotryptophan (Ellefson et al., 2018) may, in combination with multiplex screening (e.g., fluorescence-activated cell sorting), underpin the screening of larger mutant libraries for optimization of the aforementioned parameters in the intracellular environment of yeast strains.

In addition to the ever-expanding repertoire of halogenase substrate specificities, a recent study elegantly demonstrated that these halogenases can be used in combination with a tryptophanase for biosynthesis of a halogenated indole (Fräbel et al., 2018), which is a common biosynthetic precursor. While engineering *Nicotiana benthamiana* to produce chlorinated precursors of indican dyes, the authors noted that the three tryptophan halogenases (RebH, SttH, and PyrH) did not accept indole as a substrate. They therefore allowed the halogenases to target tryptophan and expressed an *E. coli*-derived tryptophanase (TnaA) to convert this into a halogenated indole, which could then be converted, with varying efficiencies, to chloro-indican *in planta*. As indole is a common biosynthetic precursor, and a privileged heterocyclic scaffold (Dhuguru and Skouta, 2020), this system may help to unlock derivative space surrounding a number of diverse metabolites.

With the recent refactoring of the *de novo* strictosidine production in yeast (**Figure 3A**; Brown et al., 2015), it is expected that there will soon exist a microbial platform in which the combinatorial effects of the above-mentioned learnings can be more systematically tested. Such strains will be invaluable tools for further study because understanding of enzyme promiscuity remains patchy for the pathway leading up to strictosidine and extremely sparse for enzymes beyond this branch point. This is principally because it is only very recently that some of these modules have been fully elucidated and enzymes are still being identified (Caputi et al., 2018). The situation is further complicated by the fact that downstream substrates become increasingly complex, making derivatives difficult and expensive to chemically synthesis, leaving enzymatic synthesis as the only alternative (**Figure 3A**). This creates a catch-22 in which it is difficult to study *in vitro* enzyme promiscuity without the substrate analogs, yet we cannot effectively produce the substrate analogs without understanding the enzyme promiscuity. If the promiscuity of these downstream modules is to be systematically assessed and engineered *in vitro* or *in vivo*, biological platforms producing substrate analogs will have to be developed first. At first glance, source plants may look like attractive targets for these platforms. However, MIA-producing plants often possess multiple competing branches downstream of strictosidine, meaning that a small drop in turnover could cause another branch to outcompete and completely remove flux from the target branch, making it appear that there is no promiscuity. This effect was neatly demonstrated by Runguphan et al. (2010), who observed that substrate halogenation altered the major MIA products in *C. roseus*. The development of dependable, strictosidine analog-producing yeast strains, into which individual downstream MIA branches can be modularly expressed and systematically studied and engineered, will greatly accelerate our progress toward probing the derivative space surrounding MIA scaffolds.

Overall, the impressive array of pharmaceutical properties and the availability of a well-studied class of halogenases targeting direct precursors has provided the motivation and the means for more extensive new-to-nature integration of halogens into MIAs, relative to other plant medicinal alkaloids. The first production of an unnatural MIA in yeast has also already been reported—Ehrenworth et al. (2015) have reported semi-synthesis of 10-hydroxystrictosidine from yeast-derived 5-hydroxytryptamine and chemically synthesized secologanin. The principle challenge of achieving this was to engineer

production of sufficient tetrahydrobiopterin cofactor for the mono-oxygenase activity yielding 5-hydroxytryptophan, which is not naturally produced in *S. cerevisiae* (Ehrenworth et al., 2015). This highlights the fact that a major challenge when microbially refactoring plant biosynthetic pathways is still often producing sufficient amounts of non-native cofactors or building blocks. A number of other significant challenges also remain, not least the enduringly low yields of microbially refactored plant biosynthetic pathways and the lack of structural information relating to enzymes downstream of strictosidine. It will therefore be some time before halogenated MIAs can be microbially produced at scale. A more attainable goal will be to produce sufficient quantities for bioactivity testing, and this would be a significant step toward unlocking the derivative space surrounding these fascinating compounds.

New-to-Nature Benzylisoquinoline Alkaloids

BIAs are an important class of specialized plant metabolites that include the antimicrobials berberine and sanguinarine as well as the opiate analgesics (Hagel and Facchini, 2013). Several semi-synthetic opiate analogs are widely used and are found on the WHO list of essential medicines (World Health Organisation Model Lists of Essential Medicines, 2019). In higher plants, all known BIAs share a common precursor, (S)-norcoclaurine, which is the product of the first committed step in the pathway. (S)-norcoclaurine is synthesized via the norcoclaurine synthase (NCS)-catalyzed Pictet–Spengler condensation of two tyrosine derivatives (4-hydroxyphenylacetaldehyde (4-HPAA and dopamine) (**Figure 3B**; Facchini, 2001). As with the MIA pathway, investigations into enzymatic production of BIA derivatives began with *in vitro* investigation of individual enzyme promiscuity. NCS has been a focus of these studies due to its central position catalyzing the committed step. This enzyme has been found to accept a variety of electron rich, electron deficient and polyfunctionalized analogs of the aldehyde 4-HPAA, including fluorine-containing (Ruff et al., 2012; Nishihachijo et al., 2014) and bromine-containing (Pesnot et al., 2012) derivatives, and ketones (Lichman et al., 2017) but excluding α-substituted aldehydes. This can be rationalized through analysis of the relatively shallow active site in which the R-group is partially solvent-exposed, while the α-carbon is more deeply buried (Ilari et al., 2009; Lichman et al., 2015). However, these studies found the substrate requirements for the dopamine to be stricter, with NCS failing to turn over phenethylamines or tryptamine.

The promiscuity of early-stage BIA pathway enzymes was also recently investigated in one pot, *in vitro* enzyme cascades converting tyrosine analogs to analogs of (S)-norcoclaurine (Wang et al., 2019b). This study identified a promiscuous tyrosine decarboxylase that accepted fluorinated, chlorinated, brominated and iodinated tyrosine analogs and observed production of six non-natural BIAs, including a fluorinated analog of (S)-norcoclaurine, when this enzyme was included in the cascade. The halogenated tyrosine used in this study was purchased commercially. However, stereoselective enzymatic synthesis of fluorinated tyrosine analogs has been reported from fluoro-phenols, which are non-chiral and significantly cheaper, using tyrosine-phenol lyases (VonTersch et al., 1996; Phillips et al., 1997). Although not the endogenous route for tyrosine biosynthesis in yeast, this opens up a potential for feeding simpler precursors as a way of introducing halogens into the BIA.

More recently, *in vivo* studies have emerged in the public domain. Pyne et al. (2020) have reported construction of a novel *S. cerevisiae* strain, containing several tens of modifications principally focusing of increasing precursor supply, capable of producing 4.6 g L^{-1} of (S)-reticuline. The authors took advantage of the improved yields of this strain to search for minor products indicative of NCS promiscuity, the enzymatic gateway to probing the derivative space surrounding the tetrahydroisoquinoline (THIQ) scaffold within norcoclaurine. By screening the liquid chromatography-mass spectrometry (LC-MS) spectra of supernatants for theoretical THIQ products, the authors identified peaks consistent with THIQs formed by the condensation of dopamine and endogenous yeast carbonyl species derived from L-phenylalanine, L-tryptophan and L-leucine (Pyne et al., 2020). By cultivating strains with single amino acids as the major nitrogen source, the authors were able to increase the yield of these derivatives but also force production of a more diverse suite of aromatic- and aliphatic-derived substituted THIQs. Interestingly, a peak corresponding to the condensation of dopamine and acetaldehyde that was independent of NCS activity was also observed. This is consistent with an earlier study reporting that inorganic phosphate can catalyze aqueous formation of 1-substituted-THIQs from dopamine and aldehydes (Pesnot et al., 2011) and is reminiscent of the pH-dependent chemical coupling of secologanin and serotonin observed by Ehrenworth et al. (2015) in their hydroxystrictosidine production study. Importantly, the chemically catalyzed reactions are not enantiospecific, thus highlighting the need for robust controls when assessing product yields of microbially refactored plant pathways. Equivalent substituted THIQs derived from L-isoleucine and L-valine were not observed due to NCS's previously reported intolerance toward α-substituted aldehydes. In a promising result for future diversification, Pesnot et al. also demonstrated that the (S)-norcoclaurine methylating enzymes, OMT and CNMT, showed activity toward all substituted THIQs.

BIA pathway engineering efforts have been concomitant with exploration of NCS promiscuity (**Figure 3B**). For example, screening of NCS variants with active site point mutations yielded two variants, A79I and A79F, with increased turnover of methyl-ketone and cyclohexanone 4-HPAA analogs, respectively, was recently reported by Lichman et al. (2017). This is in keeping with previous work from the same group suggesting that the active site entrance loop is a key determinant of NCS promiscuity toward the aldehyde substrate (Lichman et al., 2015). Furthermore, Li et al. (2018) reported *de novo* biosynthesis of noscapine, a BIA with anti-tussive and anticancer properties, in *S. cerevisiae*, achieving a final titer of 2.2 mg/L. The authors note that halogenated noscapine variants have shown improved bioactivity against cancer cell lines (DeBono et al., 2015; Tomar et al., 2016) and hence attempted microbial semi-synthesis noscapine

derivatives by supplementing the yeast media with 16 tyrosine analogs, including 3-fluoro-tyrosine, 3-chloro-tyrosine, and 3-iodo-tyrosine (Li et al., 2018). Although no noscapine derivatives were detected, peaks matching the exact masses of 8-fluoro-reticuline, 8-chloro-reticuline and 8-iodo substituted (S)-N-methylcoclaurine were observed. The authors present (i) limited promiscuities of the native enzymes, (ii) low reaction efficiencies, and/or (iii) low substrate abundances as possible explanations for missing downstream derivatives. It has been speculated that these short-comings could be addressed by either engineering tailoring enzymes to introduce "late-stage" derivatizations, or by engineering the promiscuity of BIA enzymes such that they turn over the derivatized substrates (Tomar et al., 2016; Li et al., 2018; Srinivasan and Smolke, 2019). Drawing parallels with the tryptophan halogenases supporting halogenated MIA production, enzymatic halogenation of hydroxyisoquinoline scaffolds is also an option that warrants earnest investigation. For example, direct halogenation of the THIQ scaffold by the fungal halogenase Rdc2 (Zeng et al., 2013) or of THIQ precursors by the *Homo sapiens* thyroperoxidase (Ruf and Carayon, 2006) are both options for *de novo* production of halogenated BIAs.

DISCUSSION

Recent advances in the metabolic engineering toolbox have facilitated an explosion in the number of studies reporting microbial synthesis of plant medicinal alkaloids that cannot be chemically synthesized effectively. However, key challenges with both scale up of existing pathway sections and complete refactoring of both MIA and BIA extended pathways remain. Industrially competitive yeast strains able to produce even the naturally occurring plant medicinal alkaloids are still some distance into the future. Strains capable of producing industrial amounts of new-to-nature variants are yet further off. Despite this, these strains already represent an invaluable resource for the further engineering of these pathways for production of alkaloid derivatives. As described in this review, many relevant parts have already been developed, and we envision that the experimental advantages of microbial chasses will facilitate combinatorial testing of these parts to optimize derivative turnover as well as complete pathway refactoring.

Another prominent challenge will now be to progress from elegant proof-of-principles of microbial synthesis of alkaloid derivatives to more systematic explorations of the derivative space surrounding MIAs and BIAs and expanding these capabilities to include diversification of other natural product scaffolds. General approaches for achieving this will include (i) feeding of substrate analogs, (ii) pathway modification, and (iii) addition of enzymes, as recently reviewed by Cravens et al. (2019) For these non-mutually exclusive approaches to successfully produce sufficient yields for bioactivity testing of new drug leads, a number of challenges will have to be overcome. Chief among these, improving our ability to reliably engineer enzyme specificity and promiscuity would exponentially speed progress toward improved analog turnover. New computational methods designed to support protein design, such as the online webtool FuncLib (Khersonsky et al., 2018), may also aid this process. However, these approaches will also require new high-resolution structures to be published in many cases. Conversely, structure-agnostic methodologies, such as directed evolution, have already been highly successful at engineering enzyme specificities, but are limited by our ability to screen the variants (Payne et al., 2015; Andorfer et al., 2016). New biosensors targeting analogs of alkaloid precursors or intermediates may address this and help to improve analog turnover at pathway bottlenecks (Ellefson et al., 2018). Additionally, the large datasets generated by truly high throughput technologies open the door to the application of big data techniques such as machine learning, which has recently been used to successfully guide "semi-rational" protein engineering (Saito et al., 2018; Yang et al., 2019). Bioprospecting for promiscuous homologs may also prove fruitful. In the case of MIAs, the identification of two naturally occurring chlorinated alkaloids suggests that evolution may have already provided halo-tolerant enzymes and that screening alkaloid-producing plants native to halogen-rich habitats (e.g., coastal and volcanic soils) may save a significant amount of protein engineering (Al-Khdhairawi et al., 2017; Zeng et al., 2017).

Beyond improving the catalytic activity of enzymes directly catalyzing in alkaloid production, several systems level challenges will also have to be overcome. Substrate toxicity will likely be a major hurdle on the way to producing some variants in yeast. For example, it has been shown that some tryptophan analogs interfere with tryptophan synthesis in yeast and inhibit growth (Miozzari et al., 1977), and may also be erroneously incorporated into proteins. These issues could be overcome by reconsidering the halogen entry point into the pathway (Glenn et al., 2011) or engineering tryptophan tRNA synthetases to reject halogenated tryptophan. Alternatively, inspiration could be taken from a *trans*-acting aminoacyl-tRNA deacylase that selectively decouples fluoro-threonine from tRNA to prevent its integration into protein in *Streptomyces cattleya* (McMurry and Chang, 2017). Halogen salts, which are required for enzymatic halogenation, can also inhibit yeast growth. However, a number of non-conventional, halotolerant yeast strains are currently being investigated as chassis for biotechnological applications (Zaky et al., 2014; Musa et al., 2018). Although further characterization and toolbox development is still required, these strains could allow higher salt concentrations to be utilized. Functionality of the heterologously expressed plant enzymes at high salinity also remains an open question. However, we envision that both systems-level optimizations of existing chassis and further characterization of halo-tolerant yeasts could provide routes to improve the absolute yield of halogenated alkaloids, and the yield relative to the non-halogenated product, thus simplifying extraction.

Even as our understanding of how to engineer the promiscuity of these systems improves, the small number of successful studies on this topic have demonstrated the significant effort that is required to successfully produce new-to-nature variants. In addition to this, it is often difficult or expensive to source chemically synthesized intermediate analogs (Bernhardt et al., 2007) and this becomes exponentially more difficult downstream as the compounds become more complex. It will therefore be

important to focus initial efforts on platform yeast strains that can produce usable quantities of multiple variants of branch point compounds, such as strictosidine in the MIA pathway and (S)-norcoclaurine in the BIA pathway. Downstream modules can then be expressed in a plug-and-play style that will allow them to be efficiently studied and engineered. Although a daunting task, several studies have reported microbial synthesis of unnatural strictosidine and (S)-norcoclaurine analogs (Chen et al., 2006; Bernhardt et al., 2007; Pesnot et al., 2012; Ehrenworth et al., 2015; Wang et al., 2019b). It should be noted that development of many of the parts required for this has already begun and these should be integrated into novel yeast strains with relative ease (Smith et al., 2014; Payne et al., 2015; Andorfer et al., 2016; McDonald et al., 2019; Moritzer et al., 2019). Thus, we argue that combinatorial effects of these optimizations are now ripe to be studied, hopefully yielding novel platform strains that produce sufficient amounts of specific derivatives to unlock new regions of chemical space.

In summary, although still relatively few, the growing number of studies reporting yeast-based microbial synthesis of plant medicinal alkaloids are providing experimentally amenable contexts in which these pathways can be further engineered. This has major implications for furthering our understanding of new-to-nature variants of natural products but will also allow the combinatorial effects of the many previous learnings from *in vitro* and *in planta* studies to be rapidly assessed. Although significant challenges still exist, if these challenges can be overcome, it is possible to envisage a new semi-synthetic approach to medicinal chemistry campaigns, specialized for diversifying natural product scaffolds. Such a system would involve microbial synthesis of medicinal alkaloid variants with halogen substitutions at specific points of the scaffold. These compounds can then be tested directly for pharmaceutical activities but also can be subjected to targeted, chemical cross-coupling reactions that can efficiently generate an almost infinite number of substituted variants. Thus, this system would combine natural mechanisms of generating diversity, i.e., using a small suite of organic building blocks combined through a large number of reactions, with synthetic mechanisms of generating diversity, i.e., using a wide range of building blocks combined with a small suite of reliable reactions (Ganesan, 2008). As these two approaches access very different regions of chemical space (**Figure 1D**), we foresee that this would create unprecedented opportunities for entirely new and promising regions of chemical space, possessing advantages of both the natural and synthetic spheres, to be systematically probed for pharmaceutical activities.

AUTHOR CONTRIBUTIONS

SB, JZ, and MJ conceived the scope of the review content and wrote the manuscript. All authors contributed to the article and approved the submitted version.

FUNDING

This work was supported by the Novo Nordisk Foundation, Novo Nordisk Foundation Bioscience Ph.D. Programme grant No. NNF19SA0035438, and the European Commission Horizon 2020 programme (MIAMi; No. 722287).

REFERENCES

Ajikumar, P. K., Xiao, W. H., Tyo, K. E. J., Wang, Y., Simeon, F., Leonard, E., et al. (2010). Isoprenoid pathway optimization for Taxol precursor overproduction in *Escherichia coli*. *Science* 330, 70–74. doi: 10.1126/science.1191652

Al-Khdhairawi, A. A. Q., Krishnan, P., Mai, C. W., Chung, F. F. L., Leong, C. O., Yong, K. T., et al. (2017). A bis-benzopyrroloisoquinoline alkaloid incorporating a cyclobutane core and a chlorophenanthroindolizidine alkaloid with cytotoxic activity from *Ficus fistulosa* var. *tengerensis*. *J. Nat. Prod.* 80, 2734–2740. doi: 10.1021/acs.jnatprod.7b00500

Andorfer, M. C., Belsare, K. D., Girlich, A. M., and Lewis, J. C. (2017). Aromatic halogenation by using bifunctional flavin reductase–halogenase fusion enzymes. *ChemBioChem* 18, 2099–2103. doi: 10.1002/cbic.201700391

Andorfer, M. C., Park, H. J., Vergara-Coll, J., and Lewis, J. C. (2016). Directed evolution of RebH for catalyst-controlled halogenation of indole C-H bonds. *Chem. Sci.* 7, 3720–3729. doi: 10.1039/c5sc04680g

Avalos, L., Fink, G. R., Stephanopoulos, G., Avalos, J. L., Fink, G. R., and Stephanopoulos, G. (2013). Compartmentalization of metabolic pathways in yeast mitochondria improves the production of branched-chain alcohols. *Nat. Biotechnol.* 31, 335–341. doi: 10.1038/nbt.2509

Barker, A., Kettle, J. G., Nowak, T., and Pease, J. E. (2013). Expanding medicinal chemistry space. *Drug Discov. Today* 18, 298–304. doi: 10.1016/j.drudis.2012.10.008

Becker, J. V. W., Armstrong, G. O., Van Der Merwe, M. J., Lambrechts, M. G., Vivier, M. A., and Pretorius, I. S. (2003). Metabolic engineering of *Saccharomyces* cerevisiae for the synthesis of the wine-related antioxidant resveratrol. *FEMS Yeast Res.* 4, 79–85. doi: 10.1016/S1567-1356(03)00157-0

Bernhardt, P., McCoy, E., and O'Connor, S. E. (2007). Rapid identification of enzyme variants for reengineered alkaloid biosynthesis in periwinkle. *Chem. Biol.* 14, 888–897. doi: 10.1016/j.chembiol.2007.07.008

Brown, S., Clastre, M., Courdavault, V., and O'Connor, S. E. (2015). De novo production of the plant-derived alkaloid strictosidine in yeast. *Proc. Natl. Acad. Sci. U. S. A.* 112, 3205–3210. doi: 10.1073/pnas.1423555112

Buyel, J. F., Twyman, R. M., and Fischer, R. (2015). Extraction and downstream processing of plant-derived recombinant proteins. *Biotechnol. Adv.* 33, 902–913. doi: 10.1016/j.biotechadv.2015.04.010

Caputi, L., Franke, J., Farrow, S. C., Chung, K., Payne, R. M. E., Nguyen, T. D., et al. (2018). Missing enzymes in the biosynthesis of the anticancer drug vinblastine in Madagascar periwinkle. *Science* 360, 1235–1239. doi: 10.1126/science.aat4100

Chang, F. Y., and Brady, S. F. (2013). Discovery of indolotryptoline antiproliferative agents by homology-guided metagenomic screening. *Proc. Natl. Acad. Sci. U. S. A.* 110, 2478–2483. doi: 10.1073/pnas.1218073110

Chang, M. C. Y., Eachus, R. A., Trieu, W., Ro, D. K., and Keasling, J. D. (2007). Engineering *Escherichia coli* for production of functionalized terpenoids using plant P450s. *Nat. Chem. Biol.* 3, 274–277. doi: 10.1038/nchembio875

Chen, R., Yang, S., Zhang, L., and Zhou, Y. J. (2020). Advanced strategies for production of natural products in yeast. *iScience* 23:100879. doi: 10.1016/j.isci.2020.100879

Chen, S., Galan, M. C., Coltharp, C., and O'Connor, S. E. (2006). Redesign of a central enzyme in alkaloid biosynthesis. *Chem. Biol.* 13, 1137–1141. doi: 10.1016/j.chembiol.2006.10.009

Chung, W. J., and Vanderwal, C. D. (2016). Stereoselective halogenation in natural product synthesis. *Angew. Chemie Int. Ed.* 55, 4396–4434. doi: 10.1002/anie.201506388

Corr, M. J., Sharma, S. V., Pubill-Ulldemolins, C., Bown, R. T., Poirot, P., Smith, D. R. M., et al. (2017). Sonogashira diversification of unprotected halotryptophans, halotryptophan containing tripeptides; and generation of a new to nature bromo-natural product and its diversification in water. *Chem. Sci.* 8, 2039–2046. doi: 10.1039/c6sc04423a

Courdavault, V., O'Connor, S. E., Oudin, A., Besseau, S., and Papon, N. (2020). Towards the microbial production of plant-derived anticancer drugs. *Trends Cancer* 6, 444–448. doi: 10.1016/j.trecan.2020.02.004

Cravens, A., Payne, J., and Smolke, C. D. (2019). Synthetic biology strategies for microbial biosynthesis of plant natural products. *Nat. Commun.* 10, 1–12. doi: 10.1038/s41467-019-09848-w

Dandapani, S., and Marcaurelle, L. A. (2010). Grand challenge commentary: accessing new chemical space for "undruggable" targets. *Nat. Chem. Biol.* 6, 861–863. doi: 10.1038/nchembio.479

De Luca, V., Salim, V., Thamm, A., Masada, S. A., and Yu, F. (2014). Making iridoids/secoiridoids and monoterpenoid indole alkaloids: progress on pathway elucidation. *Curr. Opin. Plant Biol.* 19, 35–42. doi: 10.1016/j.pbi.2014.03.006

DeBono, A., Capuano, B., and Scammells, P. J. (2015). Progress toward the development of noscapine and derivatives as anticancer agents. *J. Med. Chem.* 58, 5699–5727. doi: 10.1021/jm501180v

Dhuguru, J., and Skouta, R. (2020). Role of indole scaffolds as pharmacophores in the development of anti-lung cancer agents. *Molecules* 25:1615. doi: 10.3390/molecules25071615

Domergue, J., Erdmann, D., Fossey-Jouenne, A., Petit, J. L., Debard, A., de Berardinis, V., et al. (2019). XszenFHal, a novel tryptophan 5-halogenase from *Xenorhabdus* szentirmaii. *AMB Express* 9:175. doi: 10.1186/s13568-019-0898-y

Dong, C., Flecks, S., Unversucht, S., Haupt, C., Van Pée, K. H., and Naismith, J. H. (2005). Structural biology: tryptophan 7-halogenase (PrnA) structure suggests a mechanism for regioselective chlorination. *Science* 309, 2216–2219. doi: 10.1126/science.1116510

Ehrenworth, A. M., Sarria, S., and Peralta-Yahya, P. (2015). Pterin-dependent mono-oxidation for the microbial synthesis of a modified monoterpene indole alkaloid. *ACS Synth. Biol.* 4, 1295–1307. doi: 10.1021/acssynbio.5b00025

Ellefson, J. W., Ledbetter, M. P., and Ellington, A. D. (2018). Directed evolution of a synthetic phylogeny of programmable Trp repressors article. *Nat. Chem. Biol.* 14, 361–367. doi: 10.1038/s41589-018-0006-7

Facchini, P. J. (2001). Alkaloid biosynthesis in plants: biochemistry, cell biology, molecular regulation, and metabolic engineering applications. *Annu. Rev. Plant Physiol. Plant Mol. Biol.* 52, 1–26.

Fejzagić, A. V., Gebauer, J., Huwa, N., and Classen, T. (2019). Halogenating enzymes for active agent synthesis: first steps are done and many have to follow. *Molecules* 24:4008. doi: 10.3390/molecules24214008

Flecks, S., Patallo, E. P., Zhu, X., Ernyei, A. J., Seifert, G., Schneider, A., et al. (2008). New insights into the mechanism of enzymatic chlorination of tryptophan. *Angew. Chemie Int. Ed.* 47, 9533–9536. doi: 10.1002/anie.2008 02466

Fossati, E., Narcross, L., Ekins, A., Falgueyret, J.-P., and Martin, V. J. J. (2015). Synthesis of morphinan alkaloids in *Saccharomyces cerevisiae*. *PLoS One* 10:e0124459. doi: 10.1371/journal.pone.0124459

Foulston, L. C., and Bibb, M. J. (2010). Microbisporicin gene cluster reveals unusual features of lantibiotic biosynthesis in actinomycetes. *Proc. Natl. Acad. Sci. U. S. A.* 107, 13461–13466. doi: 10.1073/pnas.1008285107

Fräbel, S., Krischke, M., Staniek, A., and Warzecha, H. (2016). Recombinant flavin-dependent halogenases are functional in tobacco chloroplasts without co-expression of flavin reductase genes. *Biotechnol. J.* 11, 1586–1594. doi: 10.1002/biot.201600337

Fräbel, S., Wagner, B., Krischke, M., Schmidts, V., Thiele, C. M., Staniek, A., et al. (2018). Engineering of new-to-nature halogenated indigo precursors in plants. *Metab. Eng.* 46, 20–27. doi: 10.1016/j.ymben.2018.02.003

Frese, M., Schnepel, C., Minges, H., Voß, H., Feiner, R., and Sewald, N. (2016). Modular combination of enzymatic halogenation of tryptophan with suzuki-miyaura cross-coupling reactions. *ChemCatChem* 8, 1799–1803. doi: 10.1002/cctc.201600317

Frese, M., and Sewald, N. (2015). Enzymatic halogenation of tryptophan on a gram scale. *Angew. Chemie Int. Ed.* 54, 298–301. doi: 10.1002/anie.201408561

Fujimori, D. G., Hrvatin, S., Neumann, C. S., Strieker, M., Marahiel, M. A., and Walsh, C. T. (2007). Cloning and characterization of the biosynthetic gene cluster for kutznerides. *Proc. Natl. Acad Sci. U. S. A.* 104, 16498–16503.

Galanie, S., and Smolke, C. D. (2015). Optimization of yeast-based production of medicinal protoberberine alkaloids. *Microb. Cell Fact.* 14:144. doi: 10.1186/s12934-015-0332-3

Galanie, S., Thodey, K., Trenchard, I. J., Interrante, M. F., and Smolke, C. D. (2015). Complete biosynthesis of opioids in yeast. *Science* 349, 1095–1100. doi: 10.1126/science.aac9373

Ganesan, A. (2008). The impact of natural products upon modern drug discovery. *Curr. Opin. Chem. Biol.* 12, 306–317. doi: 10.1016/j.cbpa.2008.03.016

Gautam, L. N., Ling, T., Lang, W., and Rivas, F. (2016). Anti-proliferative evaluation of monoterpene derivatives against leukemia. *Eur. J. Med. Chem.* 113, 75–80. doi: 10.1016/j.ejmech.2016.02.034

Glenn, W. S., Nims, E., and O'Connor, S. E. (2011). Reengineering a tryptophan halogenase to preferentially chlorinate a direct alkaloid precursor. *J. Am. Chem. Soc.* 133, 19346–19349. doi: 10.1021/ja2089348

Gribble, G. W. (2003). The diversity of naturally produced organohalogens. *Chemosphere* 56, 289–297. doi: 10.1016/S0045-6535(03)00207-8

Gribble, G. W. (2018). Newly discovered naturally occurring organohalogens. *Arkivoc* 2018, 372–410. doi: 10.24820/ark.5550190.p010.610

Groot, H. J., Lubberts, S., de Wit, R., Witjes, J. A., Martijn Kerst, J., de Jong, I. J., et al. (2018). Journal of clinical oncology risk of solid cancer after treatment of testicular germ cell cancer in the platinum era. *J. Clin. Oncol.* 36, 319–325. doi: 10.1200/JCO

Hagel, J. M., and Facchini, P. J. (2013). Benzylisoquinoline alkaloid metabolism: a century of discovery and a brave new world. *Plant Cell Physiol.* 54, 647–672. doi: 10.1093/pcp/pct020

Heemstra, J. R., and Walsh, C. T. (2008). Tandem action of the O2- and FADH2-dependent halogenases KtzQ and KtzR produce 6,7-dichlorotryptophan for kutzneride assembly. *J. Am. Chem. Soc.* 130, 14024–14025. doi: 10.1021/ja806467a

Hori, K., Okano, S., and Sato, F. (2016). Efficient microbial production of stylopine using a *Pichia pastoris* expression system. *Sci. Rep.* 6:22201. doi: 10.1038/srep22201

Ignea, C., Pontini, M., Motawia, M. S., Maffei, M. E., Makris, A. M., and Kampranis, S. C. (2018). Synthesis of 11-carbon terpenoids in yeast using protein and metabolic engineering. *Nat. Chem. Biol.* 14, 1090–1098. doi: 10.1038/s41589-018-0166-5

Ilari, A., Franceschini, S., Bonamore, A., Arenghi, F., Botta, B., Macone, A., et al. (2009). Structural basis of enzymatic (S)-norcoclaurine biosynthesis. *J. Biol. Chem.* 284, 897–904. doi: 10.1074/jbc.M803738200

Ismail, M., Frese, M., Patschkowski, T., Ortseifen, V., Niehaus, K., and Sewald, N. (2019). Flavin-dependent halogenases from *Xanthomonas campestris* pv. campestris B100 Prefer bromination over chlorination. *Adv. Synth. Catal.* 361, 2475–2486. doi: 10.1002/adsc.201801591

Jakubczyk, D., Caputi, L., Hatsch, A., Nielsen, C. A. F., Diefenbacher, M., Klein, J., et al. (2015). Discovery and reconstitution of the cyclopropyl group. *Angew. Chemie Int. Ed.* 54, 5117–5121. doi: 10.1002/anie.201410002

Jungbauer, A. (2013). Continuous downstream processing of biopharmaceuticals. *Trends Biotechnol.* 31, 479–492. doi: 10.1016/j.tibtech.2013.05.011

Junker, B. H. (2004). Scale-up methodologies for *Escherichia coli* and yeast fermentation processes. *J. Biosci. Bioeng.* 97, 347–364. doi: 10.1016/S1389-1723(04)70218-2

Karabencheva-Christova, T. G., Torras, J., Mulholland, A. J., Lodola, A., and Christov, C. Z. (2017). Mechanistic insights into the reaction of chlorination of tryptophan catalyzed by tryptophan 7-halogenase. *Sci. Rep.* 7:17395. doi: 10.1038/s41598-017-17789-x

Keller, S., Wage, T., Hohaus, K., Hölzer, M., Eichhorn, E., and Van Pée, K. H. (2000). Purification and partial characterization of tryptophan 7- halogenase (PrnA) from *Pseudomonas* fluorescens. *Angew. Chemie Int. Ed.* 39, 2300–2302.

Khersonsky, O., Lipsh, R., Avizemer, Z., Ashani, Y., Goldsmith, M., Leader, H., et al. (2018). Automated design of efficient and functionally diverse enzyme repertoires. *Mol. Cell* 72, 178.e5–186.e5. doi: 10.1016/j.molcel.2018.08.033

Kong, L., Wang, Q., Deng, Z., and You, D. (2020). Flavin adenine dinucleotide-dependent halogenase xanh and engineering of multifunctional fusion

halogenases. *Appl. Environ. Microbiol.* 86:e01225-20. doi: 10.1128/AEM.01225-0

Kutchan, T. M., Gershenzon, J., Moller, B. L., and Gang, D. R. (2015). "Natural products," in *Biochemistry and Molecular Biology Of Plants*, eds B. Buchanan, W. Gruissem, and R. Jones (Hoboken, NY: Blackwell Publishing Ltd).

Lang, A., Polnick, S., Nicke, T., William, P., Patallo, E. P., Naismith, J. H., et al. (2011). Changing the regioselectivity of the tryptophan 7-halogenase PrnA by site-directed mutagenesis. *Angew. Chemie Int. Ed.* 50, 2951–2953. doi: 10.1002/anie.201007896

Latham, J., Brandenburger, E., Shepherd, S. A., Menon, B. R. K., and Micklefield, J. (2018). Development of halogenase enzymes for use in synthesis. *Chem. Rev.* 118, 232–269. doi: 10.1021/acs.chemrev.7b00032

Lee, J., Kim, J., Kim, H., Kim, E. J., Jeong, H. J., Choi, K. Y., et al. (2020). Characterization of a tryptophan 6-halogenase from *Streptomyces albus* and its regioselectivity determinants. *ChemBioChem* 21, 1446–1452. doi: 10.1002/cbic.201900723

Leggans, E. K., Duncan, K. K., Barker, T. J., Schleicher, K. D., and Boger, D. L. (2013). A remarkable series of vinblastine analogues displaying enhanced activity and an unprecedented tubulin binding steric tolerance: c20' urea derivatives. *J. Med. Chem.* 56, 628–639. doi: 10.1021/jm3015684

Li, Y., Li, S., Thodey, K., Trenchard, I., Cravens, A., and Smolke, C. D. (2018). Complete biosynthesis of noscapine and halogenated alkaloids in yeast. *Proc. Natl. Acad. Sci. U. S. A.* 115, E3922–E3931. doi: 10.1073/pnas.1721469115

Lichman, B. R., Gershater, M. C., Lamming, E. D., Pesnot, T., Sula, A., Keep, N. H., et al. (2015). Dopamine-first mechanism enables the rational engineering of the norcoclaurine synthase aldehyde activity profile. *FEBS J.* 282, 1137–1151. doi: 10.1111/febs.13208

Lichman, B. R., Zhao, J., Hailes, H. C., and Ward, J. M. (2017). Enzyme catalysed Pictet-Spengler formation of chiral 1,1'-disubstituted- A nd spiro-tetrahydroisoquinolines. *Nat. Commun.* 8:14883. doi: 10.1038/ncomms14883

Lingkon, K., and Bellizzi, J. J. (2020). Structure and activity of the thermophilic tryptophan-6 halogenase BorH. *ChemBioChem* 21, 1121–1128. doi: 10.1002/cbic.201900667

Liu, D., Ding, L., Sun, J., Boussetta, N., and Vorobiev, E. (2016). Yeast cell disruption strategies for recovery of intracellular bio-active compounds — A review. *Innov. Food Sci. Emerg. Technol.* 36, 181–192. doi: 10.1016/j.ifset.2016.06.017

Liu, X., Cheng, J., Zhang, G., Ding, W., Duan, L., Yang, J., et al. (2018). Engineering yeast for the production of breviscapine by genomic analysis and synthetic biology approaches. *Nat. Commun.* 9:448. doi: 10.1038/s41467-018-02883-z

Loris, E. A., Panjikar, S., Ruppert, M., Barleben, L., Unger, M., Schübel, H., et al. (2007). Structure-based engineering of strictosidine synthase: auxiliary for alkaloid libraries. *Chem. Biol.* 14, 979–985. doi: 10.1016/j.chembiol.2007.08.009

Luhavaya, H., Sigrist, R., Chekan, J. R., McKinnie, S. M. K., and Moore, B. S. (2019). Biosynthesis of l-4-chlorokynurenine, an antidepressant prodrug and a non-proteinogenic amino acid found in lipopeptide antibiotics. *Angew. Chemie Int. Ed.* 58, 8394–8399. doi: 10.1002/anie.201901571

Luo, X., Reiter, M. A., D'Espaux, L., Wong, J., Denby, C. M., Lechner, A., et al. (2019). Complete biosynthesis of cannabinoids and their unnatural analogues in yeast. *Nature* 567, 123–126. doi: 10.1038/s41586-019-0978-9

Ma, S. M., Li, J. W. H., Choi, J. W., Zhou, H., Lee, K. K. M., Moorthie, V. A., et al. (2009). Complete reconstitution of a highly reducing iterative polyketide synthase. *Science* 326, 589–592. doi: 10.1126/science.1175602

McCoy, E., Galan, M. C., and O'Connor, S. E. (2006). Substrate specificity of strictosidine synthase. *Bioorganic Med. Chem. Lett.* 16, 2475–2478. doi: 10.1016/j.bmcl.2006.01.098

Mccoy, E., and O'connor, S. E. (2006). Directed biosynthesis of alkaloid analogs in the medicinal plant *Catharanthus roseus*. *J. Am. Chem. Soc.* 128, 14276–14277. doi: 10.1021/ja066787w

McDonald, A. D., Perkins, L. J., and Buller, A. R. (2019). Facile in vitro biocatalytic production of diverse tryptamines. *ChemBioChem* 20, 1939–1944. doi: 10.1002/cbic.201900069

McKeague, M., Wang, Y. H., Cravens, A., Win, M. N., and Smolke, C. D. (2016). Engineering a microbial platform for de novo biosynthesis of diverse methylxanthines. *Metab. Eng.* 38, 191–203. doi: 10.1016/j.ymben.2016.08.003

McMurry, J. L., and Chang, M. C. Y. (2017). Fluorothreonyl-tRNA deacylase prevents mistranslation in the organofluorine producer Streptomyces cattleya. *Proc. Natl. Acad. Sci. U. S. A.* 114, 11920–11925. doi: 10.1073/pnas.1711482114

Menon, B. R. K., Latham, J., Dunstan, M. S., Brandenburger, E., Klemstein, U., Leys, D., et al. (2016). Structure and biocatalytic scope of thermophilic flavin-dependent halogenase and flavin reductase enzymes. *Org. Biomol. Chem.* 14, 9354–9361. doi: 10.1039/c6ob01861k

Milbredt, D., Patallo, E. P., and Van Pée, K. H. (2014). A tryptophan 6-halogenase and an amidotransferase are involved in thienodolin biosynthesis. *ChemBioChem* 15, 1011–1020. doi: 10.1002/cbic.201400016

Milne, N., Thomsen, P., Mølgaard Knudsen, N., Rubaszka, P., Kristensen, M., and Borodina, I. (2020). Metabolic engineering of Saccharomyces cerevisiae for the de novo production of psilocybin and related tryptamine derivatives. *Metab. Eng.* 60, 25–36. doi: 10.1016/j.ymben.2019.12.007

Minges, H., Schnepel, C., Böttcher, D., Weiß, M. S., Sproß, J., Bornscheuer, U. T., et al. (2020). Targeted enzyme engineering unveiled unexpected patterns of halogenase stabilization. *ChemCatChem* 12, 818–831. doi: 10.1002/cctc.201901827

Miozzari, G., Niederberger, P., and Hütter, R. (1977). Action of tryptophan analogues in *Saccharomyces cerevisiae*. *Arch. Microbiol.* 115, 307–316. doi: 10.1007/BF00446457

Moritzer, A. C., Minges, H., Prior, T., Frese, M., Sewald, N., and Niemann, H. H. (2019). Structure-based switch of regioselectivity in the flavin-dependent tryptophan 6-halogenase Thal. *J. Biol. Chem.* 294, 2529–2542. doi: 10.1074/jbc.RA118.005393

Musa, H., Kasim, F. H., Nagoor Gunny, A. A., and Gopinath, S. C. B. (2018). Salt-adapted moulds and yeasts: potentials in industrial and environmental biotechnology. *Process Biochem.* 69, 33–44. doi: 10.1016/j.procbio.2018.03.026

Neubauer, P. R., Pienkny, S., Wessjohann, L., Brandt, W., and Sewald, N. (2020). Predicting the substrate scope of the flavin-dependent halogenase BrvH. *ChemBioChem* doi: 10.1002/cbic.202000444 Online ahead of print.

Neubauer, P. R., Widmann, C., Wibberg, D., Schröder, L., Frese, M., Kottke, T., et al. (2018). A flavin-dependent halogenase from metagenomic analysis prefers bromination over chlorination. *PLoS One* 13:e0196797. doi: 10.1371/journal.pone.0196797

Newman, D. J., and Cragg, G. M. (2016). Natural products as sources of new drugs from 1981 to 2014. *J. Nat. Prod.* 79, 629–661. doi: 10.1021/acs.jnatprod.5b01055

Nielsen, C. A. F., Folly, C., Hatsch, A., Molt, A., Schröder, H., O'Connor, S. E., et al. (2014). The important ergot alkaloid intermediate chanoclavine-I produced in the yeast *Saccharomyces cerevisiae* by the combined action of EasC and EasE from aspergillus japonicus. *Microb. Cell Fact.* 13:95. doi: 10.1186/s12934-014-0095-2

Nishihachijo, M., Hirai, Y., Kawano, S., Nishiyama, A., Minami, H., Katayama, T., et al. (2014). Asymmetric synthesis of tetrahydroisoquinolines by enzymatic Pictet-Spengler reaction. *Biosci. Biotechnol. Biochem.* 78, 701–707. doi: 10.1080/09168451.2014.890039

O'Hagan, D., and Deng, H. (2015). Enzymatic fluorination and biotechnological developments of the fluorinase. *Chem. Rev.* 115, 634–649. doi: 10.1021/cr500209t

Paddon, C. J., and Keasling, J. D. (2014). Semi-synthetic artemisinin: a model for the use of synthetic biology in pharmaceutical development. *Nat. Rev. Microbiol.* 12, 355–367. doi: 10.1038/nrmicro3240

Payne, J. T., Andorfer, M. C., and Lewis, J. C. (2013). Regioselective arene halogenation using the FAD-dependent halogenase RebH. *Angew. Chemie Int. Ed.* 52, 5271–5274. doi: 10.1002/anie.201300762

Payne, J. T., Poor, C. B., and Lewis, J. C. (2015). Directed evolution of rebh for site-selective halogenation of large biologically active molecules. *Angew. Chemie Int. Ed.* 54, 4226–4230. doi: 10.1002/anie.201411901

Pesnot, T., Gershater, M. C., Ward, J. M., and Hailes, H. C. (2011). Phosphate mediated biomimetic synthesis of tetrahydroisoquinoline alkaloids. *Chem. Commun.* 47, 3242–3244. doi: 10.1039/c0cc05282e

Pesnot, T., Gershater, M. C., Ward, J. M., and Hailes, H. C. (2012). The catalytic potential of Coptis japonica NCS2 revealed - Development and utilisation of a fluorescamine-based assay ETI. *Adv. Synth. Catal.* 354, 2997–3008. doi: 10.1002/adsc.201200641

Phillips, R. S., Von Tersch, R. L., and Secundo, F. (1997). Effects of tyrosine ring fluorination on rates and equilibria of formation of intermediates in the reactions of carbon-carbon lyases. *Eur. J. Biochem.* 244, 658–663. doi: 10.1111/j.1432-1033.1997.00658.x

Pichersky, E., and Raguso, R. A. (2018). Why do plants produce so many terpenoid compounds? *New Phytol.* 220, 692–702. doi: 10.1111/nph.14178

Ping, Y., Li, X., You, W., Li, G., Yang, M., Wei, W., et al. (2019). De Novo production of the plant-derived tropine and pseudotropine in yeast. *ACS Synth. Biol.* 8, 1257–1262. doi: 10.1021/acssynbio.9b00152

Poor, C. B., Andorfer, M. C., and Lewis, J. C. (2014). Improving the stability and catalyst lifetime of the halogenase RebH by directed evolution. *ChemBioChem* 15, 1286–1289. doi: 10.1002/cbic.201300780

Pyne, M. E., Kevvai, K., Grewal, P. S., Narcross, L., Choi, B., Bourgeois, L., et al. (2020). A yeast platform for high-level synthesis of tetrahydroisoquinoline alkaloids. *Nat. Commun.* 11:3337. doi: 10.1038/s41467-020-17172-x

Qu, Y., Easson, M. L. A. E., Froese, J., Simionescu, R., Hudlicky, T., and DeLuca, V. (2015). Completion of the seven-step pathway from tabersonine to the anticancer drug precursor vindoline and its assembly in yeast. *Proc. Natl. Acad. Sci. U. S. A.* 112, 6224–6229. doi: 10.1073/pnas.1501821112

Ro, D. K., Paradise, E. M., Quellet, M., Fisher, K. J., Newman, K. L., Ndungu, J. M., et al. (2006). Production of the antimalarial drug precursor artemisinic acid in engineered yeast. *Nature* 440, 940–943. doi: 10.1038/nature04640

Ruf, J., and Carayon, P. (2006). Structural and functional aspects of thyroid peroxidase. *Arch. Biochem. Biophys.* 445, 269–277. doi: 10.1016/j.abb.2005.06.023

Ruff, B. M., Bräse, S., and O'Connor, S. E. (2012). Biocatalytic production of tetrahydroisoquinolines. *Tetrahedron Lett.* 53, 1071–1074. doi: 10.1016/j.tetlet.2011.12.089

Runguphan, W., Maresh, J. J., and O'Connor, S. E. (2009). Silencing of tryptamine biosynthesis for production of nonnatural alkaloids in plant culture. *Proc. Natl. Acad. Sci. U. S. A.* 106, 13673–13678. doi: 10.1073/pnas.0903393106

Runguphan, W., and O'Connor, S. E. (2009). Metabolic reprogramming of periwinkle plant culture. *Nat. Chem. Biol.* 5, 151–153. doi: 10.1038/nchembio.141

Runguphan, W., and O'Connor, S. E. (2013). Diversification of monoterpene indole alkaloid analogs through cross-coupling. *Org. Lett.* 15, 2850–2853. doi: 10.1021/ol401179k

Runguphan, W., Qu, X., and O'Connor, S. E. (2010). Integrating carbon-halogen bond formation into medicinal plant metabolism. *Nature* 468, 461–467. doi: 10.1038/nature09524

Saito, Y., Oikawa, M., Nakazawa, H., Niide, T., Kameda, T., Tsuda, K., et al. (2018). Machine-learning-guided mutagenesis for directed evolution of fluorescent proteins. *ACS Synth. Biol.* 7, 2014–2022. doi: 10.1021/acssynbio.8b00155

Schnepel, C., and Sewald, N. (2017). Enzymatic halogenation: a timely strategy for regioselective C-H activation. *Chem. A Eur. J.* 23, 12064–12086. doi: 10.1002/chem.201701209

Sears, J. E., and Boger, D. L. (2015). Total synthesis of vinblastine, related natural products, and key analogues and development of inspired methodology suitable for the systematic study of their structure-function properties. *Acc. Chem. Res.* 48, 653–662. doi: 10.1021/ar500400w

Seibold, C., Schnerr, H., Rumpf, J., Kunzendorf, A., Hatscher, C., Wage, T., et al. (2006). A flavin-dependent tryptophan 6-halogenase and its use in modification of pyrrolnitrin biosynthesis. *Biocatal. Biotransformation* 24, 401–408. doi: 10.1080/10242420601033738

Shepherd, S. A., Karthikeyan, C., Latham, J., Struck, A. W., Thompson, M. L., Menon, B. R. K., et al. (2015). Extending the biocatalytic scope of regiocomplementary flavin-dependent halogenase enzymes. *Chem. Sci.* 6, 3454–3460. doi: 10.1039/c5sc00913h

Shepherd, S. A., Menon, B. R. K., Fisk, H., Struck, A. W., Levy, C., Leys, D., et al. (2016). a structure-guided switch in the regioselectivity of a tryptophan halogenase. *ChemBioChem* 17, 821–824. doi: 10.1002/cbic.201600051

Smith, D. R. M. M., Willemse, T., Gkotsi, D. S., Schepens, W., Maes, B. U. W. W., Ballet, S., et al. (2014). The first one-pot synthesis of L-7-iodotryptophan from 7-iodoindole and serine, and an improved synthesis of other L-7-halotryptophans. *Org. Lett.* 16, 2622–2625. doi: 10.1021/ol5007746

Springob, K., and Kutchan, T. M. (2009). "Introduction to the different classes of natural products," in *Plant-Derived Natural Products: Synthesis, Function, and Application*, eds A. E. Osbourn and V. Lanzotti (New York, NY: Springer), 3–50. doi: 10.1007/978-0-387-85498-4_1

Srinivasan, P., and Smolke, C. D. (2019). Engineering a microbial biosynthesis platform for de novo production of tropane alkaloids. *Nat. Commun.* 10, 1–15. doi: 10.1038/s41467-019-11588-w

Tomar, V., Kukreti, S., Prakash, S., Madan, J., and Chandra, R. (2016). Noscapine and its analogs as chemotherapeutic agent: current updates. *Curr. Top. Med. Chem.* 17, 174–188. doi: 10.2174/1568026616666160530153518

VonTersch, R. L., Secundo, F., Phillips, R. S., and Newton, M. G. (1996). Preparation of fluorinated amino acids with tyrosine phenol lyase. *Biomed. Front. Fluor. Chem.* 95–104. doi: 10.1021/bk-1996-0639.ch007

Wang, Y., Ling, C., Chen, Y., Jiang, X., and Chen, G. Q. (2019a). Microbial engineering for easy downstream processing. *Biotechnol. Adv.* 37:107365. doi: 10.1016/j.biotechadv.2019.03.004

Wang, Y., Tappertzhofen, N., Méndez-Sánchez, D., Bawn, M., Lyu, B., Ward, J. M., et al. (2019b). Design and use of de novo cascades for the biosynthesis of new benzylisoquinoline alkaloids. *Angew. Chemie* 131, 10226–10231. doi: 10.1002/ange.201902761

Wilson, S. A., and Roberts, S. C. (2014). Metabolic engineering approaches for production of biochemicals in food and medicinal plants. *Curr. Opin. Biotechnol.* 26, 174–182. doi: 10.1016/j.copbio.2014.01.006

World Health Organisation Model Lists of Essential Medicines (2019). *World Health Organisation Model Lists of Essential Medicines*. Geneva: World Health Organisation. Available online at: https://apps.who.int/iris/bitstream/handle/10665/325771/WHO-MVP-EMP-IAU-2019.06-eng.pdf?ua=1

Wurtzel, E. T., and Kutchan, T. M. (2016). Plant metabolism, the diverse chemistry set of the future. *Science* 353, 1232–1236. doi: 10.1126/science.aad2062

Xu, Z., Yang, Z., Liu, Y., Lu, Y., Chen, K., and Zhu, W. (2014). Halogen bond: its role beyond drug–target binding affinity for drug discovery and development. *J. Chem. Inf. Model.* 54, 69–78. doi: 10.1021/ci400539q

Yang, K. K., Wu, Z., and Arnold, F. H. (2019). Machine-learning-guided directed evolution for protein engineering. *Nat. Methods* 16, 687–694. doi: 10.1038/s41592-019-0496-6

Yeh, E., Blasiak, L. C., Koglin, A., Drennan, C. L., and Walsh, C. T. (2007). Chlorination by a long-lived intermediate in the mechanism of flavin-dependent halogenases. *Biochemistry* 46, 1284–1292. doi: 10.1021/bi0621213

Yeh, E., Garneau, S., and Walsh, C. T. (2005). Robust in vitro activity of RebF and RebH, a two-component reductase/halogenase, generating 7-chlorotryptophan during rebeccamycin biosynthesis. *Proc. Natl. Acad. Sci. U. S. A.* 102, 3960–3965. doi: 10.1073/pnas.0500755102

Yerkes, N., Wu, J. X., McCoy, E., Galan, M. C., Chen, S., and O'Connor, S. E. (2008). Substrate specificity and diastereoselectivity of strictosidine glucosidase, a key enzyme in monoterpene indole alkaloid biosynthesis. *Bioorganic Med. Chem. Lett.* 18, 3095–3098. doi: 10.1016/j.bmcl.2007.11.063

Zaky, A. S., Tucker, G. A., Daw, Z. Y., and Du, C. (2014). Marine yeast isolation and industrial application. *FEMS Yeast Res.* 14, 813–825. doi: 10.1111/1567-1364.12158

Zehner, S., Kotzsch, A., Bister, B., Süssmuth, R. D., Méndez, C., Salas, J. A., et al. (2005). A regioselective tryptophan 5-halogenase is involved in pyrroindomycin biosynthesis in Streptomyces rugosporus LL-42D005. *Chem. Biol.* 12, 445–452. doi: 10.1016/j.chembiol.2005.02.005

Zeng, J., Lytle, A. K., Gage, D., Johnson, S. J., and Zhan, J. (2013). Specific chlorination of isoquinolines by a fungal flavin-dependent halogenase. *Bioorganic Med. Chem. Lett.* 23, 1001–1003. doi: 10.1016/j.bmcl.2012.12.038

Zeng, J., and Zhan, J. (2011). Characterization of a tryptophan 6-halogenase from *Streptomyces toxytricini*. *Biotechnol. Lett.* 33, 1607–1613. doi: 10.1007/s10529-011-0595-7

Zeng, J., Zhang, D. B., Zhou, P. P., Zhang, Q. L., Zhao, L., Chen, J. J., et al. (2017). Rauvomines A and B. Two monoterpenoid indole alkaloids from *Rauvolfia vomitoria*. *Org. Lett.* 19, 3998–4001. doi: 10.1021/acs.orglett.7b01723

Zhou, F., and Pichersky, E. (2020). More is better: the diversity of terpene metabolism in plants. *Curr. Opin. Plant Biol.* 55, 1–10. doi: 10.1016/j.pbi.2020.01.005

Zhou, Y. J., Buijs, N. A., Zhu, Z., Gómez, D. O., Boonsombuti, A., Siewers, V., et al. (2016). Harnessing yeast peroxisomes for biosynthesis of fatty-acid-derived biofuels and chemicals with relieved side-pathway competition. *J. Am. Chem. Soc.* 138, 15368–15377. doi: 10.1021/jacs.6b07394

Zydney, A. L. (2016). Continuous downstream processing for high value biological products: a review. *Biotechnol. Bioeng.* 113, 465–475. doi: 10.1002/bit.25695

Conflict of Interest: The authors declare that the research was conducted in the absence of any commercial or financial relationships that could be construed as a potential conflict of interest.

frontiers in Bioengineering and Biotechnology

MINI REVIEW
published: 19 November 2020
doi: 10.3389/fbioe.2020.594347

CRISPR/Cas9 Systems for the Development of *Saccharomyces cerevisiae* Cell Factories

*Jie Meng, Yue Qiu and Shuobo Shi**

Beijing Advanced Innovation Center for Soft Matter Science and Engineering, College of Life Science and Technology, Beijing University of Chemical Technology, Beijing, China

Synthetic yeast cell factories provide a remarkable solution for the sustainable supply of a range of products, ranging from large-scale industrial chemicals to high-value pharmaceutical compounds. Synthetic biology is a field in which metabolic pathways are intensively studied and engineered. The clustered, regularly interspaced, short, palindromic repeat-associated (CRISPR)/CRISPR-associated protein 9 (Cas9) technology has emerged as the state-of-the-art gene editing technique for synthetic biology. Recently, the use of different CRISPR/Cas9 systems has been extended to the field of yeast engineering for single-nucleotide resolution editing, multiple-gene editing, transcriptional regulation, and genome-scale modifications. Such advancing systems have led to accelerated microbial engineering involving less labor and time and also enhanced the understanding of cellular genetics and physiology. This review provides a brief overview of the latest research progress and the use of CRISPR/Cas9 systems in genetic manipulation, with a focus on the applications of *Saccharomyces cerevisiae* cell factory engineering.

Keywords: CRISPR/Cas, *Saccharomyces cerevisiae*, cell factory, genetic manipulation, synthetic biology, complex engineering

OPEN ACCESS

Edited by:
Farshad Darvishi, Alzahra University, Iran

Reviewed by:
Mario Andrea Marchisio, Tianjin University, China
Kevin Solomon, Purdue University, United States
Guokun Wang, Technical University of Denmark, Denmark

***Correspondence:**
Shuobo Shi
shishuobo@mail.buct.edu.cn

Specialty section:
This article was submitted to Synthetic Biology, a section of the journal Frontiers in Bioengineering and Biotechnology

Received: *13 August 2020*
Accepted: *19 October 2020*
Published: *19 November 2020*

Citation:
Meng J, Qiu Y and Shi S (2020) CRISPR/Cas9 Systems for the Development of Saccharomyces cerevisiae Cell Factories. Front. Bioeng. Biotechnol. 8:594347. doi: 10.3389/fbioe.2020.594347

INTRODUCTION

The development of microbial cell factories have drawn increasing attention because they allow the production in a cost-effective, renewable, and sustainable manner (Xu et al., 2020). Ever-expanding genetic toolkits and fundamental understanding have enabled biotechnologists to build or rebuild genetic pathways in many hosts, especially those of model organisms such as *Saccharomyces cerevisiae* (Chen et al., 2017). In the last decades, *S. cerevisiae* has been considered a powerful eukaryotic cell factory for the biosynthesis of many compounds (Brown et al., 2015; Billingsley et al., 2016) or biofuels (Shi et al., 2016b; Yu et al., 2017).

In practice, the Design–Build–Test–Learn (DBTL) cycle has greatly facilitated the construction of an advanced cell factory through designing a genetic modification scheme, building the designated genotypes, testing a rebuilt biosystem at various levels, and learning from systematic data analysis (Liu et al., 2015; Chen et al., 2017). The construction of a successful cell factory always needs several rounds of DBTL cycles due to the complexity of cell metabolism (Billingsley et al., 2016). "Build" can be seen as a key rate-limiting step in the execution of rapid iterative DBTL cycles in generating designated genotypes using traditional genetic tools (Chao et al., 2017). For

example, it took more than 250 human years to get a commercial strain for producing farnesene (Karim et al., 2017).

Fortunately, the clustered, regularly interspaced, short, palindromic repeat-associated (CRISPR) system has become an important tool in almost all aspects of synthetic biology and metabolic engineering, including genomic editing, heterologous expression, transcriptional regulation, and genome-wide screening. CRISPR/Cas9 has become the most popular approach in recent years. In CRISPR/Cas9 system, the effector (Cas9) is activated and targeted to specific genomic loci by forming a complex with CRISPR RNA (crRNA) and trans-activating crRNA (tracrRNA) or a single guide RNA that merged from the crRNA and tracrRNA (Jinek et al., 2012; DiCarlo et al., 2013; Mans et al., 2015). Moreover, the development of Cas9 protein variants and the availability of mutually orthogonal Cas9 proteins have greatly maximized its functions and applications (Lian et al., 2017, 2018a; Si et al., 2017). In a word, remarkable improvements in the effectiveness and scope of CRISPR/Cas9 system have made it powerful and versatile for almost all possible genetic manipulations needed for constructing microbial cell factories. Due to its countless applications, two scientists who pioneered the CRISPR technology won the Nobel Prize in Chemistry in 2020[1].

This review mainly focused on the latest advances of the CRISPR/Cas9 system in the model yeast *S. cerevisiae*. Special attention was paid to examples in four application areas: flexible and precise genetic manipulation, multiplexed editing, transcriptional regulation, and genome-scale engineering/screening. Finally, perspectives on the challenges and opportunities were discussed and highlighted.

FLEXIBLE AND PRECISE GENETIC MANIPULATION

One of the most significant advantages of the CRISPR/Cas9 system is its flexibility and efficiency for operation with high accuracy. Cas9 protein is a "scissor" to introduce double-strand breaks (DSBs), and guide RNA (gRNA) can be regarded as a "guide" for target-specific recognition (Jinek et al., 2012). The formed DSBs required intrinsic DNA repair mechanisms for editing target loci (Lian et al., 2018a). The homology-dependent recombination (HDR) in yeast can repair DSBs with flexible donors containing desired sequences (**Figure 1A**), which allows various genetic manipulations, including gene deletion (e.g., whole coding sequence knockout) (Zhang et al., 2019), gene mutation or disruption (DiCarlo et al., 2013), and gene integration (Shi et al., 2016a; Roy et al., 2018).

In the aforementioned processes, strain engineering displayed a high editing efficiency (**Table 1**). For example, DiCarlo et al. (2013) first demonstrated in yeast that both gene disruption and insertion could be achieved with nearly 100% efficiency using a 90-bp dsOligo as the donor and the CRISPR/Cas9 system. Notably, DNA integration efficiency declined rapidly when the size of the target DNA increased, which could be considered as the limiting factor in integrating large DNA fragments. Using the CRISPR/Cas9, Shi et al. (2016a) developed a Di-CRISPR platform that realized the integration of a 24-kb pathway for the production of (*R*,*R*)-2,3-butanediol. This was a significant achievement in the efficiency and multicopy integration of large DNA.

The high efficiency and flexibility also allowed the rapid generation of a mutant library (**Table 1**). Guo et al. (2018) created hundreds of mutated stains for 315 poorly characterized open reading frames (ORFs) using the CRISPR/Cas9 system, of which 68 were found to be vital for growth. Jakociunas et al. (2018) combined error-prone polymerase chain reaction (PCR) and Cas9-mediated genome integration for protein-directed evolution. The large mutagenized DNA fragments generated by error-prone PCR were integrated into the genome for creating millions of mutants without any bias in mutation frequency. Two mutant enzymes were found, resulting in the increased production of isoprenoids close to 11-fold. Because of its simplicity, flexibility, and high efficiency in knock-in, the CRISPR/Cas9 system enabled the rapid economic development of a high-throughput industrial yeast cell factory that usually required a lot of genomic integration manipulations.

The aforementioned cases showed high precision and accuracy in gene editing using the CRISPR/Cas9 system (**Table 1**). However, it is initially difficult for the CRISPR/Cas9 system to introduce mutations at single-nucleotide resolution due to its off-target effects (O'Geen et al., 2015). Various strategies have been reported to increase the fidelity and specificity, including well-designed gRNAs (Wang and Coleman, 2019), mutants of Cas proteins (Hu et al., 2018), paired nCas or fCas complexes (Shen et al., 2014; Tsai et al., 2014), and deaminase-dependent strategy (Gaudelli et al., 2017; Tan et al., 2019). For example, a two-step strategy using the CRISPR/Cas9 system was demonstrated to seamlessly introduce 17 precise single mutations in *S. cerevisiae* (Biot-Pelletier and Martin, 2016). Recently, a novel single-nucleotide resolution editing tool was reported (named as CHAnGE) by combining HDR and the CRISPR/Cas9 system that enabled the rapid engineering of *S. cerevisiae* for improved tolerance to growth inhibitors (Bao et al., 2018). Meanwhile, Tan et al. (2019) adopted a deaminase-dependent strategy that could selectively edit a single cytidine at a specific position. These high-precision tools guaranteed the introduction of specific point mutations in genome for genetic diversification, which gained special interest in terms of cell factory development using the bottom–up approach.

The CRISPR/Cas9 system has a significant advantage in its ease and wide applicability (**Table 1**). Its use is simple in designing and expressing gRNAs. In addition, it has been readily implemented in precise genome editing at an unprecedented level. Furthermore, the lethal characteristic of DSBs introduced by Cas9 endonuclease offers convenience for marker-free positive selection, which is especially useful in non-model microorganisms due to the lack of developed selectable markers.

[1]https://www.nobelprize.org/prizes/chemistry/2020/press-release/

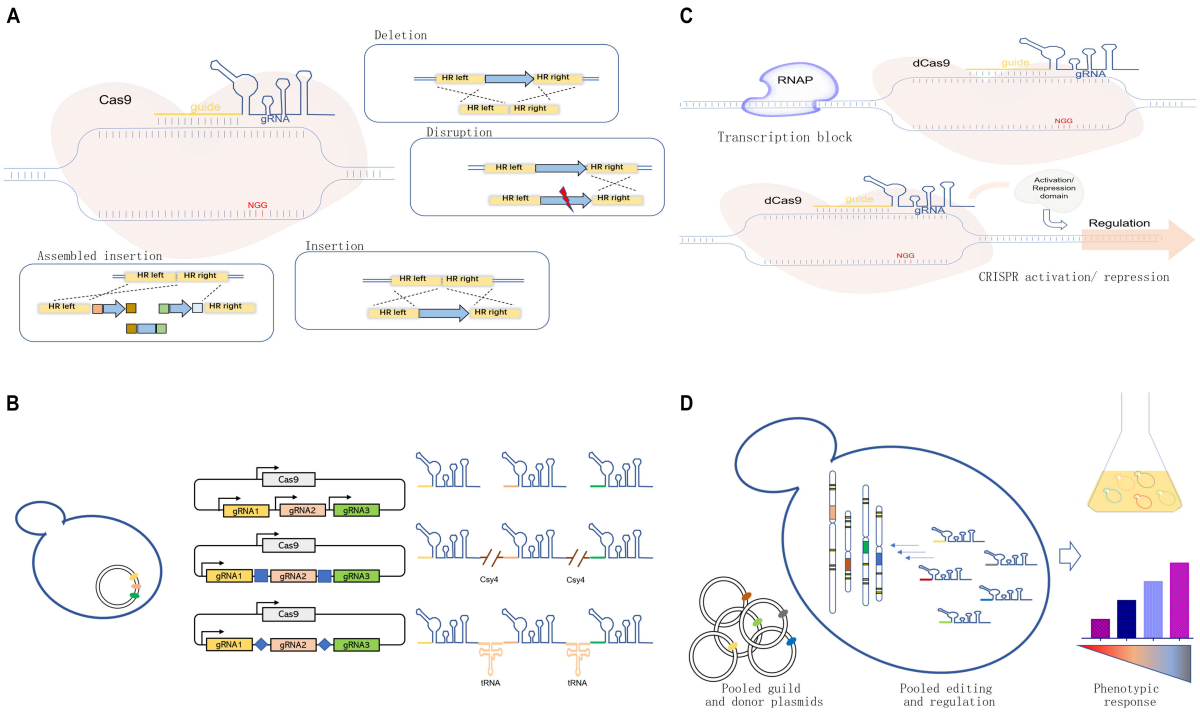

FIGURE 1 | Development and applications of the clustered, regularly interspaced, short, palindromic repeat-associated (CRISPR)/CRISPR-associated protein 9 (Cas9) systems in yeast cell factory engineering. **(A)** Scheme of the CRISPR/Cas9 system for genome editing, including gene deletion, mutation or disruption, insertion, and assembled insertion. **(B)** Guide RNA (gRNA) multiplexing strategies, including multi-single guide RNA (multi-sgRNA) expression through the use of multiple promoters or the expression of one-promoter-guided single transcript separated by different features for RNA cleavage. **(C)** dCas-meditated CRISPRi and CRISPRa systems for transcriptional regulation achieved through physically blocking RNA polymerase (RNAP) or recruiting protein effectors for target repression/activation. **(D)** Pooled gRNA-guided genome-scale engineering or screening.

MULTISITE EDITING TO ACCELERATE THE BUILDING PROCESS

The CRISPR/Cas9 system is suitable for simultaneous multigene editing in *S. cerevisiae* because of the high HDR rate (**Table 1**). The execution of multigene editing requires the expression of multiple gRNAs (**Figure 1B**), which can be transcribed individually by RNA polymerase promoters (Jakociunas et al., 2015a; Ding et al., 2020) or transcribed in a single long transcript. Then, individual gRNAs can be released through different strategies.

Using the strategy of individual expression, Jakociunas et al. (2015a) constructed a plasmid harboring multicassettes to express different gRNAs with individual promoters. This approach successfully engineered five genes in one step and achieved a 41-fold improvement in the production of mevalonate. Jakociunas et al. (2015b) further extended and updated this method to CasEMBLR by combining *in vivo* assembly and targeted editing; CasEMBLR allowed a marker-free integration of 15 exogenous DNA parts in one step. Similarly, Ronda et al. (2015) developed CrEdit to manipulate three genomic DNAs by generating three gRNAs, respectively, which completed simultaneous triple insertions of a non-native pathway for β-carotene production in *S. cerevisiae* without selection, with up to 84% targeting efficiency.

Using the single-transcript strategy for expressing gRNAs, homology-integrated CRISPR-Cas (HI-CRISPR) was developed for disrupting three genes simultaneously in the artificial hydrocortisone biosynthetic pathway with an efficiency ranging from 27 to 87%. The pre-crRNAs were transcribed by one promoter and then processed into multiple crRNAs by host RNase III and unknown nuclease(s) (Bao et al., 2015). Ferreira et al. (2018) adopted bacterial endoribonuclease Csy4 for expressing a single transcript containing multiple gRNAs fused with Csy4-cleavable RNA, contributing to a quadruple deletion with 96% efficiency.

Recently, Zhang et al. (2019) developed a gRNA–tRNA array for CRISPR-Cas9 (GTR-CRISPR) using endogenous $tRNA^{Gly}$ for gRNA processing; this method disrupted eight genes with 87% efficiency in one step, which is the best example of multigene editing. As a case study, GTR-CRISPR was adopted to obtain a 30-fold increase in free fatty acid production within 10 days.

The aforementioned studies demonstrated the ability to edit multiple genes simultaneously, with varied efficiency. The selection of gRNA sequences and the efficient expression of gRNAs seem to be critical to achieve a high efficiency. It is therefore believed that the multiple-gene manipulation of CRISPR-mediated methods and applications may greatly benefit from the study of gRNA design and efficient expression. The implementation of multiloci editing using CRISPR systems has

TABLE 1 | Selected clustered, regularly interspaced, short, palindromic repeat-associated (CRISPR)/CRISPR-associated protein 9 (Cas9)-associated applications in cell factory construction.

Types	Methods	Key features and achievements	References
Flexible and precise genetic manipulation	CRISPR/Cas9 for genome engineering (using 90-bp dsOligo donor)	First achieved site-specific mutagenesis and allelic replacement with nearly 100% efficiency	DiCarlo et al., 2013
	Di-CRISPR (delta integration CRISPR-Cas)	Assembled an unprecedented 18-copy, 24-kb pathway for the production of (*R*,*R*)-2,3-butanediol	Shi et al., 2016a
	CasPER (Cas9-mediated protein evolution reaction)	Employed error-prone PCR and CRISPR/Cas9 system for the directed evolution of key enzymes, resulting in 11-fold higher production of isoprenoids	Jakociunas et al., 2018
	Seamless site-directed mutagenesis	Introduced point mutations at 17 positions by a two-step method and constructed a target mutant for a measurable phenotype	Biot-Pelletier and Martin, 2016
	CHAnGE (CRISPR–Cas9- and homology-directed repair-assisted genome-scale engineering)	Validated single-nucleotide resolution genome editing by creating a genome-wide gene disruption collection with improved tolerance to growth inhibitors	Bao et al., 2018
	Base editor for single-nucleotide replacement using nCas9	Connected cytidine deaminase domain and the nCas9 domain and elicited C-to-T mutations with high accuracy and efficiency	Tan et al., 2019
Multisite editing	HI-CRISPR (homology-integrated CRISPR)	First example of CRISPR/Cas9 multiple disruption in *S. cerevisiae* with efficiency ranging from 27 to 87%	Bao et al., 2015
	CRISPR/Cas9 multiplex genomic editing	Realized quintuple disruption using individual gRNA cassettes in the mevalonate pathway with titers increased more than 41-fold	Jakociunas et al., 2015a
	CasEMBLR (Cas9 facilitated multiloci DNA integration assembler)	Combined *in vivo* assembly and targeted editing, allowing marker-free integration of 15 DNA parts for carotenoid production in 3 loci or 10 DNA parts for tyrosine production in 2 loci	Jakociunas et al., 2015b
	Multiplexed CRISPR/Cas9 genome editing and gene regulation	Exploited bacterial endoribonuclease Csy4 to generate multiple gRNAs from a single transcript and performed a quadruple deletion with 96% efficiency or an efficient regulation of three genes	Ferreira et al., 2018
	GTR-CRISPR (gRNA–tRNA array for CRISPR-Cas9)	Utilized endogenous tRNA-Gly processing to generate multiple gRNAs from a single transcript and disrupted eight genes with 87% efficiency in one step	Zhang et al., 2019
	Lightning GTR-CRISPR	Directly transformed the Golden Gate reaction mix into yeast and disrupted six genes in 3 days with 60% efficiency. Two-round application of Lightning GTR-CRISPR could simplify yeast lipid networks, resulting in a 30-fold increase in free fatty acid production in 10 days	Zhang et al., 2019
Transcriptional regulation for orthogonal control	Multiplex CRISPRi-mediated downregulation	CRISPRi method for simultaneously downregulating seven genes for enhancing β-amyrin production	Ni et al., 2019
	CRISPR-associated RNA scaffolds to generate synthetic multigene transcriptional programs	Realized simultaneous activation and repression of different target genes from a five-gene pathway (VioABEDC) for optimizing the production of violacein	Zalatan et al., 2015
	STEPS (systematically test enzyme perturbation sensitivities)	Established a method for fine-tuned, graded expression of pathway enzymes via dCas9 regulation by varying sgRNA target location, and identified rate-limiting steps, resulting in an increased 3-dehydroshikimate and glycerol production at 7.8- and 5.7-fold, respectively	Deaner and Alper, 2017
	SWITCH: a CRISPR-based system for rapid genetic engineering and pathway tuning	Achieved iteratively alternated genetic engineering and pathway control state for implementing and tuning the pathway for naringenin	Vanegas et al., 2017
	CRISPR-AID: an orthogonal trifunctional CRISPR system	Combined transcriptional activation, transcriptional interference, and gene deletion; the method enhanced the production of β-carotene by 3-fold in a single step and achieved a 2.5-fold improvement in endoglucanase activity in a combinatorial manner	Lian et al., 2017

(Continued)

TABLE 1 | Continued

Types	Methods	Key features and achievements	References
Genome-scale engineering/screening	CRISPR/Cas9-mediated automated platform for multiplex genome-scale engineering	Iteratively integrated mutation library into the repetitive genomic sequences using robotic automation and optimized diverse phenotypes on a genome scale, such as acetic acid tolerance	Si et al., 2017
	Cas9-mediated integration approach for tuning gene expression	Identified targets that improved protein secretion when expressed at different levels, achieving 2.2-fold improvement in amylase production	Wang et al., 2019
	CHAnGE (CRISPR–Cas9- and homology-directed repair-assisted genome-scale engineering method)	Rapidly created genome-wide disruption mutants for the directed evolution of acetic acid tolerance, achieving a 20-fold improvement	Bao et al., 2018
	MAGIC (multifunctional genome-wide CRISPR)	Combined CRISPR-AID and array-synthesized oligo pools to create comprehensive genomic libraries for obtaining furfural tolerance and surface display levels of endoglucanase, thus facilitating complete genotype–phenotype mapping	Lian et al., 2019

greatly reduced the timeline of operation. For example, the traditional method requires approximately 6 weeks for editing three genomic loci (Horwitz et al., 2015), while using multiplexed CRISPR-Cas9 needs only 1 week with one transformation step. Moreover, the GTR-CRISPR even achieved six-gene disruptions in 3 days by avoiding the cloning step in *Escherichia coli* (Zhang et al., 2019).

TRANSCRIPTIONAL REGULATION FOR ORTHOGONAL CONTROL

Besides the precise manipulation of genomic DNA, the CRISPR/Cas9 system serves as a transcriptional regulation platform with the adoption of inactive Cas protein (e.g., dCas9, with H840A and D10A mutations, loses its endonuclease activity but retains its capability of sequence-specific binding). Further, dCas9 can be combined with effector domains as artificial scaffolds, thus influencing genomic structure and transcriptional regulation (Lian et al., 2018a; Ding et al., 2020).

As shown in **Figure 1C**, the CRISPR interference (CRISPRi) used dCas9-mediated DNA recognition complex as a block in physical space to specifically interfere with transcription initiation and elongation (Qi et al., 2013). Based on this strategy, Ni et al. (2019) used a CRISPRi method for downregulating the expression of seven genes simultaneously for enhancing β-amyrin production in *S. cerevisiae*. However, the physical block alone could not always result in an efficient repression. The dCas9 can be fused with several transcriptional repressor domains or chromatin modifiers for effective repression (**Figure 1C**). In *S. cerevisiae*, the addition of dCas9 fusion domain, Mxi1, could lead to a 53-fold repression compared with 18-fold repression using dCas9 alone (Gilbert et al., 2013). Later, Lian et al. (2017) compared different repression domains in yeast and found that several native repression domains, RD2, RD5, and RD11, worked the best for CRISPRi. Similarly, CRISPR could mediate the transcription activation of target genes (CRISPRa) by recruiting transcription activators with dCas9 (**Figure 1C**). In *S. cerevisiae*, the recruitment of herpes simplex viral protein 16 (VP64) could lead to up to 70-fold activation by increasing the number of targeting sites (Farzadfard et al., 2013). Later, Chavez et al. (2015) rationally designed a tripartite activator, VP64-p65-Rta, which showed an efficient activating effect in *S. cerevisiae* (∼10-fold). Moreover, modular scaffold RNAs could also be used for CRISPRi and CRISPRa to replace the aforementioned effector domains. For example, Zalatan et al. (2015) developed a modular RNA-based system that enabled the recruitment of activators or repressors by converting the gRNA into a scaffold RNA (scRNA) for transcriptional programming. In addition, the multivalent recruitment with two RNA hairpins could produce a stronger activation effect. It is now feasible to permit programmable transcriptional regulation orthogonally by taking advantage of the binding activity of dCas and different effector domains. Besides, Wang et al. (2019) used the Cas9-mediated integration approach for tuning the transcriptional levels of multiple genes in a combinatorial manner by integrating overexpression cassettes and/or RNAi cassettes without the involvement of effector domains. The developed method was used to optimize the production of amylase.

Functional CRISPR regulatory systems have been exploited simultaneously for combinatorial genetic manipulations (**Table 1**). One particularly interesting application could tune the expression levels of a five-gene pathway (*VioABEDC*) for optimizing the production of violacein with simultaneous activation and repression (Zalatan et al., 2015). Later, Deaner and Alper (2017) established a new system called systematically test enzyme perturbation sensitivities (STEPS) to achieve a graded expression of target genes by varying gRNA-binding sites in promoter regions. STEPS was used to identify the rate-limiting steps and alleviate pathway bottlenecks, resulting in a 7.8- and 5.7-fold increased 3-dehydroshikimate and glycerol production, respectively. Similarly, SWITCH system was developed to achieve gene integration and regulation simultaneously; it was used to establish and optimize a cell factory for naringenin production (Vanegas et al., 2017). Recently, Lian et al. (2017) established orthogonal trifunctional CRISPR system (CRISPR-AID) that simultaneously enabled gene editing and transcriptional regulation. As proof of concept, this strategy was successfully

used to enhance the production of β-carotene by 3-fold and give a 2.5-fold improvement in endoglucanase activity. Combinatorial transcriptional regulation is central to developing yeast cell factories or understanding the complex behavior of synthetic biological systems. It requires not only gain- and loss-of-function genome engineering but also a fine-tuned and programmable control of the expression of multiple genes, so as to engineer or study synthetic biosystems.

GENOME-SCALE ENGINEERING/SCREENING

Libraries of strains with versatile genetic alterations at the genome level could provide invaluable knowledge for understanding genome functions or permitting a direct screening of desired traits. It is still tedious to introduce genome-wide perturbations using available techniques (Lian et al., 2019). Fortunately, the fast development and effectiveness of CRISPR tools permit researchers to build activated and/or interfered gene libraries for genome-wide perturbations in a more standardized and advanced manner compared with previous methods (**Table 1**). Recently, Si et al. (2017) reported a robotic platform for automated multiplex genome-scale engineering using a standardized workflow. With the aid of CRISPR/Cas9, this platform iteratively integrated standardized genetic parts into repetitive genomic sequences of *S. cerevisiae* and permitted functional mapping and optimization for diverse phenotypes. Wang et al. (2019) incorporated Cas9-facilitated workflow to generate a library comprising RNAi/overexpression (OE) targets for the identification and combinatorial manipulation of the expression levels of favorable gene targets.

It is now possible and convenient to generate a strain library with genetic changes across the whole genome using pooled gRNAs through efficient chip-based synthesis of oligo pools (**Figure 1D**). Bao et al. (2018) developed a CHAnGE system that could rapidly construct numerous specific genetic variants in yeast. A genome-wide gene disruption was created by this method with an average frequency of 82% and then applied to improve cell tolerance to furfural. Similarly, a gene activation library was created to screen genes for better thermotolerance in *S. cerevisiae*, which identified a key factor in thermotolerance that benefited from *OLE1* (Li et al., 2019). The genome-scale library of gRNAs could also be combined with CRISPRi and CRISPRa to generate genome-wide libraries for silencing or/and activating genes. For example, Smith et al. (2016) combined gRNA libraries with CRISPRi, establishing a screening method for functional and/or chemical genomic screens. Recently, Lian et al. (2019) combined previously reported CRISPR-AID and array-synthesized oligo pools, thus creating a comprehensive and diversified genomic library for gain/reduction/loss of function. The developed system, called multifunctional genome-wide CRISPR (MAGIC), covered almost all ORFs and RNA genes (>99%). It served as a powerful tool to uncover previously uncharacterized gene interactions or engineer complex phenotypes for different biotechnological applications.

The genome-wide CRISPR screening tactics give a significant push to complete genotype–phenotype mapping, analyze complex biological systems, and finally take a big step forward in the metabolic engineering of yeast cell factories. It is important that new knowledge and guidance be gained from the simultaneous activation and repression of various target genes.

CONCLUSION AND FUTURE PERSPECTIVES

CRISPR/Cas9-based tools are considered revolutionary and versatile platforms for genetic manipulations and synthetic biology. This review summarized recent developments and applications of the CRISPR/Cas9 system in the construction and optimization of *S. cerevisiae* cell factory. However, these tools still have some limitations and challenges.

The design and expression of gRNAs is a crucial factor severely affecting editing efficiency between genes. One possible reason could be the formation of secondary structures of gRNAs (Thyme et al., 2016). Usually, several gRNAs should be tested for a new target; however, verifying the target efficiency of each gRNA is a time-consuming process. The predictable accuracy needs further improvement. Some software, websites, rules, and algorithms have been established, for example, Zhang Lab Guide Design Resources[2], CRISPR direct[3] (Naito et al., 2015), CHOPCHOP (Montague et al., 2014), and yeast proprietary gRNA tool[4].

Another key problem limiting further applications of the CRISPR system is the yeast transformation efficiency, especially for multisite integration and genome-scale engineering. A large size and an increased number of adopted donor DNAs might reduce the likelihood to simultaneously enter the cells, thus limiting the use of repair templates for gene editing. It was also revealed that the integration efficiency facilitated by CRISPR could be enhanced if more donor DNA could enter the cells (Shi et al., 2016a). The reported HI-CRISPR (Bao et al., 2015) and multiplexed accurate genome editing with short, trackable, integrated cellular barcodes (MAGESTIC) (Roy et al., 2018) both linked HDR donors with gRNA cassette in one plasmid, providing a useful strategy to facilitate DNA delivery at high efficiency.

The currently adopted activation domain for CRISPRa could only provide a limited activation compared with inducible promoter with upregulated strength up to 1,000-fold (Lian et al., 2018b). Hence, a more efficient activation domain should be screened or engineered, or a novel strategy should be developed to activate genes.

Despite the limitations, the development of the CRISPR system has undoubtedly created a new era for genomic manipulation. The building step is time consuming in the DBTL

[2]http://crispr.mit.edu/

[3]http://crispr.dbcls.jp/

[4]http://yeastriction.tnw.tudelft.nl/

cycle of cell factory engineering, but CRISPR technology has accelerated this process. Eight genomic edits can be achieved in a week using the CRISPR/Cas9 system, which took several weeks to complete in the past. The CRISPR system might prove to be a more powerful tool in the future when integrated with new design principles learned from genome-scale metabolic models and efficient handling options from automated robotic systems.

AUTHOR CONTRIBUTIONS

JM and SS outlined this manuscript. JM drafted the manuscript. SS revised the manuscript. YQ summarized the literature. All authors contributed to the article and approved the submitted version.

FUNDING

This work was supported by the National Key Research and Development Program of China (2018YFA0900100), National Natural Science Foundation of China (21878013 and 2191101491), the Foundation of Key Laboratory of Biomass Chemical Engineering of Ministry of Education, Zhejiang University (No. 2018BCE004), the Fundamental Research Funds for the Central Universities, and Beijing Advanced Innovation Center for Soft Matter Science and Engineering.

ACKNOWLEDGMENTS

We thank Prof. Huimin Zhao (University of Illinois at Urbana-Champaign) for his very enlightening comments.

REFERENCES

Bao, Z., HamediRad, M., Xue, P., Xiao, H., Tasan, I., Chao, R., et al. (2018). Genome-scale engineering of *Saccharomyces cerevisiae* with single-nucleotide precision. *Nat. Biotechnol.* 36, 505–508. doi: 10.1038/nbt.4132

Bao, Z., Xiao, H., Liang, J., Zhang, L., Xiong, X., Sun, N., et al. (2015). Homology-integrated CRISPR-Cas (HI-CRISPR) system for one-step multigene disruption in *Saccharomyces cerevisiae*. *ACS Synth. Biol.* 4, 585–594. doi: 10.1021/sb500255k

Billingsley, J. M., DeNicola, A. B., and Tang, Y. (2016). Technology development for natural product biosynthesis in *Saccharomyces cerevisiae*. *Curr. Opin. Biotechnol.* 42, 74–83. doi: 10.1016/j.copbio.2016.02.033

Biot-Pelletier, D., and Martin, V. J. (2016). Seamless site-directed mutagenesis of the *Saccharomyces cerevisiae* genome using CRISPR-Cas9. *J. Biol. Eng.* 10:6. doi: 10.1186/s13036-016-0028-

Brown, S., Clastre, M., Courdavault, V., and O'Connor, S. E. (2015). De novo production of the plant-derived alkaloid strictosidine in yeast. *Proc. Natl. Acad. Sci. U.S.A.* 112, 3205–3210. doi: 10.1073/pnas.1423555112

Chao, R., Mishra, S., Si, T., and Zhao, H. (2017). Engineering biological systems using automated biofoundries. *Metab. Eng.* 42, 98–108. doi: 10.1016/j.ymben.2017.06.003

Chavez, A., Scheiman, J., Vora, S., Pruitt, B. W., Tuttle, M., Iyer, E. P., et al. (2015). Highly efficient Cas9-mediated transcriptional programming. *Nat. Methods* 12, 326–328. doi: 10.1038/nmeth.3312

Chen, X., Gao, C., Guo, L., Hu, G., Luo, Q., Liu, J., et al. (2017). DCEO biotechnology: tools to design, construct, evaluate, and optimize the metabolic pathway for biosynthesis of chemicals. *Chem. Rev.* 118, 4–72. doi: 10.1021/acs.chemrev.6b00804

Deaner, M., and Alper, H. S. (2017). Systematic testing of enzyme perturbation sensitivities via graded dCas9 modulation in *Saccharomyces cerevisiae*. *Metab. Eng.* 40, 14–22. doi: 10.1016/j.ymben.2017.01.012

DiCarlo, J. E., Norville, J. E., Mali, P., Rios, X., Aach, J., and Church, G. M. (2013). Genome engineering in *Saccharomyces cerevisiae* using CRISPR-Cas systems. *Nucleic Acids Res.* 41, 4336–4343. doi: 10.1093/nar/gkt135

Ding, W., Zhang, Y., and Shi, S. (2020). Development and application of CRISPR/Cas in microbial biotechnology. *Front. Bioeng. Biotechnol.* 8:711. doi: 10.3389/fbioe.2020.00711

Farzadfard, F., Perli, S. D., and Lu, T. K. (2013). Tunable and multifunctional eukaryotic transcription factors based on CRISPR/Cas. *ACS Synth. Biol.* 2, 604–613. doi: 10.1021/sb400081r

Ferreira, R., Skrekas, C., Nielsen, J., and David, F. (2018). Multiplexed CRISPR/Cas9 genome editing and gene regulation using Csy4 in *Saccharomyces cerevisiae*. *ACS Synth. Biol.* 7, 10–15. doi: 10.1021/acssynbio.7b00259

Gaudelli, N. M., Komor, A. C., Rees, H. A., Packer, M. S., Badran, A. H., Bryson, D. I., et al. (2017). Programmable base editing of AT to GC in genomic DNA without DNA cleavage. *Nature* 551, 464–471. doi: 10.1038/nature24644

Gilbert, L. A., Larson, M. H., Morsut, L., Liu, Z., Brar, G. A., Torres, S. E., et al. (2013). CRISPR-mediated modular RNA-guided regulation of transcription in eukaryotes. *Cell* 154, 442–451. doi: 10.1016/j.cell.2013.06.044

Guo, X., Chavez, A., Tung, A., Chan, Y., Kaas, C., Yin, Y., et al. (2018). High-throughput creation and functional profiling of DNA sequence variant libraries using CRISPR–Cas9 in yeast. *Nat. Biotechnol.* 36:540. doi: 10.1038/nbt.4147

Horwitz, A. A., Walter, J. M., Schubert, M. G., Kung, S. H., Hawkins, K., Platt, D. M., et al. (2015). Efficient multiplexed integration of synergistic alleles and metabolic pathways in yeasts via CRISPR-Cas. *Cell Syst.* 1, 88–96. doi: 10.1016/j.cels.2015.02.001

Hu, J. H., Miller, S. M., Geurts, M. H., Tang, W., Chen, L., Sun, N., et al. (2018). Evolved Cas9 variants with broad PAM compatibility and high DNA specificity. *Nature* 556, 57–63. doi: 10.1038/nature26155

Jakociunas, T., Bonde, I., Herrgard, M., Harrison, S. J., Kristensen, M., Pedersen, L. E., et al. (2015a). Multiplex metabolic pathway engineering using CRISPR/Cas9 in *Saccharomyces cerevisiae*. *Metab. Eng.* 28, 213–222. doi: 10.1016/j.ymben.2015.01.008

Jakociunas, T., Pedersen, L. E., Lis, A. V., Jensen, M. K., and Keasling, J. D. (2018). CasPER, a method for directed evolution in genomic contexts using mutagenesis and CRISPR/Cas9. *Metab. Eng.* 48, 288–296. doi: 10.1016/j.ymben.2018.07.001

Jakociunas, T., Rajkumar, A. S., Zhang, J., Arsovska, D., Rodriguez, A., Jendresen, C. B., et al. (2015b). CasEMBLR: Cas9-facilitated multiloci genomic integration of in vivo assembled DNA parts in *Saccharomyces cerevisiae*. *ACS Synth. Biol.* 4, 1226–1234. doi: 10.1021/acssynbio.5b00007

Jinek, M., Chylinski, K., Fonfara, I., Hauer, M., Doudna, J. A., and Charpentier, E. (2012). A programmable dual-RNA-guided DNA endonuclease in adaptive bacterial immunity. *Science* 337, 816–821. doi: 10.1126/science.1225829

Karim, A. S., Dudley, Q. M., and Jewett, M. C. (2017). Cell-free synthetic systems for metabolic engineering and biosynthetic pathway prototyping. *Ind. Biotechnol. Microorg.* 1, 125–148. doi: 10.1002/9783527807796.ch

Li, P., Fu, X., Zhang, L., and Li, S. (2019). CRISPR/Cas-based screening of a gene activation library in *Saccharomyces cerevisiae* identifies a crucial role of OLE1 in thermotolerance. *Microb. Biotechnol.* 12, 1154–1163. doi: 10.1111/1751-7915.13333

Lian, J., HamediRad, M., Hu, S., and Zhao, H. (2017). Combinatorial metabolic engineering using an orthogonal tri-functional CRISPR system. *Nat. Commun.* 8:1688. doi: 10.1038/s41467-017-01695-x

Lian, J., HamediRad, M., and Zhao, H. (2018a). Advancing metabolic engineering of *Saccharomyces cerevisiae* using the CRISPR/Cas system. *Biotechnol. J.* 13:e1700601. doi: 10.1002/biot.201700601

Lian, J., Mishra, S., and Zhao, H. (2018b). Recent advances in metabolic engineering of *Saccharomyces cerevisiae*: new tools and their applications. *Metab. Eng.* 50, 85–108. doi: 10.1016/j.ymben.2018.04.011

Lian, J., Schultz, C., Cao, M., HamediRad, M., and Zhao, H. (2019). Multi-functional genome-wide CRISPR system for high throughput genotype–phenotype mapping. *Nat. Commun.* 10:5794. doi: 10.1038/s41467-019-13621-4

Liu, R., Bassalo, M. C., Zeitoun, R. I., and Gill, R. T. (2015). Genome scale engineering techniques for metabolic engineering. *Metab. Eng.* 32, 143–154. doi: 10.1016/j.ymben.2015.09.013

Mans, R., van Rossum, H. M., Wijsman, M., Backx, A., Kuijpers, N. G., van den Broek, M., et al. (2015). CRISPR/Cas9: a molecular Swiss army knife for simultaneous introduction of multiple genetic modifications in *Saccharomyces cerevisiae*. *FEMS Yeast Res.* 15:fov004. doi: 10.1093/femsyr/fov004

Montague, T. G., Cruz, J. M., Gagnon, J. A., Church, G. M., and Valen, E. (2014). CHOPCHOP: a CRISPR/Cas9 and TALEN web tool for genome editing. *Nucleic Acids Res.* 42, W401–W407. doi: 10.1093/nar/gku410

Naito, Y., Hino, K., Bono, H., and Ui-Tei, K. (2015). CRISPRdirect: software for designing CRISPR/Cas guide RNA with reduced off-target sites. *Bioinformatics* 31, 1120–1123. doi: 10.1093/bioinformatics/btu743

Ni, J., Zhang, G., Qin, L., Li, J., and Li, C. (2019). Simultaneously down-regulation of multiplex branch pathways using CRISPRi and fermentation optimization for enhancing β-amyrin production in *Saccharomyces cerevisiae*. *Synth. Syst. Biotechnol.* 4, 79–85. doi: 10.1016/j.synbio.2019.02.002

O'Geen, H., Abigail, S. Y., and Segal, D. J. (2015). How specific is CRISPR/Cas9 really? *Curr. Opin. Chem. Biol.* 29, 72–78. doi: 10.1016/j.cbpa.2015.10.001

Qi, L. S., Larson, M. H., Gilbert, L. A., Doudna, J. A., Weissman, J. S., Arkin, A. P., et al. (2013). Repurposing CRISPR as an RNA-guided platform for sequence-specific control of gene expression. *Cell* 152, 1173–1183. doi: 10.1016/j.cell.2013.02.022

Ronda, C., Maury, J., Jakociunas, T., Jacobsen, S. A. B., Germann, S. M., Harrison, S. J., et al. (2015). CrEdit: CRISPR mediated multi-loci gene integration in *Saccharomyces cerevisiae*. *Microb. Cell. Fact.* 14:97. doi: 10.1186/s12934-015-0288-3

Roy, K. R., Smith, J. D., Vonesch, S. C., Lin, G., Tu, C. S., Lederer, A. R., et al. (2018). Multiplexed precision genome editing with trackable genomic barcodes in yeast. *Nat. Biotechnol.* 36, 512–520. doi: 10.1038/nbt.4137

Shen, B., Zhang, W., Zhang, J., Zhou, J., Wang, J., Chen, L., et al. (2014). Efficient genome modification by CRISPR-Cas9 nickase with minimal off-target effects. *Nat. Methods* 11, 399–402. doi: 10.1038/nmeth.2857

Shi, S., Liang, Y., Zhang, M. M., Ang, E. L., and Zhao, H. (2016a). A highly efficient single-step, markerless strategy for multi-copy chromosomal integration of large biochemical pathways in *Saccharomyces cerevisiae*. *Metab. Eng.* 33, 19–27. doi: 10.1016/j.ymben.2015.10.011

Shi, S., Si, T., Liu, Z., Zhang, H., Ang, E. L., and Zhao, H. (2016b). Metabolic engineering of a synergistic pathway for n-butanol production in *Saccharomyces cerevisiae*. *Sci. Rep.* 6:25675. doi: 10.1038/srep25675

Si, T., Chao, R., Min, Y., Wu, Y., Ren, W., and Zhao, H. (2017). Automated multiplex genome-scale engineering in yeast. *Nat. Commun.* 8:15187. doi: 10.1038/ncomms15187

Smith, J. D., Suresh, S., Schlecht, U., Wu, M., Wagih, O., Peltz, G., et al. (2016). Quantitative CRISPR interference screens in yeast identify chemical-genetic interactions and new rules for guide RNA design. *Genome Biol.* 17:45. doi: 10.1186/s13059-016-0900-9

Tan, J., Zhang, F., Karcher, D., and Bock, R. (2019). Engineering of high-precision base editors for site-specific single nucleotide replacement. *Nat. Commun.* 10, 1–10. doi: 10.1038/s41467-018-08034-8

Thyme, S. B., Akhmetova, L., Montague, T. G., Valen, E., and Schier, A. F. (2016). Internal guide RNA interactions interfere with Cas9-mediated cleavage. *Nat. Commun.* 7:11750. doi: 10.1038/ncomms11750

Tsai, S. Q., Wyvekens, N., Khayter, C., Foden, J. A., Thapar, V., Reyon, D., et al. (2014). Dimeric CRISPR RNA-guided FokI nucleases for highly specific genome editing. *Nat. Biotechnol.* 32, 569–576. doi: 10.1038/nbt.2908

Vanegas, K. G., Lehka, B. J., and Mortensen, U. H. (2017). SWITCH: a dynamic CRISPR tool for genome engineering and metabolic pathway control for cell factory construction in *Saccharomyces cerevisiae*. *Microb. Cell Fact.* 16:25. doi: 10.1186/s12934-017-0632-x

Wang, G., Bjork, S. M., Huang, M., Liu, Q., Campbell, K., Nielsen, J., et al. (2019). RNAi expression tuning, microfluidic screening, and genome recombineering for improved protein production in *Saccharomyces cerevisiae*. *Proc. Natl. Acad. Sci. U.S.A.* 116, 9324–9332. doi: 10.1073/pnas.1820561116

Wang, Q., and Coleman, J. J. (2019). Progress and Challenges: development and implementation of CRISPR/cas9 technology in filamentous fungi. *Comput. Struct. Biotechnol. J.* 17, 761–769. doi: 10.1016/j.csbj.2019.06.007

Xu, X., Liu, Y., Du, G., Ledesma-Amaro, R., and Liu, L. (2020). Microbial chassis development for natural product biosynthesis. *Trends Biotechnol.* 38, 779–796. doi: 10.1016/j.tibtech.2020.01.002

Yu, T., Zhou, Y. J., Wenning, L., Liu, Q., Krivoruchko, A., Siewers, V., et al. (2017). Metabolic engineering of *Saccharomyces cerevisiae* for production of very long chain fatty acid-derived chemicals. *Nat. Commun.* 8:15587. doi: 10.1038/ncomms15587

Zalatan, J. G., Lee, M. E., Almeida, R., Gilbert, L. A., Whitehead, E. H., La Russa, M., et al. (2015). Engineering complex synthetic transcriptional programs with CRISPR RNA scaffolds. *Cell* 160, 339–350. doi: 10.1016/j.cell.2014.11.052

Zhang, Y. P., Wang, J., Wang, Z. B., Zhang, Y. M., Shi, S. B., Nielsen, J., et al. (2019). A gRNA-tRNA array for CRISPR-Cas9 based rapid multiplexed genome editing in *Saccharomyces cerevisiae*. *Nat. Commun.* 10:1053. doi: 10.1038/s41467-019-09005-3

Conflict of Interest: The authors declare that the research was conducted in the absence of any commercial or financial relationships that could be construed as a potential conflict of interest.

frontiers in Bioengineering and Biotechnology

REVIEW
published: 14 December 2020
doi: 10.3389/fbioe.2020.594061

Current Challenges and Opportunities in Non-native Chemical Production by Engineered Yeasts

Jiwon Kim[1,2†], *Phuong Hoang Nguyen Tran*[1,3†] *and Sun-Mi Lee*[1,3,4*]

[1] *Clean Energy Research Center, Korea Institute of Science and Technology (KIST), Seoul, South Korea,* [2] *Department of Biotechnology, Korea University, Seoul, South Korea,* [3] *Division of Energy and Environment Technology, University of Science and Technology (UST), Daejeon, South Korea,* [4] *Green School, Korea University, Seoul, South Korea*

Yeasts are promising industrial hosts for sustainable production of fuels and chemicals. Apart from efficient bioethanol production, yeasts have recently demonstrated their potential for biodiesel production from renewable resources. The fuel-oriented product profiles of yeasts are now expanding to include non-native chemicals with the advances in synthetic biology. In this review, current challenges and opportunities in yeast engineering for sustainable production of non-native chemicals will be discussed, with a focus on the comparative evaluation of a bioethanol-producing *Saccharomyces cerevisiae* strain and a biodiesel-producing *Yarrowia lipolytica* strain. Synthetic pathways diverging from the distinctive cellular metabolism of these yeasts guide future directions for product-specific engineering strategies for the sustainable production of non-native chemicals on an industrial scale.

Keywords: non-native chemicals, *Saccharomyces cerevisiae*, *Yarrowia lipolytica*, yeast engineering, biorefinery

OPEN ACCESS

Edited by:
Farshad Darvishi,
Alzahra University, Iran

Reviewed by:
Jiazhang Lian,
Zhejiang University, China
Mario Andrea Marchisio,
Tianjin University, China
Fu-Xing Niu,
Sun Yat-sen University, China

***Correspondence:**
Sun-Mi Lee
smlee@kist.re.kr

[†] *These authors share first authorship*

Specialty section:
This article was submitted to Synthetic Biology, a section of the journal Frontiers in Bioengineering and Biotechnology

Received: *12 August 2020*
Accepted: *24 November 2020*
Published: *14 December 2020*

Citation:
Kim J, Hoang Nguyen Tran P and Lee S-M (2020) Current Challenges and Opportunities in Non-native Chemical Production by Engineered Yeasts. Front. Bioeng. Biotechnol. 8:594061. doi: 10.3389/fbioe.2020.594061

INTRODUCTION

Microorganisms have gained significant attention as cell factories for the sustainable production of fuels and chemicals, providing great opportunities for a bio-based economy in the post-petroleum era. Of the microbial cell factories, yeast has long been used as a proven industrial producer of fuels and chemicals. The robustness in a wide range of environmental conditions, the ease of separation from the culture medium, and no phage contamination related issues make the yeast more attractive industrial cell factory than bacteria. With recent advances in synthetic biology, the product profiles of yeasts have been expanding to include those that have never been produced naturally, such as cannabinoids, tropine, and amorphadiene (Luo et al., 2019; Ping et al., 2019; Srinivasan and Smolke, 2019; Marsafari and Xu, 2020). Given that synthetic pathways for non-native products commonly involve multiple enzymes from plants and/or other higher eukaryotes, which often require post-translational modification and are difficult to be functionally expressed in prokaryotic systems, the development of yeast cell factories is drawing more attention with its advantages as a eukaryotic system.

The model yeast *Saccharomyces cerevisiae* is one of the most widely developed cell factories for the production of fuels and chemicals. Industrial production of ethanol, the native product of *S. cerevisiae*, is in operation worldwide to supply alcoholic beverages and biofuels (Walker and Stewart, 2016; Parapouli et al., 2020). Industrial-scale production of β-farnesene by engineered

S. cerevisiae strains has also been reported (Gray et al., 2014; Wehrs et al., 2019). Of the non-model yeast, *Yarrowia lipolytica* has recently risen as another promising industrial cell factory with a superior capacity to accumulate lipids for biodiesel production (Ma et al., 2019). Currently, taking advantage of readily accessible genetic information and highly efficient genetic tools, an increasing number of products are being added to the product profiles of the model yeast *S. cerevisiae.* Besides being utilized for biodiesel production, *Y. lipolytica* is being transformed into a cell factory platform for the production of advanced biofuels and chemicals such as isoprenoids, polyketides, drug precursors, pigments, and organic acids (Miller and Alper, 2019).

The successful use of *S. cerevisiae* for the industrial production of bioethanol and the superior lipid production performance of *Y. lipolytica* shows that these strains can provide an economically feasible method for carbohydrate-based-biofuels production (Qiao et al., 2017). As such, there is increasing hope that these strains could be used for the production of numerous non-native chemicals on an industrial scale. Their GRAS (generally recognized as safe) status, as well as their well-known genomic characteristics and widely available engineering tools, make these yeast strains attractive microbial cell factories for the production of numerous chemicals (Darvishi et al., 2017; Markham and Alper, 2018; Ekas et al., 2019; Favaro et al., 2019). Here, the recent advances in engineering *S. cerevisiae* and *Y. lipolytica* as yeast cell factories for the production of non-native chemicals will be reviewed. Non-native chemicals were classified into four large groups, (i) terpenoids, (ii) polyketides, (iii) fatty acid-derived chemicals, and (iv) others, based on the core intermediate used as a precursor, namely acetyl-CoA, malonyl-CoA, and DHAP, which are key intermediates and diverge into branched pathways in the cellular metabolism of yeasts, such as the mevalonate or shikimate pathways (**Figure 1**). Thus, engineering strategies to produce certain groups of chemicals could be shared and more easily expanded to transform yeasts into cell factories for specific non-native chemicals. The performance of engineered yeasts as producers of specific chemical groups was analyzed and compared to that of the intensively engineered bacterial host of *E. coli* to highlight the benefits of using engineered yeasts for the industrial production of non-native chemicals by maximizing their potential, which is supported by their distinctive cellular metabolism. Finally, future directions for choosing an optimal platform strain and engineering strategies will be discussed to advance yeast cell factories for the sustainable production of non-native chemicals on an industrial scale.

PRODUCTION OF NON-NATIVE CHEMICALS IN YEAST CELL FACTORIES

Terpenoids

Terpenoids, also known as isoprenoids, are a large group of chemicals derived from five-carbon isoprene units with diverse applications in pharmaceuticals, flavors, colorants, and even liquid fuel alternatives (Vickers et al., 2017; Zhou, 2018). As naturally produced organic chemicals, terpenoids are conventionally extracted from natural sources such as plants, but the long cultivation time and inefficiency in extraction limit the sufficient supply of terpenoids to meet the increasing demand (Chang and Keasling, 2006; Wang et al., 2018). Thus, microbial terpenoid production has gained much attention as an alternative way to produce terpenoids. To achieve high productivity and yield in microbial hosts, strong metabolic flux through the mevalonate (MVA) pathway or methylerythritol 4-phosphate (MEP) pathway are required to sufficiently supply isopentenyl pyrophosphate (Pompon et al., 1996) and thus geranyl pyrophosphate (GPP), the main precursor of terpenoids (Zhang and Hong, 2020). In addition, functional expression of heterologous enzymes adapted from a source organism plays a critical role in achieving high titer production of terpenoids. Here, we discuss the engineering efforts put into *S. cerevisiae* and *Y. lipolytica* for the production of a few representative compounds in each class of terpenoids and compare their performance to that of *E. coli*, a model bacterial cell factory.

Isoprene

Isoprene (2-methyl-1,3-butadiene) is a colorless and flammable compound, and the main monomer of natural rubber. In *S. cerevisiae*, high-titer isoprene production (11.9 g/L) has been reported through protein engineering and enhanced precursor supply (Yao et al., 2018). Specifically, the authors constructed an isoprene production pathway by introducing a mutant isoprene synthase (ISPSLN), created by saturation mutagenesis, and compartmentalized a mitochondrial MVA pathway. In addition, improving the precursor supply through co-overexpression of diphosphomevalonate decarboxylase (MVD) and isopentenyl-diphosphate δ-isomerase, encoded by *MVD1* and *IDI1*, respectively, and redirection of the metabolic flux toward dimethylallyl pyrophosphate (DMAPP) contributed to improved metabolic flux through an isoprene synthetic pathway (**Figure 2**). There are no reports on the production of isoprene in *Y. lipolytica,* possibly due to its greater potential for the production of C30 or higher terpenoids (Larroude et al., 2018; Zhang et al., 2019). The isoprene titer reported by a bacterial counterpart of *E. coli* was 60 g/L. The engineered *E. coli* strongly expressed the heterologous MVA pathway and isoprene synthase (IspS) from *Populus alba* along with an enhanced pentose phosphate pathway (**Figure 2**). The isoprene productivity was 2 g/L/h with a yield of 850 mg/g DCW (Whited et al., 2010).

Geraniol (Monoterpene)

Geraniol (3,7-dimethylocta-trans-2,6-dien-1-ol) is one of the most widely used monoterpenes as a food additive, cosmetic ingredient, pesticide, and gasoline alternative. The highest titer of geraniol in *S. cerevisiae* has been reported to be 1.68 g/L through overexpression of the genes involved in the MVA pathway, tHMGR and IDI1, and the use of truncated geraniol synthase (GES) (Jiang et al., 2017; **Figure 2**). Of the nine candidates for heterologous GES, the GES from *Catharanthus roseus* (CrGES) showed the highest efficiency in geraniol production, which was further improved by truncation of a plastid targeting signal sequence required in its source organism. In addition, the

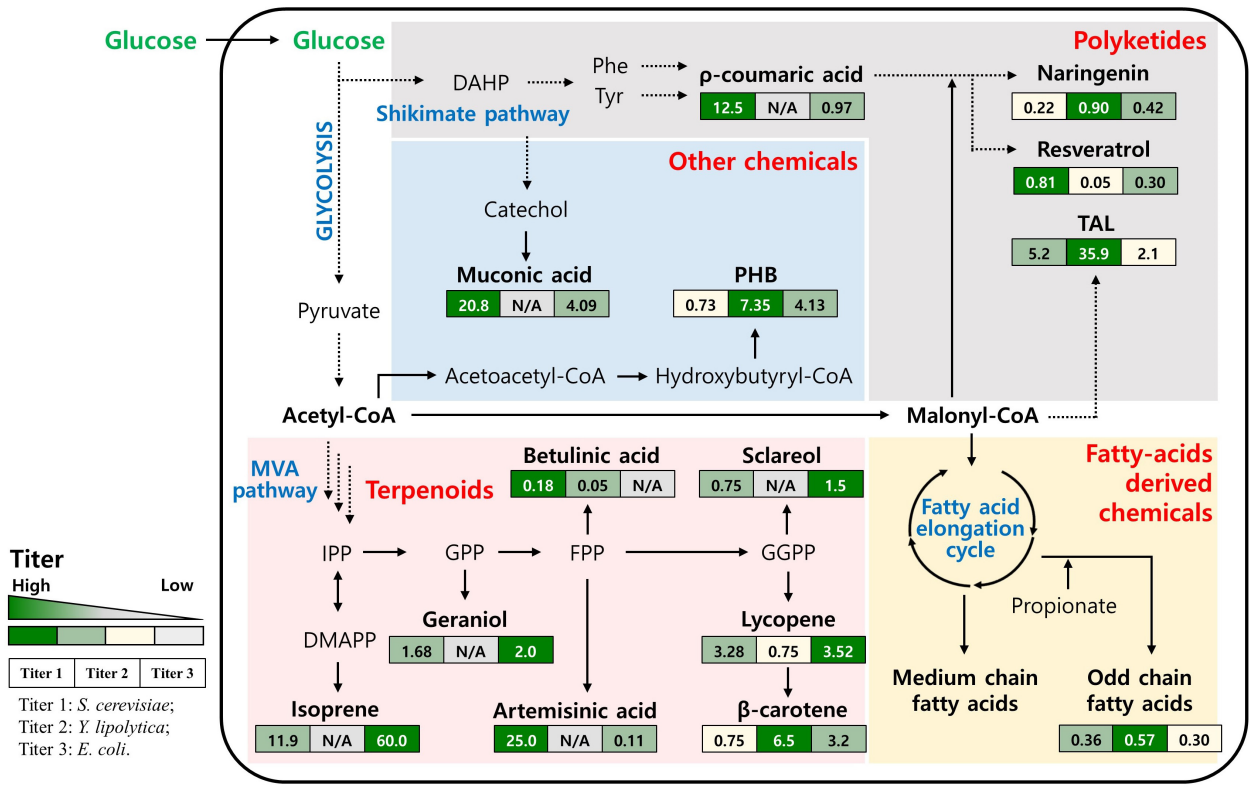

FIGURE 1 | Simplified biosynthetic pathway and the main intermediates for production of non-native chemicals in yeasts. The values in the boxes represent the production titer obtained by engineered *S. cerevisiae*, *Y. lipolytica* and *E. coli* (from left to right). N/A, not available; DAHP, 3-Deoxy-D-arabinoheptulosonate 7-phosphate; Phe, Phenylalanine; Tyr, Tyrosine; TAL, Triacetic acid lactone; PHB, Polyhydroxybutyrate; IPP, Isopentenyl pyrophosphate; DMAPP, Dimethylallyl pyrophosphate; GPP, Geranyl pyrophosphate; FPP, Farnesyl pyrophosphate; GGPP, Geranylgeranyl diphosphate.

researchers fused the ERG20ww (F96W/N126W), the modified FPPS solely generating GPP (Fischer et al., 2011; Ignea et al., 2014), into CrGES to enhance GPP accessibility (**Figure 2**). There are limited reports on monoterpene production by *Y. lipolytica* with a titer one order of magnitude lower than that by *S. cerevisiae*. Limonene and linalool have been produced at a titer of 165.3 mg/L (Cheng et al., 2019) and 6.96 mg/L (Cao et al., 2017), respectively, using minimally engineered *Y. lipolytica* strains. Geraniol production by *Y. lipolytica* has never been reported. Even with a distinctive cellular network and the lack of a native MVA pathway, the geraniol production efficiency of *E. coli* (Liu W. et al., 2016) has been shown to be similar to that of *S. cerevisiae* (2.0 vs. 1.68 g/L).

Artemisinic Acid (Sesquiterpene)

Artemisinic acid, a sesquiterpene with three isoprene units, is the precursor of artemisinin, a potent antimalarial drug (**Figure 2**). Based on the success by Ro et al. (2006), the highest titer of artemisinic acid (25 g/L) in *S. cerevisiae* has been reported through the construction of a functional biosynthetic route based on a plant-derived dehydrogenase and cytochrome P450 (Paddon et al., 2013). Possibly due to the already proven success in *S. cerevisiae*, no efforts have been devoted to the development of artemisinic acid-producing *Y. lipolytica*. Prior to the development of artemisinic acid-producing strain of *S. cerevisiae*, *E. coli* had been engineered through similar approaches involving cytochrome P450, but the titer was limited to only 105 mg/L due to the poor expression of cytochrome P450 in a prokaryotic cell factory of *E. coli* (Chang et al., 2007).

Sclareol (Diterpene)

Sclareol is a diterpene alcohol used as a cosmetic precursor in the fragrance industry. In *S. cerevisiae*, 750 mg/L of sclareol has been produced through protein engineering and deletion screening approaches (Trikka et al., 2015). To support sufficient metabolic fluxes in a sclareol synthesis pathway, a fusion protein of a modified ERG20 (F96C) and 8-hydroxycopalyl diphosphate synthase (CLS) from *Cistus creticus*, which catalyze the production of geranylgeranyl pyrophosphate (GGPP) and 8-hydroxycopalyl diphosphate (8-OH-CPP), respectively, were overexpressed in the strain harboring a sclareol synthase (SCLS), a class I diterpene synthase from *Salvia sclarea*. The engineered strain was further modified by disrupting the function of the genes selected from a heterozygous deletion screening experiments; this resulted in a 40-fold increase in the sclareol titer (750 mg/L). To our knowledge, the production of sclareol in *Y. lipolytica* has not been previously reported. In *E. coli*, a high titer (1.5 g/L) of sclareol was reportedly produced by simply

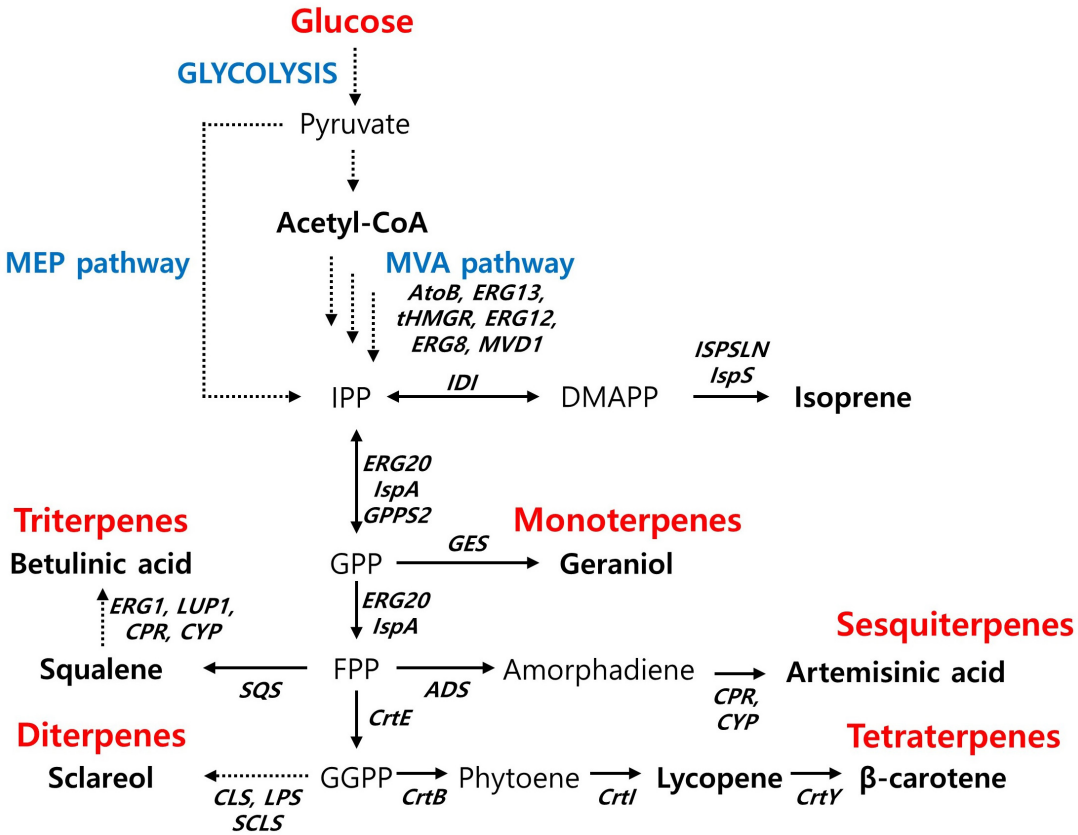

FIGURE 2 | Biosynthetic pathway for terpenoids production and main engineering targets. AtoB, acetyl-CoA acetyltransferase; ERG13, hydroxymethylglutaryl-CoA synthase; tHMGR, truncated HMG-CoA reductase; ERG12, mevalonate kinase; ERG8, phosphomevalonate kinase; MVD1, diphosphomevalonate decarboxylase; IDI, isopentenl-diphosphate δ-isomerase; IspS, isoprene synthase; ISPSLN, mutant isoprene synthase; GPPS2, geranyl diphosphate synthase; ERG20 (IspA), farnesyl pyrophosphate synthethase; SQS, squalene synthase; ADS, amorpha-4,11-diene synthase; CPR, cytochrome P450 reductase; CYP, cytochrome P450 monooxygenase; ERG1, squalene monooxygenase; LUP1, lupeol synthase; CrtE, geranylgeranyl diphosphate synthase; CLS, 8-hydroxy copalyl diphosphate synthase; LPS, LDPP synthase; SCLS, sclareol synthase; CrtB, phytoene synthase; CrtY, lycopene beta-cyclase.

introducing a heterologous pathway that converts GGPP into sclareol from *S. sclarea* (Schalk et al., 2012).

Betulinic Acid (Triterpene)

Betulinic acid is a pentacyclic triterpene and is used as an antitumor, antiviral, and anti-inflammatory agent (An et al., 2020). The highest titer of betulinic acid production obtained using *S. cerevisiae* was reported to be 182 mg/L by combining metabolic and process engineering (Czarnotta et al., 2017). The engineered strains used in the study overexpressed heterologous lupeol synthase (LUP1) and P450 reductase (CPR) from *Arabidopsis thaliana*, and P450 monooxygenase (CYP) from *Catharanthus roseus* along with homologous squalene monooxygenase (ERG1) and tHMGR. To increase the production titer of betulinic acid, these authors performed fed-batch fermentation with excess ethanol, which supports the increased supply of acetyl-CoA and NADPH for triterpene production. When combined with nitrogen-limitation conditions, metabolic flux could be directed toward betulinic acid synthesis and thereby increased the titer and yields of betulinic acid. In *Y. lipolytica*, betulinic acid titer of 51.87 mg/L has been reported during flask fermentation by adapting multimodular engineering strategy (Jin et al., 2019). To maximize betulinic acid production, they divided the betulinic acid synthesis pathway into four separate modules: the CYP/CPR, mevalonate, acetyl-CoA generation, and redox cofactor supply modules. The best combinations of heterologous CYP/CPR from five different sources, namely CYP from *Betula platyphylla* and CPR from *Medicago truncatula* were overexpressed along with ERG1, ylHMG1, and squalene synthase (ERG9); this resulted in the production of betulinic acid with a titer of 51.87 mg/L. Given that this titer was obtained from flask fermentation, the production performance of *Y. lipolytica* could be further improved when combined with process engineering approaches applied to *S. cerevisiae*. There are limited reports on the betulinic acid production in *E. coli* possibly due to the antibacterial properties of betulinic acid (Oloyede et al., 2017).

β-Carotene (Tetraterpene)

β-carotene is an orange-colored tetraterpene pigment composed of eight isoprene units, and is found in plants, photosynthetic bacteria, and algae. It exhibits antioxidant properties and serves

as a precursor of vitamin A (Arendt et al., 2016). Recent success in engineering *S. cerevisiae* has improved β-carotene titer up to 750 mg/L (López et al., 2019) through the combined efforts of adaptive laboratory evolution and metabolic engineering; the strain overexpressing the carotenoid biosynthetic genes *crtYB*, *crtI*, and *crtE* from *Xanthophyllomyces dendrorhous* with *tHMGR were evolved for improved*β-carotene production. Later, high-titer production of lycopene, a precursor of β-carotene with its own utility, was reported to be 3.28 g/L (Shi et al., 2019) by expressing the heterologous genes involved in the lycopene biosynthesis pathway (*crtE*, *crtB*, *crtI* sourced from *Pantoea ananatis*, *Pantoea agglomerans*, and *Blakeslea trispora*, respectively) under the control of various promoters with optimized gene expression levels (**Figure 2**). Given that *crtB* and *crtI* are shared in the β-carotene synthesis pathway, the production titer of β-carotene could be further improved by introducing a proper gene at the last step of the β-carotene synthesis pathway. *Y. lipolytica* has shown superior potential for the production of β-carotene, with the highest titer of 6.5 g/L (Larroude et al., 2018). The high metabolic flux through acetyl-CoA and its lipophilic depository of liposomes provided a favorable cellular system for the high production of β-carotene. Introduction of a heterologous β-carotene synthesis pathway encoded by *carRP* and *carB* from *Mucor circinelloides* with overexpression of a native MVA pathway (ylHMG1) turned a previously engineered lipid over-producing strain of *Y. lipolytica* into a superior β-carotene-producing strain. A comparable β-carotene titer has been achieved by *E. coli* (Yang and Guo, 2014). The co-expression of an optimized MEP and a hybrid MVA pathway to maximize the supply of IPP and GPP resulted in a β-carotene titer of 3.2 g/L in the strain heterologously expressing the genes involved in the β-carotene synthesis pathway from *Erwinia herbicola* and GPPS2 from *Abies grandis*.

Polyketides

Polyketides are a diverse group of secondary metabolites produced by bacteria (type I, II, III), fungi (type I, II), and plants (type III). Polyketides exhibit various bioactive properties such as anticancer, antifungal, and antiviral, and serve as important resources for pharmaceutical development (Jakočiūnas et al., 2020). Within the type III polyketides class, triacetic acid lactone, ρ-coumaric acid, naringenin, and resveratrol have been produced at high titers by fungal as well as bacterial hosts (López et al., 2019).

Triacetic Acid Lactone

Triacetic acid lactone (López et al., 2019), naturally produced by the plant *Gerbera hybrid*, is a simple polyketide used as a chemical building block for a range of value-added products such as sorbic acid, hexanoic acid, and acetylacetone (Chia et al., 2012). TAL is generated from two common metabolic precursors, acetyl-CoA and malonyl-CoA (**Figure 3A**). Recently, Markham et al. (2018) demonstrated TAL production in an engineered *Y. lipolytica* strain reaching a titer of 35.9 g/L, the highest amount obtained by recombinant strains during bioreactor operation (**Table 1**). Overexpression of *ACC1*, which encodes the enzyme that converts acetyl-CoA to malonyl-CoA, combined with overexpression of the pyruvate bypass pathway genes, *PDC2*, *ALD5*, and *ACS1*, and the β-oxidation pathway genes reinforced the already sufficient acetyl-CoA pool in *Y. lipolytica* leading to a high-titer TAL production (**Figure 3A**). In *S. cerevisiae*, the central carbon pathway is regulated toward TAL biosynthesis by blocking competing pathways and a protease enzyme activity resulting in 2.2 g/L of TAL production under bioreactor conditions (Cardenas and Da Silva, 2014). Moreover, TAL production in an engineered industrial strain of *S. cerevisiae* reached a titer of 5.2 g/L by employing fed-batch cultivation in a bioreactor with ethanol feeding (Saunders et al., 2015). In *E. coli*, a similar titer of TAL (2.1 g/L) was reported from the shake-flask culture of an engineered strain expressing a designed TAL reporter (Tang et al., 2013).

ρ-Coumaric Acid

ρ-Coumaric acid is an aromatic amino acid (AAA) that serves as a starting material for numerous high-value biochemicals such as flavors, fragrances, nutraceuticals, and pharmaceuticals. Recently, a recombinant diploid QL60 strain of *S. cerevisiae* produced 12.5 g/L of ρ-coumaric acid with a productivity of 0.13 g/L/h and a yield of 0.14 g/g sugar under glucose-limited fed-batch fermentation conditions (Liu et al., 2019). This demonstrated superior performance of *S. cerevisiae* in the production of ρ-coumaric acid over an *E. coli* strain, in which 168–974 mg/L was produced during flask culture (Kang et al., 2012; Morelli et al., 2017). This remarkable performance of ρ-coumaric acid biosynthesis in *S. cerevisiae* was achieved by intensive engineering; systematic engineering of the AAA pathway through debottlenecking a shikimate pathway, enhancing cytochrome P450 activity by overexpression of *AtCYB5* and *AtATR2*; and diverting carbon flux from glycolysis to erythrose 4-phosphate (E4P) by introducing a heterologous phosphoketolase (PHK)-based pathway. Optimization of carbon flux through interconnecting points between glycolysis and the AAA pathway was also critical for high-titer ρ-coumaric acid production (**Figure 3B**).

Naringenin

Naringenin is a key bioactive polyketide derived from ρ-coumaric acid, from which numerous flavonoids can be synthesized. Palmer et al. (2020) demonstrated *de novo* production of naringenin from *Y. lipolytica*, with the highest titer among those using *S. cerevisiae* and *E. coli*. In this study, they introduced the tyrosine-based ρ-coumaroyl-CoA- naringenin pathway and enhanced the metabolic flux from acetyl-CoA to malonyl-CoA through the overexpression of *ACC1* and *PEX10* (**Figure 3B**). The effectiveness of the upregulation of the peroxisomal matrix protein encoded by *PEX10*, previously reported to strongly improve the production of TAL, increased acetyl-CoA pool via refluxing the β-oxidation pathway. Besides, the introduction of mutant and/or heterologous enzymes, $ARO4^{K221L}$ and a tyrosine amino lyase encoded by *SeSam8* from *Saccharothrix espanaensis*, resolved the rate-limiting steps contributing to the higher titer (**Figure 3B**). The final strain of engineered *Y. lipolytica* produced 124.1 mg/L of naringenin in flask culture, which was further increased to 898 mg/L during bioreactor operation.

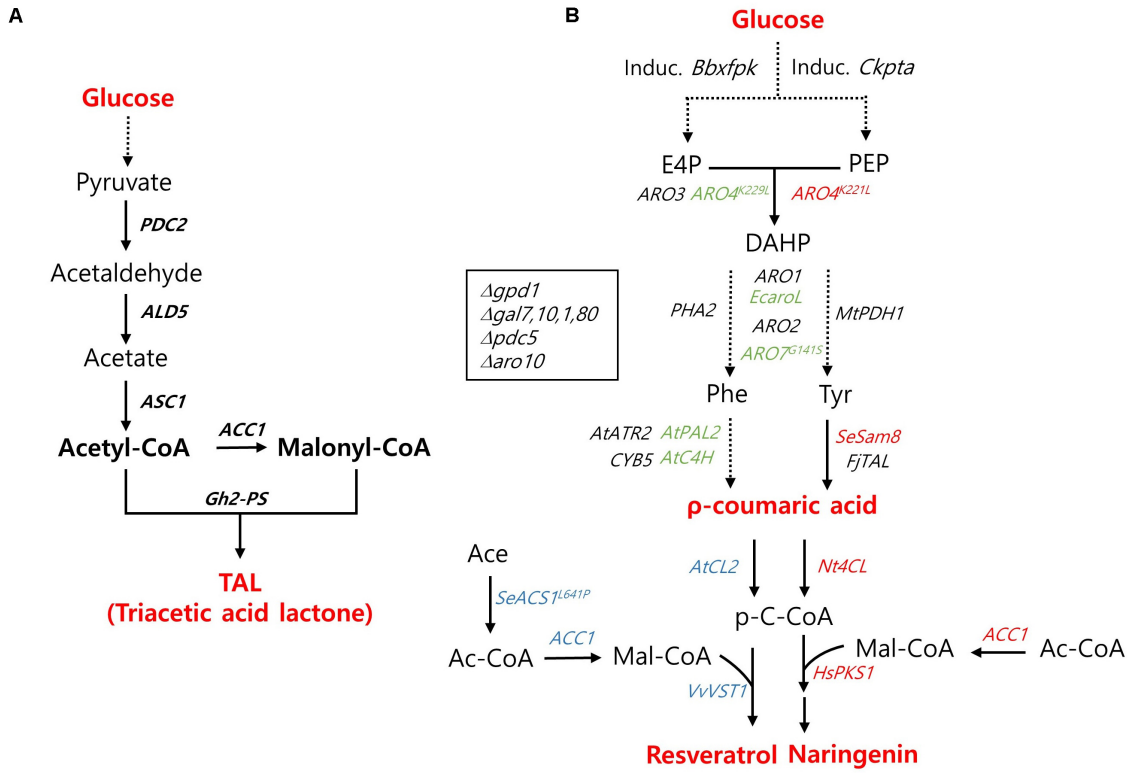

FIGURE 3 | Biosynthetic pathway for polyketides production and main engineering targets. **(A)** A pathway for triacetic acid lactone production. **(B)** A pathway for the production of ρ-coumaric acid, resveratrol, and naringenin. The genes used specifically for the production ρ-coumaric acid, resveratrol, and naringenin are indicated with green, blue, and red colors, respectively. PDC, pyruvate decarboxylase; ALD5, aldehyde dehydrogenase 5; ACS1, acetyl-CoA synthase 1; ACC1, acetyl-CoA carboxylase; Gh2-PS, *Gerbera hybrida* 2-pyrone synthase; Induc. Bbxfpk, Induc. Ckpta, The inducible phosphoketolase (PHK) pathway including a *Bifidobacterium breve* phosphoketolase (Bbxfpk) and a *Clostridium kluyveri* phosphotransacetylase (Ckpta); ARO3, DAHP synthase; $ARO4^{K229L}$, $ARO4^{K221L}$, L-tyrosine-feedback-insensitive DAHP synthase; ARO1, pentafunctional arom protein; EcaroL, *Escherichia coli* shikimate kinase; ARO2, chorismate synthase; $ARO7^{G141S}$, L-tyrosine-feedback-insensitive chorismate mutase; PHA2, prephenate dehydratase; MtPDH1, *Medicago truncatula* prephenate dehydrogenase; *At*C4H, *Arabidopsis thaliana* cinnamic acid hydroxylase; *At*PAL2, *A. thaliana* phenylalanine ammonia lyase; *At*ATR2, *A. thaliana* cytochrome P450 reductase; CYB5, Cytochrome b5; *Fj*TAL, *Flavobacterium johnsoniae* tyrosine ammonia lyase; SeSam8, *Saccharothrix espanaensis* tyrosine amino lyase; AtCL2, Nt4CL, *Arabidopsis thaliana*, *Nicotiana tabacum* 4-coumaroyl-CoA ligase; VvVST1, *Vitis vinifera* resveratrol synthase; $SeACS1^{L641P}$, *Salmonella enteric* acetyl-CoA synthetase; HsPK1, *Huperiza serrata* chalcone synthase; gpd1, Glycerol-1-phosphatase; gal7, galactose-1-phosphate uridyl transferase; gal10, UDP-glucose-4-epimerase; gal1, Galactokinase; gal80, transcriptional regulator; aro10, phenylpyruvate decarboxylase.

Lyu et al. (2019) applied multiple approaches for enhancing the metabolic flux toward naringenin via a tyrosine-based pathway. More interestingly, they investigated the beneficial effects of the co-culture system, in which the whole pathway was divided between two strains to relieve the heavy burden of complicated biosynthesis pathways and surfactant supplementation (Tween 80) on the improved naringenin production in *S. cerevisiae* (Lyu et al., 2019). In a flask culture, the naringenin titer of *S. cerevisiae* was higher than that of *Y. lipolytica* (220 vs. 124.1 mg/L), implying the potential of *S. cerevisiae* as a production host of naringenin as demonstrated in resveratrol production (discussed in the next paragraph). In *E. coli*, 421.6 mg/L of naringenin was produced in flask culture condition (Wu et al., 2015).

Resveratrol

Resveratrol shares its precursor with naringenin; ρ-coumaroyl-CoA is converted either to resveratrol or naringenin by stilbene synthase (STS) or the serial reaction of chalcone synthase (CHS) and chalcone isomerase (CHI), respectively. With the introduction of a phenylalanine-based ρ-coumaroyl-CoA—route, *S. cerevisiae* demonstrated higher resveratrol productivity over *Y. lipolytica* or *E. coli*. Li et al. adapted the engineering strategy used for ρ-coumaric acid production; overexpression of AtATR2, ARO1/2, and ARO3 encoded by *AtPAL2*, *EcaroL*/$ARO7^{G141S}$, and $RO4^{K229L}$, and enhanced availability of malonyl-CoA by overexpressing $SeACS^{L641P}$, $ACC1^{S659A,\ S1157A}$ encoding acetyl-CoA synthetase and acetyl-CoA carboxylase (Li et al., 2016) along with *ARO10* deletion (**Figure 3B**; Li et al., 2016). As mentioned above, *S. cerevisiae* efficiently produced 812 mg/L of resveratrol during fed-batch fermentation in a bioreactor, which was similar to the naringenin production of *Y. lipolytica* under bioreactor conditions (**Table 1**). Under shake-flask conditions, *Y. lipolytica* produced 48.7 mg/L of resveratrol (Palmer et al., 2020). In *E. coli*, 304.5 mg/L of resveratrol was produced in flask culture conditions (Wu et al., 2017; **Table 1**). Despite the lack of post-transcriptional

TABLE 1 | Comparison of the production titer of non-native chemicals by engineered *S. cerevisiae*, *Y. lipolytica* and *E. coli*.

Product		Strain	Performance			Fermentation			References
Class	Name		Titer (g/L)	Yields (mg/g)	Productivity (mg/L/h)	Type	Mode	Main substrate	
Terpenoids	Isoprene	*S. cerevisiae*	11.90	N/A[a]	71*	B	Fed-batch	Glucose	Yao et al., 2018
		E. coli	60.00	110	2,000	B	Fed-batch	Glucose	Whited et al., 2010
	Geraniol	*S. cerevisiae*	1.68	N/A	14*	B	Fed-batch	Glucose	Jiang et al., 2017
		E. coli	2.00	N/A	29*	B	Fed-batch	Glucose	Liu W. et al., 2016
	Artemisinic acid	*S. cerevisiae*	25.00	N/A	180*	B	Fed-batch	Glucose	Paddon et al., 2013
		E. coli	0.105	N/A	N/A	F	Batch	Glycerol	Chang et al., 2007
	Betulinic acid	*S. cerevisiae*	0.182	N/A	N/A	B	Fed-batch	Glucose, ethanol	Czarnotta et al., 2017
		Y. lipolytica	0.052	N/A	N/A	F	Batch	Glucose	Jin et al., 2019
	Sclareol	*S. cerevisiae*	0.75	N/A	N/A	F	Batch	Glucose	Trikka et al., 2015
		E. coli	1.5	N/A	N/A	B	Fed-batch	Glycerol	Schalk et al., 2012
	β-carotene	*S. cerevisiae*	0.75	N/A	9.38*	B	Fed-batch	Glucose	López et al., 2019
		Y. lipolytica	6.50	N/A	53.28*	B	Fed-batch	Glucose	Larroude et al., 2018
		E. coli	3.20	N/A	61.54*	B	Fed-batch	Glycerol	Yang and Guo, 2014
	Lycopene	*S. cerevisiae*	3.28	N/A	25*	B	Fed-batch	Glucose	Shi et al., 2019
		Y. lipolytica	0.745	N/A	7.76*	B	Fed-batch	Glucose	Zhang et al., 2019
		E. coli	3.52	N/A	35.2*	B	Fed-batch	Glycerol	Sun et al., 2014
Polyketides	Triacetic acid lactone	*S. cerevisiae*	2.20	130	N/A	B	Fed-batch	Glucose	Cardenas and Da Silva, 2014
			5.20	N/A	N/A	B	Fed-batch	Glucose, ethanol	Saunders et al., 2015
		Y. lipolytica	35.90	164	210	B	Batch	Glucose	Markham et al., 2018
		E. coli	2.10	N/A	N/A	F	Batch	Glycerol	Tang et al., 2013
			1.87	N/A	81.23*	F	Batch	Glycerol	Li et al., 2018
	ρ-coumaric acid	*S. cerevisiae*	12.50	139.6	130.1	B	Fed-batch	Glucose	Liu et al., 2019
		E. coli	0.974	N/A	27.06*	F	Batch	Glucose	Kang et al., 2012
		E. coli	0.24	N/A	5*	F	Batch	Glucose	Wu et al., 2017
	Naringenin	*S. cerevisiae*	0.22	N/A	11	F	Batch	Glucose	Lyu et al., 2019
		Y. lipolytica	0.898	N/A	N/A	B	Fed-batch	Glucose	Palmer et al., 2020
		E. coli	0.42	N/A	8.78*	F	Fed-batch	Glucose, tyrosine	Wu et al., 2015
	Resveratrol	*S. cerevisiae*	0.81	N/A	7.38*	B	Fed-batch	Glucose	Li et al., 2016
		Y. lipolytica	0.049	2.44	N/A	F	Batch	Glucose	Palmer et al., 2020
		E. coli	0.3045	75	6.34*	F	Batch	Glucose	Wu et al., 2017
FA-derived chemicals	Medium-chain fatty acids	*S. cerevisiae*	2.82	N/A	29.3	B	Fed-batch	Glucose	Zhu et al., 2020
		Y. lipolytica	N/A	N/A	N/A	F	Batch	Glucose	Rigouin et al., 2018
		E. coli	1.36	N/A	N/A	F	Batch	Glycerol	Sherkhanov et al., 2014
	Odd-chain fatty acids	*S. cerevisiae*	0.002	N/A	N/A	F	Batch	Glucose	Jin et al., 2016
		Y. lipolytica	0.36	N/A	N/A	F	Batch	Glucose	Park et al., 2020
			0.57	N/A	N/A	F	Fed-batch	Glucose, propionate	Park et al., 2018
		E. coli	0.297	N/A	N/A	F	Batch	Glucose, propionate	Wu and San, 2014
	Fatty alcohols	*S. cerevisiae*	6.00	58	N/A	B	Fed-batch	Glucose	d'Espaux et al., 2017
		Y. lipolytica	5.8	36	N/A	B	Fed-batch	Glucose	Cordova et al., 2020
		E. coli	6.33	N/A	N/A	B	Fed-batch	Glycerol	Liu Y. et al., 2016
Others	PHB	*S. cerevisiae*	0.73	13.8	4.3*	F	Batch	Xylose	Portugal-Nunes et al., 2017
		Y. lipolytica	7.35	N/A	N/A	B	Fed-batch	Glucose	Li et al., 2017
		E. coli	4.13*	360	N/A	F	Batch	Glucose	Wang J. et al., 2020
	Muconic acid	*S. cerevisiae*	20.8	66.2	139	B	Fed-batch	Glucose	Wang G. et al., 2020
		E. coli	4.09	310	56.8	F	Batch	Glucose, xylose	Fujiwara et al., 2020

[a]*Not available.*

**Calculated data. B, bioreactor; F, flask; P, 24 deep-well plate.*

modification, *E. coli* has shown a higher-titer production of plant-based polyketides. The main engineering strategies employed in *E. coli* mainly focused on increasing the malonyl-CoA pool and balancing the synthetic pathway via gene expression regulation. Recent reports on the newly developed CRISPRi system, which controls gene expression through repression rather

than conventional gene knock-out, applied in *E. coli* offered finely tuned metabolic flux effectively delivered through the newly introduced synthetic pathway (Wu et al., 2015, 2017).

Fatty Acid-Derived Chemicals

Fatty acids are essential compounds for sustaining cell membranes. With the help of synthetic biology, fatty acids are transformed into non-native chemicals with a wide range of applications. As fatty alcohols and fatty esters have been frequently discussed in previous reviews (Hu et al., 2019; Munkajohnpong et al., 2020), we focused on medium-chain and odd-chain fatty acids for which yeast engineering efforts have made noticeable progress in recent years, due to their importance as platform chemicals for the replacement of petroleum in the chemical industry.

Medium-Chain Fatty Acids (MCFAs)

MCFAs have gained attention as jet fuel replacements, platform chemicals, and ingredients for plastics and cosmetics. Recently, an MCFA-producing *S. cerevisiae* strain was developed by adapting a type I bacterial fatty acid synthesis pathway. Through the directed evolution of TPO1 transporter and laboratory adaptive evolution, the engineered strain with improved MCFA tolerances produced almost 1 g/L of MCFAs (Zhu et al., 2020; **Figure 4A**). In *Y. lipolytica*, the native FAS enzyme was simply modified to synthesize MCFAs based on its superior capacity for long-chain fatty acid (LCFA) production. Although the MCFA content (45%) in its total lipids was agreeable, the titer was insignificant, possibly because its FAS systems evolved toward a highly efficient LCFA production system (Rigouin et al., 2017). *E. coli* has also shown a similar range of MCFA titer (1.36 g/L) through metabolic engineering approaches along with enhancing the tolerance toward MCFAs (Sherkhanov et al., 2014).

Odd-Chain Fatty Acids (OCFAs)

In nature, most fatty acids derived from microorganisms contain even numbers of carbon, and rare microbes produce minute amounts of OCFAs with the exception of propionic acid. Recently, microbial production of OCFAs has also attracted considerable interest because of its potential benefits to human health, such as diabetes (Weitkunat et al., 2017) or adiposity (Aglago et al., 2017). Modifying the fatty acid synthesis pathway, in which acetyl-CoA and malonyl-CoA are used as starting materials, is not simple unless odd chain fatty acids such as propionic acid are fed as substrates. Recently, *Y. lipolytica* has shown promise as a cell factory for the production of OCFAs by harnessing the power of superior LCFA production capacity. When the metabolic flux toward LCFA production in an obese strain diverged toward OCFAs, *Y. lipolytica* produced 360 mg/L of OCFAs with a chain length of over C15. By supplying endogenous propionyl-CoA from oxaloacetate through a newly introduced synthetic pathway, the engineered strain with the genetic background for high lipid production was able to produce OCFAs without the supplementation of propionic acid (Park et al., 2020; **Figure 4B**). In *E. coli*, the overexpression of propionyl-CoA synthase from *Salmonella enterica* and acyl-ACP thioesterase from *Ricinus communis* and *Umberllularia california* enabled the production of 276 mg/L of OCFAs, with chain lengths of C11–C15, comparable to that in *Y. lipolytica*, in the presence of optimized propionate supplementation (Wu and San, 2014).

Other Chemicals

Polyhydroxybutyrate (PHB)

PHB has recently emerged as a promising candidate for the sustainable production of biodegradable thermoplastics. PHB is naturally accumulated as energy storage molecules under non-optimal conditions by several bacterial species such as *Cupriavidus necator* (previously known as *Ralstonia eutropha*) and *Methylobacterium*. However, these native producers still have drawbacks to be served as a production host for PHB commercialization due to their intracellular lysis of PHB, poor tolerance toward harsh environments, restriction of metabolic substrates, and unfamiliar genetic characterization (Madison and Huisman, 1999). Thus, the feasibility of PHB production in non-native hosts has been investigated. High-titer PHB production was achieved by an engineered oleaginous yeast *Y. lipolytica* harboring a heterologous PHB biosynthetic pathway based on *PhaA, PhaB,* and *PhaC* from a native producer of *C. necator* (**Figure 5A**; Li et al., 2017). To strengthen the availability of cytosolic acetyl-CoA, acetate, an essential precursor for PHB production, was fed as a sole carbon source, resulting in a PHB content of 10.2% with a high titer of 7.35 g/L during fed-batch fermentation in a bioreactor (Li et al., 2017). In *S. cerevisiae*, high PHB content was achieved during xylose fermentation (Portugal-Nunes et al., 2017). An engineered xylose-utilizing strain of *S. cerevisiae* with a heterologously expressed PHB pathway based on *PhaA* and *PhaC1* from *C. necator* and NADH-preferred *PhaB1* from *Allochromatium vinosum* (**Figure 5A**) produced 730 mg/L PHB with a content of 16.4% during xylose fermentation with additional nitrogen supply under an anaerobic shake-flask culture condition (Portugal-Nunes et al., 2017). PHB production in *E. coli* has been shown to be more promising than that in yeast strains. Wang et al. reported the role of truncated lipopolysaccharide (LPS) in *E. coli* in improving PHB production as a rebalanced carbon and nitrogen metabolism with increased precursors and energy levels. By introducing a PHB synthesis pathway based on PhaA, PhaB, and PhaC from *C. necator* (**Figure 5A**) as well as a truncated LPS, the engineered strain of *E. coli* produced PHB with a superior content and yield of 84.3% and 360 mg/g, respectively, under shake-flask culture conditions (Wang J. et al., 2020). In terms of PHB content and yield, the production capacity of the engineered *E. coli* was highly competitive with the natural PHB-producing strain of *C. necator*, which produced 232 g/L of PHB with a content of 80% and a yield of 380 mg/g during glucose fed-batch fermentation under phosphate limitation conditions in a bioreactor (Ryu et al., 1997).

Muconic Acid

Muconic acid is another platform chemical with the potential for production of bio-plastics, such as nylon-6,6, polyurethane and polyethylene terephthalate, as well as cosmetics and pharmaceuticals (Xie et al., 2014). Wang G. et al. (2020) developed high muconic acid-producing *S. cerevisiae* through biosensor-aided genome engineering. From a UV-mutagenesis

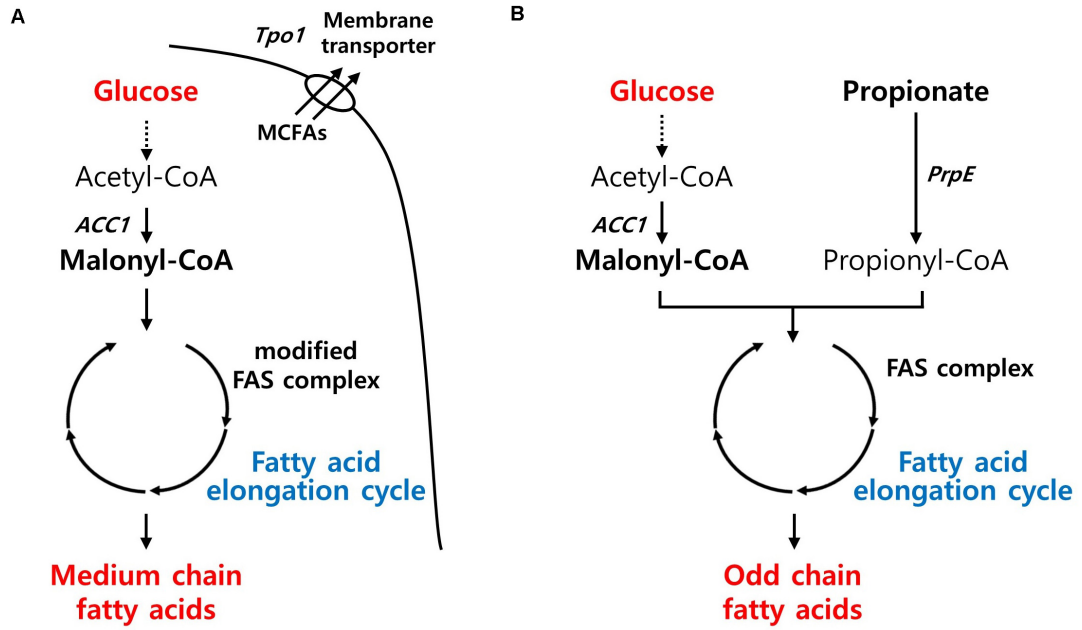

FIGURE 4 | Biosynthetic pathway for fatty-acids derived chemicals production and main engineering targets. **(A)** A pathway for MCFAs production. **(B)** A pathway for OCFAs production. ACC1, acetyl-CoA carboxylase; Tpo1, polyamine transporter; PrpE, propionate-CoA ligase; FAS, fatty acid synthase.

library, they screened out a mutant strain harboring missense mutations in several native genes, such as *PWP2*, *EST2*, *ATG1*, *DIT1*, *CDC15*, *CTS2*, and *MNE1*, duplicated *aroZ,* and *catA*, which are involved in the introduced muconic acid pathway (**Figure 5B**). The overexpression of protocatechuic acid (PCA) decarboxylase and AROM protein without the shikimate dehydrogenase domain (Aro1p$^{\Delta E}$) led to the high production of muconic acid, resulting in a muconic acid titer of 20.8 g/L during pH-controlled fed-batch fermentation. In *E. coli*, co-fermentation of glucose and xylose resulted in 4.09 g/L of muconic acid in a shake-flask condition (Fujiwara et al., 2020; **Table 1**).

CHALLENGES AND OPPORTUNITIES IN NON-NATIVE CHEMICAL PRODUCTION

Based on success as a proven industrial cell factory for biofuel production, yeasts are transforming into a cell factory for the production of non-native chemicals. In addition to the benefit from their robustness, yeasts offer ease of reactor operation and cell separation as well as low energy consumption with lower fermentation temperature (Liu et al., 2019). By exploiting the advantages of eukaryotic systems, yeast demonstrated its potential for the biosynthesis of plant-derived metabolites by better supporting the functional expression of heterologous enzymes requiring post-translational modification or providing intracellular structures for proper enzyme activity (Siddiqui et al., 2012). For instance, membrane-bound cytochrome P450 oxidase, a crucial enzyme for the biosynthesis of plant metabolites, can be functionally expressed in yeast (Pompon et al., 1996). Due to these advantages, the two main yeast cell factories, namely *S. cerevisiae* and *Y. lipolytica*, could potentially be used for the production of plant-derived chemicals, especially terpenes with three or more isoprene units and polyketides. *S. cerevisiae* has been shown to produce higher titers of artemisinic and betulinic acids. Moreover, *Y. lipolytica* has shown comparable performance with *S. cerevisiae* for the production of β-carotene and lycopene (in terms of titer), even with relatively minimal engineering. The higher titers in terpene production by *S. cerevisiae* were often based on subcellular compartmentalization using mitochondria or peroxisomes, implying the critical role of proper intracellular structures. The potential of *Y. lipolytica* in triterpene production could be improved by adapting the engineering strategy of compartmentalization applied to *S. cerevisiae*. In the strain development for the biosynthesis of β-carotene and lycopene in *S. cerevisiae* and *Y. lipolytica*, balanced enzyme expression levels played a critical role in enhancing production titer, especially at the rate-limiting steps mediated by *crtI* and *crtE*, the two main engineering targets. Even with limited attempts, *Y. lipolytica* has shown greater titer in the production of β-carotene, naringenin, and TAL by taking advantage of the high accessibility of acetyl-CoA over *S. cerevisiae* and *E. coli*. As more engineering tools are developed, and thus more sophisticated tuning of gene expression would be possible, *Y. lipolytica* could be used as a promising industrial host for the production of tetraterpene such as β-carotene. Moreover, polycistronic gene expression systems, which allow equivalent expression and regulation of multiple genes by one promoter in bacterial hosts, have been recently investigated and successfully developed for fungal hosts such as *S. cerevisiae* (Souza-Moreira et al., 2018). Therefore, the construction of a non-native chemical production pathway involving numerous heterologous genes would facilitate the

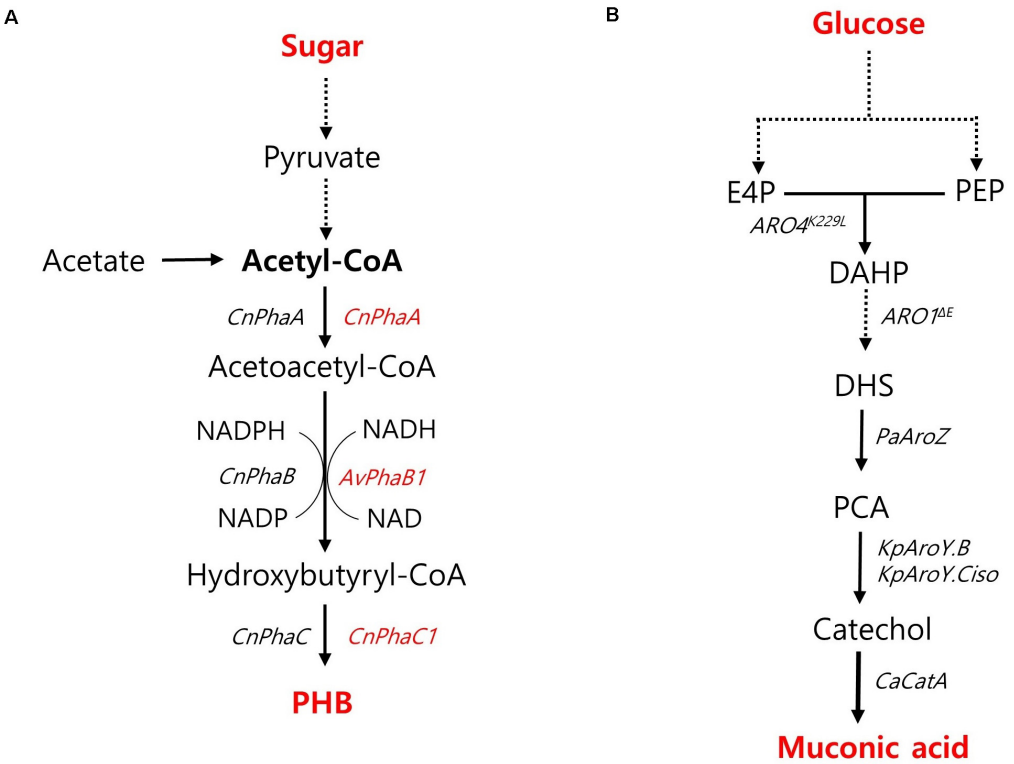

FIGURE 5 | Biosynthetic pathway for other chemicals production and main engineering targets. **(A)** A pathway for PHB production. The genes specifically used for *S. cerevisiae* and *Y. lipolytica* are indicated with red and black colors, respectively. **(B)** A pathway for muconic acid production. *Cn*, *Cupriavidus necator*; *Av, Allochromatium vinosum; PhaA*, acetyl-CoA acetyl transferase; PhaB, acetoacetyl-CoA reductase; *PhaC*, polyhydroxyalkanoate synthase. $ARO4^{K229L}$, L-tyrosine-feedback-insensitive DAHP synthase; $ARO1^{\Delta E}$, AROM protein without shikimate dehydrogenase domain; *PaAroZ*, *Podospora anserine* DHS dehydratase; *KpAroY.B*, *KpAroY.Ciso*, *Klebsiella pneumonia* PCA decarboxylase subunits; *CaCatA*, *Candida albicans* catechol 1,2-dioxygenase.

development of yeast cell factories. Interestingly, unconventional carbon sources other than glucose, such as xylose, acetate, and propionic acid, have been shown to better support metabolic flux through the biosynthesis pathway for non-native chemicals (Wu and San, 2014; Li et al., 2017; Portugal-Nunes et al., 2017; Wu et al., 2019). Thus, non-native chemical production by the engineered yeast strains with non-native carbon metabolism could offer better promises for industrial-scale production of non-native chemicals.

CONCLUSION

In this review, we discussed the current status of non-native biochemical production by model and non-model yeasts of *S. cerevisiae* and *Y. lipolytica*, respectively. The comparison of the potential of these yeasts in the production of non-native chemicals presented can serve to identify the production host of choice. By taking advantage of their distinctive cellular metabolism and characteristics as eukaryotic systems, these yeasts offer great potential for the industrial production of various non-native chemicals. Recent technological developments, such as high-throughput screening methods, are accelerating the application of synthetic biology to develop and upgrade yeast cell factories in a more efficient manner. Through target-specific engineering strategies with an expanded carbon source portfolio and optimized fermentation conditions of a single/co-culture system, yeasts could be successfully transformed into favorable industrial cell factories for the production of a wide range of non-native chemicals.

AUTHOR CONTRIBUTIONS

JK and PH wrote and edited the manuscript. S-ML provided conception of this review and edited the manuscript. All authors contributed to the article and approved the submitted manuscript.

FUNDING

This work was supported by the Korea Institute of Science and Technology (KIST) Institutional Program (Grant No. 2E30170). The authors also appreciate the additional support by the National Research Foundation of Korea (NRF) funded by the Ministry of Science and ICT (Information & Communication Technology) (Grant No. NRF-2020M1A2A2080847).

REFERENCES

Aglago, E. K., Biessy, C., Torres-Mejia, G., Angeles-Llerenas, A., Gunter, M. J., Romieu, I., et al. (2017). Association between serum phospholipid fatty acid levels and adiposity in Mexican women. *J. Lipid Res.* 58, 1462–1470. doi: 10.1194/jlr.P073643

An, T., Zha, W., and Zi, J. (2020). Biotechnological production of betulinic acid and derivatives and their applications. *Appl. Microbiol. Biotechnol.* 104, 3339–3348. doi: 10.1007/s00253-020-10495-1

Arendt, P., Pollier, J., Callewaert, N., and Goossens, A. (2016). Synthetic biology for production of natural and new-to-nature terpenoids in photosynthetic organisms. *Plant J.* 87, 16–37. doi: 10.1111/tpj.13138

Cao, X., Wei, L.-J., Lin, J.-Y., and Hua, Q. (2017). Enhancing linalool production by engineering oleaginous yeast *Yarrowia lipolytica*. *Bioresour. Technol.* 245, 1641–1644. doi: 10.1016/j.biortech.2017.06.105

Cardenas, J., and Da Silva, N. A. (2014). Metabolic engineering of *Saccharomyces cerevisiae* for the production of triacetic acid lactone. *Metab. Eng.* 25, 194–203. doi: 10.1016/j.ymben.2014.07.008

Chang, M. C. Y., Eachus, R. A., Trieu, W., Ro, D.-K., and Keasling, J. D. (2007). Engineering *Escherichia coli* for production of functionalized terpenoids using plant P450s. *Nat. Chem. Biol.* 3, 274–277. doi: 10.1038/nchembio875

Chang, M. C. Y., and Keasling, J. D. (2006). Production of isoprenoid pharmaceuticals by engineered microbes. *Nat. Chem. Biol.* 2, 674–681. doi: 10.1038/nchembio836

Cheng, B.-Q., Wei, L.-J., Lv, Y.-B., Chen, J., and Hua, Q. (2019). Elevating limonene production in oleaginous Yeast *Yarrowia lipolytica* via genetic engineering of limonene biosynthesis pathway and optimization of medium composition. *Biotechnol. Bioprocess Eng.* 24, 500–506. doi: 10.1007/s12257-018-0497-9

Chia, M., Schwartz, T. J., Shanks, B. H., and Dumesic, J. A. (2012). Triacetic acid lactone as a potential biorenewable platform chemical. *Green Chem.* 14, 1850–1853. doi: 10.1039/C2GC35343A

Cordova, L. T., Butler, J., and Alper, H. S. (2020). Direct production of fatty alcohols from glucose using engineered strains of *Yarrowia lipolytica*. *Metab. Eng. Commun.* 10:e00105. doi: 10.1016/j.mec.2019.e00105

Czarnotta, E., Dianat, M., Korf, M., Granica, F., Merz, J., Maury, J., et al. (2017). Fermentation and purification strategies for the production of betulinic acid and its lupane-type precursors in *Saccharomyces cerevisiae*. *Biotechnol. Bioeng.* 114, 2528–2538. doi: 10.1002/bit.26377

Darvishi, F., Fathi, Z., Ariana, M., and Moradi, H. (2017). *Yarrowia lipolytica* as a workhorse for biofuel production. *Biochem. Eng. J.* 127, 87–96. doi: 10.1016/j.bej.2017.08.013

d'Espaux, L., Ghosh, A., Runguphan, W., Wehrs, M., Xu, F., Konzock, O., et al. (2017). Engineering high-level production of fatty alcohols by *Saccharomyces cerevisiae* from lignocellulosic feedstocks. *Metab. Eng.* 42, 115–125. doi: 10.1016/j.ymben.2017.06.004

Ekas, H., Deaner, M., and Alper, H. (2019). Recent advancements in fungal-derived fuel and chemical production and commercialization. *Curr. Opin. Biotechnol.* 57, 1–9. doi: 10.1016/j.copbio.2018.08.014

Favaro, L., Jansen, T., and van Zyl, W. H. (2019). Exploring industrial and natural *Saccharomyces cerevisiae* strains for the bio-based economy from biomass: the case of bioethanol. *Crit. Rev. Biotechnol.* 39, 800–816. doi: 10.1080/07388551.2019.1619157

Fischer, M. J. C., Meyer, S., Claudel, P., Bergdoll, M., and Karst, F. (2011). Metabolic engineering of monoterpene synthesis in yeast. *Biotechnol. Bioeng.* 108, 1883–1892. doi: 10.1002/bit.23129

Fujiwara, R., Noda, S., Tanaka, T., and Kondo, A. (2020). Metabolic engineering of *Escherichia coli* for shikimate pathway derivative production from glucose–xylose co-substrate. *Nat. Commun.* 11:279. doi: 10.1038/s41467-019-14024-1

Gray, D., Sato, S., Garcia, F., Eppler, R., and Cherry, J. (2014). *Integrated Biorefinery Project Summary Final Report - Public Version*. Emeryville, CA: Amyris, Inc.

Hu, Y., Zhu, Z., Nielsen, J., and Siewers, V. (2019). Engineering *Saccharomyces cerevisiae* cells for production of fatty acid-derived biofuels and chemicals. *Open Biol.* 9:190049. doi: 10.1098/rsob.190049

Ignea, C., Pontini, M., Maffei, M. E., Makris, A. M., and Kampranis, S. C. (2014). Engineering monoterpene production in yeast using a synthetic dominant negative geranyl diphosphate synthase. *ACS Synthetic Biol.* 3, 298–306. doi: 10.1021/sb400115e

Jakočiūnas, T., Klitgaard, A. K., Kontou, E. E., Nielsen, J. B., Thomsen, E., Romero-Suarez, D., et al. (2020). Programmable polyketide biosynthesis platform for production of aromatic compounds in yeast. *Synth. Syst. Biotechnol.* 5, 11–18. doi: 10.1016/j.synbio.2020.01.004

Jiang, G.-Z., Yao, M.-D., Wang, Y., Zhou, L., Song, T.-Q., Liu, H., et al. (2017). Manipulation of GES and ERG20 for geraniol overproduction in *Saccharomyces cerevisiae*. *Metab. Eng.* 41, 57–66. doi: 10.1016/j.ymben.2017.03.005

Jin, C. C., Zhang, J. L., Song, H., and Cao, Y. X. (2019). Boosting the biosynthesis of betulinic acid and related triterpenoids in *Yarrowia lipolytica* via multimodular metabolic engineering. *Microb. Cell Fact.* 18:77. doi: 10.1186/s12934-019-1127-8

Jin, Z., Wong, A., Foo, J. L., Ng, J., Cao, Y.-X., Chang, M. W., et al. (2016). Engineering *Saccharomyces cerevisiae* to produce odd chain-length fatty alcohols. *Biotechnol. Bioeng.* 113, 842–851. doi: 10.1002/bit.25856

Kang, S.-Y., Choi, O., Lee, J. K., Hwang, B. Y., Uhm, T.-B., and Hong, Y.-S. (2012). Artificial biosynthesis of phenylpropanoic acids in a tyrosine overproducing *Escherichia coli* strain. *Microb. Cell Fact.* 11:153. doi: 10.1186/1475-2859-11-153

Larroude, M., Celinska, E., Back, A., Thomas, S., Nicaud, J.-M., and Ledesma-Amaro, R. (2018). A synthetic biology approach to transform *Yarrowia lipolytica* into a competitive biotechnological producer of β-carotene. *Biotechnol. Bioeng.* 115, 464–472. doi: 10.1002/bit.26473

Li, M., Schneider, K., Kristensen, M., Borodina, I., and Nielsen, J. (2016). Engineering yeast for high-level production of stilbenoid antioxidants. *Sci. Rep.* 6:36827. doi: 10.1038/srep36827

Li, Y., Qian, S., Dunn, R., and Cirino, P. C. (2018). Engineering *Escherichia coli* to increase triacetic acid lactone (TAL) production using an optimized TAL sensor-reporter system. *J. Industr. Microbiol. Biotechnol.* 45, 789–793. doi: 10.1007/s10295-018-2062-0

Li, Z.-J., Qiao, K., Liu, N., and Stephanopoulos, G. (2017). Engineering *Yarrowia lipolytica* for poly-3-hydroxybutyrate production. *J. Industr. Microbiol. Biotechnol.* 44, 605–612. doi: 10.1007/s10295-016-1864-1

Liu, Q., Yu, T., Li, X., Chen, Y., Campbell, K., Nielsen, J., et al. (2019). Rewiring carbon metabolism in yeast for high level production of aromatic chemicals. *Nat. Commun.* 10:4976. doi: 10.1038/s41467-019-12961-5

Liu, W., Xu, X., Zhang, R., Cheng, T., Cao, Y., Li, X., et al. (2016). Engineering *Escherichia coli* for high-yield geraniol production with biotransformation of geranyl acetate to geraniol under fed-batch culture. *Biotechnol. Biofuels* 9:58. doi: 10.1186/s13068-016-0466-5

Liu, Y., Chen, S., Chen, J., Zhou, J., Wang, Y., Yang, M., et al. (2016). High production of fatty alcohols in *Escherichia coli* with fatty acid starvation. *Microb. Cell Fact.* 15:129. doi: 10.1186/s12934-016-0524-5

López, J., Cataldo, V. F., Peña, M., Saa, P. A., Saitua, F., Ibaceta, M., et al. (2019). Build Your Bioprocess on a Solid Strain—β-Carotene Production in Recombinant *Saccharomyces cerevisiae*. *Front. Bioeng. Biotechnol.* 7:171. doi: 10.3389/fbioe.2019.00171

Luo, X., Reiter, M. A., d'Espaux, L., Wong, J., Denby, C. M., Lechner, A., et al. (2019). Complete biosynthesis of cannabinoids and their unnatural analogues in yeast. *Nature* 567, 123–126. doi: 10.1038/s41586-019-0978-9

Lyu, X., Zhao, G., Ng, K. R., Mark, R., and Chen, W. N. (2019). Metabolic Engineering of *Saccharomyces cerevisiae* for De Novo Production of Kaempferol. *J. Agricult. Food Chem.* 67, 5596–5606. doi: 10.1021/acs.jafc.9b01329

Ma, Y.-R., Wang, K.-F., Wang, W.-J., Ding, Y., Shi, T.-Q., Huang, H., et al. (2019). Advances in the metabolic engineering of *Yarrowia lipolytica* for the production of terpenoids. *Bioresource Technol.* 281, 449–456. doi: 10.1016/j.biortech.2019.02.116

Madison, L. L., and Huisman, G. W. (1999). Metabolic Engineering of Poly(3-Hydroxyalkanoates): from DNA to plastic. *Microbiol. Mol. Biol. Rev.* 63:21. doi: 10.1128/MMBR.63.1.21-53.1999

Markham, K. A., and Alper, H. S. (2018). Synthetic biology expands the industrial potential of *Yarrowia lipolytica*. *Trends Biotechnol.* 36, 1085–1095.

Markham, K. A., Palmer, C. M., Chwatko, M., Wagner, J. M., Murray, C., Vazquez, S., et al. (2018). Rewiring *Yarrowia lipolytica* toward triacetic acid lactone for materials generation. *Proc. Natl. Acad. Sci.* U.S.A. 115:2096. doi: 10.1073/pnas.1721203115

Marsafari, M., and Xu, P. (2020). Debottlenecking mevalonate pathway for antimalarial drug precursor amorphadiene biosynthesis in *Yarrowia lipolytica*. *Metab. Eng. Commun.* 10:e00121. doi: 10.1016/j.mec.2019.e00121

Miller, K. K., and Alper, H. S. (2019). *Yarrowia lipolytica*: more than an oleaginous workhorse. *Appl. Microbiol. Biotechnol.* 103, 9251–9262. doi: 10.1007/s00253-019-10200-x

Morelli, L., Zór, K., Jendresen, C. B., Rindzevicius, T., Schmidt, M. S., Nielsen, A. T., et al. (2017). Surface Enhanced Raman Scattering for Quantification of p-Coumaric Acid Produced by *Escherichia coli*. *Anal. Chem.* 89, 3981–3987. doi: 10.1021/acs.analchem.6b04428

Munkajohnpong, P., Kesornpun, C., Buttranon, S., Jaroensuk, J., Weeranoppanant, N., and Chaiyen, P. (2020). Fatty alcohol production: an opportunity of bioprocess. *Biofuels Bioprod. Biorefining* 14, 986–1009. doi: 10.1002/bbb.2112

Oloyede, H. O. B., Ajiboye, H. O., Salawu, M. O., and Ajiboye, T. O. (2017). Influence of oxidative stress on the antibacterial activity of betulin, betulinic acid and ursolic acid. *Microb. Pathog.* 111, 338–344. doi: 10.1016/j.micpath.2017.08.012

Paddon, C. J., Westfall, P. J., Pitera, D. J., Benjamin, K., Fisher, K., McPhee, D., et al. (2013). High-level semi-synthetic production of the potent antimalarial artemisinin. *Nature* 496, 528–532. doi: 10.1038/nature12051

Palmer, C. M., Miller, K. K., Nguyen, A., and Alper, H. S. (2020). Engineering 4-coumaroyl-CoA derived polyketide production in *Yarrowia lipolytica* through a β-oxidation mediated strategy. *Metab. Eng.* 57, 174–181. doi: 10.1016/j.ymben.2019.11.006

Parapouli, M., Vasileiadis, A., Afendra, A. S., and Hatziloukas, E. (2020). *Saccharomyces cerevisiae* and its industrial applications. *AIMS Microbiol.* 6, 1–31. doi: 10.3934/microbiol.2020001

Park, Y.-K., Dulermo, T., Ledesma-Amaro, R., and Nicaud, J.-M. (2018). Optimization of odd chain fatty acid production by *Yarrowia lipolytica*. *Biotechnol. Biofuels* 11:158. doi: 10.1186/s13068-018-1154-4

Park, Y. K., Ledesma-Amaro, R., and Nicaud, J.-M. (2020). De novo biosynthesis of odd-chain fatty Acids in *Yarrowia lipolytica* Enabled by Modular Pathway Engineering. *Front. Bioeng. Biotechnol.* 7:484. doi: 10.3389/fbioe.2019.00484

Ping, Y., Li, X., You, W., Li, G., Yang, M., Wei, W., et al. (2019). De novo production of the plant-derived tropine and pseudotropine in yeast. *ACS Synthetic Biol.* 8, 1257–1262. doi: 10.1021/acssynbio.9b00152

Pompon, D., Louerat, B., Bronine, A., and Urban, P. (1996). "Yeast expression of animal and plant P450s in optimized redox environments," in *Methods in Enzymology*, eds E. F. Johnson and M. R. Waterman (Cambridge, MA: Academic Press), 51–64. doi: 10.1016/s0076-6879(96)72008-6

Portugal-Nunes, D. J., Pawar, S. S., Lidén, G., and Gorwa-Grauslund, M. F. (2017). Effect of nitrogen availability on the poly-3-d-hydroxybutyrate accumulation by engineered *Saccharomyces cerevisiae*. *AMB Exp.* 7:35. doi: 10.1186/s13568-017-0335-z

Qiao, K., Wasylenko, T. M., Zhou, K., Xu, P., and Stephanopoulos, G. (2017). Lipid production in *Yarrowia lipolytica* is maximized by engineering cytosolic redox metabolism. *Nat. Biotechnol.* 35, 173–177. doi: 10.1038/nbt.3763

Rigouin, C., Croux, C., Borsenberger, V., Ben Khaled, M., Chardot, T., Marty, A., et al. (2018). Increasing medium chain fatty acids production in *Yarrowia lipolytica* by metabolic engineering. *Microb. Cell Fact.* 17:142. doi: 10.1186/s12934-018-0989-5

Rigouin, C., Gueroult, M., Croux, C., Dubois, G., Borsenberger, V., Barbe, S., et al. (2017). Production of medium chain fatty acids by *Yarrowia lipolytica*: combining molecular design and TALEN to engineer the fatty acid Synthase. *ACS Synthet. Biol.* 6, 1870–1879. doi: 10.1021/acssynbio.7b00034

Ro, D.-K., Paradise, E. M., Ouellet, M., Fisher, K. J., Newman, K. L., Ndungu, J. M., et al. (2006). Production of the antimalarial drug precursor artemisinic acid in engineered yeast. *Nature* 440, 940–943. doi: 10.1038/nature04640

Ryu, H. W., Hahn, S. K., Chang, Y. K., and Chang, H. N. (1997). Production of poly(3-hydroxybutyrate) by high cell density fed-batch culture of *Alcaligenes eutrophus* with phospate limitation. *Biotechnol. Bioeng.* 55, 28–32. doi: 10.1002/(sici)1097-0290(19970705)55:1<28::aid-bit4>3.0.co;2-z

Saunders, L. P., Bowman, M. J., Mertens, J. A., Da Silva, N. A., and Hector, R. E. (2015). Triacetic acid lactone production in industrial *Saccharomyces* yeast strains. *J. Industr. Microbiol. Biotechnol.* 42, 711–721. doi: 10.1007/s10295-015-1596-7

Schalk, M., Pastore, L., Mirata, M. A., Khim, S., Schouwey, M., Deguerry, F., et al. (2012). Toward a biosynthetic route to sclareol and amber odorants. *J. Am. Chem. Soc.* 134, 18900–18903. doi: 10.1021/ja307404u

Sherkhanov, S., Korman, T. P., and Bowie, J. U. (2014). Improving the tolerance of *Escherichia coli* to medium-chain fatty acid production. *Metab. Eng.* 25, 1–7. doi: 10.1016/j.ymben.2014.06.003

Shi, B., Ma, T., Ye, Z., Li, X., Huang, Y., Zhou, Z., et al. (2019). Systematic Metabolic Engineering of *Saccharomyces cerevisiae* for Lycopene Overproduction. *J. Agricult. Food Chem.* 67, 11148–11157. doi: 10.1021/acs.jafc.9b04519

Siddiqui, M. S., Thodey, K., Trenchard, I., and Smolke, C. D. (2012). Advancing secondary metabolite biosynthesis in yeast with synthetic biology tools. *FEMS Yeast Res.* 12, 144–170. doi: 10.1111/j.1567-1364.2011.00774.x

Souza-Moreira, T. M., Navarrete, C., Chen, X., Zanelli, C. F., Valentini, S. R., Furlan, M., et al. (2018). Screening of 2A peptides for polycistronic gene expression in yeast. *FEMS Yeast Res.* 18. doi: 10.1093/femsyr/foy036

Srinivasan, P., and Smolke, C. D. (2019). Engineering a microbial biosynthesis platform for de novo production of tropane alkaloids. *Nat. Commun.* 10:3634. doi: 10.1038/s41467-019-11588-w

Sun, T., Miao, L., Li, Q., Dai, G., Lu, F., Liu, T., et al. (2014). Production of lycopene by metabolically-engineered *Escherichia coli*. *Biotechnol. Lett.* 36, 1515–1522. doi: 10.1007/s10529-014-1543-0

Tang, S.-Y., Qian, S., Akinterinwa, O., Frei, C. S., Gredell, J. A., and Cirino, P. C. (2013). Screening for enhanced triacetic acid lactone production by recombinant *Escherichia coli* expressing a designed triacetic acid lactone reporter. *J. Am. Chem. Soc.* 135, 10099–10103. doi: 10.1021/ja402654z

Trikka, F. A., Nikolaidis, A., Athanasakoglou, A., Andreadelli, A., Ignea, C., Kotta, K., et al. (2015). Iterative carotenogenic screens identify combinations of yeast gene deletions that enhance sclareol production. *Microb. Cell Fact.* 14:60. doi: 10.1186/s12934-015-0246-0

Vickers, C. E., Williams, T. C., Peng, B., and Cherry, J. (2017). Recent advances in synthetic biology for engineering isoprenoid production in yeast. *Curr. Opin. Chem. Biol.* 40, 47–56. doi: 10.1016/j.cbpa.2017.05.017

Walker, G., and Stewart, G. (2016). *Saccharomyces cerevisiae* in the Production of Fermented Beverages. *Beverages* 2:30. doi: 10.3390/beverages2040030

Wang, C., Liwei, M., Park, J.-B., Jeong, S.-H., Wei, G., Wang, Y., et al. (2018). Microbial platform for terpenoid production: *Escherichia coli* and Yeast. *Front. Microbiol.* 9:2460. doi: 10.3389/fmicb.2018.02460

Wang, G., Øzmerih, S., Guerreiro, R., Meireles, A. C., Carolas, A., Milne, N., et al. (2020). Improvement of cis,cis-Muconic Acid Production in *Saccharomyces cerevisiae* through Biosensor-Aided Genome Engineering. *ACS Synth. Biol.* 9, 634–646. doi: 10.1021/acssynbio.9b00477

Wang, J., Ma, W., Fang, Y., Zhang, H., Liang, H., Li, Y., et al. (2020). Truncating the Structure of Lipopolysaccharide in *Escherichia coli* Can Effectively Improve Poly-3-hydroxybutyrate Production. *ACS Synth. Biol.* 9, 1201–1215. doi: 10.1021/acssynbio.0c00071

Wehrs, M., Tanjore, D., Eng, T., Lievense, J., Pray, T. R., and Mukhopadhyay, A. (2019). Engineering robust production microbes for large-scale cultivation. *Trends Microbiol.* 27, 524–537. doi: 10.1016/j.tim.2019.01.006

Weitkunat, K., Schumann, S., Nickel, D., Hornemann, S., Petzke, K. J., Schulze, M. B., et al. (2017). Odd-chain fatty acids as a biomarker for dietary fiber intake: a novel pathway for endogenous production from propionate. *Am. J. Clin. Nutr.* 105, 1544–1551. doi: 10.3945/ajcn.117.152702

Whited, G. M., Feher, F. J., Benko, D. A., Cervin, M. A., Chotani, G. K., McAuliffe, J. C., et al. (2010). TECHNOLOGY UPDATE: development of a gas-phase bioprocess for isoprene-monomer production using metabolic pathway engineering. *Industr. Biotechnol.* 6, 152–163. doi: 10.1089/ind.2010.6.152

Wu, H., and San, K.-Y. (2014). Engineering *Escherichia coli* for odd straight medium chain free fatty acid production. *Appl. Microbiol. Biotechnol.* 98, 8145–8154. doi: 10.1007/s00253-014-5882-5

Wu, J., Du, G., Chen, J., and Zhou, J. (2015). Enhancing flavonoid production by systematically tuning the central metabolic pathways based on a CRISPR interference system in *Escherichia coli*. *Sci. Rep.* 5:13477. doi: 10.1038/srep13477

Wu, J., Zhou, P., Zhang, X., and Dong, M. (2017). Efficient de novo synthesis of resveratrol by metabolically engineered *Escherichia coli*. *J. Industr. Microbiol. Biotechnol.* 44, 1083–1095. doi: 10.1007/s10295-017-1937-9

Wu, Y., Xu, S., Gao, X., Li, M., Li, D., and Lu, W. (2019). Enhanced protopanaxadiol production from xylose by engineered *Yarrowia lipolytica*. *Microb. Cell Fact.* 18:83. doi: 10.1186/s12934-019-1136-7

Xie, N.-Z., Liang, H., Huang, R.-B., and Xu, P. (2014). Biotechnological production of muconic acid: current status and future prospects. *Biotechnol. Adv.* 32, 615–622. doi: 10.1016/j.biotechadv.2014.04.001

Yang, J., and Guo, L. (2014). Biosynthesis of β-carotene in engineered *E. coli using the MEP and MVA pathways*. *Microb. Cell Fact.* 13:160. doi: 10.1186/s12934-014-0160-x

Yao, Z., Zhou, P., Su, B., Su, S., Ye, L., and Yu, H. (2018). Enhanced Isoprene Production by Reconstruction of Metabolic Balance between Strengthened Precursor Supply and Improved Isoprene Synthase in *Saccharomyces cerevisiae*. *ACS Synth. Biol.* 7, 2308–2316. doi: 10.1021/acssynbio.8b00289

Zhang, C., and Hong, K. (2020). Production of Terpenoids by Synthetic Biology Approaches. *Front. Bioeng. Biotechnol.* 8:347. doi: 10.3389/fbioe.2020.00347

Zhang, X.-K., Nie, M.-Y., Chen, J., Wei, L.-J., and Hua, Q. (2019). Multicopy integrants of crt genes and co-expression of AMP deaminase improve lycopene production in *Yarrowia lipolytica*. *J. Biotechnol.* 289, 46–54. doi: 10.1016/j.jbiotec.2018.11.009

Zhou, Y. J. (2018). Expanding the terpenoid kingdom. *Nat. Chem. Biol.* 14, 1069–1070. doi: 10.1038/s41589-018-0167-4

Zhu, Z., Hu, Y., Teixeira, P. G., Pereira, R., Chen, Y., Siewers, V., et al. (2020). Multidimensional engineering of *Saccharomyces cerevisiae* for efficient synthesis of medium-chain fatty acids. *Nat. Catal.* 3, 64–74. doi: 10.1038/s41929-019-0409-1

Conflict of Interest: The authors declare that the research was conducted in the absence of any commercial or financial relationships that could be construed as a potential conflict of interest.

frontiers in Bioengineering and Biotechnology

ORIGINAL RESEARCH
published: 08 January 2021
doi: 10.3389/fbioe.2020.593419

Production of Long Chain Fatty Alcohols Found in Bumblebee Pheromones by *Yarrowia lipolytica*

*Jaroslav Hambalko[1], Peter Gajdoš[1], Jean-Marc Nicaud[2], Rodrigo Ledesma-Amaro[3], Michal Tupec[4], Iva Pichová[4] and Milan Čertík[1]**

[1] Faculty of Chemical and Food Technology, Institute of Biotechnology, Slovak University of Technology, Bratislava, Slovakia, [2] French National Research Institute for Agriculture (INRAE), Food and Environment, AgroParisTech, Micalis Institute, Université Paris-Saclay, Jouy-en-Josas, France, [3] Department of Bioengineering and Imperial College Centre for Synthetic Biology, Faculty of Engineering, Imperial College London, London, United Kingdom, [4] Institute of Organic Chemistry and Biochemistry of the Czech Academy of Sciences, Prague, Czechia

OPEN ACCESS

Edited by:
M. Kalim Akhtar, United Arab Emirates University, United Arab Emirates

Reviewed by:
Matthew Wook Chang, National University of Singapore, Singapore
Marjorie A. Liénard, Lund University, Sweden
Volkmar Passoth, Swedish University of Agricultural Sciences, Sweden

***Correspondence:**
Milan Čertík, milan.certik@stuba.sk

Specialty section:
This article was submitted to Synthetic Biology, a section of the journal Frontiers in Bioengineering and Biotechnology

Received: *10 August 2020*
Accepted: *08 December 2020*
Published: *08 January 2021*

Citation:
Hambalko J, Gajdoš P, Nicaud J-M, Ledesma-Amaro R, Tupec M, Pichová I and Čertík M (2021) Production of Long Chain Fatty Alcohols Found in Bumblebee Pheromones by Yarrowia lipolytica. Front. Bioeng. Biotechnol. 8:593419. doi: 10.3389/fbioe.2020.593419

Fatty alcohols (FA-OH) are aliphatic unbranched primary alcohols with a chain of four or more carbon atoms. Besides potential industrial applications, fatty alcohols have important biological functions as well. In nature, fatty alcohols are produced as a part of a mixture of pheromones in several insect species, such as moths, termites, bees, wasps, etc. In addition, FA-OHs have a potential for agricultural applications, for example, they may be used as a suitable substitute for commercial insecticides. The insecticides have several drawbacks associated with their preparation, and they exert a negative impact on the environment. Currently, pheromone components are prepared mainly through the catalytic hydrogenation of plant oils and petrochemicals, which is an unsustainable, ecologically unfriendly, and highly expensive process. The biotechnological production of the pheromone components using engineered microbial strains and through the expression of the enzymes participating in the biosynthesis of these components is a promising approach that ensures ecological sustenance as well. The present study was aimed at evaluating the production of FA-OHs in the oleaginous yeast, *Yarrowia lipolytica*, with different lengths of fatty-acyl chains by expressing the fatty acyl-CoA reductase (FAR) *Blap*FAR4 from *B. lapidarius*, producing C16:0-OH, C16:1Δ^9-OH, and lower quantities of both C14:0-OH and C18:1Δ^9-OH, and *Bluc*FAR1 from *B. lucorum*, producing FA-OHs with a chain length of 18–26 carbon atoms, in this yeast. Among the different novel *Y. lipolytica* strains used in the present study, the best results were obtained with JMY7086, which carried several lipid metabolism modifications and expressed the *BlucFAR1* gene under the control of a strong constitutive promoter *8UAS-pTEF*. JMY7086 produced only saturated fatty alcohols with chain lengths from 18 to 24 carbon atoms. The highest titer and accumulation achieved were 166.6 mg/L and 15.6 mg/g DCW of fatty alcohols, respectively. Unlike JMY7086, the *Blap*FAR4-expressing strain JMY7090 produced only 16 carbon atom-long FA-OHs with a titer of 14.6 mg/L.

Keywords: pheromone, fatty alcohol, reductase, metabolic engineering, *Bombus*, *Yarrowia lipolytica*

INTRODUCTION

Fatty alcohols (FA-OH) are aliphatic unbranched primary alcohols with varying chain lengths ranging from 4 to 28 carbon atoms and containing either saturated or unsaturated carbon bonds (McNaught and Wilkinson, 1997). The properties and the potential applications of fatty alcohol depend on their molecular structure. Generally, fatty alcohols are used as fuels, solvents, detergents, cosmetics, lubricants, and pharmaceuticals, or may serve as precursors for other compounds such as waxes or polymers (Rutter and Rao, 2016; Wang G. et al., 2016; Wang W. et al., 2016; Borodina et al., 2018a; Cordova et al., 2019). In 2019, the global demand for fatty alcohols was estimated to be over two million tons, with an annual growth rate of 4.3%. Traditionally, these molecules are produced through the catalytic hydrogenation of petrochemicals or plant oils, which currently relies on fossil fuels or unsustainable palm farming and has significant environmental consequences such as deforestation or contribution to global warming (Rutter and Rao, 2016; Shah et al., 2016; Cordova et al., 2019). Therefore, there is an urgent requirement for a further efficient and ecologically-friendly process.

Fatty alcohols and their derivatives also have important biological functions. Insects have evolved an efficient mate-finding system that is based on volatile sex pheromones. In most species, sex pheromones are released either as a single component (Jurenka, 2004; Groot et al., 2016; Tupec et al., 2017) or as a specific blend of molecules in specific ratios, most of which are fatty acid (FA) derivatives, usually alcohols, aldehydes, or acetates. The sex pheromone blend of the bumblebees mainly comprises saturated, mono-unsaturated, and poly-unsaturated fatty alcohols with a chain length of 16–18 carbon atoms along with terpenoid compounds (Ayasse and Jarau, 2014). Sex pheromones are synthesized *de novo* in specialized cells known as pheromone glands, which have evolved from epidermal cells (Žáček et al., 2013; Tittiger and Blomquist, 2017). The pheromone biosynthesis process involves several key enzymes. In addition, the saturated FAs such as stearic and palmitic must undergo processing mediated by chain-shortening enzymes, desaturases, reductases, acetyltransferases, and oxidases, among others (Tillman et al., 1999; Jurenka, 2004; Matoušková et al., 2008; Matsumoto, 2010; Buček et al., 2013; Koutroumpa and Jacquin-Joly, 2014; Tupec et al., 2017).

The first pheromone to be identified and purified was a fatty alcohol named bombykol (10*E*,12*Z*- hexadeca-10,12-dien-1-ol), which was isolated from the silkmoth *Bombyx mori* (Butenandt et al., 1961). Enzymes involved in bombykol biosynthesis were described later (Moto et al., 2003, 2004). Since then, pheromones have been identified in several thousands of insect species and are known for their potential as attractants or repellents in agriculture (Koutroumpa and Jacquin-Joly, 2014; El-Sayed, 2019). Pheromones represent the most suitable substitute for insecticides. Insecticides have been in use in agriculture for over 50 years. However, the environmental damage caused by the insecticides and the development of insecticide resistance among insects and pests are emerging as serious threats. The most significant problems associated with the use of insecticides include: (a) harmful effects on other organisms, including humans and the plants that rely on insects for pollination, (b) persistence of the insecticides in the biosphere, (c) worldwide spread, and (d) significant levels of pollution associated with the current methods of insecticide production (Hagström et al., 2013; Borodina et al., 2018b). In order to resolve some of these issues, synthetic pheromones were developed to control the pest insects in a species-specific manner and to maintain healthy agricultural practices (Hagström et al., 2013). For instance, tetradec-9-enyl acetate (C14:1Δ^9-OAc) was reported to disrupt the mating efficiency of the fall armyworm when applied alone (Mitchell and McLaughlin, 1982). However, most agricultural applications of pheromones are limited by their high cost. Pheromones are expensive because their purity is paramount for eliciting a response in an insect, and the production of pheromones with such high levels of purity through chemical processes requires expensive and complicated methods while generating waste in huge quantities, which again requires disposal and increases costs (Borodina et al., 2018b).

The development of various genetic tools has allowed the characterization of heterologously produced fatty acyl-CoA reductases (FARs), which catalyze the reduction of fatty acyl-CoA precursors into the corresponding alcohols (Moto et al., 2003; Liénard et al., 2010; Antony et al., 2016; Ding et al., 2016; Tupec et al., 2019). The FAR genes are present in several species, including vertebrates, non-insect invertebrates, and fungi, with a particularly high number of FAR gene families reported in plant and insect genomes (Eirín-López et al., 2012; Buček et al., 2016; Tupec et al., 2019). Within the class Insecta, large quantities of long-chain alcohols have been identified in the pheromone mixtures of different bumblebees, including *Bombus lucorum*, *Bombus lapidarius*, and *Bombus terrestris*. Tupec et al. (2019) used heterologous expression in *S. cerevisiae* to demonstrate that bumblebees have evolved a specific FAR gene group that encodes reductases with unusual specificities and contributes to the biosynthesis of different fatty alcohols that form a part of bumble-specific pheromones.

The recent advancements in metabolic engineering and synthetic biology have enabled an environment-friendly production of FA-derived compounds, including FA-OHs and the biofuels from renewable feedstock using microbial biomass (Guo et al., 2016; Rutter and Rao, 2016). *Yarrowia lipolytica* is an oleaginous non-pathogenic yeast belonging to the Ascomycota phylum of kingdom Fungi (Abdel-Mawgoud et al., 2018), which could serve as a perfect cell factory for industrial applications (Groenewald et al., 2014). This yeast species is of great importance to researchers due to its high tolerance to a variety of organic substrates, higher salt levels in the environment, and a broad range of pH (Miller and Alper, 2019). Since the genome of *Y. lipolytica* was unraveled long ago and the tools for manipulating genomes and the knowledge of genetic engineering has also progressed dramatically, *Y. lipolytica* has become a suitable representative model organism for the production of natural biosynthetic products in the laboratory (Ledesma-Amaro and Nicaud, 2016). In this context, the present study was aimed to evaluate the ability of *Y. lipolytica* in the production of FA-OHs of different lengths, for which two

bumblebee FARs (Tupec et al., 2019) were expressed in this yeast. The *Blap*FAR4 from *B. lapidarius* is capable of preferentially catalyzing the production of shorter FA-OHs (14–16 carbons), while *Bluc*FAR1 from *B. lucorum* prefers acyl chains containing 18–26 carbon atoms.

In the present study, we engineered multiple strains of *Y. lipolytica* for a redesigned lipid metabolism, with genes encoding *Bluc*FAR1 and *Blap*FAR4, to produce the FARs and obtain the corresponding fatty alcohols. The expression of *Bluc*FAR1 (JMY7086) stimulated the production of 18–24 carbon atom-long fatty alcohols, presenting the highest fatty alcohol production among all the strains (166.6 mg/L). Unlike JMY7086, the *Blap*FAR4-expressing strain (JMY7090) produced only 14.6 mg/L of fatty alcohols with a chain length of 16 carbons.

MATERIALS AND METHODS

Strains, Media Composition, and Culture Conditions

All the strains of *Escherichia coli* and *Y. lipolytica* used in the present study are listed in **Table 1**. The recombinant strains of *Y. lipolytica* were constructed by engineering the wild type strain W29 (ATCC 20 460). The *E. coli* strains were cultured in a lysogeny broth medium containing a suitable antibiotic (100 μg/mL of ampicillin or 50 μg/mL of kanamycin), according to the standard protocol described by Sambrook and Russell (2001). Minimal YNB, YNBUra, and YNBLeu media agar plates were used for the selection of *Y. lipolytica* transformants. The minimal YNB medium comprised 1.7 g/L yeast nitrogen base (without amino acids and ammonium sulfate; BD, Erembodegem, Belgium), 5 g/L NH4Cl, 50 mM phosphate buffer (pH 6.8), and 20 g/L glucose. The YNBUra and YNBLeu media were prepared by adding 0.1 g/L of uracil and leucine, respectively, to the YNB medium. The agar plates were prepared by adding 20 g/L agar to the respective medium. A rich YPD medium containing 10 g/L yeast extract (BD, Erembodegem, Belgium), 10 g/L peptone (BD, Erembodegem, Belgium), and 20 g/L glucose (Mikrochem, Pezinok, Slovakia) was prepared for obtaining the inoculum of *Y. lipolytica*. The medium for lipid production ($MedA^+$) comprised 1.5 g/L yeast extract, 0.5 g/L NH_4Cl, 7 g/L KH_2PO_4, 5 g/L $Na_2HPO_4.12H_2O$, 0.1 g/L $CaCl_2$, 1.5 g/L $MgSO_4.7H_2O$, 10 mg/L $ZnSO_4.7H_2O$, 0.6 mg/L $FeCl_3.6H_2O$, 0.07 mg/L $MnSO_4.H_2O$, and 0.04 mg/L $CuSO_4.5H_2O$. The carbon source used was either glucose or crude glycerol (Mikrochem, Pezinok, Slovakia) in the concentration of 60 g/L. Owing to its high C/N ratio, this medium was suitable for the accumulation of lipids in yeasts. The $MedA^+$ growth medium was prepared by modifying the MedA medium reported by Holdsworth et al. (1988). The yeast inoculum was prepared in 20 mL of the YPD medium in 100 mL flasks. Subsequently, 50 mL production medium in 250 mL baffled flasks was inoculated with a 24-h inoculum which had an optical density (OD_{600}) of 0.1. The cells were cultured at 28°C and 130 rpm inside an orbital shaker (Innova 40R, NB, Canada). In order to confirm fatty alcohol production, the strains of *Y. lipolytica* were cultured for 3 days, while the cultivation of the selected strain continued for 5 days, with 24-h interval sampling, to describe the kinetics of fatty alcohol formation. All the experiments were performed in three independent biological replicates.

TABLE 1 | The *Escherichia coli* and *Yarrowia lipolytica* strains and plasmids used in the present study.

Strain (host strain)	Plasmid/genotype	References
Escherichia coli		
JME1046	*JMP62-pTEF-URA3ex*	Lazar et al. (2013)
JME2563	*JMP62-pTEF-LEU2ex*	Dulermo et al. (2017)
JME2607	*JMP62–8UAS-pTEF-RedStar2-LEU2ex*	Dulermo et al. (2017)
JME3048	*JMP62–8UAS-pTEF-URA3ex*	Dulermo et al. (2017)
JME4149	*JMP1046-BlucFAR1*	This work
JME4151	*JMP1046-BlapFAR4*	This work
JME4303	*JMP3048-BlucFAR1*	This work
JME4305	*JMP2607-BlapFAR4*	This work
Yarrowia lipolytica		
W29	*MATA, wild type*	Barth and Gaillardin (1996)
Po1d	*MATA leu2–270 ura3–302 xpr2–322+pXPR2-SUC2*	Barth and Gaillardin (1996)
JMY6697	*Po1d, pTEF-BlucFAR1-URA3ex, LEU2*	This work
JMY6698	*Po1d, pTEF-BlapFAR4-URA3ex, LEU2*	This work
JMY3501	*W29 ura3–302 leu2–270 xpr2–322 Δpox1–6 Δtgl4+pXPR2-SUC2+pTEF-DGA2-LEU2ex+pTEF-GPD1-URA3ex*	Lazar et al. (2014)
JMY3820	*W29 ura3–302 leu2–270 xpr2–322 Δpox1–6 Δtgl4+pXPR2-SUC2+pTEF-DGA2+pTEF-GPD1*	Lazar et al. (2014)
JMY7086	*JMY3820, 8UAS-pTEF-BlucFAR1-URA3ex, LEU2*	This work
JMY7090	*JMY3820, 8UAS-pTEF-BlapFAR4-LEU2ex, URA3*	This work
JMY7094	*JMY3820, 8UAS-pTEF-BlucFAR1-URA3ex, 8UAS-pTEF-BlapFAR4-LEU2ex*	This work

Plasmid and Strain Construction

The genes *BlucFar1* and *BlapFar4* were codon-optimized for *Yarrowia lipolytica* (**Supplementary Figure 1**). The synthetic fragments were digested using BamHI/AvrII, followed by insertion into the corresponding BamHI/AvrII sites of the already-available plasmids JME2607 and JME3048, which contained the *8UAS-pTEF* promoter (Dulermo et al., 2017). The *JMP62-pTEF-LEU2ex* and *JMP62-pTEF-URA3ex* vectors were employed to complement the LEU and URA auxotrophy, respectively, in the final strain. The plasmids were digested with NotI prior to being used for *Y. lipolytica* transformation using the lithium acetate method (Le Dall et al., 1994). The transformants were selected on the YNBUra, YNBLeu, or YNB media, depending on their genotypes. Subsequently, the genomic DNA was derived from the yeast transformants as described by Querol et al. (1992). The positive transformants were confirmed using PCR. The PCR amplifications were performed in an Eppendorf 2720 thermal cycler using GoTaq DNA polymerases (Promega). The obtained PCR fragments were purified using a

QIAgen Purification Kit (Qiagen, Hilden, Germany), followed by verification through gel electrophoresis and sequencing. All the reactions were performed in accordance with the respective manufacturers' instructions.

Analytical Methods

In order to isolate the biomass, the cell suspensions were centrifuged (2,880 × *g*, 5 min), washed twice with the saline solution (NaCl, 9 g/L), and then once with deionized water, and finally freeze-dried. The freeze-dried cells were subjected to lipid analysis and dry cell weight (DCW) determination. DCW was determined gravimetrically.

The residual glycerol amounts during growth profile analysis were determined by performing HPLC (Agilent Technologies, Santa Clara, CA, United States) using an Aminex HPX87H column (Bio-Rad, Hercules, CA, United States) coupled with an RI detector and a DAD detector. H_2SO_4 (5 mM) was used as the mobile phase with a flow rate of 0.6 mL/min, as described by Lazar et al. (2011).

The freeze-dried cells (approximately 10 mg) were added to a mixture of 1 mL CH_2Cl_2 (containing 0.1 mg of C13:0 as the internal standard) and 2 mL anhydrous methanolic HCl solution, and the suspension was incubated at 50°C for 3 h. After the incubation, 1 mL of water and 1 mL of hexane were added, and the whole suspension was vortexed vigorously. The organic layer containing fatty alcohols and fatty acid methyl esters (FAME) was separated through centrifugation (2,880 × *g*, 5 min) and analyzed using GC-6890 N (Agilent Technologies, Santa Clara, CA, United States). The samples (1 μL) were injected automatically into the DB-23 column (50% cyanopropyl-methylpolysiloxane, length 60 m, diameter 0.25 mm, film thickness 0.25 μm) and analyzed. The analysis conditions were: carrier gas–hydrogen, inlet (230°C; hydrogen flow: 37 mL/min; split–10:1), FID detector (250°C, hydrogen flow: 40 mL/min, air flow: 450 mL/min.), gradient (150°C–0 min; 150–170°C–5,0°C/min; 170–220°C–6,0°C/min; 220°C–6 min; 220–230°C–6°C/min; 230°C–1 min; 230–240°C–30°C/min; 240°C–6 min). The chromatograms were analyzed using the Agilent Open LAB CDS software. The fatty alcohols and fatty acids were quantified according to the individual peak area normalized with the internal standard (C13:0). Individual fatty acids were identified according to the C4–C24 FAME standard (Supelco, Bellefonte, PA, United States). The fatty alcohol standards were obtained from Nu-Chek Prep and Sigma-Aldrich. GC-MS (EI at 70 eV) was performed to confirm the identity of the obtained peaks according to their MS spectra.

RESULTS

Insertion of FAR Genes Into Wild Type *Y. lipolytica*

The genes *BlucFAR1* from *B. lucorum* and *BlapFAR4* from *B. lapidarius* were overexpressed, under the control of the *pTEF* promoter, in the genetic background of Po1d strain (**Supplementary Figure 2**). Po1d was constructed from the wild type strain W29 in an earlier study (Barth and Gaillardin, 1996). Both new strains JMY6697 (*Bluc*FAR1) and JMY6698 (*Blap*FAR4) were cultured in YPD and two MedA$^+$ media, supplemented with either glycerol or glucose as the carbon source. The W29 strain was used as a control as it has the same genetic background as the host Po1d. All the strains were quite similar in terms of growth and did not differ significantly regarding the amount of accumulated lipids. The lowest lipid accumulation was obtained with the YPD medium, which is consistent with the assumption that the YPD medium is not suitable for lipid overproduction as it does not have a high C/N ratio. In both the MedA$^+$ media, the lipid accumulation amounts were similar (**Supplementary Table 1**). However, trace amounts of FA-OHs were observed only under oleaginous conditions. The JMY6697 strain (*Bluc*FAR1) produced saturated FA-OHs with a chain length of 18 or more carbon atoms, while the JMY6698 strain (*Blap*FAR4) produced saturated FA-OH with a 16 carbon atom-long chain only. No FA-OHs were secreted into the medium. Since insect FA-OHs were produced in low quantities in these strains, it was decided to construct *Y. lipolytica* strains with further improved lipid metabolism to achieve higher FA-OH production by the expressed FARs.

Metabolic Redesigning of *Y. lipolytica* for Effective Fatty Alcohol Production

New strains capable of accumulating higher amounts of lipids were constructed. The JMY3820 strain, which had all the 6 *POX* genes and *TGL4* lipase deleted and the *DGA2* and *GPD1* overexpressed using the *pTEF* promoter, was selected as the host strain for FAR expression. The JMY3820 strain is an auxotrophic version of the JMY3501 strain. Both these strains were constructed from the JMY1233 (Beopoulos et al., 2008) strain in an earlier study (Lazar et al., 2014). In both these strains, the FARs were expressed under a stronger hybrid constitutive promoter named *8UAS-pTEF* (Dulermo et al., 2017). Therefore, in total, three new strains were constructed (**Supplementary Figure 3**): JMY7086 (*8UAS-pTEF-BlucFAR1*), JMY7090 (*8UAS-pTEF-BlapFAR4*), and JMY7094 (*8UAS-pTEF-BlucFAR1* and *8UAS-pTEF-BlapFAR4*). Changes in lipid metabolism are displayed in **Figure 1**.

Biomass, Fatty Acid, and Fatty Alcohol Production

The yeast strains were cultured in two MedA$^+$ media with different carbon sources (glucose or glycerol) for 3 days. The C/N ratio of both the media was 80 and the concentration of carbon source was 60 g/L. The non-alcohol producing JMY3501 strain was cultured under the same conditions as the control for evaluating the influence of the alcohols on cell growth and lipid accumulation. Glycerol promoted higher biomass growth and total fatty acid including fatty alcohol accumulation (TFA) in all the strains, compared to glucose (**Figure 2**). Whether growing on glucose or glycerol, all the alcohol-producing strains produced quite similar amounts of lipid-free biomass, and the amount of lipid-free biomass produced by the control strain was lower compared to that of the alcohol-producing strains (5.8 g/L vs. approx. 6.8 g/L on glucose and 5.8 g/L vs. approx.

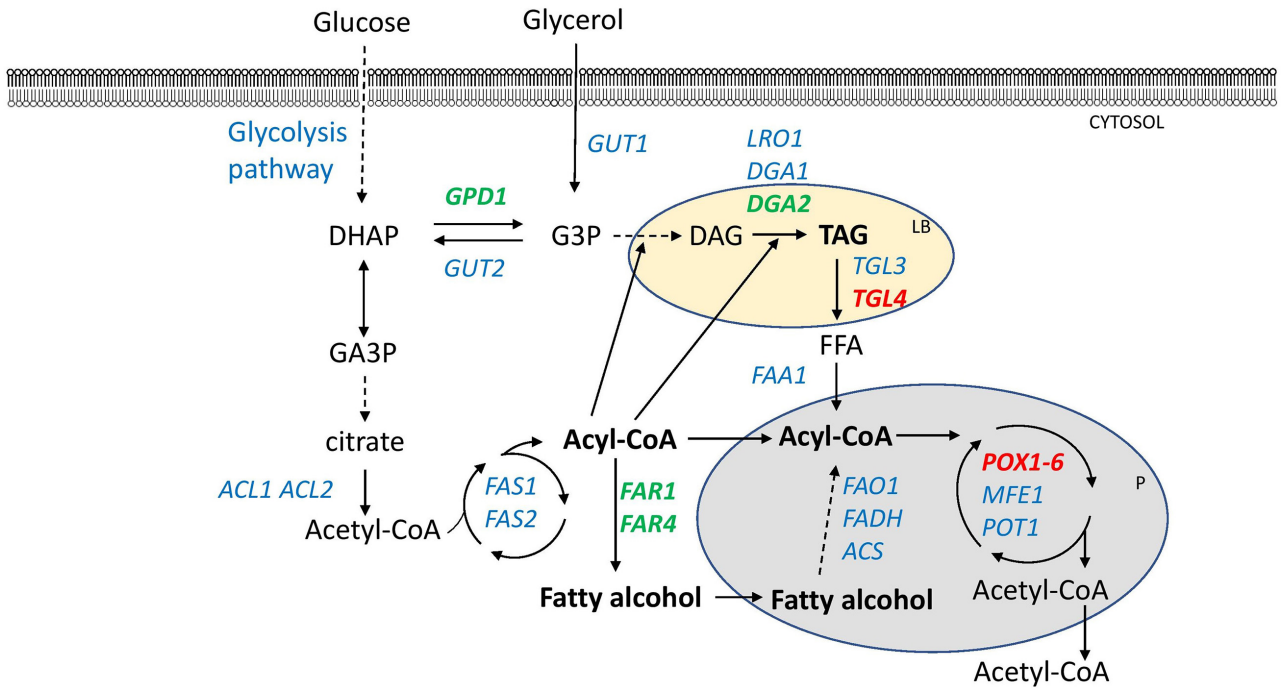

FIGURE 1 | Lipid metabolism of manipulated *Y. lipolytica* strains producing fatty alcohols. Overexpressed genes are shown in green. Deleted genes are shown in red. Dashed lines indicate multiple steps. DHAP-dihydroxycetone phosphate, G3P-glycerol-3-phosphate, GA3P-glyceraldehyde-3-phosphate, DAG-diacylglycerol, TAG-triacylglycerol, FFA-free fatty acid, LB-lipid body, P-peroxisome. Enzymes: GPD1-glycerol-3-phosphate dehydrogenase, GUT1-glycerol kinase, GUT2-glycerol-3-phosphate dehydrogenase, ACL1-ATP-citrate lyase 1, ACL2-ATP citrate lyase 2, FAS1-fatty acid synthase 1, FAS2-fatty acid synthase, LRO1-phospholipid:diacylglycerol acyltransferase, DGA1 and DGA2-acyl-CoA:diacylglycerol acyltransferases 1, TGL3 and TGL4-intracellular lipases, FAA1-fatty acyl-CoA synthetase, FAO1-fatty alcohol oxidase, FADH-fatty alcohol oxidase, ACS-acyl-CoA synthase, POX1-6-acyl-CoA oxidases, MFE1-multifunctional enzyme, POT1-thiolase, and FAR1 and FAR4-fatty acyl-CoA reductases.

7.5 g/L on glycerol). The most remarkable difference was observed in the FAs accumulation in yeasts, which was inversely proportional to the FA-OH accumulation. The control strain JMY3501 accumulated approximately 60% of TFA/DCW, while the alcohol-producing strains accumulated only 17–45% of it. Even a higher production of fatty alcohols did not promote the secretion of fatty alcohols into the medium.

After 3 days of cultivation, all the yeast strains grown on glycerol accumulated more FA-OHs compared to the yeast growing on glucose (9.77 mg/g in JMY7086 on glycerol vs. 6.17 mg/g in JMY7086 on glucose) (**Table 2**). The titer of FA-OH was also higher on glycerol (104.78 mg/L on glycerol vs. 49.97 mg/L on glucose in JMY7086). The rates of the biosynthesis of individual FA-OHs facilitated by *Bluc*FAR1 reductase were different, although the final amounts of FA-OH produced were quite similar, as evidenced by the growth profile (**Table 3**). The JMY7086 strain (*Bluc*FAR1) could produce only saturated fatty alcohols with chain length ranging from C18 to C24. All the FA-OHs were produced in similar final amounts, with C22:0-OH being the most abundant one. When the *BlapFAR4* expression was driven by a stronger promoter *8UAS-pTEF* in the JMY7090 and JMY7094 strains accumulating higher amounts of lipids, an additional unsaturated FA-OH C16:1Δ^9-OH was identified compared to the previous experiment in which only C16:0-OH was produced. The best FA-OH-producing strain was the JMY7086 strain expressing the *BlucFAR1* gene and yielding 9.77 mg/g DCW of FA-OH (104.78 mg/L). JMY7090 (*Blap*FAR4) produced the least amount of FA-OH at 1.04 mg/g DCW (14.6 mg/L). The expected higher FA-OH production in the JMY7094 strain expressing both the reductases could not be achieved as this strain produced only 5.68 mg/g DCW and 65.04 mg/L yield. On the basis of these results, only glycerol was selected for use as the carbon source, while JMY7086 was selected as the FA-OH-producing strain for subsequent experiments.

Fatty Acid Profile

The FA profiles of the new strains and a control strain were compared (**Figure 3**). In all strains, oleic acid was determined as the major FA in the intracellular lipids. The FA analysis clearly demonstrated that the expression of FARs influenced the FA profile. The FAR-expressing yeast strains that produced higher amounts of FA-OHs presented a greater change in the FA profiles. The biggest change was observed for the JMY7086 strain, which accumulated the highest levels of FA-OH among all the strains. With the increasing FA-OH amount, the stearic acid content increased dramatically (8.9% in JMY3501 vs. 27.7% in JMY7086), while the oleic acid content decreased (54.3% in JMY 3501 vs. 35.4% in JMY7086). In addition, the palmitoleic acid level decreased and reached up to 1.9% in JMY7086 vs. 6.7% in JMY3501. When comparing JMY3501 and JMY7086, the ratio

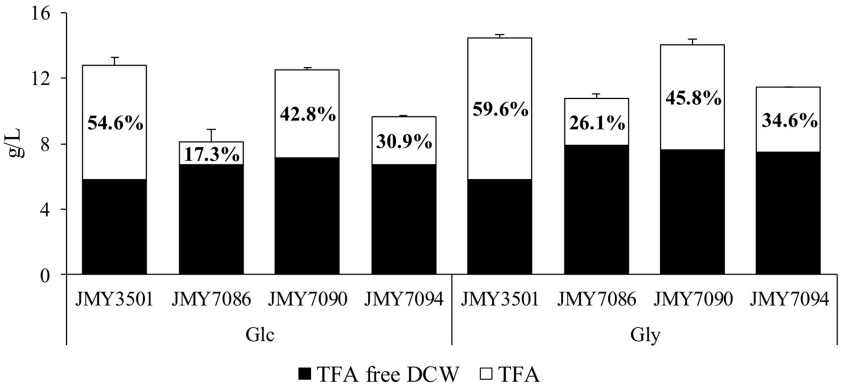

FIGURE 2 | Biomass and lipid accumulation of JMY3501 (control), JMY7086 (*8UAS-pTEF-BlucFAR1*), JMY7090 (*8UAS-pTEF-BlapFAR4*), and JMY7094 (*8UAS-pTEF-BlucFAR1*, *8UAS-pTEF-BlapFAR4*) cultured in two different media. The yeast cells were cultured in a medium with a C/N ratio of 80 and 60 g/L of the carbon substrate. The carbon source was either glucose or glycerol. ■ Lipid free biomass (g/L) and □ total fatty acids, including fatty alcohols (g/L). The number inside the TFA is lipid accumulation, expressed as the TFA to DCW ratio. Each value is an average of the values obtained from three independent experiments.

TABLE 2 | Fatty alcohol production in JMY7086 (*8UAS-pTEF-BlucFAR1*), JMY7090 (*8UAS-pTEF-BlapFAR4*), and JMY7094 (*8UAS-pTEF-BlucFAR1*, *8UAS-pTEF-BlapFAR4*) cultivated for 72 h using different carbon sources.

	JMY7086	JMY7090	JMY7094	JMY7086	JMY7090	JMY7094
	Glucose			Glycerol		
FA-OH (mg/g DCW)						
C16:0-OH	–	0.13	0.53	–	0.68	1.65
C16:1Δ^9-OH	–	0.09	0.18	–	0.36	0.49
C18:0-OH	0.82	–	0.44	2.58	–	0.93
C20:0-OH	0.82	–	0.66	2.09	–	0.78
C22:0-OH	2.02	–	1.56	2.93	–	1.13
C24:0-OH	2.51	–	0.93	2.17	–	0.70
Total	6.17	0.22	4.29	9.77	1.04	5.68
FA-OH (mg/L)						
C16:0-OH	–	1.66	5.09	–	9.61	18.92
C16:1Δ^9-OH	–	1.07	1.74	–	4.99	5.64
C18:0-OH	6.66	–	4.27	27.69	–	10.62
C20:0-OH	6.61	–	6.35	22.38	–	8.96
C22:0-OH	16.33	–	15.05	31.44	–	12.94
C24:0-OH	20.36	–	9.02	23.26	–	7.96
Total	49.97	2.73	41.52	104.78	14.60	65.04

of FAs with chains longer than 20 carbon atoms rose by 2.6-fold for C20:0, 3.4-fold for C22:0, and 2-fold for C24:0. All these changes could be observed in all the FA-OH-producing strains, depending on the amount of FA-OH. The decrease in the palmitic acid level and increase in the linoleic acid level were obvious in JMY7086 and JMY 7094 (both expressing *Bluc*FAR1), while no such dependence was observed in JMY7090 (expressing only *Blap*FAR4).

Daily Production Levels of the Individual Fatty Acids and Fatty Alcohols in the Strain JMY7086

The alcohol-producing JMY7086 strain and the control strain JMY3501 were cultured in the MedA$^+$ medium containing glycerol as a carbon source for 5 days, with sample retrieval every 24 h (**Figure 4**). After the first 24 h, no alcohol was detected in JMY7086, and the cells behaved similar to those in the control. Both the strains produced 7 g/L of DCW, of which a slightly lower FA content was accumulated in JMY7086 (15% in JMY7086 vs. 19% in JMY3501). The residual glycerol in the medium was 46 g/L. After 48 h, alcohol production had begun and differences among the strains could be observed. JMY7086 consumed less glycerol (22 g/L) compared to JMY3501 (25 g/L), the lipid-free biomass was approximately the same as that in the control (JMY3501 7.4 g/L vs. JMY7086 7.8 g/L), the DCW value was lower (JMY3501 12 g/L vs. JMY7086 10 g/L), and the accumulated TFA was less than that of the control strain (37% in JMY3501 vs. 20% in JMY7086). After 72 h, both the strains reached the respective stationary phases, and

TABLE 3 | Kinetics of the individual fatty acids and fatty alcohols in *Y. lipolytica*.

Strain	JMY7086					JMY3501				
Time (days)	**1**	**2**	**3**	**4**	**5**	**1**	**2**	**3**	**4**	**5**
FA	**FA (mg/g DCW)**									
C14:0	0.33	0.32	0.42	0.44	0.45	0.36	0.83	1.10	1.30	1.35
C15:0	0.20	0.18	0.54	0.69	0.83	0.22	0.37	0.80	0.95	1.09
C16:0	26.48	25.90	42.65	45.51	48.83	32.49	81.38	123.88	136.32	139.45
C16:1Δ^9	5.64	4.09	5.19	5.29	5.30	7.46	23.92	40.11	44.46	44.74
C16:0-OH	0.00	0.00	0.00	0.00	0.00	0.00	0.00	0.00	0.00	0.00
C17:0	0.51	0.54	0.62	0.76	0.85	0.67	1.03	3.26	3.65	3.77
C16:1 Δ^9-OH	0.00	0.00	0.00	0.00	0.00	0.00	0.00	0.00	0.00	0.00
C18:0	28.06	50.83	69.34	80.88	81.26	30.13	48.59	53.24	58.55	56.07
C18:1Δ^9	57.62	66.54	93.81	97.81	96.68	65.84	180.29	323.85	347.97	341.47
C18:1Δ^{11}	0.63	0.68	0.80	0.89	0.94	0.75	1.63	2.70	2.96	3.08
C18:2$\Delta^{9,12}$	19.18	19.31	24.04	26.01	30.72	18.01	18.14	27.88	29.69	31.93
C18:0-OH	0.00	0.54	2.12	4.72	1.59	0.00	0.00	0.00	0.00	0.00
C20:0	1.89	4.29	5.67	7.07	6.81	1.79	3.15	5.10	5.35	5.05
C20:0-OH	0.00	0.66	1.92	3.27	1.06	0.00	0.00	0.00	0.00	0.00
C22:0	2.11	5.25	4.60	5.95	5.04	1.83	2.91	3.81	4.13	3.86
C22:0-OH	0.00	1.57	3.05	4.41	2.71	0.00	0.00	0.00	0.00	0.00
C24:0	5.89	13.00	8.55	9.92	8.52	6.10	10.25	10.46	11.65	10.99
C24:0-OH	0.00	2.17	2.31	3.17	0.79	0.00	0.00	0.00	0.00	0.00
TFA	148.55	195.87	265.63	296.78	292.38	165.66	372.50	596.21	646.98	642.86

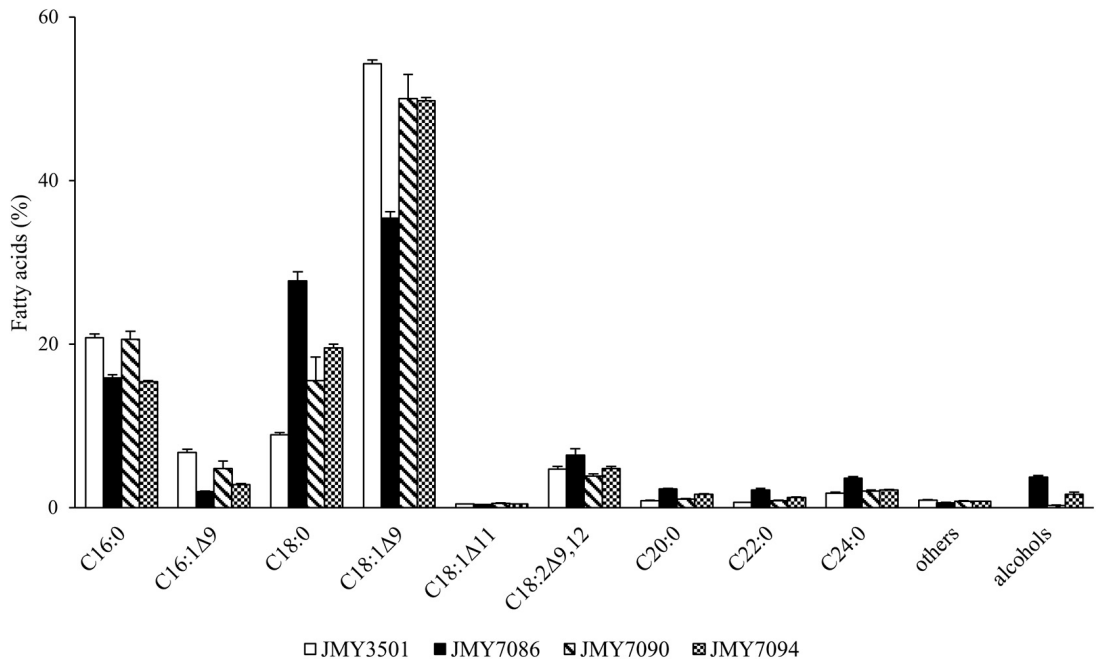

FIGURE 3 | Fatty acid profiles of the strains JMY3501 (control), JMY7086 (*8UAS-pTEF-BlucFAR1*), JMY7090 (*8UAS-pTEF-BlapFAR4*), and JMY7094 (*8UAS-pTEF-BlucFAR1*, *8UAS-pTEF-BlapFAR4*) cultivated on glycerol. The column "others" includes fatty acids C14:0, C15:0, and C17:0. The column "alcohols" presents the total amount of all the alcohols produced together. The values provided are an average of the values obtained in three parallel experiments.

the amount of DCW reached its highest value and remained nearly the same for the next few days. Interestingly, the peak for the lipid-free biomass was observed on the second day in JMY3501, which decreased on the third day and then remained constant in the following days (approx. 5.6 g/L). Meanwhile, the amount of lipid-free biomass in JMY7086 increased to

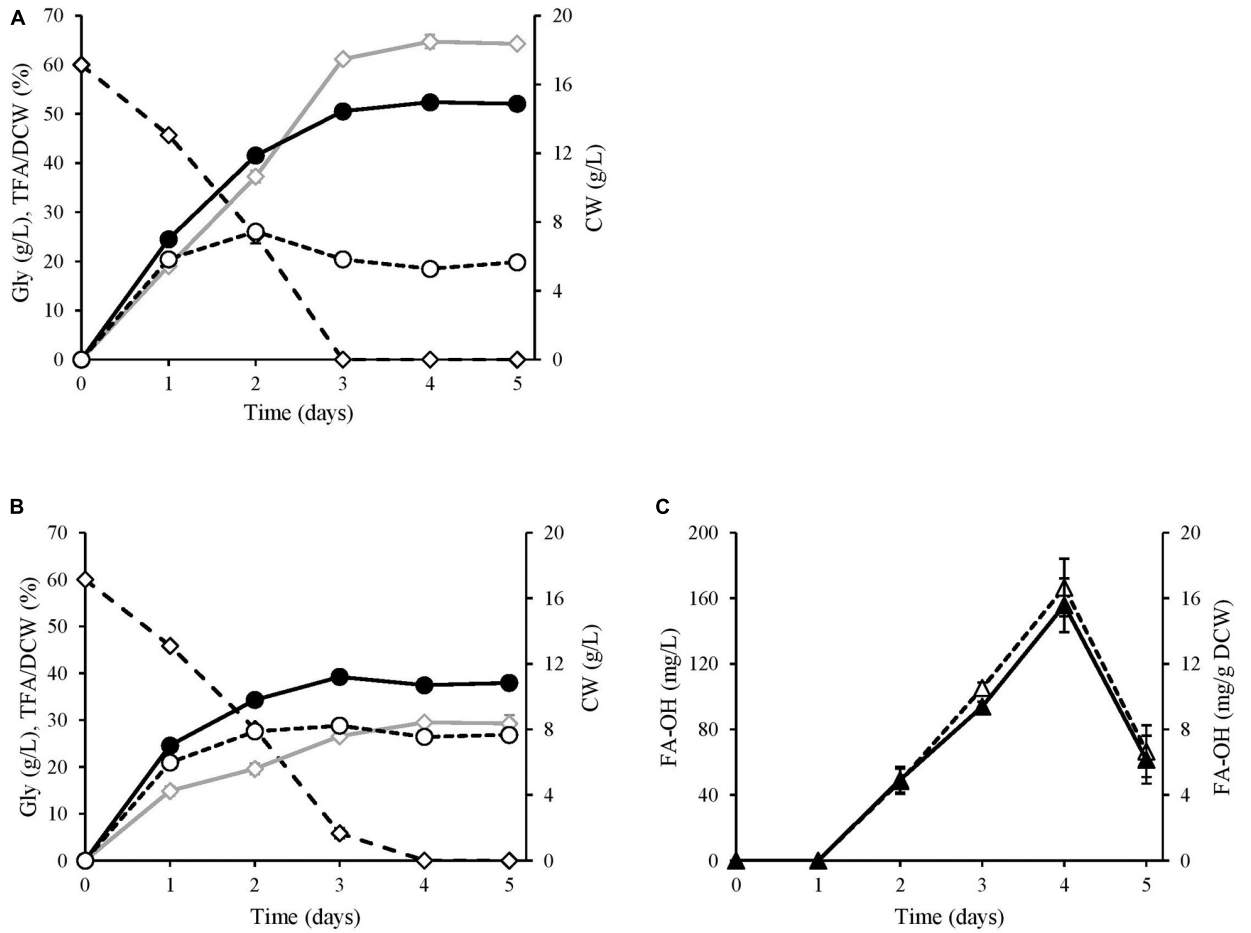

FIGURE 4 | Kinetics of alcohol production. **(A)** JMY3501 (control) and **(B,C)** JMY7086 (*8UAS-pTEF-BlucFAR1*). Both the strains were cultivated for 5 days in a glycerol medium with an initial glycerol concentration of 60 g/L. Gly, kinetics of substrate consumption (◊); CW (cell weight), DCW biomass growth (●), TFA free DCW (○), TFA, total fatty acid accumulation, including that of fatty alcohols (◊), FA-OH, fatty alcohols, mg/g DCW (▲), mg/L (Δ).

8.2 g/L on the third day. At this time, glycerol was completely consumed by JMY3501, while 6 g/L of residual glycerol remained in the medium with JMY7086. The TFA accumulation reached its maximum value 24 h later, i.e., on the fourth day, with the FA-OH-producing strain accumulating less than half of the TFA amount accumulated by the control strain (65 vs. 29%). After the fourth day, no significant change in the lipid content was observed. The peak of FA-OH production was achieved on the 4th day. The yeast cells accumulated 5% FA-OH of TFA, which represented 15.6 mg/g DCW and a 166.6 mg/L titer of alcohols. On the 5th day, the FA-OH content decreased, which occurred most probably due to the depletion of the carbon substrate in the medium. In order to survive, the cells attempted to derive energy from the fat stored inside the lipid bodies. The deletion of the genes encoding lipase (TFL4) and acyl-CoA oxidases (POX1–6) prevented the cells from consuming lipids, although the presence of functional fatty alcohol oxidase (FAO1) and fatty alcohol dehydrogenase (HFD4) continued converting the fatty alcohols into fatty acids.

The effect of fatty alcohols on fatty acid accumulation is best described in **Table 3**. On the first day of cultivation, no huge difference was observed between the two strains. While JMY7086 accumulated slightly fewer FAs, its FA profile was quite similar to the FA profile of JMY3501. On the second day and beyond, the differences between the strains began deepening. JMY3501 began accumulating higher amounts of palmitic acid, palmitoleic acid, and oleic acid, while the increased amounts of palmitic and oleic acids accumulated in JMY7086 were much lower than those in the control. In addition, from the second day onward, JMY7086 did not accumulate palmitoleic acid at all. On the contrary, JMY7086 exhibited an increased amount of accumulated stearic acid, which was higher than that of the control. Although the relative contents of other FAs were different, the absolute amounts did not differ significantly.

DISCUSSION

Fatty alcohol production using microorganisms could reduce the production costs for insect pheromones and render the

TABLE 4 | Comparison of pheromone production between *Y. lipolytica* and *S. cerevisiae* expressing the same genes.

	***Bluc*FAR1**		***Blap*FAR4**	
	JMY7086	***S. cerevisiae***	**JMY7090**	***S. cerevisiae***
	Fatty alcohols (mg/L)			
C16:0-OH	–	0.1	9.61	35
C16:1-OH	–	–	4.99	44
C18:0-OH	50.5	3.3	–	–
C20:0-OH	35.0	1	–	–
C22:0-OH	47.2	1.3	–	–
C24:0-OH	33.9	0.7	–	–
C26:0-OH	–	0.5	–	–

production process environmentally safer (Borodina et al., 2018b; Petkevicius et al., 2020). Although the literature has reported several approaches for producing fatty alcohols using *E. coli* and *S. cerevisiae*, one promising tool is the use of oleaginous microorganisms. So far, among all the oleaginous yeasts, *Y. lipolytica* is the most researched one (Borodina et al., 2018a). Host systems, either bacterial (*E. coli* or cyanobacteria) or yeast (*S. cerevisiae*, *R. toruloides,* or *Y. lipolytica*) that express non-insect enzyme sequences are reported to have reached several grams of fatty alcohols per liter of cultivation medium after optimization (Tupec et al., 2017). A fatty alcohol titer of 6.33 g/L was achieved in fed-batch fermentation in *E. coli via* the deletion of all fatty acyl-CoA thioestarases and *ldhA*, *pta*, and *ackA* genes, to starve cells of fatty acids and remove competing pathways (Liu et al., 2016). The expression of *Tyto alba* FAR (TaFAR1) in *Y. lipolytica* resulted in the production of 690 mg/L of hexadecan-1-ol (Wang G. et al., 2016), while the *Y. lipolytica* transformed with the *MhFAR* gene encoding the reductase from *Marinobacter hydrocarbonoclasticus* produced 6 g/L of alcohols representing an accumulation of 36 mg alcohols/g of cells (Cordova et al., 2019). The same reductase stimulated the production of 770 mg/L of fatty alcohols in *L. starkeyi* (Wang W. et al., 2016) and 8 g/L of fatty alcohols in *Rhodosporidium toruloides* (Fillet et al., 2015). Since the pheromone blends often contain unusual components, it is an advantage to use insect fatty acyl biosynthetic enzymes for their production.

In the present work, *Y. lipolytica* strains were engineered to have different genetic backgrounds with genes encoding reductases from *Bombus lucorum* (*BlucFAR1*) and *Bombus lapidarius* (*BlapFAR4*). When these genes were introduced into the Po1d strain under the control of the *pTEF* promoter, alcohols were detected only in trace amounts (in strains JMY6697 and JMY6698). Therefore, the second strategy was adopted, which involved redesigning the strain JMY3820, which had all the six *POX* genes and *TGL4* lipase deleted and the *DGA2* and *GPD1* overexpressed using the *pTEF* promoter, with the incorporation of *FAR* genes driven by a stronger promoter *8UAS-pTEF*. This genotype is particularly effective in accumulating high amounts of lipids (Dulermo et al., 2015). Deletions of *POX* genes and *TGL4* gene prevents degradation of storage lipids and oxidation of fatty acids. On the other hand, overexpression of the *DGA2* and *GPD1* drives the formation of the TAGs and incorporation of fatty acids into the TAGs. The premise was to implement the push and pull strategy (Tai and Stephanopoulos, 2013), with the higher lipid production as the driving force for the higher fatty acid synthesis. With the higher fatty acyl-CoA pool, more fatty acyl-CoAs can be redirected to the reduction by FARs. As the cells become more saturated with TAGs, more fatty acyl-CoA becomes available as a substrate for reductases. This strategy produced three new strains: JMY7086 (*8UAS-pTEF-BlucFAR1*), JMY7090 (*8UAS-pTEF-BlapFAR4*), and JMY7094 (*8UAS-pTEF-BlucFAR1*, *8UAS-pTEF-BlapFAR4*). A co-expression of both the reductases (JMY7094) did not meet the expectations. It might have affected the FA profiles or reduced the activity of the elongases (**Figure 3**). This could have led to limited availability of the substrate and ultimately a lower yield of alcohols. For instance, co-expression of *Bluc*FAR1 and *Blap*FAR4 resulted in a higher level of C16:0-OH and C16:1Δ^9-OH and a decreased level of longer FA-OHs (**Table 2**). Another explanation could be as a consequence of an increased degree of FA-OH degradation. **Table 3** presents the degradation of long-chain fatty alcohol between Day 4 and Day 5, which might have been induced by the presence of C16 fatty alcohols, which would also explain the lower level of total FA-OHs in JMY7090. It may also be interpreted by the level of *Bluc*FAR1 expression, possibly due to the integration site of *Bluc*FAR1 in the double mutant or titration of the *pTEF* promoter. All of the results did not indicate alcohol toxicity on the cells and rather indicated the inhibition of FA formation and lipid accumulation by the alcohols or the by-products of their metabolism. It is also possible that in addition to being affected by the total FA-OH amount, the FA profile is affected by the FA-OH composition as well. For example, **Figure 3** clearly shows that the JMY7086 strain produces more long chain fatty acids (>C18). Indirectly, this tells us that the production of long-chain fatty alcohols may well be driving the elongation of fatty acids - the so-called metabolic driving force. This also corresponds to the push and pull strategy described by Tai and Stephanopoulos (2013). If FAR is taking substrates (long-chain fatty acyl-CoAs) from lipid metabolism, the cells are overcompensating by producing more long-chain fatty acyl-CoAs. Although the metabolic engineering of the selected *Y. lipolytica* strains enabled the production of the desired FA-OHs, there is scope for further improvement. A combination of lipid metabolism manipulation in *Y. lipolytica* and engineering of the FA-OH metabolism could produce higher amounts of specific FA-OHs synthesized by a particular FAR in low concentrations. It is well recognized that in certain cases, *Y. lipolytica* secretes fatty acids and fatty alcohols into the medium, which increases the production while simplifying the purification. Most often, this occurs spontaneously when the cells accumulate high amounts of toxic products that they are unable to degrade. The excretion of fatty alcohols may also be achieved by optimizing the fermentation process. The deletion of *FAO1* (fatty alcohol oxidase) and *HFD4* (fatty alcohol dehydrogenase) could prevent product degradation by the cells (Dahlin et al., 2019; Holkenbrink et al., 2020). Another approach is to manipulate the *FAA1* gene

(fatty acyl-CoA synthetase) or the lipases to increase the substrate availability for the functioning of FARs, or to use dodecane-mediated extraction fermentation for the secretion of alcohols into the medium (Cordova et al., 2019).

In a previous study, the FARs used in the present work were expressed in *Saccharomyces cerevisiae* (Tupec et al., 2019), and several discrepancies were observed between the composition of FA-OH synthesized by the FARs in labial gland of bumblebee and in the *S. cerevisiae* expression system. The reductase *Blap*FAR4 produced poly-unsaturated fatty alcohols in the yeast cells, which are not present in the labial gland of male *B. lapidarius*. It is possible that a pool of fatty acyl CoA precursors in the yeasts differs from those present in the labial gland. The concentrations of C18:1Δ^9-CoA, C18:2$\Delta^{9,12}$-CoA, and C18:3$\Delta^{9,12,15}$-CoA in the labial gland of *B. lapidarius* might be extremely low, to the extent that detectable accumulation of the corresponding alcohols is not possible. This implies that the ratio of fatty alcohols in the pheromones is dependent not only on the FAR substrate specificity, rather also on substrate availability, which is affected greatly by the other mechanisms such as the conversion of fatty acyls into fatty acyl-CoAs, fatty acyl-CoAs hydrolysis, etc. The differences in the quantity and ratio of fatty alcohols between *Y. lipolytica* and *S. cerevisiae* (**Table 4**) most likely reflects the differences in metabolism of these species. While *Y. lipolytica* is considered as oleaginous yeast, *S. cerevisiae* do not accumulate significant quantities of lipids. FA composition of lipids of these two yeast species is also different. While *Y. lipolytica* naturally prefers to accumulate the FAs with a chain length of 18 carbon atoms, *S. cerevisiae* prefers 16 carbon atom-long FAs. It could, therefore, be assumed that this difference in the accumulation of FAs was reflected in the fatty acyl-CoA pool as well. Since the fatty acyl-CoA pool is the source of substrates for FAR, a higher quantity of either 16 or 18 carbon long FA could influence the quantity and quality of FA-OHs. While the enzyme *Bluc*FAR1 produced the highest FA-OH content in *Y. lipolytic*a (166.6 mg/L), the same enzyme produced only a small amount of FA-OH in *S. cerevisiae* (6.9 mg/L). On the contrary, *Blap*FAR4 worked much better in *S. cerevisiae* (79 mg/L) than in *Y. lipolytica* (14.6 mg/L). Therefore, variations in yields could be attributed to the difference in the substrate availability between *Y. lipolytica* and *S. cerevisiae*. However, the expression level of the enzymes and in particular their activities also might have an effect on the synthesis of FA-OH.

Taken together, the results of the present work demonstrated that bioengineered *Y. lipolytica* strain with deleted *POX* and *TGL4* lipase genes and overexpressed *DGA2* and *GPD1* genes is suitable for the efficient production of FA-OHs with different chain lengths. To our knowledge, this is the first study showing the ability of *Y. lipolytica* to produce FA-OHs of different lengths and the first study achieving production of FA-OHs longer than 20 carbons by *Y. lipolytica*.

DATA AVAILABILITY STATEMENT

The raw data supporting the conclusions of this article will be made available by the authors, without undue reservation.

AUTHOR CONTRIBUTIONS

IP, RL-A, J-MN, and MC defined the concept of the study. MT isolated the genes. IP provided the gene sequences. RL-A designed and prepared the constructs. PG and JH designed and performed the cultivation experiments and performed the GC MS analyses. JH prepared the manuscript. IP, MT, RL-A, J-MN, MC, and PG revised the manuscript. All authors contributed to the article and approved the submitted version.

FUNDING

The work was supported by grant (APVV–17–0262) from the Slovak Research and Development Agency, Slovak Republic.

ACKNOWLEDGMENTS

We thank Tatiana Klempová for valuable comments and Aleš Buček for discussion.

SUPPLEMENTARY MATERIAL

The Supplementary Material for this article can be found online at: https://www.frontiersin.org/articles/10.3389/fbioe.2020.593419/full#supplementary-material

REFERENCES

Abdel-Mawgoud, A. M., Markham, K. A., Palmer, C. M., Liu, N., Stephanopoulos, G., and Alper, H. S. (2018). Metabolic engineering in the host *Yarrowia lipolytica*. *Metab. Eng.* 50, 192–208. doi: 10.1016/j.ymben.2018.07.016

Antony, B., Ding, B. J., Moto, K., Aldosari, S. A., and Aldawood, A. S. (2016). Two fatty acyl reductases involved in moth pheromone biosynthesis. *Sci. Rep.* 6:29927. doi: 10.1038/srep29927

Ayasse, M., and Jarau, S. (2014). Chemical ecology of bumble bees. *Ann. Rev. Entomol.* 59, 299–319. doi: 10.1146/annurev-ento-011613-161949

Barth, G., and Gaillardin, C. (1996). "*Yarrowia lipolytica*," in *Nonconventional Yeasts in Biotechnology*, ed. K. Wolf, (Berlin: Springer), 313–388.

Beopoulos, A., Mrozova, Z., Thevenieau, F., Le Dall, M. Z., Hapala, I., Papanikolaou, S., et al. (2008). Control of lipid accumulation in the yeast *Yarrowia lipolytica*. *Appl. Environ. Microbiol.* 74:24. doi: 10.1128/AEM.01412-08

Borodina, I., Holkenbrink, C., Dam, M. I., and Löfstedt, C. (2018a). *Methods for Producing Fatty Alcohols and Derivatives Thereof in Yeast*. Patent No WO2018109163. Geneva: World Intellectual Property Organization.

Borodina, I., Holkenbrink, C., Dam, M. I., Löfstedt, C., Ding, B., and Wang, H. (2018b). *Production of Desaturated Fatty Alcohols and Desaturated Fatty*

Acyl Acetates in Yeast. Patent No WO2018109167. Geneva: World Intellectual Property Organization.

Buček, A., Brabcová, J., Vogel, H., Prchalová, D., Kindl, J., Valterová, I., et al. (2016). Exploring complex pheromone biosynthetic processes in the bumblebee male labial gland by RNA sequencing. *Insect Mol. Biol.* 25, 295–314. doi: 10.1111/imb.12221

Buček, A., Vogel, H., Matoušková, P., Prchalová, D., Žáèek, P., Vrkoslav, V., et al. (2013). The role of desaturases in the biosynthesis of marking pheromones in bumblebee males. *Insect biochemistry and molecular biology* 43, 724–731. doi: 10.1016/j.ibmb.2013.05.003

Butenandt, A., Beckmann, R., and Hecker, E. (1961). Über den sexuallockstoff des seidenspinners, I. Der biologische test und die isolierung des reinen sexuallockstoffes bombykol. *Biol. Chem.* 324, 71–83. doi: 10.1515/bchm2.1961.324.1.71

Cordova, L. T., Butler, J., and Alper, H. S. (2019). Direct production of fatty alcohols from glucose using engineered strains of *Yarrowia lipolytica*. *Metab. Eng. Commun.* 10:e00105. doi: 10.1016/j.mec.2019.e00105

Dahlin, J., Holkenbrink, C., Marella, E. R., Wang, G., Liebal, U., Lieven, C., et al. (2019). Multi-omics analysis of fatty alcohol production in engineered yeasts *Saccharomyces cerevisiae* and *Yarrowia lipolytica*. *Front. Genet.* 10:747. doi: 10.3389/fgene.2019.00747

Ding, B. J., Lager, I., Bansal, S., Durrett, T. P., Stymne, S., and Löfstedt, C. (2016). The yeast ATF1 acetyltransferase efficiently acetylates insect pheromone alcohols: implications for the biological production of moth pheromones. *Lipids* 51, 469–475. doi: 10.1007/s11745-016-4122-4

Dulermo, R., Brunel, F., Dulermo, T., Ledesma-Amaro, R., Vion, J., Trassaert, M., et al. (2017). Using a vector pool containing variable-strength promoters to optimize protein production in *Yarrowia lipolytica*. *Microb. Cell Fact.* 16:31.

Dulermo, T., Lazar, Z., Dulermo, R., Rakicka, M., Haddouche, R., and Nicaud, J.-M. (2015). Analysis of ATP-citrate lyase and malic enzyme mutants of *Yarrowia lipolytica* points out the importance of mannitol metabolism in fatty acid synthesis. *Biochim. Biophys. Acta* 1851, 1107–1117. doi: 10.1016/j.bbalip.2015.04.007

Eirín-López, J. M., Rebordinos, L., Rooney, A. P., and Rozas, J. (2012). The birth-and-death evolution of multigene families revisited. *Genome Dynamics* 7, 170–196. doi: 10.1159/000337119

El-Sayed, A. M. (2019). *The Pherobase: Database of Pheromones and Semiochemicals*. Available online at: http://www.pherobase.com (accessed October 20, 2020).

Fillet, S., Gibert, J., Suárez, B., Lara, A., Ronchel, C., and Adrio, J. L. (2015). Fatty alcohols production by oleaginous yeast. *J. Indust. Microbiol. Biotechnol.* 42, 1463–1472. doi: 10.1007/s10295-015-1674-x

Groenewald, M., Boekhout, T., Neuvéglise, C., Gaillardin, C., van Dijck, P. W., and Wyss, M. (2014). *Yarrowia lipolytica*: safety assessment of an oleaginous yeast with a great industrial potential. *Crit. Rev. Microbiol.* 40, 187–206. doi: 10.3109/1040841X.2013.770386

Groot, A. T., Dekker, T., and Heckel, D. G. (2016). The genetic basis of pheromone evolution in moths. *Annu. Rev. Entomol.* 61, 99–117. doi: 10.1146/annurev-ento-010715-023638

Guo, W., Sheng, J., Zhao, H., and Feng, X. (2016). Metabolic engineering of *Saccharomyces cerevisiae* to produce 1-hexadecanol from xylose. *Microb. Cell Fact.* 15:24. doi: 10.1186/s12934-016-0423-9

Hagström, ÅK., Wang, H. L., Liénard, M. A., Lassance, J. M., Johansson, T., and Löfstedt, C. (2013). A moth pheromone brewery: production of (*Z*)-11-hexadecenol by heterologous co-expression of two biosynthetic genes from a noctuid moth in a yeast cell factory. *Microb. Cell Fact.* 12:125. doi: 10.1186/1475-2859-12-125

Holdsworth, J. E., Veenhuis, M., and Ratledge, C. (1988). Enzyme activities in oleaginous yeasts accumulating and utilizing exogenous or endogenous lipids. *J. Gen. Microbiol.* 1988, 2907–2915. doi: 10.1099/00221287-134-11-2907

Holkenbrink, C., Ding, B.-J., Wang, H.-L., Dam, M. I., Petkevicius, K., Kildegaard, K., et al. (2020). Production of moth sex pheromones for pest control by yeast fermentation. *Metab. Eng.* 62, 312–321. doi: 10.1101/2020.07.15.205047

Jurenka, R. (2004). Insect pheromone biosynthesis. *Top. Curr. Chem.* 239, 97–132. doi: 10.1007/b95450

Koutroumpa, F. A., and Jacquin-Joly, E. (2014). Sex in the night: fatty acid-derived sex pheromones and corresponding membrane pheromone receptors in insects. *Biochimie* 107, 15–21. doi: 10.1016/j.biochi.2014.07.018

Lazar, Z., Dulermo, T., Neuvéglise, C., Crutz-Le Coq, A. M., and Nicaud, J. M. (2014). Hexokinase—A limiting factor in lipid production from fructose in *Yarrowia lipolytica*. *Metab. Eng.* 26, 89–99. doi: 10.1016/j.ymben.2014.09.008

Lazar, Z., Rossignol, T., Verbeke, J., Crutz-Le Coq, A. M., Nicaud, J.-M., Robak, M. (2013). Optimized invertase expression and secretion cassette for improving *Yarrowia lipolytica* growth on sucrose for industrial applications. *J. Ind. Microbiol. Biotechnol.* 40, 1273–1283. doi: 10.1007/s10295-013-1323-1

Lazar, Z., Walczak, E., and Robak, M. (2011). Simultaneous production of citric acid and invertase by *Yarrowia lipolytica* SUC+ transformants. *Bioresour. Technol.* 102, 6982–6989. doi: 10.1016/j.biortech.2011.04.032

Le Dall, M.-T., Nicaud, J.-M., Gaillardin, C. (1994). Multi-copy integration in the yeast Yarrowia lipolytica. *Curr. Genet.* 26, 38–44. doi: 10.1007/BF00326302

Ledesma-Amaro, R., and Nicaud, J.-M. (2016). *Yarrowia lipolytica* as a biotechnological chassis to produce usual and unusual fatty acids. *Prog. Lipid Res.* 61, 40–50. doi: 10.1016/j.plipres.2015.12.001

Liénard, M. A., Hagström, ÅK., Lassance, J.-M., and Löfstedt, C. (2010). Evolution of multi-component pheromone signals in small ermine moths involves a single fatty-acyl reductase gene. *Proc. Natl. Acad. Sci. U.S.A.* 107, 10955–10960. doi: 10.1073/pnas.1000823107

Liu, Y., Chen, S., Chen, J., Zhou, J., Wang, Y., Yang, M., et al. (2016). High production of fatty alcohols in *Escherichia coli* with fatty acid starvation. *Microb. Cell Fact.* 15:129. doi: 10.1186/s12934-016-0524-5

Matoušková, P., Luxová, A., Matoušková, J., Jiroš, P., Svatoš, A., Valterová, I., et al. (2008). A delta(9) desaturase from *Bombus lucorum* males: investigation of the biosynthetic pathway of marking pheromones. *Chembiochem* 9, 2534–2541. doi: 10.1002/cbic.200800374

Matsumoto, S. (2010). Molecular mechanisms underlying sex pheromone production in moths. *Biosci. Biotechnol. Biochem.* 74, 223–231. doi: 10.1271/bbb.90756

McNaught, A. D., and Wilkinson, A. (1997). *IUPAC. Compendium of Chemical Terminology*, 2 Edn. Oxford: Blackwell Scientific Publications. doi: 10.1351/goldbook

Miller, K. K., and Alper, H. S. (2019). *Yarrowia lipolytica*: more than an oleaginous workhorse. *Appl. Microbiol. Biotechnol.* 103, 9251–9262. doi: 10.1007/s00253-019-10200-x

Mitchell, E. R., and McLaughlin, J. R. (1982). Suppression of mating and oviposition by fall armyworm and mating by corn earworm in corn, using the air permeation technique. *J. Econom. Entomol.* 75, 270–274. doi: 10.1093/jee/75.2.270

Moto, K., Suzuki, M. G., Hull, J. J., Kurata, R., Takahashi, S., Yamamoto, M., et al. (2004). Involvement of a bifunctional fatty-acyl desaturase in the biosynthesis of the silkmoth, *Bombyx mori*, sex pheromone. *Proc. Natl. Acad. Sci. U.S.A.* 101, 8631–8636. doi: 10.1073/PNAS.0402056101

Moto, K., Yoshiga, T., Yamamoto, M., Takahashi, S., Okano, K., Ando, T., et al. (2003). Pheromone gland-specific fatty-acyl reductase of the silkmoth, *Bombyx mori*. *Proc. Natl. Acad. Sci. U.S.A.* 100, 9156–9161. doi: 10.1073/pnas.1531993100

Petkevicius, K., Löfstedt, C. h, and Borodina, I. (2020). Insect sex pheromone production in yeasts and plants. *Curr. Onin. Biotechnol.* 65, 259–267. doi: 10.1016/j.copbio.2020.07.011

Querol, A., Barrio, E., Ramon, D. (1992). A comparative study of different methods of yeast strain characterization. *Syst. Appl. Microbiol.* 15, 439–446. doi: 10.1016/S0723-2020(11)80219-5

Rutter, C. D., and Rao, C. V. (2016). Production of 1-decanol by metabolically engineered *Yarrowia lipolytica*. *Metab. Eng.* 38, 139–147. doi: 10.1016/j.ymben.2016.07.011

Sambrook, J., and Russell, D. W. (2001). *Molecular Cloning: A Laboratorymanual*, 3 Edn. Cold Spring Harbor, NY: Cold Spring Harbor Laboratory Press.

Shah, J., Arslan, E., Cirucci, J., O'Brien, J., and Moss, D. (2016). Comparison of oleo− *vs* petro−sourcing of fatty alcohols via cradle−to−gate life cycle assessment. *J. Surfact. Deterg.* 19, 1333–1351. doi: 10.1007/s11743-016-1867-y

Tai, M., and Stephanopoulos, G. (2013). Engineering the push and pull of lipid biosynthesis in oleaginous yeast *Yarrowia lipolytica* for biofuel production. *Metab. Eng.* 15, 1–9. doi: 10.1016/j.ymben.2012.08.007

Tillman, J. A., Seybold, S. J., Jurenka, R. A., and Blomquist, G. J. (1999). Insect pheromones—an overview of biosynthesis and endocrine regulation. *Insect Biochem. Mol. Biol.* 29, 481–514. doi: 10.1016/s0965-1748(99)00016-8

Tittiger, C., and Blomquist, G. J. (2017). Pheromone biosynthesis in bark beetles. *Curr. Opin. Insect Sci.* 24, 68–74. doi: 10.1016/j.cois.2017.09.005

Tupec, M., Buček, A., Janoušek, V., Vogel, H., Prchalová, D., Kindl, J., et al. (2019). Expansion of the fatty acyl reductase gene family shaped pheromone communication in Hymenoptera. *eLife* 8:e39231. doi: 10.7554/eLife.39231

Tupec, M., Buček, A., Valterová, I., and Pichová, I. (2017). Biotechnological potential of insect fatty acid-modifying enzymes. *Zeitschr. Naturfors. C* 72, 387–403. doi: 10.1515/znc-2017-0031

Wang, G., Xiong, X., Ghogare, R., Wang, P., Meng, Y., and Chen, S. (2016). Exploring fatty alcohol-producing capability of Yarrowia lipolytica. *Biotechnol. Biof.* 9:107. doi: 10.1186/s13068-016-0512-3

Wang, W., Wei, H., Knoshaug, E., Van Wychen, S., Xu, Q., Himmel, M. E., et al. (2016). Fatty alcohol production in *Lipomyces starkeyi* and *Yarrowia lipolytica*. *Biotechnol. Biof.* 9:227. doi: 10.1186/s13068-016-0647-2

Žáček, P., Prchalová-Horòáková, D., Tykva, R., Kindl, J., Vogel, H., Svatoš, A., et al. (2013). De novo biosynthesis of sexual pheromone in the labial gland of bumblebee males. *Chembiochem* 14, 361–371. doi: 10.1002/cbic.201200684

Conflict of Interest: The authors declare that the research was conducted in the absence of any commercial or financial relationships that could be construed as a potential conflict of interest.

frontiers in Bioengineering and Biotechnology

MINI REVIEW
published: 09 February 2021
doi: 10.3389/fbioe.2021.606795

Successful Enzyme Colocalization Strategies in Yeast for Increased Synthesis of Non-native Products

*Hannah C. Yocum†, Anhuy Pham† and Nancy A. Da Silva**

Department of Chemical and Biomolecular Engineering, University of California, Irvine, CA, United States

Yeast cell factories, particularly *Saccharomyces cerevisiae*, have proven valuable for the synthesis of non-native compounds, ranging from commodity chemicals to complex natural products. One significant challenge has been ensuring sufficient carbon flux to the desired product. Traditionally, this has been addressed by strategies involving "pushing" and "pulling" the carbon flux toward the products by overexpression while "blocking" competing pathways via downregulation or gene deletion. Colocalization of enzymes is an alternate and complementary metabolic engineering strategy to control flux and increase pathway efficiency toward the synthesis of non-native products. Spatially controlling the pathway enzymes of interest, and thus positioning them in close proximity, increases the likelihood of reaction along that pathway. This mini-review focuses on the recent developments and applications of colocalization strategies, including enzyme scaffolding, construction of synthetic organelles, and organelle targeting, in both *S. cerevisiae* and non-conventional yeast hosts. Challenges with these techniques and future directions will also be discussed.

Keywords: enzyme colocalization, organelle targeting, enzyme scaffolds, yeast, *Saccharomyces cerevisiae*

OPEN ACCESS

Edited by:
Mark Blenner,
University of Delaware, United States

Reviewed by:
Jiazhang Lian,
Zhejiang University, China
Mingfeng Cao,
University of Illinois at Urbana-Champaign, United States

***Correspondence:**
Nancy A. Da Silva
ndasilva@uci.edu

†These authors have contributed equally to this work

Specialty section:
This article was submitted to Synthetic Biology, a section of the journal Frontiers in Bioengineering and Biotechnology

Received: *15 September 2020*
Accepted: *11 January 2021*
Published: *09 February 2021*

Citation:
Yocum HC, Pham A and Da Silva NA (2021) Successful Enzyme Colocalization Strategies in Yeast for Increased Synthesis of Non-native Products. Front. Bioeng. Biotechnol. 9:606795. doi: 10.3389/fbioe.2021.606795

INTRODUCTION

A main goal of metabolic engineering is to increase production of non-native products built from native precursors. Traditionally, this has been done by "pushing" or "pulling" the carbon flux toward the product-producing pathway by overexpression of pathway enzymes or by deletion of competing pathways (Ostergaard et al., 2000). Recently, many novel molecular engineering tools and synthetic biology strategies have been successfully employed to improve the production of desired compounds in microbial cell factories (Lian et al., 2018; Liu and Nielsen, 2019; Guirimand et al., 2020; Xu et al., 2020). This review focuses on the latest successful attempts to localize the metabolic pathway enzymes in close proximity for redirection of flux through the pathway of interest and, subsequently, increase synthesis of the products in *Saccharomyces cerevisiae* and other yeast species. The methods include enzyme fusion, enzyme scaffolding, organelle targeting, and construction of synthetic organelles (**Figure 1**).

ENZYME FUSIONS

Construction of synthetic fusion proteins is perhaps the most obvious strategy to enhance the substrate channeling effect in metabolic engineering. By physically fusing successive enzymes in the production pathway together, substrates can be localized in the same vicinity. However, despite the straightforward nature of the approach, fusion proteins are not always successful in improving

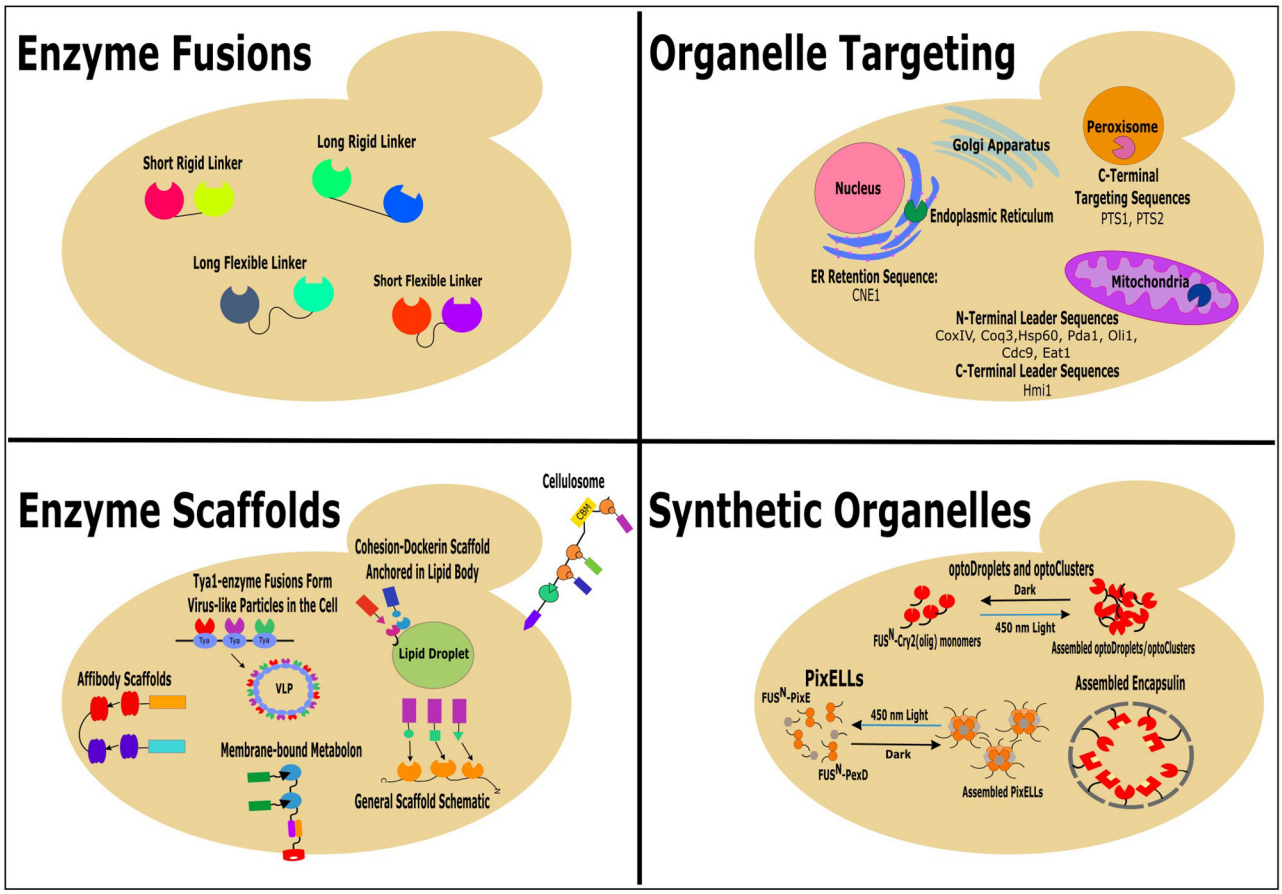

FIGURE 1 | Successful colocalization strategies: enzyme fusions, enzyme scaffolds, organelle targeting, and synthetic organelles, for increasing the production of non-native products in yeast.

final product titer, as fusion can lower the enzymatic activities or hinder the folding processes (Jia et al., 2014). Therefore, optimization of the fusion protein construct is often needed.

One critical factor in designing a multi-enzyme complex is the choice of linker. Albertsen et al. (2011) demonstrated the effect of different linkers on the production of patchoulol for a two-enzyme fusion of farnesyl diphosphate synthase (FPPS) and patchoulol synthase (PTS). A short flexible linker (GSG) resulted in the highest titer (9.5 mg/L, representing a 2-fold increase over the free enzyme system) whereas a very long linker (the entire CFP protein sequence) resulted in the lowest titer (one third of that with the flexible linker). This study showed a decrease in patchoulol titer as the length of the linker increased; however, since the optimal linker is often dependent on the specific protein, this finding may not translate to other proteins. A comprehensive review of different linkers and their properties (such as length and structural integrity) can be found in Chen et al. (2013).

Interestingly, the order in which the enzymes are fused may also affect the performance of the fusion protein complex. By fusing *Petroselinum crispum* coumarate-CoA ligase (Pc4CL) and *Rheum palmatum* benzalacetone synthase (RpBAS) using either a flexible (VDGGSGR) or rigid (VDEAAAKSGR) linker, Lee et al. (2016) achieved a 6.5-fold improvement in raspberry ketone titer relative to the free enzymes. However, this improvement was only observed with the orientation Pc4CL-RpBAS and not with RpBAS-Pc4CL; for the latter, the final titer was similar to that obtained when expressing free enzymes. Similar findings were also reported in Hu et al. (2017) for the synthesis of germacrene A when fusing the farnesyl diphosphate synthase (*ERG20*) and a *Lactuca sativa* germacrene A synthase ($LTC2_{opt}$) with two different flexible linkers, GSG and GGGGS. No significant differences were observed for the linkers used and both protein orientations resulted in higher germacrene A production relative to free enzymes. However, the *ERG20-*$LTC2_{opt}$ configuration resulted in 97.7 mg/L germacrene A production compared to approximately 60 mg/L for the $LTC2_{opt}$*-ERG20* configuration.

Recently, Rabeharindranto et al. (2019) reconfirmed the importance of both linkers and domain order when constructing a synthetic fusion protein for carotenoid synthesis. A tri-domain enzyme containing the full β-carotene synthesis pathway (CrtY, CrtB, and CrtI) was constructed using different domain orders and linkers. The best tri-domain enzyme [CrtY linked with CrtB by their natural 27 residue linkers and CrtB linked with

CrtI by an $(EAAAK)_4$ linker] resulted in a 2-fold increase in β-carotene production relative to the native system. Another successful three-enzyme fusion protein in *S. cerevisiae* was a trifunctional cellulase complex, with each enzyme connected by the flexible $GGGGS_3$ linker (Liu et al., 2018). This fusion protein had a 46, 6.7, and 46% increase in β-glucosidase, exoglucanase, and endoglucanase activity, respectively, when compared to individual free enzymes.

ENZYME SCAFFOLDS

Protein scaffolds, where specific enzymes are recruited onto synthetic constructs, have been used to localize desired biosynthetic pathway enzymes to improve product formation via substrate channeling. Dueber et al. (2009) successfully demonstrated the use of synthetic scaffolds comprised of metazoan protein-protein interaction domains and ligands in *Escherichia coli*, increasing mevalonate production 77-fold. There were concerns about the efficiency of this approach for *S. cerevisiae*, since native proteins may interact with the scaffold domains (Siddiqui et al., 2012). However, the metazoan synthetic scaffold improved the production of resveratrol in *S. cerevisiae* by 5-fold relative to the non-scaffold system and by 2.7-fold relative to a protein fusion strategy (Zhang et al., 2006; Wang and Yu, 2012). Nonetheless, optimization of the system was still important; depending on the stoichiometry of the SH3 and pDZ domains in the protein scaffold, the increase in resveratrol production varied from 1.2 to 5-fold over the control.

Another successful synthetic scaffold in *S. cerevisiae* is based on the cohesin and dockerin-enzyme interaction found in the surface cellulosomes of *Clostridium cellulovorans* and other microorganisms (Mechaly et al., 2001). Engineered cellusome-like complexes localizing cellulases have been successfully expressed on the surface of *S. cerevisiae* to improve ethanol production (Fan et al., 2012; Tsai et al., 2013; Tang et al., 2018). Recently, the "largest cellulolytic complex" was successfully constructed on the surface of the yeast *Kluyveromyces marxianus* (Anandharaj et al., 2020). However, utilization of the dockerin-cohesin interaction as an intracellular metabolic scaffold in yeast has been limited. Kim and Hahn (2014) took advantage of the high binding affinity between cohesion and dockerin (Kd $<10^{-11}$ M) (Stahl et al., 2012) to create a substrate channeling module in the cytosol of *S. cerevisiae*. Increasing numbers (2, 3, or 7) of cohesin domains were included on the scaffold and the C terminal dockerin fusion proteins of heterologous AlsS, AlsD, and endogenous Bdh1 proteins were overexpressed. 2,3-Butanediol production increased by 37% compared to the scaffold-free system in fed-batch fermentation with occasional glucose feeding; although the increase was limited, this was the first study to utilize the interaction between cohesin and dockerin in the yeast cytosol and for metabolic engineering. In a follow-up study (Kim et al., 2016), this synthetic substrate channeling strategy was used to redirect carbon flux from pyruvate to 2,3-butanediol using a heterologous AlsS or to lactate using heterologous LdhA, rather than to ethanol. The native Pyk1 (for pyruvate synthesis) was fused to a cohesin domain and AlsS to a dockerin domain colocalizing the two enzymes, resulting in a 38% increase in 2,3-butanediol production and a 46% decrease in ethanol production compared to the native strain. However, this strategy was unsuccessful in redirecting the flux toward lactate formation; the dockerin-fused LdhA had a >2-fold lower specific activity relative to wildtype LdhA (11.6 and 27.9 U/nmol, respectively). As discussed in the previous section, the reduction of enzymatic activity presents a significant challenge to fusion-based colocalization strategies.

The dockerin-cohesin interaction was also utilized to colocalize the ethyl acetate biosynthesis enzymes onto the surface of lipid droplets (thus combining both scaffolding and organelle targeting strategies), resulting in 2-fold increase in the production rate (Lin et al., 2017). In *S. cerevisiae*, ethyl acetate is synthesized by the enzymes Ald6, Acs1, and Atf1, with only Atf1 targeted to the lipid droplets. To target Ald6 and Acs1, the authors screened and identified the protein oleosin as a promising candidate to direct enzymes of interest to the lipid droplets. Cohesin domains were fused to the oleosin proteins while the corresponding dockerin domains were fused to Ald6 and Acs1. After an extensive screening of promoters and scaffold optimization, the ethyl acetate specific titer increased 1.7-fold compared to the strain without scaffold.

An alternate scaffolding strategy is based on the interactions between affibodies and anti-idiotypic affibodies. The 58-residues affibodies (or Z-domains) are a class of non-immunoglobulin affinity proteins derived from *Staphylococcus aureus* protein A (Löfblom et al., 2010). They possess high specificity and binding affinity toward their target proteins (0.3 pM−10 μM) (Ståhl et al., 2017). In a recent study, Tippmann et al. (2017), utilized the Z_{Taq}:anti-Z_{Taq} (Kd = 0.7 μM) and Z_{IgA}:anti-Z_{IgA} (Kd = 0.9 μM) interactions to create a functional synthetic scaffold in *S. cerevisiae*. A scaffold linked anti-Z_{Taq} and anti-Z_{IgA}, and Z_{IgA} and Z_{Taq} were fused with farnesyl diphosphate synthase and farnesene synthase, respectively. By optimizing the amino acid linkers and the enzyme:scaffold ratio, a 135% increase in the yield of farnesene on glucose was achieved. This affibody scaffold was also functional in *E. coli*, in which its utilization resulted in a 7-fold increase in PHB production, demonstrating its versatility as a scaffold platform for metabolic engineering.

Scaffolds were also used to create an artificial Gal2-xylose isomerase complex to improve xylose utilization in *S. cerevisiae* (Thomik et al., 2017). In this study, WASP-homology 1 (WH1) from rat N-WASP was used as the scaffold construct and a xylose isomerase (XI) was fused with WH1 ligand (WH1L) at the N-terminus. To recruit the XI-WH1 scaffold complex to the Gal2 transmembrane protein, a pair of synthetic coiled-coil zippers with high binding affinity for one another was used: SYNZIP1 (SZ1) and SYNZIP2 (SZ2) (Reinke et al., 2010). In this configuration, Gal2 was fused with SZ2 at the N-terminus by either the flexible or helical linker, while the WH1 scaffold was used with SZ1 at the N-terminus by the flexible linker. The synthetic scaffold allowed the Gal2-xylose isomerase complex to form, enabled the yeast strain to uptake and process xylose, and resulted in higher ethanol/xylitol ratio, a proxy measurement for xylose consumption. Kang et al. (2019) used an alternate means to localize pathway enzymes into a multienzyme complex

via RIDD and RIAD, short peptides with high binding affinity ($K_D = 1.2$ nM), to improve lycopene production in *S. cerevisiae*. The two key enzymes Idi and CrtE, were tagged with RIAD and RIDD, respectively. The resulting complex yielded 2.3 g/L of lycopene after 144 h fermentation, 58% higher than the control strains.

In a recent study, Han et al. (2018) utilized Tya, a part of the Ty1 retrotransposon, to spatially recruit the key enzymes to improve farnesene and farnesol production in *S. cerevisiae*. Tya is a 49-kDa protein that self-assembles into a shell, similar to virus-like particles (VLPs) (Marchenko et al., 2003). Tya was fused to either the C-terminus or the N-terminus of three key isoprenoid enzymes: tHMG1 (a truncated form of HMG-CoA reductase from *S. cerevisiae*), IspA (from *E. coli*), and AFS1 (from *Malus domestica*) or DPP1 (from *S. cerevisiae*) to create synthetic metabolons to drive carbon flux toward farnesene or farnesol. Titer reached 930 ± 40 mg/L in the best-performing strain, a 3.1-fold increase relative to 300 ± 11 mg/L for free enzymes. The best-performing strain for farnesol production produced 882 ± 15 mg/L, 3.8-fold higher than the control strains expressing free enzymes (231 ± 14 mg/L).

With increased interest in scaffolds to channel substrates toward formation of desired products, additional protein interactions have been screened for their scaffolding potential. Curvature Thylakoid1A (CURT1A) protein, isolated from the thylakoid membrane of *Arabidopsis thaliana*, has been identified as a prospective membrane-bound scaffolding module (Behrendorff et al., 2019). CURT1A can form homo-oligomers in the membrane. By fusing fluorescence proteins to several variants of CURT1A, CURT1A fusion proteins were shown to scaffold onto the endoplasmic reticulum of *S. cerevisiae,* resulting in the fluorescence signal being localized to the membrane.

ORGANELLE TARGETING

Another strategy to colocalize enzymes is to target the enzyme pathway to an organelle. This is done by fusing specific leader sequences to the enzymes, allowing the transporters of the respective organelles to recognize and facilitate entry of the enzymes. Once in the organelles, the semipermeable membrane prevents enzymes from diffusing out to the cytosol and localizes them in a smaller volume, increasing the chances of reaction along the enzymatic pathway. Furthermore, some organelles have different local conditions than the cytosol and those conditions may be advantageous to product formation for a given pathway. The mitochondria and the peroxisomes are the most popular organelles for pathway targeting for the production of non-native products, though the endoplasmic reticulum has also been utilized (Hammer and Avalos, 2017).

Mitochondria

The mitochondrial matrix is enclosed by two membranes and has a higher reducing redox potential, higher pH, and lower oxygen concentration than the cytosol (Hu et al., 2008; Orij et al., 2009). The mitochondrion is the cellular location for heme and iron-sulfur cluster biosynthesis (Mühlenhoff and Lill, 2000), formation of several amino acids, and the TCA cycle, and also houses a large number of cofactors and metabolites [NADP(H), NADP+, acetyl-CoA, FAD, TCA cycle intermediates] (Malina et al., 2018). In particular, mitochondria are an attractive location for pathways utilizing acetyl-CoA as the acetyl-CoA pool is 20–30 times greater than the cytosolic pool in *S. cerevisiae* (Wagner and Alper, 2016). A mitochondrial leader sequence (MLS) is required for an enzyme to enter the mitochondria, with the CoxIV MLS as the most commonly used (Hurt et al., 1985; Farhi et al., 2011; Avalos et al., 2013). In addition, several other leader sequences, Hmil (Lee et al., 1999), Coq3 (Yuan and Ching, 2016), Hsp60, Pda1, Oli1 (Ehrenworth et al., 2017), Cdc9 (Willer et al., 1999), and Eat1 (Löbs et al., 2018), have been characterized for targeting of non-native enzymes.

Exploiting the high acetyl-CoA pool in the mitochondria has allowed for increased production of terpenes and sesquiterpenes, products that come directly from acetyl-CoA. Introduction of the farnesyl pyrophosphate biosynthetic pathway to the mitochondria resulted in production of 427 mg/l of amorpha-4,11-diene and provided evidence that the mitochondrial membranes prevented diffusion of intermediates to competing cytosolic pathways (Yuan and Ching, 2016). Similarly, targeting the entire mevalonate pathway along with the genes *FPS* and *GES* resulted in a 6-fold improvement in geraniol production; when coupled with cytosolically expressed *G8H*, *GOR*, and *ISY*, the compounds 8-hydroxygeraniol and nepetalactol were produced in yeast for the first time (Yee et al., 2019). Interestingly, targeting part of the isoprene pathway to the mitochondria resulted in a 2.1 or 1.6-fold increase in isoprene production relative to purely mitochondrial or cytosolic expression, respectively (Lv et al., 2016), highlighting the importance of local environment on enzyme expression.

In addition to acetyl-CoA, there are many other substrates present in the mitochondria in high concentration that can be utilized. Farhi et al. (2011) took advantage of the high concentration of farnesyl diphosphate (FDP) in the mitochondria to increase production of valencene and amorphadiene by 8- and 20-fold, respectively over a cytosolic expression strain. Targeting the entire isobutanol pathway to the mitochondria and utilizing mitochondrial pyruvate increased isobutanol production by 2.6-fold over cytosolic expression (Avalos et al., 2013). Additionally, targeting the 2-ketoacid elongation enzymes Leu4, Leu1, and Leu2 (responsible for the cyclic elongation of iso-alcohol products by one carbon per cycle) to the mitochondria increased isopentanol production over isobutanol by 53% relative to cytosolic production (Hammer et al., 2020). In the non-conventional yeast *Kluyveromyces marxianus*, targeting of the isobutanol pathway to the mitochondria resulted in 1.1 g/l isobutanol in 250 ml shake flasks compared to 0.03 g/l for the cytosolic pathway, and a titer of 21.6 g/l isobutanol for the mitochondrial-targeted pathway in fed-batch reactors (Patent Application: Buelter et al., 2010).

Peroxisomes

The yeast peroxisome is the site of β-oxidation as well as the organelle responsible for the removal and degradation of hydrogen peroxide (Van Der Klei and Veenhuis, 1997). Peroxisomes are enclosed by a single membrane and are

selectively permeable, with all entering and exiting proteins receiving assistance by membrane-bound proteins called porins (Sibirny, 2016). The size and number of peroxisomes present in a cell is also dynamically controlled and varies with growth conditions (Saraya et al., 2010). Since the peroxisome is the site of fatty acid degradation by β-oxidation and acetyl-CoA is a byproduct of β-oxidation (Poirier et al., 2006), this organelle is promising for the targeting of lipidic product pathways and acetyl-CoA utilizing pathways.

Proteins enter the peroxisome by the use of peroxisomal targeting sequences, PTS1, PTS2, and mPTS (Sibirny, 2016). The need for a quick, efficient peroxisomal targeting sequence can be important to prevent reactions in the cytosol prior to peroxisomal compartmentalization. DeLoache et al. (2016) developed an enhanced efficiency PTS1 (ePTS1) by adding basic residues upstream of the PTS1 targeting sequence. This new ePTS1 was found to import proteins quicker than PTS1 and with less interaction with cytosolic pathways. Additionally, ePTS1 can be used to target multiple enzymes to the peroxisome with minimal decrease of import efficiency.

Synthesis of the mevalonate pathway derived cytosolic product squalene was compartmentalized to the peroxisome, leading to titers of 1.3 g/l, a 138-fold improvement over cytosolic production; when simultaneously produced in both the peroxisome and the cytosol, titers were as high as 11 g/l in fed-batch culture (Liu et al., 2020). Additionally, the peroxisome acts as a storage vessel for squalene produced in both the cytosol and the peroxisome, leading to reduced degradation of squalene. Synthesis of fatty acid derived products (fatty alcohols and alkanes) was also increased by targeting heterologous pathway enzymes to the peroxisome. Fatty alcohol titers were more than 2-fold higher and alkane titers up to 2-fold higher, shorter chain lengths were observed, and there was a higher alkane to fatty alcohol ratio when enzymes were targeted to the peroxisome (Zhou et al., 2016). Additionally, the carboxylic acid reductase, MmCAR, has 45% higher activity in the peroxisome over the cytosol, demonstrating that the peroxisome has favorable conditions for this enzyme. The titer of olefins, a heterologous product class synthesized from a P450 fatty acid decarboxylase, increased 40% when this enzyme was targeted to the peroxisome, indicating that the peroxisome is a promising location for fatty acid derived products.

Targeting enzymes for the production of fatty acid-derived compounds to the peroxisome also increased product titers in *Yarrowia lipolytica*. There was an 11-fold increase in fatty acid ethyl ester (FAEE) titers and a 3-fold increase in alkane titers, with shorter chain length alkanes being produced (Xu et al., 2016). Titers of methyl ketones were 6.5-fold higher when the pathway enzymes were targeted to the peroxisome relative to cytosolic expression (Hanko et al., 2018).

Endoplasmic Reticulum

The endoplasmic reticulum (ER) works in conjunction with the Golgi apparatus to sort, transport, and modify newly synthesized proteins and lipids. The ER lumen has an oxidative environment (Tu and Weissman, 2004) and a pH similar to that of the cytosol (Paroutis et al., 2004) making it a possible advantageous location for enzymes requiring an oxidative environment. Targeting to the ER is primarily done by a co-translational mechanism involving an ER recognition signal that facilitates entry to the ER (Young et al., 2001) and additional ER retention sequences are necessary for the enzyme to remain in the ER (Pagny et al., 1999). The ER also has the ability to utilize triacyl glycerides and other neutral lipids (Markgraf et al., 2014) resulting in the presence of acyl-CoA and ACP intermediates, making it a possible location for production of fatty acid-derived compounds from those metabolites (Xu et al., 2016).

Targeting a key enzyme in the opioid production pathway (COR from *Papaver somniferum*) to the ER increased the production of morphine by almost 2-fold while also reducing the amount of the undesirable side product, neomorphine, in *S. cerevisiae* (Thodey et al., 2014). In *Y. lipolytica*, targeting select enzymes in the fatty acid ethyl ester (FAEE) and alkane pathways to the ER led to 19- and 5-fold increases in FAEE and alkane production, respectively (Xu et al., 2016).

SYNTHETIC ORGANELLES

A new emerging technique to colocalize enzymes in yeast is through the use of synthetic organelles. Synthetic organelles are clusters of enzymes that are encapsulated away from the cytosol, similar to an organelle but not a native structure of the cells. Advantages are similar to those of native organelles (smaller volume, separation from the cytosol, and possible different pH conditions) but with the added advantage of avoiding native organelle processes that may compete or interfere with the actions of the localized enzymes.

Many prokaryotes have native intracellular protein compartments that sequester enzymes from the cytoplasm. An example is the encapsulin nanocompartment native to several different bacteria (Giessen, 2016). Encapsulins are constructed by self-assembly of 60 or 180 identical subunits (20–24 nm or 30–32 nm) depending on the source bacterium. Encapsulins were first used as non-native enzyme sequestering organelles in *E. coli* (Kang et al., 2008; Tanaka et al., 2010; Moon et al., 2014; Giessen, 2016; Nichols et al., 2017), but have since been tested in *S. cerevisiae*. In an initial study, use of the encapsulin nanocompartment from *Myxococcus xanthus* in *S. cerevisiae* resulted in the colocalization of split mVenus, resulting in fluorescence (Lau et al., 2018). This yeast encapsulin can also protect enzymes from native cell proteases.

Another method of constructing synthetic organelles in yeast is via light-inducible enzyme clustering techniques (Zhao et al., 2018). The light-inducible optoCluster and the light-repressible PixELL systems create rigid enzyme clusters that place two or more enzymes in close proximity with little to no diffusion away from the cluster. Both systems were used to direct flux at a branch point in the deoxyviolacein pathway toward deoxyviolacein rather than prodeoxyviolacein (which is formed from the diffuse cytosolic enzymes). These light-inducible synthetic organelles both form and dissociate rapidly, pointing to their possible future use as dynamic synthetic organelles for the production of diverse products (Zhao et al., 2019). Synthetic organelles are

TABLE 1 | Enzyme colocalizations studies in yeast and the resulting improvements in product titer.

Products	Strategy	Final titer	Fold improvement*	Organism	References
Amorpha-4,11-diene	Mitochondria targeting (COX4)	427 mg/L	26.5	*S. cerevisiae*	Yuan and Ching, 2016
Geraniol	Mitochondria targeting (COX4)	43.3 mg/L	6	*S. cerevisiae*	Yee et al., 2019
Isoprene	Mitochondria targeting (COX4)	246 mg/L	1.6	*S. cerevisiae*	Lv et al., 2016
Valencene	Mitochondria targeting (COX4)	1.5 mg/L	8	*S. cerevisiae*	Farhi et al., 2011
Amorphadiene	Mitochondria targeting (COX4)	20 mg/L	20	*S. cerevisiae*	Farhi et al., 2011
Isobutanol	Mitochondria targeting (COX4)	635 mg/L	2.6	*S. cerevisiae*	Avalos et al., 2013
Isopentanol	Mitochondria targeting (COX4)	1.24 g/L	7.3	*S. cerevisiae*	Hammer et al., 2020
Isobutanol	Mitochondria targeting (COX4)	21.6 g/L	36.5	*K. marxianus*	Buelter et al., 2010
Squalene	Peroxisome targeting (ePTS1)	11 g/L	138	*S. cerevisiae*	Liu et al., 2020
Olefins	Peroxisome targeting (PTS1)	0.18 mg/L	1.4	*S. cerevisiae*	Zhou et al., 2016
Alkane	Peroxisome targeting (PTS1)	3.5 mg/L	2	*S. cerevisiae*	Zhou et al., 2016
Fatty alcohol	Peroxisome targeting (PTS1)	193 mg/L	2	*S. cerevisiae*	Zhou et al., 2016
Fatty acid ethyl ester	Peroxisome targeting (SKL)	110.9 mg/L	20	*Y. lipolytica*	Xu et al., 2016
Alkane	Peroxisome targeting (SKL)	11 mg/L	3.4	*Y. lipolytica*	Xu et al., 2016
Methyl Ketone	Peroxisome targeting (SKL)	314.8 mg/L	6.5	*Y. lipolytica*	Hanko et al., 2018
Fatty acid ethyl ester	ER targeting	136.5 mg/L	15	*Y. lipolytica*	Xu et al., 2016
Alkane	ER targeting	16.8 mg/L	5	*Y. lipolytica*	Xu et al., 2016
Morphine	ER Targeting (CNE1)	4.7 mg/L	2	*S. cerevisiae*	Thodey et al., 2014
Patchoulol	Fusion protein (GSG)	9.5 mg/L	2	*S. cerevisiae*	Albertsen et al., 2011
Raspberry ketone	Fusion protein (VDEAAAKSGR)	2.81 mg/L	6.5	*S. cerevisiae*	Lee et al., 2016
Germacrene A	Fusion protein (GGGGS)	190.7 mg/L	3	*S. cerevisiae*	Hu et al., 2017
β-carotene	Tridomain fusion protein	2.7 mg/gDCW	2	*S. cerevisiae*	Rabeharindranto et al., 2019
Resveratrol	Metazoan synthetic scaffold	14.4 mg/L	5	*S. cerevisiae*	Wang and Yu, 2012
2,3-Butanediol	Dockerin-Cohesin scaffold	13.6 g/L	1.4	*S. cerevisiae*	Kim et al., 2016
Ethyl Acetate	Lipid droplet scaffold	15 mg/(L*OD)	1.7	*S. cerevisiae*	Lin et al., 2017
Farnesene	Affibodies scaffold	16 mg/L	1.9	*S. cerevisiae*	Tippmann et al., 2017
Farnesene	Tya scaffold	930 mg/L	3.1	*S. cerevisiae*	Han et al., 2018
Farnesol	Tya scaffold	882 mg/L	3.8	*S. cerevisiae*	Han et al., 2018
Lycopene	Peptide tags	2.3 g/L	1.6	*S. cerevisiae*	Kang et al., 2019

**Fold improvement reported is due to enzyme colocalization (not other metabolic engineering strategies).*

thus an emerging technology with potential to influence yeast metabolic engineering.

CONCLUSIONS

Immobilization and colocalization of enzymes are effective ways to increase production of both native and heterologous compounds in yeast. These strategies, including enzyme fusion, scaffolding, and organelle targeting have successfully improved product titers (**Table 1**) without adversely affecting the cell growth and metabolism. Initial studies with synthetic organelles demonstrated both successful colocalization and redirection of a model pathway, indicating the promise of this emerging technology. Nonetheless, the success of these strategies remains somewhat enzyme-specific and extensive optimization (e.g., enzyme-scaffold ratio) or screening (e.g., linker choice, domain order, and targeting sequence) are needed for successful application. Additional studies should allow more general principles to emerge. It is expected that these colocalization synthetic biology approaches will continue to impact metabolic pathway engineering as more strategies are discovered and optimized.

AUTHOR CONTRIBUTIONS

HY and AP conducted the literature survey. All authors wrote and edited the manuscript.

REFERENCES

Albertsen, L., Chen, Y., Bach,L. S., Rattleff, S., Maury, J., Brix, S., et al. (2011). Diversion of flux toward sesquiterpene production in *Saccharomyces cerevisiae* by fusion of host and heterologous enzymes. *Appl. Environ. Microbiol.* 77, 1033–1040. doi: 10.1128/AEM.01361-10

Anandharaj, M., Lin, Y., Rani, R. P., Nadendla, E. K., Ho, M.-C., Huang, C.-C., et al. (2020). Constructing a yeast to express the largest cellulosome complex on the cell surface. *Proc. Natl. Acad. Sci. U.S.A.* 117, 2385–2394. doi: 10.1073/pnas.1916529117

Avalos, J. L., Fink, G. R., and Stephanopoulos, G. (2013). Compartmentalization of metabolic pathways in yeast mitochondria improves the production of branched-chain alcohols. *Nat. Biotechnol.* 31, 335–341. doi: 10.1038/nbt.2509

Behrendorff, J. B. Y. H., Sandoval-Ibanez, O. A., Sharma, A., and Pribil, M. (2019). Membrane-bound protein scaffolding in diverse hosts using thylakoid protein CURT1A. *ACS Synth. Biol.* 8, 611–620. doi: 10.1021/acssynbio.8b00418

Buelter, T., Meinhold, P., Smith, C., Aritiduo, A., Dundon, C. A., and Urano, J. (2010). *Engineered Microrganisms for the Production of one or more Target Compounds*. World Intellectual Property Organization. International Publication Number WO 2010/075504 A2.

Chen, X., Zaro, J. L., and Shen, W.-C. (2013). Fusion protein linkers: property, design and functionality. *Adv. Drug Deliv. Rev.* 65, 1357–1369. doi: 10.1016/J.ADDR.2012.09.039

DeLoache, W. C., Russ, Z. N., and Dueber, J. E. (2016). Towards repurposing the yeast peroxisome for compartmentalizing heterologous metabolic pathways. *Nat. Commun.* 7:11152. doi: 10.1038/ncomms11152

Dueber, J. E., Wu, G. C., Malmirchegini, G. R., Moon, T. S., Petzold, C. J., Ullal, A. V., et al. (2009). Synthetic protein scaffolds provide modular control over metabolic flux. *Nat. Biotechnol.* 27, 753–759. doi: 10.1038/nbt.1557

Ehrenworth, A. M., Haines, M. A., Wong, A., and Peralta-Yahya, P. (2017). Quantifying the efficiency of *Saccharomyces cerevisiae* translocation tags. *Biotechnol. Bioeng.* 114, 2628–2636. doi: 10.1002/bit.26376

Fan, L.-H., Zhang, Z.-J., Yu, X.-Y., Xue, Y.-X., and Tan, T.-W. (2012). Self-surface assembly of cellulosomes with two miniscaffoldins on *Saccharomyces cerevisiae* for cellulosic ethanol production. *Proc. Natl. Acad. Sci. U.S.A.* 109, 13260–13265. doi: 10.1073/pnas.1209856109

Farhi, M., Marhevka, E., Masci, T., Marcos, E., Eyal, Y., Ovadis, M., et al. (2011). Harnessing yeast subcellular compartments for the production of plant terpenoids. *Metab. Eng.* 13, 474–481. doi: 10.1016/j.ymben.2011.05.001

Giessen, T. W. (2016). Encapsulins: microbial nanocompartments with applications in biomedicine, nanobiotechnology and materials science. *Curr. Opin. Chem. Biol.* 34, 1–10. doi: 10.1016/j.cbpa.2016.05.013

Guirimand, G., Kulagina, N., Papon, N., Hasunuma, T., and Courdavault, V. (2020). Innovative tools and strategies for optimizing yeast cell factories. *Trends Biotechnol.* doi: 10.1016/J.TIBTECH.2020.08.010. [Epub ahead of print].

Hammer, S. K., and Avalos, J. L. (2017). Harnessing yeast organelles for metabolic engineering. *Nat. Chem. Biol.* 13, 823–832. doi: 10.1038/nchembio.2429

Hammer, S. K., Zhang, Y., and Avalos, J. L. (2020). Mitochondrial compartmentalization confers specificity to the 2-ketoacid recursive pathway: increasing isopentanol production in *Saccharomyces cerevisiae*. *ACS Synth. Biol.* 9, 546–555. doi: 10.1021/acssynbio.9b00420

Han, J. Y., Song, J. M., Seo, S. H., Wang, C., Lee, S.-G., Lee, H., et al. (2018). Ty1-fused protein-body formation for spatial organization of metabolic pathways in *Saccharomyces cerevisiae*. *Biotechnol. Bioeng.* 115, 694–704. doi: 10.1002/bit.26493

Hanko, E. K. R., Denby, C. M., Sànchez i Nogu,é, V., Lin, W., Ramirez, K. J., Singer, C. A., et al. (2018). Engineering β-oxidation in yarrowia lipolytica for methyl ketone production. *Metab. Eng.* 48, 52–62. doi: 10.1016/j.ymben.2018.05.018

Hu, J., Dong, L., and Outten, C. E. (2008). The redox environment in the mitochondrial intermembrane space is maintained separately from the cytosol and matrix. *J. Biol. Chem.* 283, 29126–29134. doi: 10.1074/jbc.M803028200

Hu, Y., Zhou, Y. J., Bao,. J., Huang, L., Nielsen, J., and Krivoruchko, A. (2017). Metabolic Engineering of *Saccharomyces cerevisiae* for production of germacrene a, a precursor of beta-elemene. *J. Industr. Microbiol. Biotechnol.* 44, 1065–1072. doi: 10.1007/s10295-017-1934-z

Hurt, E. C., Pesold-Hurt, B., Suda, K., Oppliger, W., and Schatz, G. (1985). The first twelve amino acids (less than half of the pre-sequence) of an imported mitochondrial protein can direct mouse cytosolic dihydrofolate reductase into the yeast mitochondrial matrix. *EMBO J.* 4, 2061–2068. doi: 10.1002/j.1460-2075.1985.tb03892.x

Jia, F., Narasimhan, B., and Mallapragada, S. (2014). Materials-based strategies for multi-enzyme immobilization and co-localization: a review. *Biotechnol. Bioeng.* 111, 209–222. doi: 10.1002/bit.25136

Kang, S., Lucon, J., Varpness, Z. B., Liepold, L., Uchida, M., Willits, D., et al. (2008). Monitoring biomimetic platinum nanocluster formation using mass spectrometry and cluster-dependent H2 production. *Angew. Chem. Int. Ed.* 47, 7845–7848. doi: 10.1002/anie.200802481

Kang, W., Ma, T., Liu, M., Qu, J., Liu, Z., Zhang, H., et al. (2019). Modular enzyme assembly for enhanced cascade biocatalysis and metabolic flux. *Nat. Commun.* 10:4248. doi: 10.1038/s41467-019-12247-w

Kim, S., Bae, S. J., and Hahn, J. S. (2016). Redirection of pyruvate flux toward desired metabolic pathways through substrate channeling between pyruvate kinase and pyruvate-converting enzymes in *Saccharomyces cerevisiae*. *Sci. Rep.* 6:24145. doi: 10.1038/srep24145

Kim, S., and Hahn, J. S. (2014). Synthetic scaffold based on a cohesin-dockerin interaction for improved production of 2,3-butanediol in *Saccharomyces cerevisiae*. *J. Biotechnol.* 192(Part A), 192–96. doi: 10.1016/j.jbiotec.2014.10.015

Lau, Y. H., Giessen, T. W., Altenburg, W. J., and Silver, P. A. (2018). Prokaryotic nanocompartments form synthetic organelles in a eukaryote. *Nat. Commun.* 9:1311. doi: 10.1038/s41467-018-03768-x

Lee, C. M., Sedman, J., Neupert, W., and Stuart, R. A. (1999). The DNA helicase, Hmi1p, is transported into mitochondria by a C- terminal cleavable targeting signal. *J. Biol. Chem.* 274, 20937–20942. doi: 10.1074/jbc.274.30.20937

Lee, D., Lloyd, N. D. R., Pretorius, I. S., and Borneman, A. R. (2016). Heterologous production of raspberry ketone in the wine yeast *Saccharomyces cerevisiae* via pathway engineering and synthetic enzyme fusion. *Microb. Cell Fact.* 15:49. doi: 10.1186/s12934-016-0446-2

Lian, J., Mishra, S., and Zhao, H. (2018). Recent advances in metabolic engineering of *Saccharomyces cerevisiae*: New tools and their applications. *Metab. Eng.* 50, 85–108. doi: 10.1016/j.ymben.2018.04.011

Lin, J. L., Jie, Z., and Ian, W. (2017). Synthetic protein scaffolds for biosynthetic pathway colocalization on lipid droplet membranes. *ACS Synth. Biol* 6, 1534–1544. doi: 10.1021/acssynbio.7b00041

Liu, G.-S., Li, T., Zhou, W., Jiang, M., Tao, X., Liu, M., et al. (2020). The yeast peroxisome: a dynamic storage depot and subcellular factory for squalene overproduction. *Metab. Eng. 57,* 151–161. doi: 10.1016/j.ymben.2019.11.001

Liu, Y., and Nielsen, J. (2019). Recent trends in metabolic engineering of microbial chemical factories. *Curr. Opin. Biotechnol.* 60, 188–197. doi: 10.1016/J.COPBIO.2019.05.010

Liu, Z. L., Li, H. N., Song, H. T., Xiao, W. J., Xia, W. C., Liu, X. P., et al. (2018). Construction of a trifunctional cellulase and expression in *Saccharomyces cerevisiae* using a fusion protein. *BMC Biotechnol.* 18:43. doi: 10.1186/s12896-018-0454-x

Löbs, A. K., Schwartz, C., Thorwall, S., and Wheeldon, I. (2018). Highly multiplexed CRISPRi repression of respiratory functions enhances mitochondrial localized ethyl acetate biosynthesis in kluyveromyces marxianus. *ACS Synth. Biol.* 7, 2647–2655. doi: 10.1021/acssynbio.8b00331

Löfblom, J., Feldwisch, J., Tolmachev, V., Carlsson, J., Ståhl, S., and Frejd, T. Y. (2010). Affibody molecules: engineered proteins for therapeutic, diagnostic and biotechnological applications. *FEBS Lett.* 584, 2670–2680. doi: 10.1016/j.febslet.2010.04.014

Lv, X., Wang, F., Zhou, P., Ye, L., Xie, W., Xu, H., et al. (2016). Dual regulation of cytoplasmic and mitochondrial acetyl-CoA utilization for improved isoprene production in *Saccharomyces cerevisiae*. *Nat. Commun* 7:12851. doi: 10.1038/ncomms12851

Malina, C., Larsson, C., and Nielsen, J. (2018). Yeast mitochondria: an overview of mitochondrial biology and the potential of mitochondrial systems biology. *FEMS Yeast Res.* 18, 1–17. doi: 10.1093/femsyr/foy040

Marchenko, A. N., Kozlov, D. G., Svirshchevskaya, E. V., Viskova, N. Y., and Benevolensky, S. V. (2003). The P1 protein of the yeast transposon Ty1 can be used for the construction of bi-functional virus-like particles. *J. Mol. Microbiol. Biotechnol.* 5, 97–104. doi: 10.1159/000069980

Markgraf, D. F., Klemm, R. W., Junker, M., Hannibal-Bach, H. K., Ejsing, C. S., and Rapoport, T. A. (2014). An ER protein functionally couples neutral lipid

metabolism on lipid droplets to membrane lipid synthesis in the ER. *Cell Rep.* 6, 44–55. doi: 10.1016/j.celrep.2013.11.046

Mechaly, A., Fierobe, H. P., Belaich, A., Belaich, J. P., Lamed, R., Shoham,Y., et al. (2001). Cohesin-dockerin interaction in cellulosome assembly: a single hydroxyl group of a dockerin domain distinguishes between nonrecognition and high affinity recognition. *J. Biol. Chem.* 276, 9883–9888. doi: 10.1074/jbc.M009237200

Moon, H., Lee, J., Kim, H., Heo, S., Min, J., and Kang, S. (2014). Genetically engineering encapsulin protein cage nanoparticle as a SCC-7 cell targeting optical nanoprobe. *Biomater. Res.* 18:21. doi: 10.1186/2055-7124-18-21

Mühlenhoff, U., and Lill, R. (2000). Biogenesis of iron-sulfur proteins in eukaryotes: a novel task of mitochondria that is inherited from bacteria. *Bioch. Biophys. Bioenerget.* 1459, 370–382. doi: 10.1016/S0005-2728(00)00174-2

Nichols, R. J., Cassidy-Amstutz, C., Chaijarasphong, T., and Savage, D. F. (2017). Encapsulins: molecular biology of the shell. *Crit. Rev. Biochem. Mol. Biol.* 52, 583–594. doi: 10.1080/10409238.2017.1337709

Orij, R., Postmus, J., Ter Beek, A., Brul, S., and Smits, G. J. (2009). *In vivo* measurement of cytosolic and mitochondrial ph using a PH-sensitive gfp derivative in *Saccharomyces cerevisiae* reveals a relation between intracellular PH and growth. *Microbiology* 155, 268–278. doi: 10.1099/mic.0.022038-0

Ostergaard, S., Olsson, L., and Nielsen, J. (2000). Metabolic Engineering of *Saccharomyces cerevisiae*. *Microbiol. Mol. Biol. Rev.* 64, 34–50. doi: 10.1128/mmbr.64.1.34-50.2000

Pagny, S., Lerouge, P., Faye, L., and Gomord, V. (1999). Signals and mechanisms for protein retention in the endoplasmic reticulum. *J. Exp. Bot.* 50, 157–164. doi: 10.1093/jxb/50.331.157

Paroutis, P., Toure, N., and Grinstein, S. (2004). The PH of the secretory pathway: measurement, determinants, and regulation. *Physiology* 19, 207–215. doi: 10.1152/physiol.00005.2004

Poirier, Y., Antonenkov, V. D., Glumoff, T., and Hiltunen, J. K. (2006). Peroxisomal β-oxidation-A metabolic pathway with multiple functions. *Biochim. Biophys. Acta Mol. Cell Res.* 1763, 1413–1426. doi: 10.1016/j.bbamcr.2006.08.034

Rabeharindranto, H., Castaño-Cerezo, S., Lautier, T., Garcia-Alles, L. F., Treitz, C., Tholey, A., et al. (2019). Enzyme-fusion strategies for redirecting and improving carotenoid synthesis in *S. cerevisiae*. *Metab. Eng. Commun.* 8:e00086. doi: 10.1016/j.mec.2019.e00086

Reinke, A. W., Grant, R. A., and Keating, A. E. (2010). A synthetic coiled-coil interactome provides heterospecific modules for molecular engineering. *J. Am. Chem. Soc.* 132, 6025–6031. doi: 10.1021/ja907617a

Saraya, R., Veenhuis, M., and Van Der Klei, I. J. (2010). Peroxisomes as dynamic organelles: peroxisome abundance in yeast. *FEBS J.* 277, 3279–3288. doi: 10.1111/j.1742-4658.2010.07740.x

Sibirny, A. A. (2016). Yeast peroxisomes: structure, functions and biotechnological opportunities. *FEMS Yeast Res.* 16, 1–14. doi: 10.1093/femsyr/fow038

Siddiqui, M. S., Thodey, K., Trenchard, I., and Smolke, C. D. (2012). Advancing secondary metabolite biosynthesis in yeast with synthetic biology tools. *FEMS Yeast Res.* 18, 21. doi: 10.1111/j.1567-1364.2011.00774.x

Ståhl, S., Gräslund, T., Karlström, A. E., Frejd, F. Y., Nygren,P.-A., and Löfblom, J. (2017). Affibody molecules in biotechnological and medical applications. *Trends Biotechnol.* 35, 691–712. doi: 10.1016/J.TIBTECH.2017.04.007

Stahl, S. W., Nash, M. A., Fried, D. B., Slutzki, M., Barak, Y., Bayer, E. A., et al. (2012). Single-Molecule Dissection of the High-Affinity Cohesin-Dockerin Complex. *Proc. Natl. Acad. Sci. U.S.A.* 109, 20431–20436. doi: 10.1073/pnas.1211929109

Tanaka, S., Sawaya, M. R., and Yeates, T. O. (2010). Structure and mechanisms of a protein-based organelle in *Escherichia coli*. *Science* 327, 81–84. doi: 10.1126/science.1179513

Tang, H., Wang, J., Wang, S., Shen, Y., Petranovic, D., Hou, J., et al. (2018). Efficient Yeast surface-display of novel complex synthetic cellulosomes. *Microb. Cell Fact.* 17:122. doi: 10.1186/s12934-018-0971-2

Thodey, K., Galanie, S., and Smolke, C. D. (2014). A microbial biomanufacturing platform for natural and semisynthetic opioids. *Nat. Chem. Biol.* 10, 837–844. doi: 10.1038/nchembio.1613

Thomik, T., Wittig, I., Choe, J.-Y., Boles, E., and Oreb, M. (2017). An artificial transport metabolon facilitates improved substrate utilization in yeast. *Nat. Chem. Biol.* 13, 1158–1163. doi: 10.1038/nchembio.2457

Tippmann, S., Anfelt, J., David, F., Rand, J. M., Siewers, V., Uhlén, M., et al. (2017). Affibody scaffolds improve sesquiterpene production in *Saccharomyces cerevisiae*. *ACS Synth. Biol.* 6, 19–28. doi: 10.1021/acssynbio.6b00109

Tsai, S.-L., DaSilva, N. A., and Chen, W. (2013). Functional display of complex cellulosomes on the yeast surface via adaptive assembly. *ACS Synth. Biol.* 2, 14–21. doi: 10.1021/sb300047u

Tu, B. P., and Weissman, J. S. (2004). Oxidative protein folding in eukaryotes: mechanisms and consequences. *J. Cell Biol.* 164, 341–346. doi: 10.1083/jcb.200311055

Van Der Klei, I. J., and Veenhuis, M. (1997). Yeast peroxisomes: function and biogenesis of a versatile cell organelle. *Trends Microb.* 5, 502–509. doi: 10.1016/S0966-842X(97)01156-6

Wagner, J. M., and Alper, H. S. (2016). Synthetic biology and molecular genetics in non-conventional yeasts: current tools and future advances. *Fungal Genet Biol.* 89, 126–136. doi: 10.1016/j.fgb.2015.12.001

Wang, Y., and Yu, O. (2012). Synthetic scaffolds increased resveratrol biosynthesis in engineered yeast cells. *J. Biotechnol.* 157, 258–260. doi: 10.1016/j.jbiotec.2011.11.003

Willer, M., Rainey, M., Pullen, T., and Stirling, C. J. (1999). The yeast CDC9 gene encodes both a nuclear and a mitochondrial form of DNA ligase I. *Curr. Biol.* 9, 1085–1094. doi: 10.1016/S0960-9822(99)80477-1

Xu, P., Qiao, K., Ahn, W. S., and Stephanopoulos, G. (2016). Engineering yarrowia lipolytica as a platform for synthesis of drop-in transportation fuels and oleochemicals. *Proc. Natl. Acad. Sci. U.S.A.* 113, 10848–10853. doi: 10.1073/pnas.1607295113

Xu, W., Klumbys, E., Ang, E. L., and Zhao, H. (2020). Emerging molecular biology tools and strategies for engineering natural product biosynthesis. *Metab. Eng. Commun.* 10:e00108. doi: 10.1016/J.MEC.2019.E00108

Yee, D. A., DeNicola, A. B., Billingsley, J. M., Creso, J. G., Subrahmanyam, V., and Tang, Y. (2019). Engineered mitochondrial production of monoterpenes in *Saccharomyces cerevisiae*. *Metab. Eng.* 55, 76–84. doi: 10.1016/j.ymben.2019.06.004

Young, B. P., Craven, R. A., Reid, P. J., Willer, M., and Stirling, C. J. (2001). Sec63p and Kar2p are recquired for the translocation of SRP-dependent precursors into the yeast endoplasmic reticulum *in vivo*. *EMBO J.* 20, 262–71. doi: 10.1093/emboj/20.1.262

Yuan, J., and Ching, C. B. (2016). Mitochondrial acetyl-CoA utilization pathway for terpenoid productions. *Metab. Eng.* 38, 303–309. doi: 10.1016/j.ymben.2016.07.008

Zhang, Y., Li, S. Z., Li, J., Pan, X., Cahoon, R. E., Jaworski, J. G., et al. (2006). Using unnatural protein fusions to engineer resveratrol biosynthesis in yeast and mammalian cells. *J. Am. Chem. Soc.* 128, 13030–13031. doi: 10.1021/ja0622094

Zhao, E. M., Suek, N., Wilson, M. Z., Dine, E., Pannucci, N. L., Gitai, Z., et al. (2019). Light-based control of metabolic flux through assembly of synthetic organelles. *Nat. Chem. Biol.* 15, 589–597. doi: 10.1038/s41589-019-0284-8

Zhao, E. M., Zhang, Y., Mehl, J., Park, H., Lalwani, M. A., Toettcher, J. E., et al. (2018). Optogenetic regulation of engineered cellular metabolism for microbial chemical production. *Nature* 555, 683–687. doi: 10.1038/nature26141

Zhou, Y. J., Buijs, N. A., Zhu, Z., Gómez, D. O., Boonsombuti, A., Siewers, V., et al. (2016). Harnessing yeast peroxisomes for biosynthesis of fatty-acid-derived biofuels and chemicals with relieved side-pathway competition. *J. Am. Chem. Soc.* 138, 15368–15377. doi: 10.1021/jacs.6b07394

Conflict of Interest: The authors declare that the research was conducted in the absence of any commercial or financial relationships that could be construed as a potential conflict of interest.

frontiers in Bioengineering and Biotechnology

ORIGINAL RESEARCH
published: 22 February 2021
doi: 10.3389/fbioe.2021.624838

Application of Random Mutagenesis and Synthetic FadR Promoter for *de novo* Production of ω-Hydroxy Fatty Acid in *Yarrowia lipolytica*

*Beom Gi Park[1,2], Junyeob Kim[1,2], Eun-Jung Kim[3], Yechan Kim[1,2], Joonwon Kim[4], Jin Young Kim[2,5] and Byung-Gee Kim[1,2,3,5]**

[1] School of Chemical and Biological Engineering, Seoul National University, Seoul, South Korea, [2] Institute of Molecular Biology and Genetics, Seoul National University, Seoul, South Korea, [3] Bio-MAX/N-Bio, Seoul National University, Seoul, South Korea, [4] Department of Chemical Engineering, Soongsil University, Seoul, South Korea, [5] Interdisciplinary Program in Bioengineering, Seoul National University, Seoul, South Korea

OPEN ACCESS

Edited by:
Rodrigo Ledesma-Amaro, Imperial College London, United Kingdom

Reviewed by:
Jingyu Wang, Westlake Institute for Advanced Study (WIAS), China
Shuobo Shi, Beijing University of Chemical Technology, China

***Correspondence:**
Byung-Gee Kim
byungkim@snu.ac.kr

Specialty section:
This article was submitted to Synthetic Biology, a section of the journal Frontiers in Bioengineering and Biotechnology

Received: 01 November 2020
Accepted: 12 January 2021
Published: 22 February 2021

Citation:
Park BG, Kim J, Kim E-J, Kim Y, Kim J, Kim JY and Kim B-G (2021) Application of Random Mutagenesis and Synthetic FadR Promoter for de novo Production of ω-Hydroxy Fatty Acid in Yarrowia lipolytica. Front. Bioeng. Biotechnol. 9:624838. doi: 10.3389/fbioe.2021.624838

As a means to develop oleaginous biorefinery, *Yarrowia lipolytica* was utilized to produce ω-hydroxy palmitic acid from glucose using evolutionary metabolic engineering and synthetic FadR promoters for cytochrome P450 (CYP) expression. First, a base strain was constructed to produce free fatty acids (FFAs) from glucose using metabolic engineering strategies. Subsequently, through ethyl methanesulfonate (EMS)-induced random mutagenesis and fluorescence-activated cell sorting (FACS) screening, improved FFA overproducers were screened. Additionally, synthetic promoters containing bacterial FadR binding sequences for CYP expression were designed to respond to the surge of the concentration of FFAs to activate the ω-hydroxylating pathway, resulting in increased transcriptional activity by 14 times from the third day of culture compared to the first day. Then, endogenous *alk5* was screened and expressed using the synthetic FadR promoter in the developed strain for the production of ω-hydroxy palmitic acid. By implementing the synthetic FadR promoter, cell growth and production phases could be efficiently decoupled. Finally, in batch fermentation, we demonstrated *de novo* production of 160 mg/L of ω-hydroxy palmitic acid using FmeN3-TR1-alk5 in nitrogen-limited media. This study presents an excellent example of the production of ω-hydroxy fatty acids using synthetic promoters with bacterial transcriptional regulator (i.e., FadR) binding sequences in oleaginous yeasts.

Keywords: *Yarrowia lipolytica*, evolutionary metabolic engineering, synthetic promoter, FadR, ω-hydroxy fatty acid

INTRODUCTION

Construction of biorefinery using microorganisms and biomass can be competitive to that of oil refinery, only when the cost of carbon resource substrates is economical enough to that of petroleum (Cherubini, 2010). Therefore, if the current world petroleum price is persistent at around 35$, the biorefinery using biomass is very difficult to compete with the current petroleum-based

economy except for waste carbon resources. Along the same line, biotransformation of fatty acid or fatty acid methyl ester (FAME) hydrolyzed from vegetable oils, mainly palm oil, into bulk chemicals have no price advantage over petroleum-derived fatty acids (Harahap et al., 2019). However, waste vegetable oils and glycerol from food industries are excellent and cheap enough carbon sources to compete with petroleum, since not only the price of the resources but also sustainable society maintenance in terms of carbon recycling give sufficient legitimacy to develop various bioprocesses utilizing the cheap carbon sources (da Silva et al., 2009; Chen et al., 2018). In this regard, unlike *Saccharomyces cerevisiae*, which is characterized to efficiently produce bioethanol from simple sugars such as glucose and sugar cane/beet (Sarkar et al., 2012), non-conventional yeasts have drawn our attention as they have unique traits such as methylotroph or oleaginous yeast strains (Houard et al., 2002; Radecka et al., 2015; Rebello et al., 2018). Among the non-conventional yeasts, *Yarrowia lipolytica* is recognized as a promising industrial strain due to its ability to convert a broad range of carbon substrates such as not only glucose but also glycerol, fructose, fatty acids, and hydrophobic hydrocarbon compounds into high content of intracellular neutral lipids (Barth and Gaillardin, 1996; Mori et al., 2013; Workman et al., 2013; Abghari and Chen, 2014; Lazar et al., 2014) [substrate range of *Y. lipolytica* is well-reviewed herein (Ledesma-Amaro and Nicaud, 2016)]. Primarily, it is notable that waste glycerol from various industries using vegetable oils such as hydrolysis of fats and oil or soap manufacturing could be converted into single-cell oil using *Y. lipolytica* (Dobrowolski et al., 2016). Thus, *Y. lipolytica* is well-suited for the bioproduction of lipid-derived bulk chemicals, as it can assimilate cheap carbon sources, even industrial wastes, into intracellular lipids.

To date, there have been many efforts to utilize *Y. lipolytica* as cell factories for the production of lipid-derived chemicals such as single-cell oil, fatty alcohols, dicarboxylic acids, fatty acid ethyl esters, and medium-chain fatty acids (Gajdoš et al., 2015, 2017; Gao et al., 2018; Mishra et al., 2018; Rigouin et al., 2018; Cordova et al., 2020). Also, since *Y. lipolytica* is notable as a "generally regarded as safe (GRAS)" strain among oleaginous yeasts, it becomes a good cell factory candidate to produce food-grade commercial chemicals such as polyunsaturated fatty acids (Xue et al., 2013; Gemperlein et al., 2019). With these pioneering studies, *Y. lipolytica* showed its potential to be developed as oleo-biorefineries producing a broad range of lipid-derived chemicals, such as detergent, adhesive, dye, lubricant, cosmetics, and polymer and monomer. In parallel with well-developed molecular biology and metabolic engineering tools, now we are entering an era of developing oleaginous biorefinery using *Y. lipolytica*.

The development of synthetic biology, molecular biology tools, and systems biology has remarkably expanded our understanding of non-conventional microorganisms and broadened their applications to design cell factories for industrial biotechnology (Wagner and Alper, 2016; Park et al., 2017). Such new biological and theoretical approaches provided various useful analytical and methodological tools such as metabolic flux analysis, metabolite profiling, promoter engineering, and clusters of regularly interspaced short palindromic repeats (CRISPR)/Cas9 system, enabling us to understand detailed metabolic properties of the microorganisms and industrial host strain development, which are otherwise very tedious and challenging due to dominant non-homologous end-joining (Liu et al., 2016; Weninger et al., 2016; Tredwell et al., 2017; Xiong and Chen, 2020). In particular, non-conventional yeasts, such as *Pichia pastoris*, *Kluyveromyces lactis*, and *Y. lipolytica*, have been recently studied for their potential to implement feasible cell factories for the production of commodity and fine chemicals (Zhu and Jackson, 2015; Wagner and Alper, 2016; Schwarzhans et al., 2017; Abdel-Mawgoud et al., 2018; Cernak et al., 2018).

Recent metabolic engineering and systems biology studies of *Y. lipolytica* revealed underlying mechanisms on how excess carbon sources could be accumulated as neutral lipids in nutrient-limited conditions and how such a metabolic phase shift occurs in *Y. lipolytica* (Beopoulos et al., 2008; Lazar et al., 2018; Wang et al., 2020). In brief, in the absence of nutrients such as nitrogen, intracellular adenosine monophosphate (AMP) decreases as AMP deaminase activity increases. AMP's low levels inhibit AMP-dependent mitochondrial isocitrate dehydrogenase, accumulating citrate in the mitochondria (Kerkhoven et al., 2016). The accumulated citrate is then transported to the cytoplasm via citrate-malate transporter, and ATP-citrate lyase converts cytoplasmic citrate into oxaloacetate acetyl-CoA. *Y. lipolytica* converts excess carbon sources into cytoplasmic acetyl-CoA throughout the above mechanism and further synthesizes fatty acids and intracellular neutral lipids. If the enriched acetyl-CoA pool is channeled into other valuable chemicals, fatty acid or lipid-derived biorefinery could be easily constructed using the oleaginous yeast as a platform strain.

To construct the biorefinery systems producing fatty acid derivatives, it is essential to design strains that prevent excess carbon sources from being channeled into the synthesis of neutral lipids and to separate cell growth and product production phases since the high expression of heterologous genes for the production of lipid-derived chemicals causes cellular burden to fitness for cell growth. Metabolic engineering of *Y. lipolytica* for the production of free fatty acids (FFAs) has been studied with diverse approaches such as blocking metabolic pathways for synthesis of neutral lipids or degradation of synthesized fatty acids through β-oxidation (Ledesma-Amaro et al., 2016), pushing metabolic flux toward fatty acid synthesis (Ghogare et al., 2020), impairing glycerol metabolism to prevent the synthesis of neutral lipids (Yuzbasheva et al., 2018), expressing heterogeneous thioesterases (Xu et al., 2016), or breaking down lipids to fatty acids and glycerol with overexpression of lipases (Ledesma-Amaro et al., 2016). Also, chimeric eukaryotic type I fatty acid synthase (FAS-I) fused with heterologous thioesterase was applied to release fatty acids directly from acyl-carrier-protein along with genome manipulation using transcription activator-like effector nucleases (TALEN) (Rigouin et al., 2017).

To properly convert the produced fatty acids into target products, it is necessary to induce tailoring enzymes' expression

when fatty acids are accumulated in the cell. In general, according to a desired specific metabolic state, synchronized gene expression is critical to reducing metabolic burdens resulting from the overexpression of the tailoring enzymes. For the synchronization of the enzyme expression, perhaps chemical induction is the easiest method. However, there are drawbacks to finding out inexpensive proper inducers, the need for optimization of induction condition, and low reproducibility because of non-homogeneous mixing of inducers in bioreactors. Moreover, screening inducible promoters responding to the desired cell state is a prerequisite, so that systems biological understanding of the inducible promoters should be preceded. The other alternative method would be using a genetic switch. If a simple genetic switch responding to changes in fatty acid concentrations exists, dynamic control of the tailoring enzymes' gene expression would be possible for the production of target fatty acid derivatives. Then, cell growth can be easily decoupled with the production phase.

The bacterial FadR is a master regulator involved in lipid biosynthesis and its degradation and regulates the transcription of the related genes by binding to the FadR operator according to the intracellular concentration of fatty acyl-CoA. Studies have been carried out to design genetic circuits or to change the ratio of intracellular saturated or unsaturated fatty acids by redesigning FadR regulon by utilizing characteristics of the bacterial FadR (Teo et al., 2013; Kim et al., 2018). In particular, the previous report investigated the changes in the profile of FadR promoter activity depending on the concentration of externally treated fatty acid, the expression level of FadR, and the number of FadR binding sequences in *S. cerevisiae*. These results showed the possibility of implementing FadR synthetic promoters in *Y. lipolytica* to respond to intracellular fatty acids produced in various nutrient-limited conditions.

ω-Hydroxy fatty acids are valuable chemicals for adhesives, lubricants, and potential anticancer agents (Abe and Sugiyama, 2005; Lu et al., 2010). It can mostly be utilized for renewable monomers for polymers with high resistance to heat and chemicals and biocompatibility (Seo et al., 2015). Also, ω-hydroxylated long-chain fatty acids are essential components of esterified omega-hydroxy ceramides derived from glucosylceramide and sphingomyelin in epithermal cells (LLC, 2017). Since the esterified omega-hydroxy ceramides' deficiency is strongly correlated with skin diseases such as ichthyosis or atopic dermatitis (Sandhoff, 2010; Breiden and Sandhoff, 2014), the ω-hydroxylated long-chain fatty acids are one of the key components of the skin lipids.

In this study, to develop *Y. lipolytica* as a platform for producing fatty acid derivatives rather than neutral lipids, strains producing FFAs were constructed and improved via random library construction using ethyl methanesulfonate (EMS) mutagenesis and fluorescence-activated cell sorting (FACS) screening, and FadR synthetic promoters were constructed for gene expression responding to the accumulation of fatty acids. To evaluate the developed system, cytochrome P450 (CYP) was used as a model enzyme to convert palmitic acid to ω-hydroxy palmitic acid.

MATERIALS AND METHODS

Strains and Plasmids

All plasmids used in this study were constructed and amplified in *Escherichia coli* DH5α. *Y. lipolytica* Po1g *ku70*Δ strain with weakened homologous recombination was used as the base strain, annotating as wild type (WT) (Verbeke et al., 2013). A list of strains used in this study is summarized in **Supplementary Table 1**. pCRISPRyl (Addgene #70007) was used to remove genes for strain design as following a protocol from the supplier. N20 sequences of the gene of interest were predicted from "Benchling"[1] and cloned into pCRISPRyl. Primers used in this study are listed in **Supplementary Table 1**.

To construct replicating yeast vectors, pCRISPRyl_v1.0 was constructed by deleting the sgRNA expression cassette from pCRISPRyl, and restriction enzymes such as *Sgs*I and *Nhe*I (Thermo Scientific, United States) were used to secure the overexpression vector by replacing the *cas9* gene with the gene of interest.

Media and Culture Conditions

When culturing *E. coli* DH5α for vector construction and amplification, ampicillin as an antibiotic for selection was added in Luria-Bertani (LB) broth. Yeast Extract-Peptone-Dextrose (YPD) medium containing yeast extract 1% (w/v), peptone 2% (w/v), and glucose 2% (w/v) were used for non-selective seed cultivation of *Y. lipolytica*. For selective cultivation or enrichment of *Y. lipolytica*, synthetic dextrose (SD) media containing glucose 2% (w/v), Yeast Nitrogen Base without amino acids 0.68% (w/v), and 0.05% (w/v) of amino acids and nucleotide mixture without selection marker was used. To induce lipid accumulation in *Y. lipolytica*, CN medium containing glucose 6% (w/v), Yeast Nitrogen Base without amino acids and ammonium sulfate 0.17% (w/v), set amount of ammonium chloride for variation of carbon/nitrogen ratio (CN ratio), and 60 mM phosphate buffer (pH 6.8) was used. If needed, 0.05% (w/v) of amino acids were supplemented to CN medium. For batch fermentation, CN medium having a 60 carbon/nitrogen ratio was used. The batch fermentation's operation condition proceeded as follows: 1 L working volume, 30°C, 600 rpm, one vvm (vol/vol), and pH was titrated with 3 M KOH to 5.00. All experiments expressing CYP were supplemented with 0.5 mM of 5-aminolevulinic acid and 0.1 mM of ferric sulfate.

General Molecular Biology Techniques

The transformation of constructed plasmids and relevant editing templates for deleting target genes using the CRISPR/Cas9 system was conducted using a standard lithium acetate protocol (Chen et al., 1997). Briefly, fresh cells from YPD plates and DNAs were mixed with a buffer containing 88 μl of 50% (w/v) PEG 4000, 5 μl of 2 M dithiothreitol, 5 μl of lithium acetate (pH 6.0), and 2 μl of single-strand carrier DNA (10 μg/μl) purchased from Thermo Fisher Scientific. The mixture was incubated at 37°C for 1 h and plated on selective agar plates. To identify positive transformants, 3 μl of 0.02 M sodium hydroxide and a freshly picked colony

[1] http://benchling.com

was boiled at 99°C for 10–15 min. The boiled mixture was then mixed with a PCR reaction mixture containing Taq polymerase (nTaq, Enzynomics).

Gene amplification from genomic DNA was performed by Herculase II Fusion DNA polymerase (Agilent) based on standard recombinant DNA techniques and a supplier's protocol. For the construction of desired vectors, an amplified DNA and a template vector were cut by restriction enzymes (Thermo Fisher Scientific) and ligated by T4 ligase (Promega). If there were no appropriate restriction enzymes to cut specified DNAs, the circular polymerase extension cloning (CPEC) method was applied (Quan and Tian, 2009).

In detail, promoters with FadR operator sequences were cloned from genomic DNA of *Y. lipolytica* Po1g or in-house vectors. First, GPD promoter (pGPD) was amplified from genomic DNA using pGPD-F and pGPD-front-R, and 17 bp of *E. coli* FadR operator sequence was inserted at the end of pGPD using pGPD-Back-F and pGPD-R, which was fused with overlap extension using primer pGPD-F and pGPD-R. Also, for constructing the same three FadR operator sequences, pGPD was amplified with pGPD-3O-F and pGPD-3O-R, then fused with an amplified fragment using pGPD-BB-F and pGPD-BB-R from pGPD with one FadR operator sequence. For the construction of TEF and LEU promoters harboring FadR operator sequences, each promoter was amplified using primers with the number of operators added. Each fragment was digested with *Pac*I and *Avr*II and ligated to the digested vector harboring pGPD and one or three FadR operator sequences. Humanized *Renilla reniformis* GFP (hrGFP) was amplified from an in-house vector to construct hrGFP-expressing cassette with pGPD using hrGFP-F and hrGFP-R. The digested promoter sequence with *Xba*I and *Eco*RI was ligated with amplified hrGFP digested with *Eco*RI and *Hin*dIII, then subcloned into a pUC19 vector. To construct the yeast-replicating plasmid (YRp) expressing *fadR*, FadR-F and FadR-R were used as primers to amplify *fadR* from an in-house vector. The backbone of YRp was amplified using primers YRp-F and YRp-R from pCRISPRyl v1.0. Then, amplified fragments were ligated using the CPEC method yielding FadR-YRp. Insertion of the hrGFP-expressing cassettes harboring pGPD, pTEF, or pLEU into pFadR-YRp was done by amplifying the hrGFP-expressing cassette from pUC19-hrGFP with hrGFP-YRp-F and hrGFP-YRp-R and ligated with FadR-YRp digested with *Pac*I and *Spe*I.

Analyses of FFAs and Determination of Lipid Classes

There have been many studies to report analytical methods of FFA quantification. Among them, the following method was performed (Ferreira et al., 2018). Briefly, 5% (v/v) of 40% (w/v) tetrabutylammonium hydroxide was added to the whole broth as a base catalyst, and the same volume of dichloromethane containing 200 mM of methyl iodide was used to convert and extract FFA into FAMEs. The extracted mixture was centrifugated for phase separation. Then, dichloromethane layer was transferred to a new Eppendorf tube for evaporation. Extracted FAMEs were resuspended with hexane and further analyzed in GC/FID (Agilent). Methyl heptadecanoate was used as an internal standard, and analytic standards purchased from Sigma-Aldrich Chemical Co. (St. Louis, MO, United States) were used to obtain standard curves of each FAME. Operation condition for GC/FID was as follows: a non-polar capillary column (5% phenyl methyl siloxane capillary 30 m × 250 m i.d., 0.25 μm film thicknesses) and a linear temperature gradient (60°C 1 min, temperature gradient of 15°C/min to 180°C, hold for 10 min, the temperature gradient of 15°C/min to 200°C, hold for 10 min, the temperature gradient of 15°C/min to 250°C, hold for 10 min) was used.

Lipid classification was performed using thin-layer chromatography (TLC) (Athenstaedt et al., 1999; Schneiter and Daum, 2006). Lipids extracted from lyophilized cells using hexane were applied on silica gel plates, then the plates were developed twice with petroleum ether/diethyl ether/acetic acid [25:25:1 (vol/vol/vol)] and petroleum ether/diethyl ether [49:1 (vol/vol)]. Separated lipids were dyed with iodine vapor for visualization, then additionally charred using the heat gun. Visualized lipids were identified based on the migration of standards purchased from Sigma-Aldrich Chemical Co. (St. Louis, MO, United States).

Ethyl Methanesulfonate Mutagenesis and Library Screening Using FACS

The random library was constructed via EMS mutagenesis based on a previous study (Liu et al., 2015), and the process was as follows. Overnight seed culture was diluted into 10 OD_{600} units and resuspended in sodium phosphate buffer (pH 7.4). After treating EMS in the buffer to a final concentration of 0.6% (v/v), cells were incubated in a shaking incubator at 30°C for 1 h. Then, the EMS-treated cells were washed with 5% (w/v) sodium thiosulfate, and the cell pellet was resuspended in sterile water. An OD_{600} value of the constructed random library was measured, a small moiety of the sample solution was spread on plates to calculate the size of the random library, and the rest was inoculated into an appropriate medium. All laboratory equipment with contact with EMS were washed thoroughly with 5% (w/v) sodium thiosulfate.

Nile Red was used to stain intracellular lipids, and the following staining method was used: one OD_{600} unit of seed culture was harvested and resuspended in 500 μl of phosphate-buffered saline solution. The resuspended cells were stained with 6 μl of 1 mM Nile Red dissolved in dimethyl sulfoxide and incubated for 15 min in the dark at room temperature. The stained cells were harvested and washed twice with ice-cold sterile water. The stained cells were diluted to 0.1 OD_{600} units for FACS operation (Bio-Rad, S3e Cell Sorter). The FL2 filter was used to determine the fluorescence of stained cells. The filter's voltage was adjusted to obtain an appropriate chromatogram, and fluorescence was measured under the same conditions for each cycle of iterative enrichment culture and FACS screening. The library was inoculated and cultured in YPD overnight and diluted to a 0.1 OD_{600} unit using the induction medium for lipid accumulation. After the seed culture was fully grown, the cells were harvested and stained with Nile Red. Among the stained cells, the top 5% cells with the highest fluorescence intensity were

sorted through FACS machine and inoculated into YPD media for regeneration. The above steps of processes were combined and defined as one cycle (**Figure 2A**).

Evaluation of Strength of the Synthetic FadR Promoters via Fluorescence Spectrometry and Quantitative Reverse Transcription-Polymerase Chain Reaction

For evaluation of the strength of synthetic FadR promoters, the fluorescence intensity of hrGFP was measured. The plasmids containing *fadR*-expressing genetic cassette, called pTEF-FadR-Cyc1t, and synthetic FadR promoters expressing hrGFP were transformed into host strains, and transformants were cultured in 2-ml selective media for 24 h at 30°C. The cells were transferred to a 100-ml flask containing 20 ml selective medium. After 12 h of incubation at 30°C, cells were harvested and washed with sterile water. Each strain was diluted to two OD_{600} units in a 4-ml SD medium. Synthetic FadR promoter was induced with exogenously added fatty acid dissolved in dimethyl sulfoxide and Tween-80. After 8 h of incubation at 30°C, OD_{600} was measured using a Labino spectrophotometer (Labotec), and 200 μl of cells were loaded to 96-well microplates (Corning), and their fluorescence was measured with Spark multimode microplate reader (Tecan). Excitation was done with a 485/20 filter, and emission was measured with a monochromator at the wavelength of 520/20.

RNA preparation for quantitative reverse transcription-polymerase chain reaction (qRT-PCR) was conducted using the phenol extraction method (Collart and Oliviero, 2001). Briefly, samples were washed with lysis buffer containing 10 mM Tris–HCl (pH 7.4), 10 mM ethylene diamine tetraacetic acid (EDTA), and 0.5% (w/v) sodium dodecyl sulfate (SDS), and incubated at −70°C for 30 min. After treating with the same amount of acidic phenol, the samples were incubated at 65°C for 20 min. At this time, the samples were vortexed every 5 min. After 10 min of incubation in ice, the samples were centrifuged at 4°C, and supernatant was transferred to new Eppendorf tubes. The same volume of chloroform was added and vortexed. After centrifugation, the supernatant of samples was transferred to new Eppendorf tubes containing 1/10 volume of 3 M sodium acetate and two-volume of 100% ethanol and incubated at −70°C for 30 min. After repetitive washing with 70% ethanol and centrifugation at 4°C, extracted RNA was processed with aspiration and air-drying and eluted with RNase-free water at 65°C.

cDNA was synthesized using M-MLV Reverse Transcriptase (Promega) from the extracted RNA following the supplier's protocol. For qRT-PCR, TOPreal^{TM} qPCR 2X Premix (Enzynomics, SYBR Green with low ROX) was used as a reaction buffer, and Light Cycler 480 system (Roche) was used to measure relative expression levels of mRNA. To quantify the mRNA level of the gene of interest, *act1* was used as a housekeeping gene, and the temperature gradient was set as follows: preincubation was conducted with a temperature gradient of 4.4°C/min to 95°C and held for 5 min. Amplification was conducted with a temperature gradient of 4.4°C/min to 95°C and held for 20 s, 2.2°C/min to 60°C and held for 20 s, and 4.4°C/min to 72°C and held for 20 s. A total of 40 cycles were repeated for the amplification step. Primers used for qRT-PCR were listed in **Supplementary Table 1**.

RESULTS

Development of *Y. lipolytica* Strains for FFA Production by Iterative Serial Cultures and FACS Screening

Based on pioneering studies on FFA production, metabolic engineering and an evolutionary approach were adopted to improve the FFA production *of Y. lipolytica*. To generate a platform strain to start, a metabolically engineered strain of *Y. lipolytica* was constructed by blocking the biosynthesis of neutral lipids, as the Nicaud group reported (Ledesma-Amaro et al., 2016). To minimize the use of selection markers for further transformation, six genes related to neutral lipids' biosynthesis were deleted following the previous report (**Figure 1A**). For rewiring of carbon flux toward FFA production instead of synthesis of neutral lipids, four genes, i.e., two diacylglycerol O-acyltransferases (Dga1 and Dga2), acyl-CoA: sterol acyltransferase (Are1), and acyl-CoA: phospholipid acyltransferase (Lro1) involved in the last step of the biosynthesis of triacylglyceride, were deleted. Also, the two genes involved in activation or degradation of FFA, i.e., acyl-CoA synthetase (Faa1) and peroxisomal multifunctional enzyme (Mfe1), respectively, were deleted for prevention of using FFA-consuming metabolic pathways (**Supplementary Figure 1**). As a result, based on the constructed strains, i.e., M and MF, hindering FFA consumption, deletion of the genes involved in neutral lipid synthesis were added to MF, yielding D1/2MF and F6.

Each mutant's productivity during the construction of the F6 strain was evaluated in a nitrogen-limited growth medium to induce FFA overproduction (**Figure 1B**). The F6 strain showed improved productivity about 15 times compared to that of the WT strain. Other strains, such as MF or D1/2MF, also showed improved productivities, about 17 times higher than that of the WT strain. During the construction of the platform strain, one thing to note was that cell growth of the three strains decreased by 20, 30, and 40% compared to that of the WT strain (**Supplementary Table 2**). Also, to identify lipid classes, TLC analysis revealed that F6 strain accumulated major FFAs in the cytoplasm and minor ones in the supernatant, unlike the WT strain that mainly accumulated neutral lipids in the cell (**Figure 1C**).

Furthermore, the F6 strain cultured in the nitrogen-deficient medium showed filamentous growth after 100 h (**Supplementary Figure 2**). As dimorphism of *Y. lipolytica* was reported in the previous studies (Ruiz-Herrera and Sentandreu, 2002), it was hypothesized that filamentous growth could influence growth defect of the F6 strain. To reduce the heterogeneity induced by filamentous growth, Mhy1, i.e., C_2H_2-type zinc-finger protein, which is involved in regulating lipid biosynthesis,

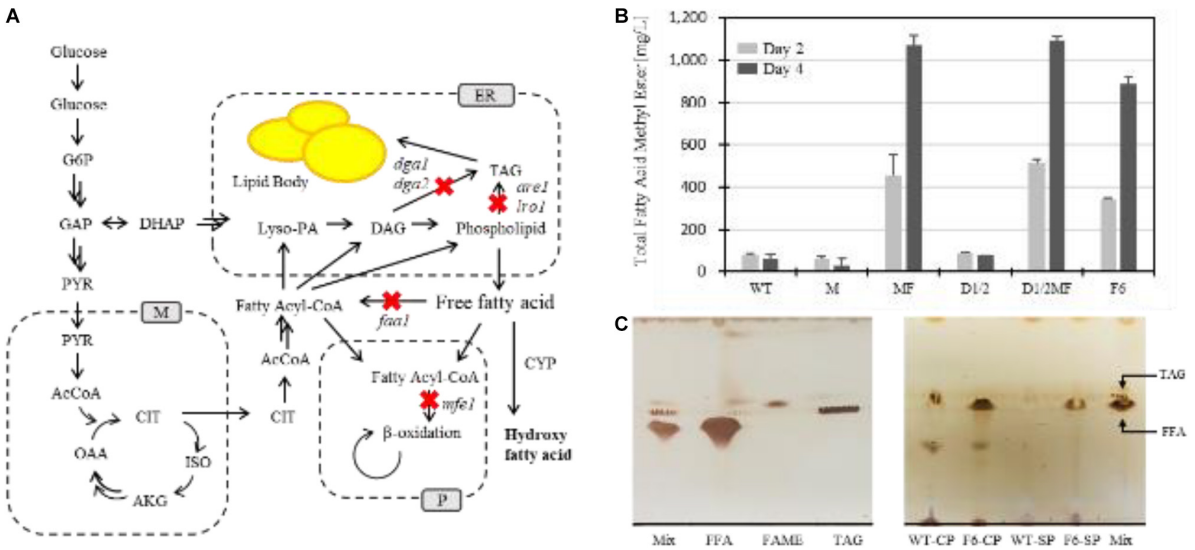

FIGURE 1 | Scheme of metabolic engineering of *Y. lipolytica* for FFA production and evaluation of its production of the constructed strains **(A,B)** and lipid identification using thin-layer chromatography (TLC) analysis **(C)**. Red cross represented deletion of genes involved in marked pathways. Abbreviations used in this figure were as follows: glucose 6-phosphate (G6P), glyceraldehyde 3-phosphate (GAP), dihydroxyacetone phosphate (DHAP), pyruvate (PYR), acetyl-CoA (AcCoA), oxaloacetate (OAA), citrate (CIT), alpha-ketoglutarate (AKG), isocitrate (ISO), lysophosphatidic acid (Lyso-PA), diglyceride (DAG), triglyceride (TAG), mitochondria (M), endoplasmic reticulum (ER), peroxisome (P) free fatty acid (FFA), fatty acid methyl ester (FAME), cell pellet (CP), and supernatant (SP). The strains used in panels **(B)** were as follows: Po1g *ku70*Δ (WT), Po1g *ku70*Δ *mfe1*Δ (M), Po1g *ku70*Δ *mfe1*Δ *faa1*Δ (MF), Po1g *ku70*Δ *dga1*Δ dga2Δ (D1/2), Po1g *ku70*Δ *dga1*Δ dga2Δ *mfe1*Δ *faa1*Δ (D1/2MF), and Po1g *ku70*Δ *dga1*Δ dga2Δ *mfe1*Δ *faa1*Δ *are1*Δ lro1Δ (F6). For quantification, total free fatty acids in the strains were converted into total fatty acid methyl esters using the transesterification method described in the "Materials and Methods" section.

amino acid and nitrogen metabolism, and cell cycle (Hurtado and Rachubinski, 1999), was additionally deleted, yielding Fm strain. The Fm strain showed unicellular yeast growth and increased its cell growth by 30% (**Supplementary Figures 2a,c**). Throughout the above metabolic engineering of *Y. lipolytica*, the productivity of FFA in the Fm strain increased significantly (**Supplementary Figure 2b**). To further overcome the growth defect of the Fm strain, an evolutionary metabolic engineering strategy was attempted. Therefore, it was aimed to screen the strains with recovered cell growth and comparable FFA production. To accelerate the natural evolutionary process for metabolic engineering, a random mutation library of the Fm strain was constructed via EMS mutagenesis. As a result, the experimental group treated with EMS for an hour showed a death rate of 98.9%, and the size of the constructed random library was approximately 8×10^6 cells. A two-step screening method was also designed for screening strains with enhanced growth but with comparable productivity of FFA. It was presumed that iterative serial culture and FACS screening with Nile Red staining could screen robust strains with high yields of FFAs. As the screening cycles proceeded, the mean value of the screened library's fluorescence intensity increased but started to decrease at the fourth cycle (**Figure 2B**). Thus, further evaluation was carried out with the strains after the third cycle. After a total of 10 colonies were secured in the screened library, their cell growth rate and fluorescence intensity of the colonies were compared with those of the Fm strain (**Table 1**). Among them, two strains, annotated as FmeN3 and FmeN4, showed about twofold enhanced fluorescence intensity, and FmeN3 and FmeN6 showed increased cell growth yields by 40 and 90%, respectively. Three candidates (FmeNXs) were selected and further evaluated in the media with different CN ratios.

First, FmeN3, FmeN4, and FmeN6 were cultured in media with a high and low CN ratio, i.e., 120 (C mol/N mol) and 30 (C mol/N mol), respectively, and evaluated for their profiles of cell growth and FFA production under such limiting conditions. It was confirmed that the FmeN3 and FmeN6 showed enhanced cell growth rate and FFA production yields in the medium with low CN ratio, whereas the FmeN4 strain showed lower cell growth rate and FFA production yields under all the conditions examined (**Supplementary Figure 3**). The experimental results concluded that FmeN4 was false positive. FmeN3 and FmeN6 were further evaluated in the medium with 60 (C mol/N mol) ratio (CN60), inducing the best FFA accumulation when the Fm strain was cultured. After 5 days of culture, the cell growths of FmeN3 and FmeN6 strains were fast by about 50 and 70%, respectively, compared to that of the Fm strain. Also, each strain's FFA production increased by about 20 and 40%, respectively (**Figure 3**). In summary, through EMS random mutagenesis and FACS screening method, two strains, FmeN3 and FmeN6, were selected based on the increased cell growth rate and FFA production yields and were further utilized as platform strains for the production of hydroxy fatty acid.

Construction of FadR Synthetic Promoter Responsive to FFA Production

In order to evaluate whether FadR can be used in *Y. lipolytica*, FadR-dependent promoters were constructed and evaluated

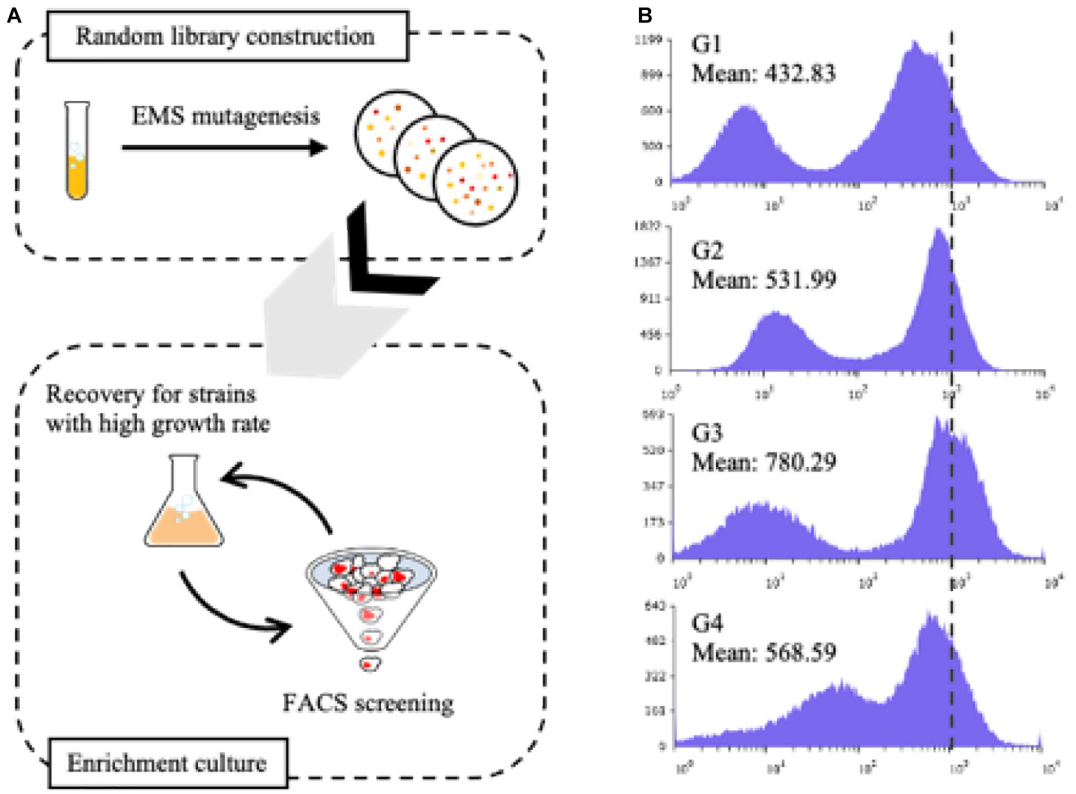

FIGURE 2 | Schematic representation of constructing random library and screening **(A)**. Fluorescence intensity on *X*-axis and cell counts on *Y*-axis were demonstrated in chromatograms acquired from fluorescence-activated cell sorting (FACS) **(B)**. Each cycle of the screening step was annotated as GXs, and the mean value of each cycle's fluorescence intensity was displayed in the figure. As cycles of screening and enrichment proceeded, G3 showed the highest mean value of fluorescence, and after G3, the value decreased. Thus, further evaluation was conducted using the mutants acquired from G3.

TABLE 1 | Colonies from the screened library were compared with the Fm strain.

	Fm 1	Fm 2	N1	N2	N3	N4	N5	N6	N7	N8	N9	N10
OD_{600}	1.16	0.78	1.00	1.21	1.38	1.01	1.05	1.81	0.99	1.24	1.05	0.98
Intensity of fluorescence	213.29	208.4	254.03	279.56	419.78	494.86	210.91	244.88	237.32	273.65	305.19	227.75
Fold change compared to mean value of OD_{600}			1.03	1.25	1.43	1.04	1.08	1.87	1.02	1.28	1.09	1.01
Fold change compared to mean value of intensity of fluorescence			1.20	1.33	1.99	2.35	1.00	1.16	1.13	1.30	1.45	1.08
Total	1.00		1.24	1.65	2.84	2.45	1.08	2.17	1.15	1.66	1.57	1.09

OD_{600} and fluorescence-activated cell sorting (FACS) analysis were carried out with samples at 24 h, cultured in the CN 60 media. Mean values acquired from the control strain were used to compare fold changes with growth and fluorescence acquired from 10 colonies. The intensity of fluorescence was measured using FACS. The total change was calculated by multiplying fold changes of OD_{600} and fluorescence intensity. Among 10 colonies, N3, N4, and N6 showed improved growth and fluorescence by about twofold compared to that of the Fm strain.

with an expression of *hrgfp* in FadR-expressing strains. Three well-characterized promoters in *Y. lipolytica*, i.e., glyceraldehyde-3-phosphate dehydrogenase (pGPD), translational elongation factor (pTEF), and 3-isopropyl malate dehydrogenase (pLEU), were used as templates. FadR binding sequences were inserted between the promoters and the start codon. First, FadR-dependent TEF promoters were constructed by harboring varying numbers (i.e., 0, 1, and 3) of FadR binding sequences, yielding $pTEF_{R0}$, $pTET_{R1}$, and $pTEF_{R3}$, respectively. To evaluate the sufficient binding of FadR to its binding sequences, the intrinsic transcription levels of hrGFP of the three promoters were compared in *mfe1* deletion mutant (**Figure 4A**). $pTEF_{R1}$ and $pTEF_{R3}$ showed decreased transcription as fluorescence intensity of hrGFP decreased by 80 and 90%, respectively, compared to $pTEF_{R0}$ (**Figure 4B**), suggesting that the transcription of *hrgfp* was inhibited by the constitutively expressed FadR and the presence of the FadR binding sequences. Based on these FadR synthetic promoters, we attempted to confirm whether externally treated fatty acids induced gene expression.

To confirm that externally treated fatty acids can activate the designed synthetic promoters, myristic acid showing a good binding affinity to the FadR was fed with varying concentrations (Teo et al., 2013). pGPD promoters showed about 10% increased

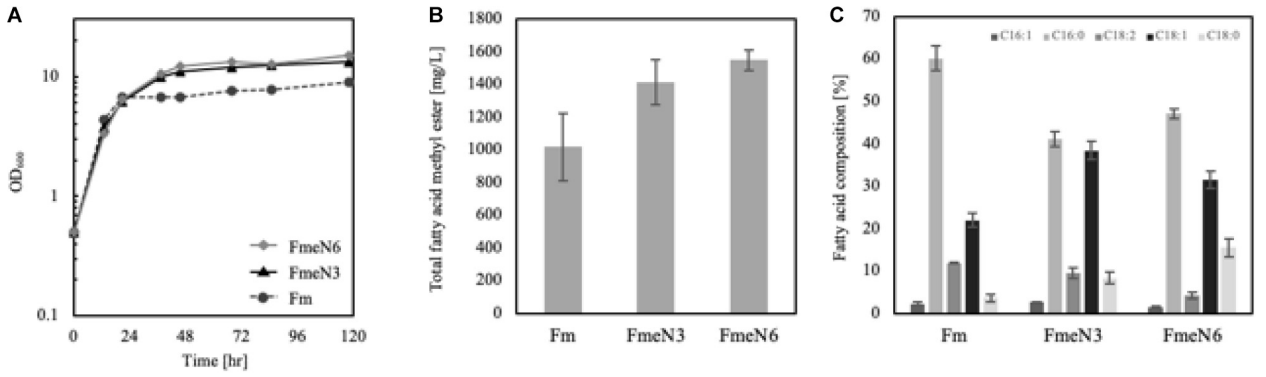

FIGURE 3 | Growth curve **(A)**, free fatty acid (FFA) production **(B)**, and fatty acid composition **(C)** of Fm and the screened mutants cultured in the CN60 medium. Experiments were carried out with biological duplicates. The screened mutants showed better growth and improved FFA production in the nutrient-deficient media than the Fm strain. The composition of fatty acids was calculated by the proportion of each fatty acid over total fatty acid concentration. Each fatty acid was represented in the number of the carbon chain and unsaturated bonds. Error bars represented the standard deviation of biological duplicates.

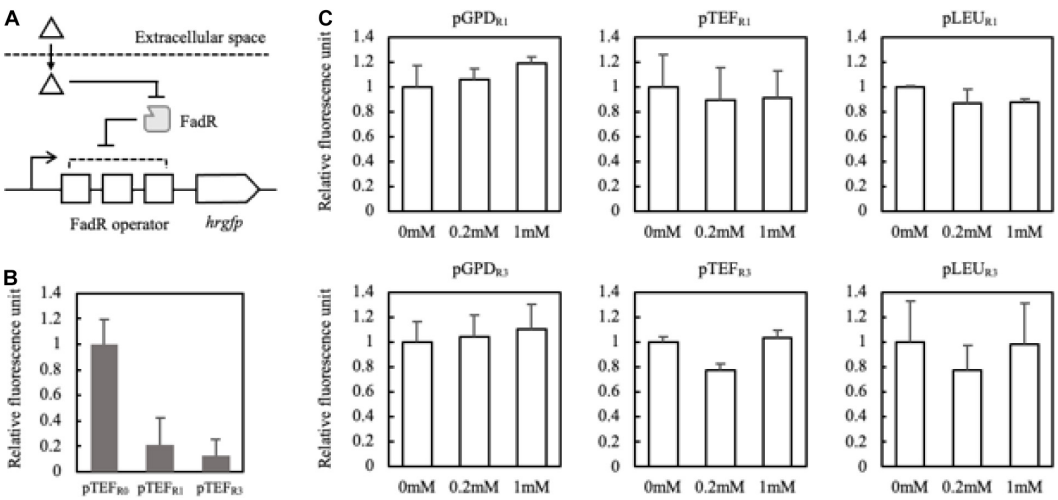

FIGURE 4 | Schematic representation of the FadR synthetic promoters and their induction by extracellularly treated fatty acids **(A)**. Triangle and gray rectangle represented fatty acids and FadR, respectively. The number of FadR binding sequences (R0, R1, and R3) and promoters (pTEF, pGPD, and pLEU) was varied with the construction of the FadR synthetic promoters. Fluorescence intensities of $pTEF_{R0}$, $pTEF_{R1}$, and $pTEF_{R3}$ without extracellularly treated fatty acid were measured **(B)**. Relative fluorescence unit was presented by the concentration of myristic acid on the *X*-axis, which was extracellularly treated, and the synthetic FadR promoters **(C)**. The relative fluorescence unit was calculated based on the synthetic FadR promoters' fluorescence intensity without inducers (0 mM). Standard deviation was measured in triplicates.

fluorescence activity regardless of the copies of binding sequences (**Figure 4C**). Also, there were no significantly activated promoters among the constructs. The careful examination confirmed that the six FadR promoters' activity was fully inhibited even in the presence of the added fatty acid, suggesting that externally treated myristic acid did not effectively induce the FadR synthetic promoters. Therefore, to reduce the effect of other factors on FadR promoter strength except FFA concentration, the synthetic promoters' profile was evaluated in the strains such as Fm endogenously producing FFA *in vivo*.

To analyze and evaluate the promoters' transcriptional activity *per se*, quantification of mRNA expression levels of synthetic promoters on the first and third days was carried out as FFA production started from the second day of the culture in the nitrogen-deficient medium. It was revealed that 150 mg/L and 520 mg/L of FFA were produced in the Fm strain on days 1 and 3, respectively (**Supplementary Figure 4**). On day 3, the relative mRNA expression level of the $pTEF_{R0}$ was significantly reduced compared to day 1 (**Figure 5B**). However, $pTEF_{R1}$ and $pTEF_{R3}$ displayed about 14 and 11 times higher mRNA expression levels of hrGFP on day 3, respectively (**Figure 5C**). Even in the cases of $pLEU_{R1}$ and $pLEU_{R3}$, the mRNA expression levels decreased by 10% and increased by about 70% on day 3, respectively, compared to day 1 (**Figure 5C**). The expression profiles of the $pGPD_{R1}$ and $pGPD_{R3}$ appeared to be quite different (**Figure 5C**). For the $pGPD_{R1}$, the mRNA expression increased by 30% on day 3 compared to day 1. However, the relative mRNA expression level of $pGPD_{R3}$ decreased by 10% as time passed.

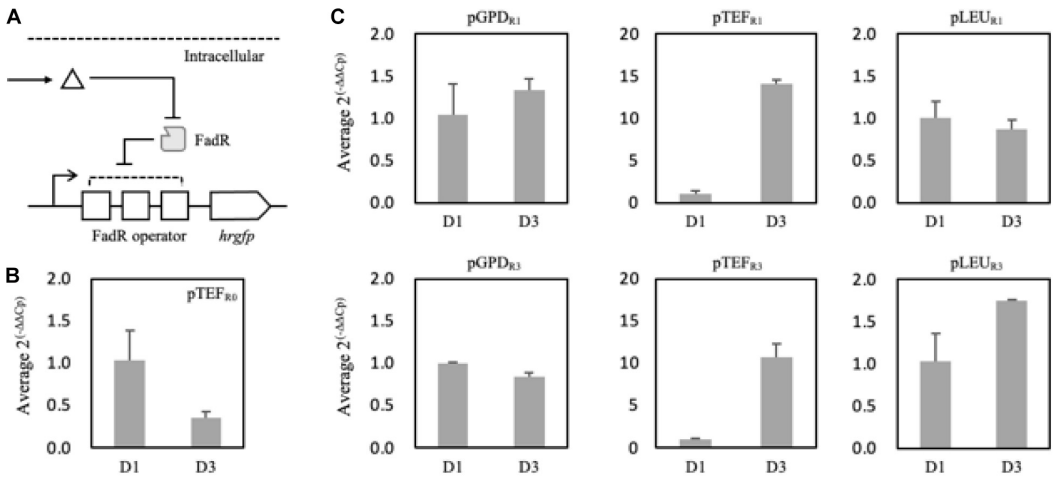

FIGURE 5 | Schematic representation of the FadR synthetic promoters and its induction by intracellularly produced fatty acid **(A)**. Triangle and gray rectangle represented fatty acid and FadR, respectively. The relative mRNA expression level of hrGFP expressed via pTEF without FadR operator (pTEF$_{R0}$) was compared on days 1 and 3 **(B)**. In panel **(C)**, pGPD, pTEF, and pLEU represented varying promoters constituting the synthetic FadR promoters. R1 and R3 represented the number of FadR operators in the synthetic FadR promoters with varying promoters. mRNAs from each construct were prepared from samples from days 1 and 3. C_p values were acquired from qRT-PCR, and average $2^{(-\Delta\ \Delta\ Cp)}$ was calculated using ΔC_p, i.e., $C_{p,\,hrGFP} - C_{p,\ Act1}$, of days 1 and 3 of each construct varying promoters and FadR binding sites **(B,C)**. Relative mRNA expression level and standard deviation were measured in triplicate.

Taken together, the transcriptional activities of the FadR synthetic promoters depend not only on the effector molecule concentrations, i.e., intracellular fatty acid concentrations but also on the strength of promoters in a specific metabolic state. In conclusion, among the various FadR synthetic promoters, pTEF$_{R1}$ could only decouple cell growth and production of fatty acid derivatives as its transcriptional activity dramatically (i.e., 14 times) increased as FFAs accumulated. Thus, further experiments proceeded with pTEF$_{R1}$ promoter for the expression of desired enzymes.

De novo Biosynthesis of ω-Hydroxy Palmitic Acid Using FmeN3 Strain Producing FFAs and Expression of *alk5* Under the Control of the FadR Synthetic Promoter

Previously, biotransformation of fatty acids or FAMEs into their corresponding ω-hydroxy fatty acids was carried out using yeasts (Lu et al., 2010; Durairaj et al., 2015) or *E. coli* (van Nuland et al., 2016; He et al., 2019; Yoo et al., 2019) where overexpression of alkane monooxygenase or CYP was attempted to introduce a hydroxy group to the substrates. CYPs drew our attention for their ability to introduce a hydroxy group into many complex structures with high regioselectivity (Urlacher and Girhard, 2019), and their application to the production of fatty acid derivatives in *Y. lipolytica* was quite promising. Firstly, we sought to express several CYPs known as having hydroxylating activity on the omega position of fatty acids in the Fm strain.

According to the Fm platform strains' profiles of fatty acids, palmitic acid, and oleic acid were the major ones (**Figure 3C**). To introduce proper CYPs accepting long-chain fatty acids as a substrate into the platform strains, two bacterial CYP153 family members, CYP153A33 and CYP153A35, and one CYP52A family in *Y. lipolytica*, Alk5, were chosen, and they were individually overexpressed in the Fm strain (Scheps et al., 2013; Jung et al., 2018). When cultured in CN60 medium for 2 days, a small amount of ω-hydroxy palmitic acid was produced, and Alk5 showed the highest production yield (5 mg/L) among the three CYPs (**Figure 6B**). Thus, Alk5 was chosen to further study the production of ω-hydroxy palmitic acid in the screened strains, FmeN3 and FmeN6. Unfortunately, any transformants could not be acquired from FmeN6 for unknown reasons, so that FmeN3 was used as the improved platform strain for the production of ω-hydroxy palmitic acid.

To assess the production of ω-hydroxy palmitic acid using Fm strain and FmeN3 strain containing *alk5* in pTEF$_{R0}$, yielding Fm_TR0_alk5 and FmeN3_TR0_alk5, respectively, test tube culture was conducted with CN60 medium. After 4 days of cultivation, FmeN3_TR0_alk5 produced about 40 mg/L of ω-hydroxy palmitic acid, which was about a 50% increase in production, compared to Fm_TR0_alk5 (**Figure 6C**). This result showed that the FmeN3_TR0_alk5 strain is a better performer than the Fm_TR0_alk5 for the production of ω-hydroxy palmitic acid. Next, *alk5* was expressed by pTEF$_{R1}$ in FmeN3, yielding the FmeN3_TR1_alk5 strain. It was compared with FmeN3_TR0_alk5 to assess its response to FFA accumulated in the nutrient-limited condition, which could decouple cell growth and production of ω-hydroxy palmitic acid (**Figure 6D**). FmeN3_TR1_alk5 displayed a somewhat (ca. 24 h) delayed product production but resulting in a comparable titer (55 mg/L). Since FFA started to accumulate after the depletion of nitrogen source, in the case of the Fm strain, it took ca. 48 h using the CN60 medium (**Figure 1B**). Our results also confirmed that the decoupling of cell growth and production of fatty acid derivatives was implemented using FadR synthetic promoters.

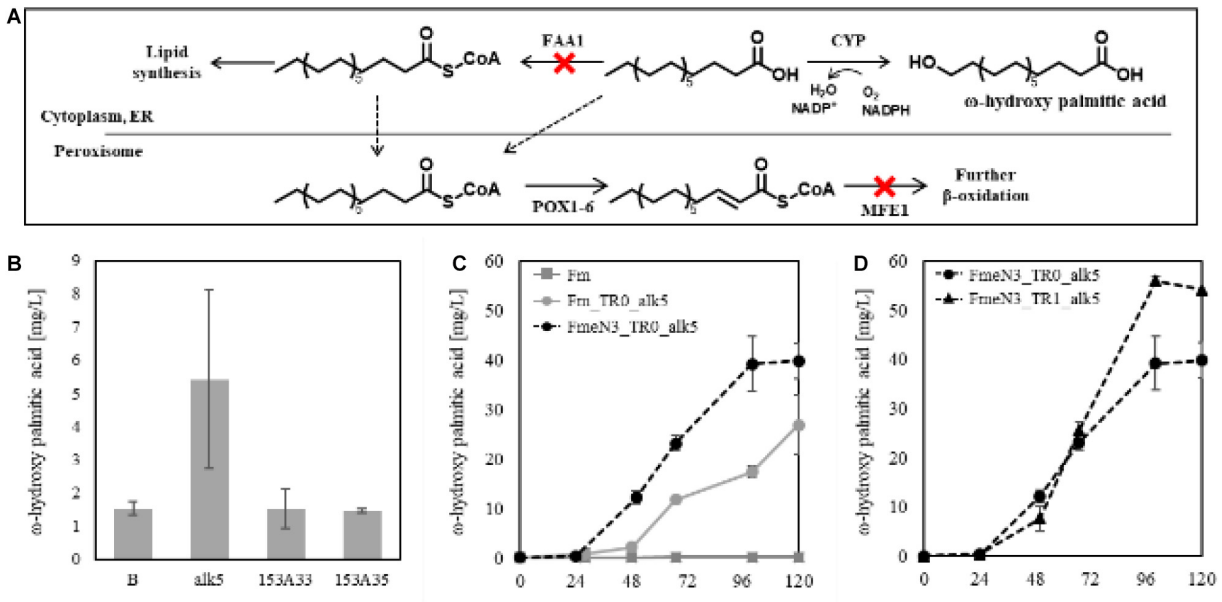

FIGURE 6 | Schematic representation of terminal hydroxylation via CYPs **(A)** and evaluating CYPs in the Fm strain. **(B)** represented the control strain in which the blank vector transformed, and alk5, 153A33, 153A35 represented the experimental strains expressing each CYP in the Fm strain **(B)**. Each CYP was expressed under the UAS1B8-TEF promoter. ω-hydroxy palmitic acid was analyzed using the samples from 2 days after the culture started. Endogenous Alk5 was the most active to palmitic acid produced in the Fm strain. The ω-hydroxy palmitic acid production using the screened mutants and the FadR synthetic promoter was evaluated, respectively **(C,D)**. For the appropriate expression of CYP, 0.5 mM of 5-aminolevulinic acid and 0.1 mM of ferrous sulfate were added when the cultures started. Experiments were carried out with biological duplicates. Error bars represented the standard deviation of biological duplicates. Abbreviations used in panel **(A)** were as follows: Acyl-CoA synthetase (FAA1), cytochrome P450 (CYP), endoplasmic reticulum (ER), Acyl-CoA oxidase (POX), and multifunctional peroxisomal enzyme 1 (MFE1).

Batch Fermentation

Lipid accumulation in *Y. lipolytica* was greatly influenced by the degree of aeration so that to synthesize more cellular lipids, non-baffled flask culture was more favorable than baffled flask culture (Xu et al., 2017) (data not shown). However, since the Alk5 reaction requires oxygen as a substrate, to achieve enough oxygen supply for cell growth and maintain a high CYP reaction rate, FmeN3_TR1_alk5 was cultured in a bioreactor. According to the cell growth and FFA production profiles, ω-hydroxy palmitic acid started to be produced in the cell from the stationary phase, around 24 h after the culture started (**Figure 7**). Here, 160 mg/L of ω-hydroxy palmitic acid, which is about threefold higher titer than that from test tube culture, was yielded at the end of the fermentation run. This result showed that the FadR synthetic promoter strength, the number of FadR binding sites, and oxygen supply were essential parameters to change hydroxy fatty acid production in *Y. lipolytica*.

DISCUSSION

When *Y. lipolytica* was designed to produce FFA instead of neutral lipid in nutrient-limited conditions, the deletion of acyl-CoA synthetase gene (faa1), involved in modifying fatty acid to fatty acyl-CoA, showed the most significant effect on the production of FFA (**Figure 1B**). According to some previous studies, there are FAA isozymes in *S. cerevisiae*, and the deletion of multiple faa genes showed increased FFA production (Michinaka et al., 2003; Scharnewski et al., 2008; Chen et al., 2014). We also confirmed that activation of fatty acid synthesis to fatty acyl-CoA and channeling into other pathways consuming fatty acyl-CoA should be avoided to accumulate FFA instead of triacylglyceride (**Figure 1C**). Also, during our construction of the Fm platform strain, the cell growth rate reduction was somewhat observed as more FFAs were accumulated in the cell.

Previously, EMS was a well-known mutagen for constructing a random library to produce point mutations on the entire microbial genome of interest at a rate of 5×10^{-4}–5×10^{-2} per gene (Wloch et al., 2001; Willensdorfer et al., 2007). According to one of the representative studies from the Alper group, if the mutated *Y. lipolytica* strains accumulate more neutral lipids in the cell, the cells' specific gravity would decrease and tend to float above liquid media. The floated cells were iteratively screened, and the mutants of enhanced lipogenesis genotype were identified (Liu et al., 2015). To acquire any desired phenotype, it was essential to implement a suitable and optimized screening method. Thus, it was hypothesized that screening fatty acid overproducer with FACS and recovering the cells with higher growth rate among the constructed library should be needed for securing mutants with robust cell growth and comparable accumulation of FFA (**Figure 2A**). After three generations of iterative FACS screening and EMS mutagenesis, several mutants displaying better cell growth and comparable FFA production were selected (**Figure 2B**). To identify the mutated genes

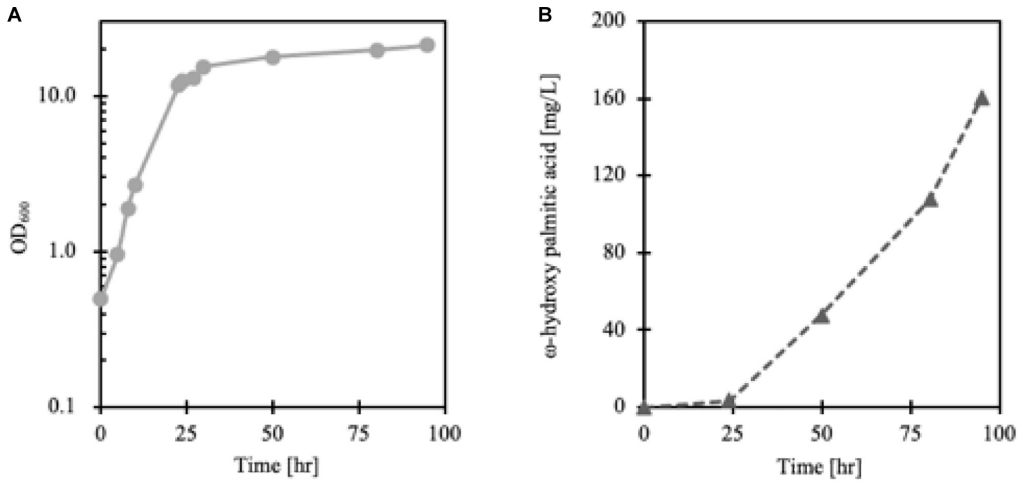

FIGURE 7 | Growth curve **(A)** and production **(B)** of FmeN3_TR1_alk5 cultured in the bioreactor. The dissolved oxygen level of the culture was maintained at over 50% compared to the initial Dissolved Oxygen (DO) level. As cell growth entered the stationary phase after 24 h, ω-hydroxy palmitic acid started to be produced in FmeN3_TR1_alk5.

caused by EMS mutagenesis, the screened mutants will be further subjected to next-generation sequencing (NGS) sequence analysis. Moreover, cell-to-cell variation in all fluorescence results was identified. According to the study, this heterogeneity could be further engineering target to improve FFA production that minimized cell-to-cell variation by implementing a FadR genetic circuit expressing antibiotic transporter in *E. coli* (Xiao et al., 2016).

For implementation of FadR synthetic promoters, FadR protein itself was constitutively expressed under TEF promoter, whereas reporter gene hrGFP was expressed under the modified FadR synthetic promoters in response to the amount of produced fatty acid. We have examined three promoters with different numbers of FadR binding sites and compared their response profiles to the accumulated fatty acid in the Fm strain (**Figure 5A**). It was confirmed that the response profile significantly changed according to the type of promoter and the number of binding sites constituting the FadR synthetic promoters. We thought this might be influenced by characteristics of the promoter responding to the metabolic status. According to a transcriptomic study on lipid-accumulating conditions in *Y. lipolytica*, there were five clusters categorized by the response profiles of metabolic genes (Morin et al., 2011). Among the study's identified genes, glyceraldehyde 3-phosphate dehydrogenase (YALI0C06369g, GPD) belonged to cluster 3, which was repressed when lipid started to accumulate. Therefore, the FadR synthetic promoter containing pGPD might be repressed by other factors instead of the FadR/fatty acyl-CoA complex. Also, the dynamic range of FadR synthetic promoters could be controlled by FadR expression level (Teo et al., 2013) and the numbers of FadR binding sites, so that our data showed that various designs would be possible depending upon types and strength of promoter expressing a gene of interest. Also, FmeN3_TR1_alk5 produced a lower amount of ω-hydroxy palmitic acid than FmeN3_TR0_alk5 after 48 h, whereas the maximum productivity of FmeN3_TR1_alk5 increased by 40% than that of FmeN3_TR0_alk5 (**Figure 6**). The results indicated that as FFA started to be accumulated, the expression of Alk5 by $pTEF_{R1}$ increased significantly (**Figure 5C**). After 72 h, the productivity of ω-hydroxy palmitic acid from FmeN3_TR1_alk5 surpassed that of FmeN3_TR0_alk5, where the activity of $pTEF_{R0}$ would decrease on day 3 (**Figure 5B**).

Comparing FFA production with or without the introduction of CYPs and the synthetic FadR promoter (**Supplementary Figure 5b**), Fm_TR0_alk5 and FmeN3_TR0_alk5 showed comparable FFA production with the strains without the introduction of Alk5 (**Figure 3B**). However, for FmeN3_TR1_alk5, FFA production decreased by 35% compared to that of FmeN3_TR0_alk5. As FadR was constitutively expressed in FmeN3_TR1_alk5, there could be a cellular burden of expressing FadR with the strong promoter, i.e., UAS1B8-pTEF, or FadR might interact with the fatty acid production system in *Y. lipolytica*. In fact, according to fatty acid profiles produced by FmeN3_TR0_alk5 and FmeN3_TR1_alk5 (**Supplementary Figure 5c**), oleic acid proportion decreased dramatically by about 15% when FadR was expressed in FmeN3_TR1_alk5. FFA production in batch fermentation using FmeN3_TR1_alk5 was about 400 mg/L, which showed lower productivity than FmeN3_TR0_alk5. Based on FFA production results in FmeN3_TR1_alk5, even production of ω-hydroxy palmitic acid increased, FadR expression on FFA production in *Y. lipolytica* needs to be examined in further studies.

This study also showed that FACS analysis and optimization of the bacterial transcriptional regulators as a genetic switch could be preferably utilized to construct oleaginous yeast producing ω-hydroxy fatty acid. Furthermore, this study demonstrated that evolutionary engineering approaches combined with synthetic biology could easily increase oleaginous biorefinery's potential capacity to higher levels beyond the metabolic engineering approach alone. These approaches can be easily adopted in constructing oleaginous biorefinery producing various chemicals.

DATA AVAILABILITY STATEMENT

The strains, plasmids, and raw data constructed or generated in this study can be requested from the authors.

AUTHOR CONTRIBUTIONS

BP and B-GK conceived the study. BP designed and carried out evolutionary metabolic engineering, FACS screening and application of the synthetic promoters to produce hydroxy fatty acid. BP and E-JK constructed the mutant strains. JuK and BP designed and constructed the synthetic FadR promoters. BP and JuK performed evaluation of the synthetic promoters in *Y. lipolytica*. YK and JYK provided experimental assistance in developing FACS screening and constructing mutants. BP, JoK, and B-GK organized the manuscript. All authors contributed to the article and approved the submitted version.

FUNDING

This research was supported by the National Research Foundation of Korea (NRF) funded by the Ministry of Science, ICT & Future Planning (NRF-2017R1E1A1A01073523), and Industrial Strategic technology development program (20002734) funded by the Ministry of Trade, Industry & Energy (MI, South Korea).

SUPPLEMENTARY MATERIAL

The Supplementary Material for this article can be found online at: https://www.frontiersin.org/articles/10.3389/fbioe.2021.624838/full#supplementary-material

REFERENCES

Abdel-Mawgoud, A. M., Markham, K. A., Palmer, C. M., Liu, N., Stephanopoulos, G., and Alper, H. S. (2018). Metabolic engineering in the host *Yarrowia lipolytica*. *Metab. Eng.* 50, 192–208. doi: 10.1016/j.ymben.2018.07.016

Abe, A., and Sugiyama, K. (2005). Growth inhibition and apoptosis induction of human melanoma cells by omega-hydroxy fatty acids. *Anticancer Drugs* 16, 543–549. doi: 10.1097/00001813-200506000-00010

Abghari, A., and Chen, S. (2014). *Yarrowia lipolytica* as an oleaginous cell factory platform for production of fatty acid-based biofuel and bioproducts. *Front. Energy Res.* 2:21. doi: 10.3389/fenrg.2014.00021

Athenstaedt, K., Zweytick, D., Jandrositz, A., Kohlwein, S. D., and Daum, G. (1999). Identification and characterization of major lipid particle proteins of the yeast *Saccharomyces cerevisiae*. *J. Bacteriol.* 181, 6441–6448.

Barth, G., and Gaillardin, C. (1996). *Yarrowia lipolytica*. *Nonconventional Yeasts in Biotechnology: A Handbook*. Heidelberg: Springer.

Beopoulos, A., Mrozova, Z., Thevenieau, F., Le Dall, M.-T., Hapala, I., Papanikolaou, S., et al. (2008). Control of lipid accumulation in the yeast *Yarrowia lipolytica*. *Appl. Environ. Microbiol.* 74, 7779–7789.

Breiden, B., and Sandhoff, K. (2014). The role of sphingolipid metabolism in cutaneous permeability barrier formation. *Biochim. Biophys. Acta* 1841, 441–452. doi: 10.1016/j.bbalip.2013.08.010

Cernak, P., Estrela, R., Poddar, S., Skerker, J. M., Cheng, Y. F., Carlson, A. K., et al. (2018). Engineering *Kluyveromyces marxianus* as a robust synthetic biology platform host. *mBio* 9, e1410–e1418. e01410-18,

Chen, C., Sun, N., Li, D., Long, S., Tang, X., Xiao, G., et al. (2018). Optimization and characterization of biosurfactant production from kitchen waste oil using *Pseudomonas aeruginosa*. *Environ. Sci. Pollut. Res. Int.* 25, 14934–14943. doi: 10.1007/s11356-018-1691-1

Chen, D. C., Beckerich, J. M., and Gaillardin, C. (1997). One-step transformation of the dimorphic yeast *Yarrowia lipolytica*. *Appl. Microbiol. Biotechnol.* 48, 232–235. doi: 10.1007/s002530051043

Chen, L., Zhang, J., Lee, J., and Chen, W. N. (2014). Enhancement of free fatty acid production in *Saccharomyces cerevisiae* by control of fatty acyl-coa metabolism. *Appl. Microbiol. Biotechnol.* 98, 6739–6750. doi: 10.1007/s00253-014-5758-8

Cherubini, F. (2010). The biorefinery concept: using biomass instead of oil for producing energy and chemicals. *Energy Convers. Manage.* 51, 1412–1421. doi: 10.1016/j.enconman.2010.01.015

Collart, M. A., and Oliviero, S. (2001). Preparation of yeast RNA. *Curr. Protoc. Mol. Biol.* Chapter 13:Unit13.12.

Cordova, L. T., Butler, J., and Alper, H. S. (2020). Direct production of fatty alcohols from glucose using engineered strains of *Yarrowia lipolytica*. *Metab. Eng. Commun.* 10:E00105.

da Silva, G. P., Mack, M., and Contiero, J. (2009). Glycerol: a promising and abundant carbon source for industrial microbiology. *Biotechnol. Adv.* 27, 30–39. doi: 10.1016/j.biotechadv.2008.07.006

Dobrowolski, A., Mituła, P., Rymowicz, W., and Mirończuk, A. M. (2016). Efficient conversion of crude glycerol from various industrial wastes into single cell oil by yeast *Yarrowia lipolytica*. *Bioresour. Technol.* 207, 237–243. doi: 10.1016/j.biortech.2016.02.039

Durairaj, P., Malla, S., Nadarajan, S. P., Lee, P. G., Jung, E., Park, H. H., et al. (2015). Fungal cytochrome P450 monooxygenases of *Fusarium oxysporum* for the synthesis of Ω-Hydroxy fatty acids in engineered *Saccharomyces cerevisiae*. *Microb. Cell Fact.* 14, 45.

Ferreira, R., Teixeira, P. G., Siewers, V., and Nielsen, J. (2018). Redirection of lipid flux toward phospholipids in yeast increases fatty acid turnover and secretion. *Proc. Natl. Acad. Sci. U.S.A.* 115, 1262–1267. doi: 10.1073/pnas.1715282115

Gajdoš, P., Nicaud, J. M., and Èertïk, M. (2017). Glycerol conversion into a single cell oil by engineered *Yarrowia lipolytica*. *Eng. Life Sci.* 17, 325–332. doi: 10.1002/elsc.201600065

Gajdoš, P., Nicaud, J. M., Rossignol, T., and Èertïk, M. (2015). Single cell oil production on molasses by *Yarrowia lipolytica* strains overexpressing Dga2 in multicopy. *Appl. Microbiol. Biotechnol.* 99, 8065–8074. doi: 10.1007/s00253-015-6733-8

Gao, Q., Cao, X., Huang, Y. Y., Yang, J. L., Chen, J., Wei, L. J., et al. (2018). Overproduction of fatty acid ethyl esters by the oleaginous yeast *Yarrowia lipolytica* through metabolic engineering and process optimization. *ACS Synth. Biol.* 7, 1371–1380. doi: 10.1021/acssynbio.7b00453

Gemperlein, K., Dietrich, D., Kohlstedt, M., Zipf, G., Bernauer, H. S., Wittmann, C., et al. (2019). Polyunsaturated fatty acid production by *Yarrowia lipolytica* employing designed myxobacterial pufa synthases. *Nat. Commun.* 10:4055.

Ghogare, R., Chen, S., and Xiong, X. (2020). Metabolic engineering of oleaginous yeast *Yarrowia lipolytica* for overproduction of fatty acids. *Front. Microbiol.* 11:1717. doi: 10.3389/fmicb.2020.01717

Harahap, F., Silveira, S., and Khatiwada, D. (2019). Cost competitiveness of palm oil biodiesel production in Indonesia. *Energy* 170, 62–72. doi: 10.1016/j.energy.2018.12.115

He, Q., Bennett, G. N., San, K. Y., and Wu, H. (2019). Biosynthesis of medium-chain Ω-Hydroxy fatty acids by Alkbgt of *Pseudomonas putida* Gpo1 with native Fadl in engineered *Escherichia coli*. *Front Bioeng Biotechnol* 7:273. doi: 10.3389/fbioe.2019.00273

Houard, S., Heinderyckx, M., and Bollen, A. (2002). Engineering of non-conventional yeasts for efficient synthesis of macromolecules: the methylotrophic genera. *Biochimie* 84, 1089–1093. doi: 10.1016/s0300-9084(02)00011-1

Hurtado, C. A., and Rachubinski, R. A. (1999). Mhy1 encodes a C2h2-type zinc finger protein that promotes dimorphic transition in the yeast *Yarrowia lipolytica*. *J. Bacteriol.* 181, 3051–3057. doi: 10.1128/jb.181.10.3051-3057.1999

Jung, E., Park, B. G., Yoo, H. W., Kim, J., Choi, K. Y., and Kim, B. G. (2018). Semi-rational engineering of Cyp153a35 to enhance Ω-Hydroxylation activity toward palmitic acid. *Appl. Microbiol. Biotechnol.* 102, 269–277. doi: 10.1007/s00253-017-8584-y

Kerkhoven, E. J., Pomraning, K. R., Baker, S. E., and Nielsen, J. (2016). Regulation of amino-acid metabolism controls flux to lipid accumulation in *Yarrowia lipolytica*. *NPJ Syst. Biol. Appl.* 2:16005.

Kim, J., Yoo, H. W., Kim, M., Kim, E. J., Sung, C., Lee, P. G., et al. (2018). Rewiring Fadr regulon for the selective production of Ω-Hydroxy palmitic acid from glucose in *Escherichia coli*. *Metab. Eng.* 47, 414–422. doi: 10.1016/j.ymben.2018.04.021

Lazar, Z., Dulermo, T., Neuvëglise, C., Crutz-Le Coq, A. M., and Nicaud, J. M. (2014). Hexokinase–a limiting factor in lipid production from fructose in *Yarrowia lipolytica*. *Metab. Eng.* 26, 89–99. doi: 10.1016/j.ymben.2014.09.008

Lazar, Z., Liu, N., and Stephanopoulos, G. (2018). Holistic approaches in lipid production by *Yarrowia lipolytica*. *Trends Biotechnol.* 36, 1157–1170. doi: 10.1016/j.tibtech.2018.06.007

Ledesma-Amaro, R., Dulermo, R., Niehus, X., and Nicaud, J. M. (2016). Combining metabolic engineering and process optimization to improve production and secretion of fatty acids. *Metab. Eng.* 38, 38–46. doi: 10.1016/j.ymben.2016.06.004

Ledesma-Amaro, R., and Nicaud, J. M. (2016). Metabolic engineering for expanding the substrate range of *Yarrowia lipolytica*. *Trends Biotechnol.* 34, 798–809. doi: 10.1016/j.tibtech.2016.04.010

Liu, L., Pan, A., Spofford, C., Zhou, N., and Alper, H. S. (2015). An evolutionary metabolic engineering approach for enhancing lipogenesis in *Yarrowia lipolytica*. *Metab. Eng.* 29, 36–45. doi: 10.1016/j.ymben.2015.02.003

Liu, N., Qiao, K., and Stephanopoulos, G. (2016). 13c metabolic flux analysis of acetate conversion to lipids by *Yarrowia lipolytica*. *Metab. Eng.* 38, 86–97. doi: 10.1016/j.ymben.2016.06.006

LLC, M. (2017). The essential role of esterified omega-hydroxy ceramides as skin lipids. *Newsletter For Glyco/Sphingolipidresearch*. (Matreya Llc, 2nd October 2017).

Lu, W., Ness, J. E., Xie, W., Zhang, X., Minshull, J., and Gross, R. A. (2010). Biosynthesis of monomers for plastics from renewable oils. *J. Am. Chem. Soc.* 132, 15451–15455. doi: 10.1021/ja107707v

Michinaka, Y., Shimauchi, T., Aki, T., Nakajima, T., Kawamoto, S., Shigeta, S., et al. (2003). Extracellular secretion of free fatty acids by disruption of a fatty acyl-coa synthetase gene in *Saccharomyces cerevisiae*. *J. Biosci. Bioeng.* 95, 435–440. doi: 10.1016/s1389-1723(03)80041-5

Mishra, P., Lee, N. R., Lakshmanan, M., Kim, M., Kim, B. G., and Lee, D. Y. (2018). Genome-scale model-driven strain design for dicarboxylic acid production in *Yarrowia lipolytica*. *BMC Syst Biol* 12(Suppl. 2):12. doi: 10.1186/s12918-018-0542-5

Mori, K., Iwama, R., Kobayashi, S., Horiuchi, H., Fukuda, R., and Ohta, A. (2013). Transcriptional repression by glycerol of genes involved in the assimilation of N-Alkanes and fatty acids in yeast *Yarrowia lipolytica*. *FEMS Yeast Res.* 13, 233–240. doi: 10.1111/1567-1364.12025

Morin, N., Cescut, J., Beopoulos, A., Lelandais, G., Le Berre, V., Uribelarrea, J. L., et al. (2011). Transcriptomic analyses during the transition from biomass production to lipid accumulation in the oleaginous yeast *Yarrowia lipolytica*. *PLoS One* 6:E27966. doi: 10.1371/journal.pone.0027966

Park, B. G., Kim, M., Kim, J., Yoo, H., and Kim, B. G. (2017). Systems biology for understanding and engineering of heterotrophic oleaginous microorganisms. *Biotechnol. J.* 12:1600104. doi: 10.1002/biot.201600104

Quan, J., and Tian, J. (2009). Circular polymerase extension cloning of complex gene libraries and pathways. *PLoS One* 4:E6441. doi: 10.1371/journal.pone.0006441

Radecka, D., Mukherjee, V., Mateo, R. Q., Stojiljkovic, M., Foulquië-Moreno, M. R., and Thevelein, J. M. (2015). Looking beyond *Saccharomyces*: the potential of non-conventional yeast species for desirable traits in bioethanol fermentation. *FEMS Yeast Res.* 15:fov053. doi: 10.1093/femsyr/fov053

Rebello, S., Abraham, A., Madhavan, A., Sindhu, R., Binod, P., Karthika Bahuleyan, A., et al. (2018). Non-conventional yeast cell factories for sustainable bioprocesses. *FEMS Microbiol. Lett.* 365:fny222.

Rigouin, C., Croux, C., Borsenberger, V., Ben Khaled, M., Chardot, T., Marty, A., et al. (2018). Increasing medium chain fatty acids production in *Yarrowia lipolytica* by metabolic engineering. *Microb. Cell Fact.* 17:142.

Rigouin, C., Gueroult, M., Croux, C., Dubois, G., Borsenberger, V., Barbe, S., et al. (2017). Production of medium chain fatty acids by *Yarrowia lipolytica*: combining molecular design and talen to engineer the fatty acid synthase. *ACS Synth. Biol.* 6, 1870–1879. doi: 10.1021/acssynbio.7b00034

Ruiz-Herrera, J., and Sentandreu, R. (2002). Different effectors of dimorphism in *Yarrowia lipolytica*. *Arch. Microbiol.* 178, 477–483. doi: 10.1007/s00203-002-0478-3

Sandhoff, R. (2010). Very long chain sphingolipids: tissue expression, function and synthesis. *FEBS Lett.* 584, 1907–1913. doi: 10.1016/j.febslet.2009.12.032

Sarkar, N., Ghosh, S. K., Bannerjee, S., and Aikat, K. (2012). Bioethanol production from agricultural wastes: an overview. *Renew. Energy* 37, 19–27. doi: 10.1016/j.renene.2011.06.045

Scharnewski, M., Pongdontri, P., Mora, G., Hoppert, M., and Fulda, M. (2008). Mutants of *Saccharomyces cerevisiae* deficient in acyl-coa synthetases secrete fatty acids due to interrupted fatty acid recycling. *FEBS J.* 275, 2765–2778. doi: 10.1111/j.1742-4658.2008.06417.x

Scheps, D., Honda Malca, S., Richter, S. M., Marisch, K., Nestl, B. M., and Hauer, B. (2013). Synthesis Of Ω-Hydroxy dodecanoic acid based on an engineered Cyp153a fusion construct. *Microb. Biotechnol.* 6, 694–707. doi: 10.1111/1751-7915.12073

Schneiter, R., and Daum, G. (2006). Analysis of yeast lipids. *Methods Mol. Biol.* 313, 75–84.

Schwarzhans, J. P., Luttermann, T., Geier, M., Kalinowski, J., and Friehs, K. (2017). Towards Systems metabolic engineering in *Pichia pastoris*. *Biotechnol. Adv.* 35, 681–710. doi: 10.1016/j.biotechadv.2017.07.009

Seo, J. H., Lee, S. M., Lee, J., and Park, J. B. (2015). Adding value to plant oils and fatty acids: biological transformation of fatty acids into Ω-Hydroxycarboxylic, A,Ω-Dicarboxylic, And Ω-Aminocarboxylic acids. *J. Biotechnol.* 216, 158–166. doi: 10.1016/j.jbiotec.2015.10.024

Teo, W. S., Hee, K. S., and Chang, M. W. (2013). Bacterial fadr and synthetic promoters function as modular fatty acid sensor- regulators in *Saccharomyces cerevisiae*. *Eng. Life Sci.* 13, 456–463. doi: 10.1002/elsc.201200113

Tredwell, G. D., Aw, R., Edwards-Jones, B., Leak, D. J., and Bundy, J. G. (2017). Rapid screening of cellular stress responses in recombinant *Pichia pastoris* strains using metabolite profiling. *J. Ind. Microbiol. Biotechnol.* 44, 413–417. doi: 10.1007/s10295-017-1904-5

Urlacher, V. B., and Girhard, M. (2019). Cytochrome P450 monooxygenases in biotechnology and synthetic biology. *Trends Biotechnol.* 37, 882–897. doi: 10.1016/j.tibtech.2019.01.001

van Nuland, Y. M., Eggink, G., and Weusthuis, R. A. (2016). Application of Alkbgt and Alkl from *Pseudomonas putida* Gpo1 for selective Alkyl ester Ω-Oxyfunctionalization in *Escherichia coli*. *Appl. Environ. Microbiol.* 82, 3801–3807. doi: 10.1128/aem.00822-16

Verbeke, J., Beopoulos, A., and Nicaud, J. M. (2013). Efficient homologous recombination with short length flanking fragments in Ku70 deficient *Yarrowia lipolytica* strains. *Biotechnol. Lett.* 35, 571–576. doi: 10.1007/s10529-012-1107-0

Wagner, J. M., and Alper, H. S. (2016). Synthetic biology and molecular genetics in non-conventional yeasts: current tools and future advances. *Fungal Genet. Biol.* 89, 126–136. doi: 10.1016/j.fgb.2015.12.001

Wang, J., Ledesma-Amaro, R., Wei, Y., Ji, B., and Ji, X.-J. (2020). Metabolic engineering for increased lipid accumulation in *Yarrowia lipolytica* – a review. *Bioresour. Technol.* 313:123707. doi: 10.1016/j.biortech.2020.123707

Weninger, A., Hatzl, A.-M., Schmid, C., Vogl, T., and Glieder, A. (2016). Combinatorial optimization of Crispr/Cas9 expression enables precision genome engineering in the methylotrophic yeast *Pichia pastoris*. *J. Biotechnol.* 235, 139–149. doi: 10.1016/j.jbiotec.2016.03.027

Willensdorfer, M., B??rger, R., and Nowak, M. A. (2007). Phenotypic mutation rates and the abundance of abnormal proteins in yeast. *PLoS Comput. Biol.* 3:E203. doi: 10.1371/journal.pcbi.0030203

Wloch, D. M., Szafraniec, K., Borts, R. H., and Korona, R. (2001). Direct estimate of the mutation rate and the distribution of fitness effects in the yeast *Saccharomyces cerevisiae*. *Genetics* 159, 441–452.

Workman, M., Holt, P., and Thykaer, J. (2013). Comparing cellular performance of *Yarrowia lipolytica* during growth on glucose and glycerol in submerged cultivations. *Amb. Express* 3:58. doi: 10.1186/2191-0855-3-58

Xiao, Y., Bowen, C. H., Liu, D., and Zhang, F. (2016). Exploiting nongenetic cell-to-cell variation for enhanced biosynthesis. *Nat. Chem. Biol.* 12, 339–344. doi: 10.1038/nchembio.2046

Xiong, X., and Chen, S. (2020). Expanding toolbox for genes expression of *Yarrowia lipolytica* to include novel inducible, repressible, and hybrid promoters. *ACS Synth. Biol.* 9, 2208–2213. doi: 10.1021/acssynbio.0c00243

Xu, P., Qiao, K., Ahn, W. S., and Stephanopoulos, G. (2016). Engineering *Yarrowia lipolytica* as a platform for synthesis of drop-in transportation fuels and oleochemicals. *Proc. Natl. Acad. Sci. U.S.A.* 113, 10848–10853. doi: 10.1073/pnas.1607295113

Xu, P., Qiao, K., and Stephanopoulos, G. (2017). Engineering oxidative stress defense pathways to build a robust lipid production platform in *Yarrowia lipolytica*. *Biotechnol. Bioeng.* 114, 1521–1530. doi: 10.1002/bit.26285

Xue, Z., Sharpe, P. L., Hong, S. P., Yadav, N. S., Xie, D., Short, D. R., et al. (2013). Production of omega-3 Eicosapentaenoic acid by metabolic engineering of *Yarrowia lipolytica*. *Nat. Biotechnol.* 31, 734–740.

Yoo, H. W., Kim, J., Patil, M. D., Park, B. G., Joo, S. Y., Yun, H., et al. (2019). Production of 12-Hydroxy dodecanoic acid methyl ester using a signal peptide sequence-optimized transporter Alkl and a novel monooxygenase. *Bioresour. Technol.* 291:121812. doi: 10.1016/j.biortech.2019.121812

Yuzbasheva, E. Y., Mostova, E. B., Andreeva, N. I., Yuzbashev, T. V., Fedorov, A. S., Konova, I. A., et al. (2018). A metabolic engineering strategy for producing free fatty acids by the *Yarrowia lipolytica* yeast based on impairment of glycerol metabolism. *Biotechnol. Bioeng.* 115, 433–443. doi: 10.1002/bit.26402

Zhu, Q., and Jackson, E. N. (2015). Metabolic engineering of *Yarrowia lipolytica* for industrial applications. *Curr. Opin. Biotechnol.* 36, 65–72. doi: 10.1016/j.copbio.2015.08.010

Conflict of Interest: The authors declare that the research was conducted in the absence of any commercial or financial relationships that could be construed as a potential conflict of interest.

Advantages of publishing in Frontiers

OPEN ACCESS
Articles are free to read for greatest visibility and readership

FAST PUBLICATION
Around 90 days from submission to decision

HIGH QUALITY PEER-REVIEW
Rigorous, collaborative, and constructive peer-review

TRANSPARENT PEER-REVIEW
Editors and reviewers acknowledged by name on published articles

Frontiers
Avenue du Tribunal-Fédéral 34
1005 Lausanne | Switzerland

Visit us: www.frontiersin.org
Contact us: frontiersin.org/about/contact

REPRODUCIBILITY OF RESEARCH
Support open data and methods to enhance research reproducibility

DIGITAL PUBLISHING
Articles designed for optimal readership across devices

FOLLOW US
@frontiersin

IMPACT METRICS
Advanced article metrics track visibility across digital media

EXTENSIVE PROMOTION
Marketing and promotion of impactful research

LOOP RESEARCH NETWORK
Our network increases your article's readership